

The GTPase DRG1 controls microtubule dynamics and is involved in chromatin decondensation

Dissertation

der Mathematisch-Naturwissenschaftlichen Fakultät

der Eberhard Karls Universität Tübingen

zur Erlangung des Grades eines

Doktors der Naturwissenschaften

(Dr. rer. nat.)

vorgelegt von

Anna Katharina Schellhaus

aus Hannover

Tübingen

2017

Tag der mündlichen Prüfung:

20. Juli 2017

Dekan:

Prof. Dr. Wolfgang Rosenstiel

1. Berichterstatter:

Prof. Dr. Wolfram Antonin

2. Berichterstatter:

Prof. Dr. Ralf-Peter Jansen

Acknowledgements

There are several people who have been vital for me and this project.

First of all, I want to thank my supervisor Prof. Dr. Wolfram Antonin for his continuous support and guidance. I am deeply grateful that he taught me to become a real scientist during the past years: from performing experiments to scientific thinking and designing projects. I learned a lot from his experience but in the same time he also taught me scientific independence.

I would also like to thank my TAC members, Prof. Dr. Jansen and Prof. Dr. Rapaport for their support and suggestions throughout the years.

I am also very grateful to Dr. Claudia Walther, Sandra Schedler, Dr. Anja Hoffmann and all the other members of the Boehringer Ingelheim Fonds team for giving me an amazing PhD fellowship, great opportunities, support, access to a network full of great scientists and always kind and personal contact.

I had many amazing colleagues throughout the years. I am thankful to every Antonin lab member I worked with. There are some colleagues I would like to mention personally: Allana, for loving science, always having great scientific ideas and being my frog buddy; Paola, for being my other frog buddy, it was great to have a colleague who went with me through the same stages – including ups and downs – of PhD; Dani, for great work and help on the DRG project, endless discussions and always being helpful and supportive in moments that needed it; Marion, for being an amazingly supportive colleague and for great lunch breaks; Susanne, for all the help on the project and the lab organization which made work so much easier for us; Ben & Micha, for the coffee breaks and being the experienced PhD guys I learned a lot from; Ada, for developing the great decondensation assay and answering my questions and emails before even knowing me; Hideki, for all the microtubule expertise; Rabia, for taking care of the frog and decondensation future of the lab; Franzi & Mario, for all the gels; Cathrin for the fun!!!

Beside the Antonin lab members, there are a lot of scientific colleagues & friends in FML who made work even more fun: Thanks to Alex, Maria, Luciano, Jelena, David, Stan, JP and Stefano for making a great working atmosphere!

I am grateful to Nadine for her lovely care for the frogs. Thanks to Veronika and Herta for their supportive work, to Christian for a very helpful and friendly microscope facility & to Sarah and the IMPRS program for the support.

Last but not least I also want to thank my family - especially my parents. Although I was probably really bad in explaining why I want to study Biochemistry, what chromatin decondensation and spindle assembly is and why I use frogs– you still trusted and believed in me and always supported me. I wouldn't be where I am today without you.

Most importantly I want to thank my husband Fritz. You always support and trust me. You always understand me, you motivate me when I am demotivated, you celebrate with me, and most important, you believe in me and convince me to continue when I don't believe in myself.

Table of contents

1.1	Summary	1
1.2	Zusammenfassung	2
2	Abbreviations	3
3	List of publications	4
4	Personal contribution	5
5	Introduction	7
5.1	Mitosis	7
5.2	Microtubules and the mitotic spindle	7
5.3	Chromatin decondensation at the end of mitosis	12
5.4	Developmentally-regulated GTP binding protein 1	14
6	Thesis objectives	17
7	Results	18
7.1	DRG1, DRG2, DFRP1 & DFRP2 are involved in chromatin decondensation	18
7.1.1	<i>In vitro</i> reconstitution of chromatin decondensation	18
7.1.2	Immunodepletion of DRG1, DRG2, DFRP1 & DFRP2 inhibits chromatin decondensation	19
7.1.3	Dominant mutants of DRG1 & DRG2 inhibit chromatin decondensation	20
7.1.4	DRGs and DFRPs form at least two complexes	21
7.2.	DRG1 is involved in microtubule dynamics	23
7.2.1	DRG1 binds microtubules directly via different domains independently of a functional G-domain	23
7.2.2	Full-length DRG1 bundles, polymerizes and stabilizes microtubules independently of GTP hydrolysis	24
7.2.3	DRG1 is involved in spindle assembly in HeLa cells	25
8	Discussion	27
8.1	DRGs & DFRPs function as chromatin decondensation factors	27
8.2	DRG1 is a microtubule-associated protein	29
8.3	Possible connections of the chromatin- and microtubule-associated functions of DRG1	34
9	References	38
10	Appendix	43

1.1 Summary

The cell undergoes dramatic structural rearrangements during the cell cycle, particularly the nucleus and the microtubule cytoskeleton. While, in the beginning of mitosis, the nucleus needs to condense its genomic content and to disassemble the nuclear envelope, microtubules build the elaborate and highly dynamic structure of the mitotic spindle. At the end of mitosis all these events need to be reversed in order to re-establish an interphase cell fully functional for gene expression and further tasks.

Microtubules, the highly dynamic building blocks of the mitotic spindle are regulated by several different classes of microtubule-associated proteins. In this study, the Developmentally regulated GTP binding protein (DRG1) was identified as new player in this network. DRG1 is a highly conserved GTPase with not yet well understood functions. Here, I show that DRG1 binds to microtubules via several domains. Not only immobile binding was observed but also diffusive binding modes on the microtubule lattice were observed. Furthermore, DRG1 bundles and stabilizes microtubules as well as promotes microtubule polymerization *in vitro*. The GTP hydrolysis activity of DRG1 is not necessary for these functions, while the full-length protein is necessary for all microtubule-associated functions but binding. Consistent with the *in vitro* observations, knock down of DRG1 in HeLa cells slows down the regrowth of the mitotic spindle after cold shock as well as extends mitotic progression.

Beside the newly described microtubule-associated functions, DRG1 seems also to be involved in chromatin decondensation as it happens at the end of mitosis. Depletion of DRG1 from *Xenopus* egg extract or addition of recombinant DRG1 mutants to untreated egg extract, inhibits chromatin decondensation *in vitro*.

In summary, two novel functions of DRG1 were identified in this study. If the spindle assembly and chromatin decondensation functions of DRG1 are connected to each other or independent, so called moonlighting functions, and thus, if these pathways are in general directly connected or not remains an exciting topic for future research.

1.2 Zusammenfassung

Während des Zellzyklus durchläuft die Zelle enorme strukturelle Reorganisationen, besonders hervorzuheben sind hierbei die starken Veränderungen des Zellkerns und des Mikrotubuli-Zytoskeletts. Am Anfang der Mitose kondensiert das Chromatin im Zellkern und die Kernmembran löst sich auf. Das Mikrotubuli-Zytoskelett muss die aufwendige und sehr dynamische Struktur des mitotischen Spindelapparates aufbauen. Am Ende der Mitose müssen all diese Abläufe wieder umgekehrt werden, um einen funktionstüchtigen Interphase-Zustand herzustellen, der unter anderem die Expression der Gene möglich macht.

Mikrotubuli, die dynamischen Bausteine des mitotischen Spindelapparates, werden durch vielfältige Mikrotubuli-assoziierte Proteine modifiziert und reguliert. In dieser Arbeit wurde das „Developmentally regulated GTP binding protein 1“ (DRG1) als ein solches identifiziert. DRG1 ist eine hoch konservierte GTPase mit bislang wenig verstandenen Funktionen. In dieser Arbeit konnte ich zeigen, dass verschiedene Domänen von DRG1 Mikrotubuli binden. DRG1 ist nicht nur statisch, sondern auch mobil durch Diffusion auf den Mikrotubuli gebunden. Weiterhin bündelt, stabilisiert und polymerisiert DRG1 Mikrotubuli *in vitro*. Die GTPase-Aktivität von DRG1 ist nicht notwendig für die erwähnten Funktionen, allerdings die volle Länge des Proteins, mit Ausnahme der Mikrotubuli-Bindung. Übereinstimmend mit diesen *in vitro* Beobachtungen, führt die Herunterregulierung von DRG1 in HeLa Zellen zu einem verlangsamten Wiederaufbau des Spindelapparates nach Kälteschock, sowie zu einer Verzögerung im mitotischen Ablauf, von Pro- zu Anaphase.

Neben diesen neu entdeckten Mikrotubuli-assoziierten Funktionen, scheint DRG1 auch an der Dekondensierung des Chromatins am Ende der Mitose beteiligt zu sein. Depletion von DRG1 in *Xenopus* Eiextrakten oder Hinzufügen von rekombinantem DRG1 zu unbehandelten Eiextrakten, inhibiert die Chromatin-Dekondensierung *in vitro*.

Zusammenfassend wurden in dieser Arbeit zwei neue Funktionsbereiche für DRG1 entdeckt. Ob die unterschiedlichen Aufgaben von DRG1, den Aufbau des Spindel-Apparates und die Chromatin-Dekondensierung betreffend, abhängig oder unabhängig voneinander sind bleibt eine spannende Frage für zukünftige Forschung.

2 Abbreviations

DRG	Developmentally regulated GTP binding protein
DFRP	DRG family regulatory protein
ER	endoplasmic reticulum
γ -TURC	γ -tubulin ring complex
γ -TuSC	γ -tubulin small complex
GAP	GTPase activating protein
GCP	γ -tubulin complex protein
G-domain	GTPase domain
GEF	guanine nucleotide exchange factor
HTH	helix-turn-helix
IgG	immunoglobulin G
kDa	kilo Dalton
Ncd	non-claret disjunctional
NE	nuclear envelope
NPC	nuclear pore complex
Npl4	nuclear protein localization 4
Rbg1	Ribosome binding GTPase 1
SA	spindle assembly
TIRF	Total internal reflection microscopy
Ufd1	Ubiquitin fusion degradation 1
VCP	valosin-containing protein

3 List of publications

3.1 Accepted papers

I. RuvB-like ATPases function in chromatin decondensation at the end of mitosis

Magalska A, **Schellhaus AK**, Moreno-Andrés D, Zanini F, Schooley A, Sachdev R, Schwarz H, Madlung J, Antonin W.

Developmental Cell (2014) 31, 305-18

II. A Cell Free Assay to Study Chromatin Decondensation at the End of Mitosis

Schellhaus AK*, Magalska A*, Schooley A, Antonin W.

Journal of Visualized Experiments (2015) e53407

III. Nuclear Reformation at the End of Mitosis.

Schellhaus AK*, De Magistris P*, Antonin W.

Journal of Molecular Biology (2016) 428, 1962-1985. (Review.)

3.2 Manuscript in revision

IV. Developmentally Regulated GTP binding protein 1 (DRG1) controls microtubule dynamics

Schellhaus AK, Moreno-Andrés D, Chugh M, Yokoyama H, Moschopoulou A, De S, Bono F, Hipp K, Schäffer E, Antonin W

Currently in revision for Scientific Reports

*contributed equally

4 Personal contributions

I. RuvB-like ATPases function in chromatin decondensation at the end of mitosis

Magalska A, **Schellhaus AK**, Moreno-Andrés D, Zanini F, Schooley A, Sachdev R, Schwarz H, Madlung J, Antonin W.

Developmental Cell (2014) 31, 305-18

As a co-author of this publication I contributed several chromatin decondensation experiments to this study, including microscopy of several immunofluorescence staining. Further decondensation experiments were performed by AM, AS and WA. AM and WA designed the experiments and developed the chromatin decondensation assay. AM and DM-A performed live-cell imaging. FZ designed and wrote the image analysis software for quantifying chromatin decondensation. RS purified recombinant RuvBL1/2 complexes, HS performed electron microscopy, and JM performed mass spectrometry. WA wrote the manuscript and supervised the study.

II. A Cell Free Assay to Study Chromatin Decondensation at the End of Mitosis

Schellhaus AK*, Magalska A*, Schooley A, Antonin W.

Journal of Visualized Experiments (2015) e53407

I designed the outline of the article and wrote the manuscript under critical supervision from AM and WA. The methods described in this article were designed by AM with help from AS and supervision from WA, as described in *Magalska et al.* (2014) (see I.). Figure 1 and 2 were reprinted from *Magalska et al.* (2014), figure 3 was contributed from AS. I showed and explained the experimental procedure in the accompanying video.

III. Nuclear Reformation at the End of Mitosis

Schellhaus AK*, De Magistris P*, Antonin W.

Journal of Molecular Biology (2016) 428, 1962-1985. (Review.)

Together with PDM, I designed the outline and scope of this review supervised by WA. I wrote the parts about “Mitotic exit regulation” and “Chromatin decondensation” and contributed with comments and suggestions to the other parts, written by PDM and WA. I made figure 1 and 2, PDM made figure 3-5. WA supervised the whole manuscript preparation.

IV. Developmentally Regulated GTP binding protein 1 (DRG1) controls microtubule dynamics

Schellhaus AK, Moreno-Andrés D, Chugh M, Yokoyama H, Moschopoulou A, De S, Bono F, Hipp K, Schäffer E, Antonin W

In revision

As a first author of this study I designed the experiments and wrote the manuscript under the supervision of WA. I cloned the DNA constructs with the help of AM. I purified the proteins and established as well as performed the bundling, polymerization and stabilization experiments. For the bundling and polymerization experiments HY gave helpful input about the experimental conditions. I performed microtubule co-sedimentation assays with recombinant proteins, while HY made co-sedimentation assays with cell extracts. MC performed TIRF experiments, supervised by ES using a microscope built by SD and proteins purified by me. DM-A performed all experiments in HeLa cells. KH made the electron microscopy with bundled microtubules prepared by me. FB performed the structure modelling.

5 Introduction

5.1 Mitosis

In order to divide, cells have to undergo enormous structural rearrangements. In metazoans, the nuclear envelope breaks down, chromatin condenses and the mitotic spindle forms in the beginning of mitosis. After chromatin segregation into the two emerging daughter cells, performed by the mitotic spindle, these processes need to be reversed. The nuclear envelope including the nuclear pore complexes reforms, the mitotic spindle disassembles and the chromatin decondenses in order to be accessible for gene expression and DNA replication during interphase (reviewed in Schellhaus et al., 2016).

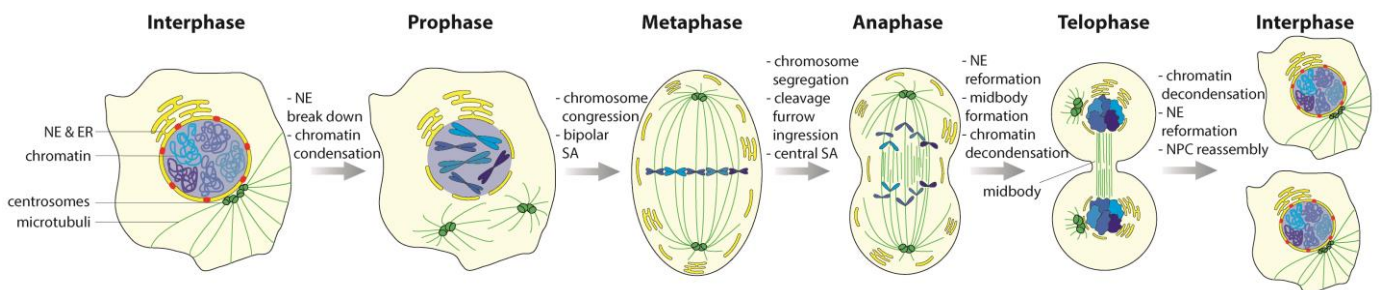


Figure 1: Structural rearrangements of the cell during mitosis. Modified from (Schellhaus et al., 2016). NE: nuclear envelope, ER: endoplasmic reticulum, SA: spindle assembly, NPC: nuclear pore complex.

5.2 Microtubules and the mitotic spindle

The mitotic spindle is built from microtubules, highly dynamic cytoskeletal filaments. The basic building blocks of microtubules are the well conserved GTPases α - and β -tubulin. These tubulin heterodimers assemble in a head-to-tail manner into protofilaments, which gives the microtubules a polarity. Protofilaments in turn associate laterally to form a hollow tube structure, *in vivo* mostly consisting of 13 protofilaments (Chretien et al., 1992; Tilney et al., 1973). The most prominent feature of microtubules is their dynamic instability. Especially at the plus-end, microtubules can rapidly change from growth phases into shrinkage or pause phases and vice versa. The transition from different phases, known as catastrophe and rescue, is usually governed by the nucleotide state of β -tubulin which faces the plus end of the microtubule (Kirschner and Mitchison, 1986;

Nogales et al., 1999). Upon microtubule polymerization, GTP-bound tubulin dimers are added to the end of the microtubule. While the GTP that is bound to α -tubulin does not hydrolyse, the GTP bound to β -tubulin slowly hydrolyses in the polymerized microtubule. GTP hydrolysis and phosphate release causes a conformational rearrangement in the tubulin dimer altering longitudinal interfaces which generates strain in the microtubule lattice (Alushin et al., 2014). The nucleotide is only exchangeable for the last tubulin at the plus-end. If the growth rate exceeds the GTP hydrolysis rate, the microtubule continues to grow, while it depolymerizes if the GTP hydrolyses before more GTP-tubulins are added to the end. GTP-tubulin at the end serves as a protective “GTP-tubulin cap”, respectively. Using laser ablation to cut the mitotic spindle parallel to the metaphase plate leads to rapid depolymerization of the newly generated plus ends while the minus ends remain stable, highlighting the faster dynamics of the plus ends (Brugues et al., 2012). If a microtubule is damaged at the site of its lattice, GTP-tubulin can be inserted directly into the shaft (Aumeier et al., 2016). Interestingly, this laterally added “GTP-tubulin islands” serve also as the side of rescue if a microtubule depolymerizes up to this location before GTP-hydrolysis has happened at this site.

In cells, the behavior of microtubules is spatially and temporally regulated by many microtubule-associated proteins, e.g. polymerases and depolymerases that directly influence the growth and shrinkage rate by favouring a straight tubulin conformation or by supporting intrinsic curvature which is the favourable tubulin conformation in solution, respectively; nucleation factors; stabilizing factors that perform their function e.g. by bundling microtubules or that form a cap structure at the microtubule ends; severing enzymes that cut microtubules and motor proteins that move on the microtubules often carrying cargoes like certain molecular assemblies, organelles or other microtubules (reviewed in Petry, 2016). In addition, tubulins exist in many isoforms and are target of many posttranslational modifications (reviewed in Gadadhar et al., 2017). Well-known protein modifications like acetylation and phosphorylation are observed on tubulins but also rather rare events like glutamylation and glycylation. De-/tyrosination are specific for tubulin. Both, the different tubulin isoforms and posttranslational-modifications together, form the “tubulin code” resembling the well-known histone

code, which is readable by microtubule-associated and motor proteins, thus also influencing microtubule dynamics.

Microtubules are not only important during mitosis in the form of the mitotic spindle but also during interphase when they are less dynamic. Microtubules are involved in the overall organization of the cell by positioning, organizing and maintaining different organelles. Microtubules are crucial for intracellular transport processes, for cell motility, cell shape and cell polarity regulation e.g. for the formation and maintenance of neuronal axons or the polarization of asymmetric epithelial cells (reviewed in de Forges et al., 2012). Disruption of the interphase microtubule cytoskeleton was observed in diseases. For instance, in many neurodegenerative diseases hyperphosphorylation of the microtubule-associated protein tau which promotes assembly and stabilization of microtubules, leads to the disassembly of tau from microtubules and formation of prion-like tau aggregates accompanied by microtubule disassembly (reviewed in Alonso et al., 2016).

The mitotic spindle consists of three different kind of microtubules (reviewed in Prosser and Pelletier, 2017): roughly 20-30 (in Ptk cells (McDonald et al., 1992)) kinetochore microtubules bundle into each k-fiber which connect the centrosomes at their minus ends with the kinetochores at the plus ends. Kinetochores are protein complexes assembled on centromeric chromatin. Proper attachment of the k-fibers, meaning the two kinetochores of sister chromatids are connected to the two opposite centrosomes, is monitored by the spindle assembly checkpoint pathway.

The majority of the mitotic spindle consists of non-kinetochore microtubules, which are part of the spindle itself but not connected to the kinetochores. In *C.elegans* early embryos only roughly 200 of the 8331 microtubules in each half spindle were classified as kinetochore microtubules (Redemann et al., 2017). Non-kinetochore microtubules give stability to the spindle, are involved in the separation of the spindle poles and in elongation of the spindle during anaphase. Lastly, astral microtubules radiating from the centrosome to the cell cortex, position the spindle properly.

In contrast and as extension to the classical model, it was recently shown that k-fibers associate with bundles of overlapping non-kinetochore fibers connecting the two spindle poles (Kajtez et al., 2016; Polak et al., 2017). These bundles bridge

the two k-fibers of sister kinetochores and are hence termed bridging fibers. Bridging fibers are suggested to be involved in balancing forces acting on the k-fibers. Laser ablation of a k-fiber and consequent movement of the kinetochore that was separated from the pole showed that the bridging fiber, the intact sister kinetochore fiber and the broken kinetochore fiber move together as a stable entity.

Another recent study challenging the classical model of the mitotic spindle demonstrated that in *C.elegans* early embryos kinetochore microtubules are not directly connected to centrosomes but rather anchored into the spindle network (Redemann et al., 2017). According to this model, kinetochore microtubules nucleate from centrosomes, followed either by catastrophe or attaching to a kinetochore. Microtubules that attached to the kinetochores then transit into a shrinking state, depolymerizing from the minus end. However, *C.elegans* has holocentric kinetochores, meaning that kinetochore microtubules can bind to the entire chromosomal surface, and thus most likely differ in certain spindle assembly dynamics compared to mammals.

Microtubules in the spindle are usually shorter than the spindle itself. Their individual half-lives are likewise shorter. Although microtubule minus ends always face towards the spindle poles while plus ends are facing away, minus and plus ends are found throughout the spindle. Especially the minus ends of the non-kinetochore microtubules are more distributed throughout the spindle than the k-fiber minus ends (Mastrorade et al., 1993). Microtubules in the center of the spindle are longer compared to microtubules at the poles (Brugues et al., 2012). The classical "Search & capture" spindle assembly model suggested that microtubules nucleate from the centrosomes and grow towards the cell equator searching for kinetochores (Kirschner and Mitchison, 1986; Mitchison and Kirschner, 1984). Dynamic instability increases the chances that a microtubule finds a kinetochore. Additionally, the microtubules can change their angle of growing and if they attach laterally to a kinetochore they can position it in a way that increases the chances of an end-on attachment. Nevertheless, the model is nowadays extended by several nucleation pathways, favorable cell mechanic advantages like cell rounding and factors involved in spindle assembly which would otherwise be much slower (reviewed in Heald and Khodjakov, 2015).

Nucleation does not only occur at the centrosome but also close to chromatin. Most prominent in this context is the Ran-pathway, resembling the regulation of the nuclear-cytoplasmic transport during interphase: spindle assembly factors are sequestered by importins but get released once RanGTP binds these transport factors instead (Kalab et al., 2002). RanGTP is highly increased around chromosomes because the guanine nucleotide exchange factor (GEF) of Ran, RCC1, is associated with chromatin (Carazo-Salas et al., 1999). RCC1 facilitates the exchange from GDP to GTP on Ran. The released spindle assembly factors can then nucleate microtubules around chromatin.

Furthermore microtubules also nucleate from already existing microtubules.

The spindle is further organized by motor proteins. A main player in this context is dynein, which transports microtubules on another microtubule, called microtubule sliding, constantly towards the minus ends focusing the spindle poles and also forming two poles in the absence of centrosomes, respectively (Heald et al., 1997). But also plus end directed motors are involved in generating a bipolar array e.g. by cross-linking and sorting the plus ends. Molecular motors are furthermore important for the proper positioning of the chromosome arms and kinetochores (reviewed in Heald and Khodjakov, 2015). Microtubule sliding also plays crucial roles during interphase, such as for neuronal differentiation when the molecular motors kinein-1 and dynein establish the prominent neuronal cell shape (reviewed in Lu and Gelfand, 2017).

The α - and β -tubulin homolog, γ -tubulin, is essential for microtubule nucleation. Together with the γ -tubulin complex proteins 2 and 3 (GCP) it forms the γ -tubulin small complex (γ TuSC) which further assembles, with the exception of many yeasts, with additional factors (GCP4, GCP5, MOZART1 and in some organisms GCP6, MOZART2A and 2B) into the ring shaped γ -tubulin ring complex (γ TuRC). γ TuRC serves as a template for microtubule nucleation when attached to the centrosome or pre-existing microtubules (reviewed in Kollman et al., 2011). α - and β -tubulin heterodimers most likely attach longitudinally to the γ -tubulin ring. The nucleation capacity of the centrosome is increased during mitosis by recruiting more γ -TURC and further centrosomal components as well as by phosphorylation of centrosomine, one of these components (reviewed in Petry, 2016). Although the

centrosome is often considered to be the main microtubule nucleation site in metazoans, the other mentioned pathways can take over its function, shown by experiments in which the centrosomes were artificially removed. Naturally it also occurs that cells do not have centrosomes e.g. in vertebrate eggs. Therefore, these pathways are partially redundant. The same accounts for the numerous factors involved in spindle assembly. Many of them can take over each other's function if necessary. For example, while the small GTPase Ran and the kinesin Eg5 are essential for spindle assembly in *X.laevis*, they are not in *X.tropicalis*. The latter has a threefold excess of Xklp2 (TPX2) and much smaller mitotic spindles compared to the first. The phenotype caused by inhibition of Ran and Eg5 in *X.laevis* can be reduced by increasing the TPX2 concentration showing how the importance of individual factors can vary between organisms and cell types by the individual protein levels, also reflected in different spindle sizes and morphologies (Helmke and Heald, 2014).

Nevertheless, even if partially replaced by others, each missing pathway and factor increases the chance of chromosome missegregation. In line with this, deregulation of spindle assembly is observed in many types of cancer (Du et al., 2016; Kumar et al., 2016; Schneider et al., 2017). Thus, this multi-layered regulation of spindle assembly seems to be a security mechanism of the cell, decreasing the chance of errors as much as possible, best summarized in the words of Rebecca Heald and Alexey Khodjakov: "Thus, the complexity of numerous nonessential mechanisms sustains the wonderfully simple principle of S&C [Search and Capture]"(Heald and Khodjakov, 2015).

5.3 Chromatin decondensation at the end of mitosis

Once the sister chromatids are successfully segregated by the mitotic spindle, the two daughter nuclei need to reform. The nuclear envelope reassembles around the chromatin including the nuclear pore complexes, but also the chromatin itself undergoes significant structural rearrangements (reviewed in Schellhaus et al., 2016). While it needs to be highly compacted in order to enable segregation during mitosis, it has to be much less densely packed to be accessible for DNA replication and gene expression during interphase. The grade of chromatin

compaction during mitosis is highly controversial, ranging from 2 to 50-fold (Belmont, 2006; Vagnarelli, 2012). Thus, chromatin needs to decondense at the end of mitosis. This process is highly under-investigated. It can be reconstituted *in vitro* incubating isolated, mitotic chromatin clusters with interphase *Xenopus laevis* egg extracts (Magalska et al., 2014). Using this *in vitro* reconstitution, it was shown that chromatin decondensation is an active process, requiring ATP and GTP hydrolysis. In this assay, chromatin decondenses to a certain extent in the absence of membranes, but it further decondenses in the presence of membranes –suggesting that for the second level of decondensation a nucleus capable of importing cytoplasmic factors is necessary.

Not many factors involved in chromatin decondensation are known to date. RuvBL1 and RuvBL2 (also known as Pontin/Tip49 and Reptin/Tip48) are AAA+ATPases that form a double hexameric complex. Immunodepletion of RuvBL1/2 impairs chromatin decondensation *in vitro* (Magalska et al., 2014). Rescue experiments showed that either RuvBL1 or RuvBL2 is sufficient for chromatin decondensation, however ATPase mutants are not. Next to other diverse functions, RuvBL1/2 are known to be associated with chromatin remodeling complexes (reviewed in Nano and Houry, 2013) and it is tempting to speculate that they directly act on remodeling the chromatin at the end of mitosis.

Another AAA+ATPase involved in chromatin decondensation is p97 (also known as valosin-containing protein (VCP) in vertebrates and CDC48 in yeast) forming a complex with its co-factors UFD1 (ubiquitin fusion degradation 1) and NPL4 (nuclear protein localization 4) (Ramadan et al., 2007). p97 removes the kinase Aurora B from chromatin and thus seems to have rather a regulatory instead of a direct role on chromatin. If Aurora B is removed to function at a different localization, to prevent phosphorylation at this site or to make chromatin more accessible is not known.

RuvBL1/2 are not sufficient to decondense isolated mitotic chromatin (Magalska et al., 2014) and it is very likely that such a fundamental process, involving the global decompaction and rearrangement of chromatin at the end of mitosis, depends on a multi-step process with numerous factors. One of these is most likely a GTPase as chromatin decondensation requires GTP hydrolysis (Magalska et al., 2014). It is also conceivable that histone modifications are involved in the process. Histone modifications play important roles in local chromatin rearrangements during

interphase but to which extend they are involved in global rearrangements at the transition from mitosis to interphase is not known and controversial. As an example, histone H3 phosphorylation at serine 10 correlates with chromatin condensation during mitosis and its removal with chromatin decondensation. It was therefore long believed that this mitotic histone mark might even be able to cause chromatin condensation (e.g. Hendzel et al., 1997). However, while it was recently suggested again to be involved in mitotic chromatin condensation in yeast (Wilkins et al., 2014), it can clearly be uncoupled from chromatin decondensation (Hsu et al., 2000; MacCallum et al., 2002; Magalska et al., 2014; Murnion et al., 2001).

In conclusion, chromatin decondensation at the end of mitosis is a highly under-investigated process that still awaits major explorations to achieve deeper knowledge.

5.4 Developmentally-regulated GTP binding protein 1

In this work, Developmentally regulated GTP binding protein 1 (DRG1) was identified to bundle, polymerize and stabilize microtubules and to be involved in spindle dynamics in HeLa cells. Furthermore, it might function as a chromatin decondensation factor at the end of mitosis.

DRG1 is a GTPase that belongs to the Obg subfamily of GTPases (Leipe et al., 2002) and is highly conserved between different species (Hudson and Young, 1993; Kumar et al., 1993; Lee et al., 1998; Sazuka et al., 1992; Schenker et al., 1994; Shimmin and Dennis, 1989; Sommer et al., 1994). Archeobacteria usually contain one DRG, while eukaryotes from yeast to human contain two isoforms (Li and Trueb, 2000), DRG1 and DRG2, which are highly homologous (58 % identity on the protein level for human proteins). Plants even contain three DRGs (O'Connell et al., 2009). DRGs are associated with the DRG family regulatory proteins (DFRPs) 1 and 2 (Ishikawa et al., 2009; Ishikawa et al., 2005). While DFRP1 binds only to DRG1, it is under debate if DFRP2 binds only DRG2 or also DRG1 (Ishikawa et al., 2009; Ishikawa et al., 2005; Wout et al., 2009). The association with DFRPs prevents that the DRGs get ubiquitinated and degraded by the proteasome and therefore DFRPs are considered to be the stabilizing

factors of DRGs. In agreement with this, downregulation of DFRP1 also causes down-regulation of DRG1.

Not much is known about the functions of the DRGs and DFRPs although the high interspecies conservation of the DRGs suggested early that they might have a function in a highly fundamental pathway. First, DRG1 was suggested to function as developmental factor as its expression was observed to be upregulated in mouse embryonic brain, hence its name (Sazuka et al., 1992). However, DRGs are also widely expressed in adult tissues (Ishikawa et al., 2003; Lee et al., 1998; Li and Trueb, 2000). DRG1 and DFRP1 co-sediment with polysomes (Daugeron et al., 2011; Francis et al., 2012; Ishikawa et al., 2009; Wout et al., 2009) and DRG1 binds RNA (Ishikawa et al., 2003) suggesting that they play a role in translation or other functions connected to ribosomes. Nevertheless, this still remains obscure. The same obscurity remains for DRGs' repeatedly suggested involvement in cell growth (Devitt et al., 1999; Lu et al., 2016).

The crystal structure of the yeast DRG1 homolog, Rbg1 (Ribosome binding GTPase 1), together with a C-terminal fragment of the yeast homolog of DFRP1 (Tma46) showed that DRG1 has an N-terminal helix-turn-helix (HTH) motif and a C-terminal TGS-domain. In between a canonical GTPase domain (G-domain) performing the GTP hydrolysis is found (Francis et al., 2012). This G-domain is surprisingly interrupted by a S5D2L-domain. An insertion in the G-domain is usually found in the α -subunits of G-protein coupled receptors. In the latter case they are inserted between the canonical G1 and G2 box, while the insertion in DRG1 lies between the G3 and G4 boxes (Sommer et al., 1994). The G-domain of DRG1 is the only domain that shares some similarities with other GTPase families. DRG1 hydrolysis GTP under a wide range of pHs and temperatures with optimums at pH 8 to 9 and 42°C (Perez-Arellano et al., 2013). DRG1 does not require a GTPase activating protein (GAP) (Francis et al., 2012; O'Connell et al., 2009; Perez-Arellano et al., 2013). In fact DFRP1 stimulates the GTPase activity but binds on the opposite site of the GTP binding pocket and rather stimulates the GTP hydrolysis by different mechanisms compared to a classical GAP, e.g. by increasing the affinity for potassium ions which stimulate the GTP hydrolysis activity.

Despite all these exciting characteristics, not much about the functions of the DRGs has been elucidated since their discovery 30 years ago but the high interspecies conservation most certainly suggests an important function in a conserved cell biology pathway.

6 Thesis objectives

The cell undergoes enormous structural rearrangements during cell division. Especially the nucleus including the chromatin passes through dramatic morphological changes but also the cytoskeleton, particularly the microtubules, experiences major transformations. Errors in these processes can have dramatic consequences for the cell making it important to understand every individual detail. Some pathways are rather well studied, while others are highly under-investigated.

One of the less studied structural changes happening at the end of mitosis is chromatin decondensation necessary to make chromatin accessible for replication and transcription during interphase. Chromatin decondensation relies on GTP hydrolysis (Magalska et al., 2014) and prior to this thesis work, I identified the GTPase Developmentally regulated GTP binding protein 1 (DRG1) as a possible candidate to be involved in the process. DRG1 is highly conserved between different species but its function is unclear.

The goal of this work was to find out if and how DRG1 is involved in chromatin decondensation and further mitotic processes. Chromatin decondensation was reconstituted in a cell-free assay using *Xenopus laevis* egg extracts. This approach was combined with immunodepletion of DRG1, DRG2 and the interaction partners DFRP1 and DFRP2, or with the addition of recombinant dominant mutants of DRG1 and 2.

In the process of characterizing DRG1 further, it was found to be also associated with microtubule functions. Cell-free assays using recombinant tubulin and DRG1 were used to test the functions of DRG1 in the context of microtubule binding, bundling, polymerization and stabilization activities. DRG1 not only shows these various functions in minimal *in vitro* systems, it is also involved in mitotic spindle dynamics in HeLa cells.

DRG1 is directly involved in the rearrangements occurring during mitosis, respectively. If the chromatin- and microtubule-associated functions of DRG1 are functionally connected or independent of each other is unknown and remains an exciting topic for future investigations.

7 Results

7.1 DRG1, DRG2, DFRP1 & DFRP2 are involved in chromatin decondensation

7.1.1 *In vitro* reconstitution of chromatin decondensation

Xenopus laevis egg extracts have been long used to reconstitute nuclear envelope reassembly *in vitro* (reviewed in Gant and Wilson, 1997). The advantages of *Xenopus* egg extracts are versatile. Extracts can be prepared in the mitotic or interphasic state, they can be easily manipulated e.g. by depleting or adding proteins or chemicals like inhibitors, and cellular proteins are highly enriched as transcription and translation do not start until the 4000 cell embryo is reached and therefore, the eggs store enough necessary factors for the first rounds of cell divisions (reviewed in Murray, 1991; Newmeyer and Wilson, 1991; Powers et al., 2001). In the context of studying nuclear envelope assembly, sperm chromatin is usually used which decondenses first by exchanging sperm specific protamines to histones performed by nucleoplasmin (Philpott and Leno, 1992; Philpott et al., 1991). This represents the process that is happening after fertilization but not what happens at the end of mitosis as mitotic chromatin is already bound to histones and nucleoplasmin is only expressed in oocytes (Burglin et al., 1987). Therefore, a novel cell-free assay was established to study chromatin decondensation using isolated mitotic chromatin from HeLa cells. These chromatin clusters decondensed upon incubation with interphase *Xenopus* egg extract in a time-dependent manner. The samples were fixed at indicated time points and stained with DAPI (Fig. 1 in (Magalska et al., 2014)). Furthermore, chromatin decondensed to a certain extent in the absence of membranes but even more in the presence of membranes suggesting that nuclear import of specific factors is necessary for the second level of decondensation (Fig. 3 in (Schellhaus et al., 2015)). Indeed, using this *in vitro* approach yielded fully functional nuclei capable of import and export. Chromatin decondensation required ATP and GTP hydrolysis suggesting that one or more ATPases and GTPases are involved (Fig. 3 in (Magalska et al., 2014)).

7.1.2 Immunodepletion of DRG1, DRG2, DFRP1 & DFRP2 inhibits chromatin decondensation

In order to find a GTPase that is involved in chromatin decondensation, previously, I did a biochemical fractionation approach combined with the cell-free assay described in 7.1.1 which suggested that the GTPase DRG1 might be a possible candidate. DRG1, DRG2 as well as their stabilizing interaction partners DFRP1 and DFRP2 were immunodepleted from *Xenopus* egg extracts (Fig.2 A & C).

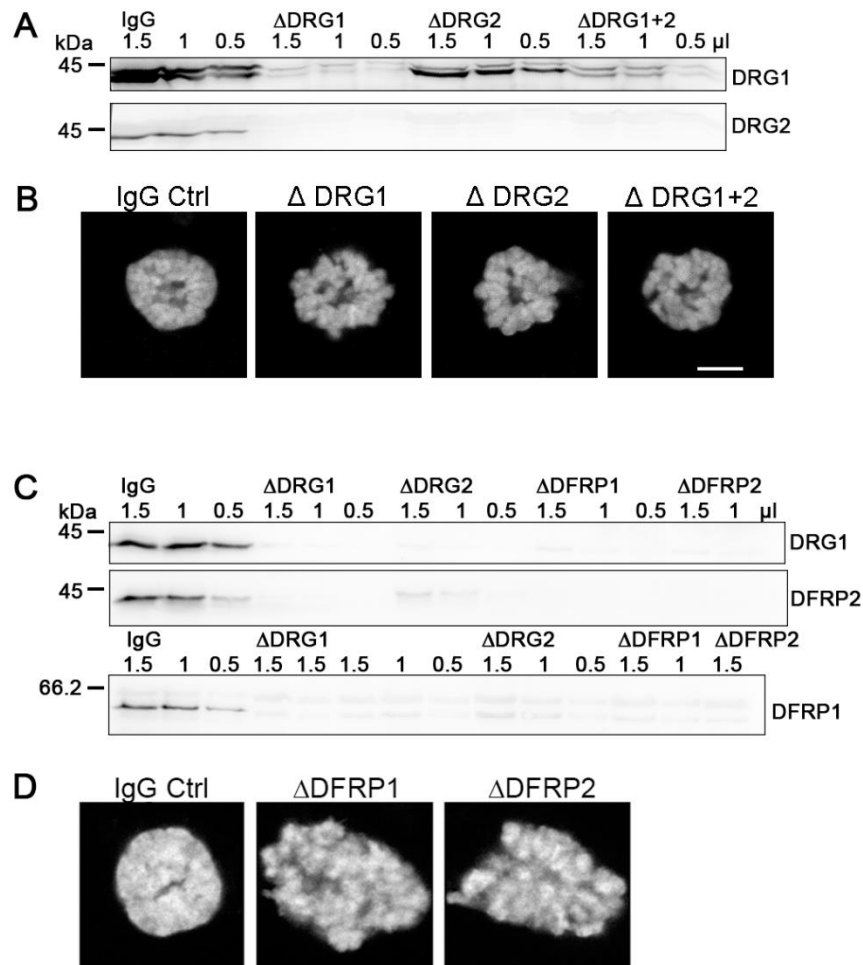


Figure 2: Immunodepletion of DRG1, DRG2, DFRP1 and DFRP2 from *Xenopus laevis* egg extracts. The depleted extracts were analyzed by Western blotting (A and C) and used for *in vitro* reconstitution of chromatin decondensation (B and D). Note that the antibody against DRG1 recognized DRG1 (lower band) and DRG2 (upper band) in the Western blot in A. Scale bar: 5 μm.

Individual antibodies against one of these proteins co-depleted the other three proteins as well which can be explained with cross-reactivity of the antibodies in the case of DRG1 and DRG2. However, DFRP1 and DFRP2 share only some

sequence conservation in the DFRP domain and are otherwise not similar suggesting that the four proteins might form a tetrameric complex in contrast to previously suggested specific DRG1-DFRP1 and DRG2-DFRP2 heterodimers. Immunodepletion of the DRGs and DFRPs inhibited chromatin decondensation *in vitro* (Fig. 2 B & D) suggesting that they are indeed involved in chromatin decondensation at the end of mitosis.

7.1.3 Dominant mutants of DRG1 & DRG2 inhibit chromatin decondensation

To further confirm that DRGs are involved in chromatin decondensation, dominant GTPase mutants were designed, expressed and purified. A dominant positive GTPase mutant is locked in its GTP-bound state while a dominant negative mutant is either nucleotide-free or GDP-bound. The dominant mutants of DRG1 and 2 were designed by sequence comparison to other known GTPase mutants (Fig. 3): in the case of the dominant-negative mutant, a point mutation was introduced similar to dominant-negative mutants of the small GTPase Ran (Dasso et al., 1994) and of the yeast homolog of DRG1, Rbg1 ((Daugeron et al., 2011; Francis et al., 2012). The dominant-positive mutant was created according to the mutant of the *Streptomyces coelicolor* GTPase Obg which belongs to the same GTPase subfamily as the DRGs (Okamoto and Ochi, 1998).

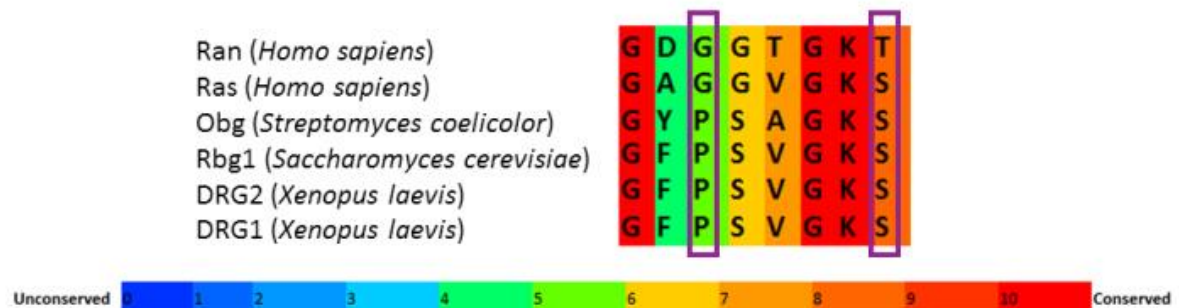


Figure 3: Sequence alignment of the G1 boxes of DRG1, DRG2 and other small GTPases. Purple boxes highlight the residues that were mutated to gain dominant mutants. Alignment was done using the “PRALINE multiple sequence alignment” software (<http://www.ibi.vu.nl/programs/pralinewww/>).

Addition of the recombinant dominant positive mutants, DRG1 P73V and DRG2 P71V (Fig. 4A), the dominant negative mutants, DRG1 S78N (Fig. 4B) and DRG2 S76N (Fig. 4C) but also of wild-type DRG1 (Fig. 4B) and DRG2 (Fig 4C) to *Xenopus* egg extract impaired chromatin decondensation as well.

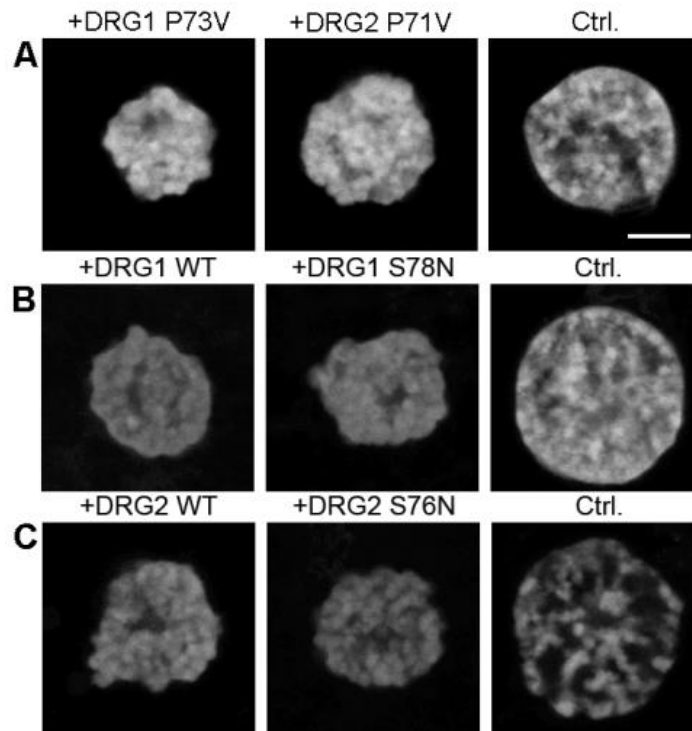


Figure 4: Chromatin decondensation was reconstituted in the presence of recombinant, dominant positive mutants of DRG1 and DRG2 (A), the wild-type and dominant negative mutant of DRG1 (B) or DRG2 (C). Scale bar: 5 μ m.

7.1.4 DRGs and DFRPs form at least two complexes

Following the co-depletion of DRG1, DRG2, DFRP1 & DFRP2 in the immunodepletion experiments, *Xenopus* egg extracts were fractionated by gel filtration. The fractions were analyzed by Western blotting. The concentration of DRG2 and DRP2 peaked in a fraction corresponding to approximately 180 kDa (Fig. 5, fraction 7). DRG1 and DFRP1 showed two concentration peaks, one in the same fraction as DRG2 and DFRP2 (Fig. 5, fraction 7), and another one in a fraction corresponding to approximately 440 kDa (Fig. 5, fraction 3).



Figure 5: *Xenopus laevis* egg extracts were fractionated by gel filtration and analyzed by Western blotting using primary antibodies against DRG1, DRG2, DFRP1 or DFRP2.

This suggested that DRG1, DRG2, DFRP1 and DFRP2 might indeed form a tetramer complex. Additionally, DRG1 and DFRP1 seem to be involved in a second bigger complex. If this complex consists solely of several copies of DRG1 and DFRP1 or if other factors are involved remains open. The existence of at least two different complexes could explain the different observations described concerning interaction specificity of the DRGs and DFRPs.

To characterize the DRGs further, immunoprecipitations were done (data not shown). Interaction partners of DRGs were analyzed by mass spectrometry (performed by the Proteome Center Tübingen). DRG1 interacts with several proteins involved in the dynamics of the mitotic spindle like XMAP215, ISWI and tacc3 (interaction was not confirmed yet) which suggests that DRG1 might also play a role in this context.

7.2 DRG1 is involved in microtubule dynamics

7.2.1 DRG1 binds microtubules directly via different domains independently of a functional G-domain

As DRG1 was observed to interact with many microtubule-associated proteins, it was analyzed if DRG1 interacts itself also with microtubules. Indeed, DRG1 as well as DFRP1 co-sedimented with microtubules when *Xenopus* egg extracts, HeLa nuclear extract or recombinant DRG1 and DFRPs were incubated with taxol-stabilized microtubules while it was not the case for DFRP2 (Fig. 1 in (Schellhaus et al., in revision)). This showed that the binding was direct. Sensitivity of the binding to high salt further showed that the binding was specific and occurred via polar/ionic interactions. Applying the GTPase mutants of DRG1, DRG1 P73V and DRG1 S78N, in the co-sedimentation assay showed that these as well bound to microtubules (Fig. 6a in (Schellhaus et al., in revision)). The same accounts for truncated versions of DRG1 lacking the HTH, the TGS domain or both, as well as the TGS or HTH domain individually. The only non-binding fragment was the S5D2L domain (Fig. 3 b,c in (Schellhaus et al., in revision)). Many microtubule-associated proteins are highly positively charged and bind microtubules via the highly negatively charged, acidic C-terminus of tubulin which is also the main target of posttranslational modifications ((Redeker et al., 1992); (reviewed in Cooper and Wordeman, 2009)). Modelling of the DRG1 structure based on the known crystal structure of the yeast homolog Rbg1 (Francis et al., 2012) showed that DRG1 has a highly positively charged surface area opposite of the GTP binding pocket (Fig. 3d in (Schellhaus et al., in revision)). This surface involves all four domains and could explain why various different fragments bound to microtubules. That the S5D2L-domain is included in this area but did not bind to microtubules could simply be because it was not properly folded or the affinity without the neighbouring domains was not high enough.

To test if DRG1 binds tubulin via its acidic C-terminal tail, taxol-stabilized microtubules were digested with subtilisin, a protease that removes the C-terminus. DRG1 interacted also with microtubules lacking the extreme C-terminus although with a reduced affinity (Fig. 3e in (Schellhaus et al., in revision)).

A more detailed characterization of DRG1 binding to microtubules using an approach based on Total internal reflection microscopy (TIRF) enabled the detection of the binding in a mobile way with single molecule resolution. DRG1 not only bound microtubules transiently in an immobile way but also diffused on the microtubules in a fast or slow manner (Fig. 2 in (Schellhaus et al., in revision)). The slow diffusion resembled the diffusive behaviour of the depolymerase MCAK (Helenius et al., 2006), the fast movement that of the plus-end tracking protein EB1 (Chen et al., 2014). Both proteins perform their functions at the microtubule ends and the diffusion on the microtubule lattice increases the chances to find the ends compared to simple diffusion in solution. Why DRG1 binds microtubules in three different modes is currently unclear. It cannot be explained by the different nucleotide states, GTP-bound, GDP-bound and nucleotide free, as all three binding populations were also observed in the presence of the non-hydrolysable GTP analog, GTP γ S (Supplementary Fig. S1 in (Schellhaus et al., in revision)). The proportions of the different binding populations as well as the interaction times of the immobile fraction were concentration-dependent: the lower the DRG1 concentration, the higher was the proportion of immobile binding DRG1 and the longer were the interaction times (Fig. 2 & Supplementary Fig. S1 in (Schellhaus et al., in revision)). The interaction times were also slightly decreased in the presence of GTP γ S (Supplementary Fig. S1 in (Schellhaus et al., in revision)).

7.2.2 Full-length DRG1 bundles, polymerizes and stabilizes microtubules independently of GTP hydrolysis

Microtubule-associated proteins are often directly involved in regulating microtubule dynamics and possible microtubule-associated functions of DRG1 were further tested. Upon incubation of DRG1 with fluorescently-labeled, taxol-stabilized microtubules, bundling was observed by confocal (Fig. 4a in (Schellhaus et al., in revision)) and electron microscopy (Fig. 4b in (Schellhaus et al., in revision)). Bundling of microtubules can give the microtubules more stability as it is for example the case in k-fibers which are bundles of kinetochore microtubules. Polymerization of tubulin for one hour at 37 °C followed by incubation on ice for 30 minutes induced disassembly of the before assembled microtubules. Indeed, DRG1 stabilized microtubules *in vitro* and prevented disassembly on ice (Fig. 5a in

(Schellhaus et al., in revision)). This observation was further confirmed in HeLa cells stably expressing histone H2B-mCherry and eGFP-tubulin, in which DRG1 was knocked-down by siRNA (Fig. 5b in (Schellhaus et al., in revision)). 72 hours post-transfection, these cells were incubated on ice for one hour. After adding fresh, warm medium, the regrowth of microtubules in the mitotic population was observed by fixing the cells at different time points. Microtubules regrew much slower in cells lacking DRG1 (Fig. 5c & d in (Schellhaus et al., in revision)) which can be either explained by little remnants of the mitotic spindles which were more often retained in control cells upon incubation on ice (Fig. 5c & insert 5d in (Schellhaus et al., in revision)). These remnants could have facilitated a faster re-assembly of the mitotic spindle. Another possibility is that DRG1 in some way accelerated microtubule polymerization. Indeed, incubation of Cy3-labeled tubulin below the critical concentration that is necessary for self-assembly of microtubules (Fygenson et al., 1994) with DRG1 induced microtubule polymerization (Fig. 4c in (Schellhaus et al., in revision)) which was also confirmed in light-scattering experiments (Fig. 4d in (Schellhaus et al., in revision)). In the latter case, tubulin in a concentration as little as 2.5 μ M was incubated with DRG1 and GTP and the absorption at 340 nm was measured over time. Thus, DRG1 not only bundles but also stabilizes and polymerizes microtubules.

The described experiments were repeated using the recombinant dominant GTPase mutants as well as the truncated versions of DRG1. While the GTPase mutants were able to bundle, stabilize and polymerize microtubules (Fig. 6b-d in (Schellhaus et al., in revision)), the truncated versions were not (Supplementary Fig. S2 a-c in (Schellhaus et al., in revision)). Thus, DRG1 does not require its GTPase activity for its microtubule-associated functions but it needs to be the full-length protein.

7.2.3 DRG1 is involved in spindle assembly in HeLa cells

While the *in vitro* approaches were not feasible to distinguish between mitotic and interphase microtubule functions, the cold shock experiment in HeLa cells suggested that DRG1 performs its microtubule-associated functions in mitosis. This was further confirmed by the observation that DRG1 knock-down in HeLa cells, stably expressing histone H2B-mCherry and eGFP-tubulin, indeed showed a

prolonged timing from prophase to anaphase onset, evaluated by analyzing the chromatin shape (based on histone H2B-mCherry staining) (Fig. 7 a & b in (Schellhaus et al., in revision)) and of the timing from aster to anaphase spindle formation (based on eGFP-tubulin staining) (Fig. 7 a & c in (Schellhaus et al., in revision)). Although this clearly showed, that DRG1 is involved in the dynamics of the mitotic spindle, it does not exclude that DRG1 might also function at the interphase microtubule cytoskeleton.

8 Discussion

In this work, the highly conserved GTPase DRG1 was identified as microtubule-associated protein with microtubule bundling, polymerization and stabilization activities as well as potential chromatin decondensation factor, possibly linking mitotic spindle assembly in the beginning of mitosis with chromatin decondensation as it happens at the end of mitosis.

8.1 DRGs & DFRPs function as chromatin decondensation factors

Chromatin decondensation as it happens at the end of mitosis is an active process requiring, next to ATP hydrolysis, GTP hydrolysis, suggesting that a GTPase is involved (Magalska et al., 2014). Using a biochemical fractionation approach combined with *in vitro* reconstitution of chromatin decondensation with *Xenopus laevis* egg extract, DRG1 was identified as possible candidate for this GTPase prior to this work.

Immunodepletions with antibodies against DRG1, DRG2, DFRP1 or DFRP2 co-depleted all four proteins from *Xenopus* egg extract. This depleted extract was not able to decondense mitotic chromatin as much as the mock depleted control, suggesting that at least one of the factors is involved in chromatin decondensation. Co-depletion of all four proteins was an unexpected observation as it was so far suggested that DFRP1 exclusively interacts with DRG1 while it is under debate if DFRP2 only binds DRG2 or also DRG1 (Ishikawa et al., 2009; Ishikawa et al., 2005; Wout et al., 2009). A tetramer complex was not described to date. Co-depletion of DRG1 and DRG2 can be explained by cross-reactivity of the polyclonal antibodies used, as the two proteins are highly similar, sharing 58 % sequence identity on the protein level in the case of the human proteins. However, DFRP1 and DFRP2 share only some homology in a small part of the protein, the DFRP domain which constitutes the main part of the DRG binding site. Thus, co-depletion of all four proteins by using DFRP1 or DFRP2 antibodies happened most likely because of the formation of a tetramer complex.

It has to be mentioned that little inconsistencies were observed over the course of immunodepletions and an add-back experiment of the depleted protein would be necessary to show the specificity of the observation. The main problem was that

the conditions necessary to deplete the DRGs and DFRPs were so strong that the control depletion (rabbit IgG) was often not fully decondensed as well, owing to decreased egg extract quality under such strong experimental conditions. Additionally, due to the high sequence similarities of DRG1 and DRG2 it was not possible to generate antibodies that do not cross-react. Nevertheless, the control was obviously more decondensed than the depleted samples, supporting the idea that DRGs and/or DFRPs are acting as chromatin decondensation factors.

This observation was confirmed by adding recombinant dominant mutants but also wild-type DRG1 and DRG2 to the *in vitro* reconstitution reaction of chromatin decondensation. All recombinant proteins inhibited chromatin decondensation, suggesting, in the case of the dominant mutants, that a functional GTPase domain of the DRGs is necessary. GTP hydrolysis might be necessary in order to undergo a conformational change in the protein that re-shapes chromatin in parallel.

Inhibition of decondensation by addition of wild-type DRGs could be caused by disturbing the GTP-bound to GDP-bound DRG ratios. This is for instance also observed for the small GTPase Ran which functions by gradients of its GTP- to GDP-bound state. GTP-bound Ran is enriched around chromatin during mitosis, releasing spindle assembly factors from importins by binding these transport factors instead (Carazo-Salas et al., 1999; Kalab et al., 2002). The same is true during interphase, when Ran-GTP accumulates in the nucleus, releasing cargos from imported importins, while Ran-GDP accumulates in the cytosol (reviewed in Cavazza and Vernos, 2015). These gradients are regulated by specific and differing localization of Ran GEFs and GAPs. Adding excess amounts of RanGTP to an *in vitro* reconstitution of nuclear envelope assembly leads to accumulations of membrane stacks in the cytosol due to impairment of the ratio of the different nucleotide states of Ran (Walther et al., 2003). This could also be the case for the DRGs.

While the immunodepletion experiments did not answer the question, which of the four proteins functions as chromatin decondensation factor, the dominant mutants showed that, as expected, the DRGs are involved. The DFRPs could also have a chromatin decondensation function, although it is more likely that they rather function as stabilizer or support of the DRGs. The mentioned inconsistencies in

the immunodepletion experiments as well as the effect of the addition of recombinant wild-type DRG1 and DRG2 might also suggest that the ratio of DRG1 to DRG2 plays an important role. The ratio of DRGs to DFRPs could similarly be crucial. It is also unclear, if DRG1 and DRG2 function redundantly, in association or antagonistically.

8.2 DRG1 is a microtubule-associated protein

In this work, DRG1 and DFRP1 were shown to bind directly to microtubules. Microtubule-associated proteins are often highly positively charged and bind tubulins at the highly acidic, negatively charged C-terminus. The C-terminal tails are unstructured, exposed at the microtubule surface and are the main site of posttranslational modifications ((Redeker et al., 1992); (reviewed in Cooper and Wordeman, 2009)). The only known crystal structure of DRG1 exist from its yeast homolog Rbg1 and showed a highly positively charged area upon electrostatic surface potential analysis (Francis et al., 2012). Modelling the structure of *Xenopus* DRG1 based on the Rbg1 structure, showed a similar surface. The positive charges stretch over the HTH, TGS, S5D2L and the G-domain opposite of the GTP binding pocket. It is likely that this area is the binding site for microtubules, in agreement with the fact that the HTH and TGS domain individually but also the truncated version of DRG1 lacking the TGS and/or HTH domain bound microtubules. The recombinant S5D2L domain alone did not bind microtubules, either it was not folded properly or its affinity was too low without the neighbouring areas. Concomitant with many individually binding domains, a functional GTPase domain of DRG1 was not necessary for microtubule binding. Surprisingly, DRG1 also bound to microtubules lacking the extreme C-terminus, removed by the protease subtilisin. Although the binding affinity might have been a bit reduced. For the *drosophila* non-claret disjunctional (Ncd) kinesin-like protein binding to two acidic patches in each tubulin monomer was observed. Both acidic clusters are in the C-terminal part of tubulin but the cleavage site for subtilisin lies in between these, thus, keeping and removing one acidic cluster each by subtilisin digestion. Thus, Ncd binding to subtilisin-digested microtubules was decreased but present (Karabay and Walker, 2003). Considering that the positively charged

surface of DRG1 stretches over the whole molecule and additionally, that many domains bound microtubules, it seems reasonable that the DRG1 binding site/s in the tubulins stretches over an extended area, from the extreme C-terminus further down.

DRG1 bound microtubules in three different ways: immobile, slow or fast diffusive. It was excluded that the three states represented different nucleotide-binding states as all three binding populations were also observed in the presence of GTP γ S, even if overall binding was slightly reduced. The different binding populations could either represent different functions such as bundling versus polymerization or different oligomeric states. These scenarios could also be linked: different oligomeric states could induce different ways of binding and could be linked each to a specific function. The proportions of the different binding populations were concentration dependent. The lower the DRG1 concentration, the more DRG1 molecules bound in an immobile way. This fits to the idea that different binding populations could represent different oligomeric states: if the concentration is higher, more DRG1 molecules might oligomerize into bigger complexes. Why the interaction times increased with smaller DRG1 concentrations remains currently unclear. In general, the diffusion on the microtubule lattice resembled other proteins that target the microtubule ends, facilitated by the diffusion on the microtubule, to perform their functions there, e.g. MCAK and EB1 (Chen et al., 2014; Helenius et al., 2006).

As expected for a protein with several microtubule binding domains, full-length DRG1 bundled microtubules, while DRG1 fragments did not. Microtubule bundling is often involved in stabilizing microtubules, for instance, in Ptk cells, roughly 20-30 kinetochore microtubules bundle into each k-fiber (McDonald et al., 1992); neuronal axons contain microtubule bundles that serve as their structural backbone as well as transport track between the cell body and the distal synapse (reviewed in Voelzmann et al., 2016) and crosslinking at the microtubule ends can form microtubule asters (reviewed in Subramanian and Kapoor, 2012).

DRG1 was indeed able to prevent microtubule disassembly on ice shown in a minimal *in vitro* system in which tubulin was first polymerized in the presence of DRG1 followed by incubation on ice. But also in mitotic HeLa cells, DRG1 knock-down by siRNA slowed down microtubule re-growth after cold shock. Small

spindle remnants were more often observed in control cells after cold shock. These remnants could facilitate re-assembly of the mitotic spindle. Acceleration of microtubule re-polymerization catalyzed by DRG1 is also possible.

DRG1 indeed polymerized tubulin into microtubules in a concentration below the critical concentration which is necessary for tubulin to polymerize without additional factors (Fyngenson et al., 1994). The *in vitro* microtubule polymerization assays used, did not allow to distinguish between microtubule nucleation and elongation. As for the bundling activity, truncated versions of DRG1 showed no polymerization or stabilization activities if the same conditions as for the wild-type were used. It is possible that some fragments would be able to bundle, polymerize or stabilize microtubules in higher concentrations, but the activities were definitely reduced compared to the wild-type. It was previously described in a different context that DRG1 needs its full-length protein to function properly: triple deletion of the DRG1 and 2 homologs, Rbg1 and 2, together with the ATPase Slh1 caused a severe growth effect in yeast that could only be rescued by full-length Rbg1 but not by any of its truncations (Daugeron et al., 2011).

In contrast to the necessity for all domains, the GTPase activity was not necessary for microtubule bundling, polymerization or stabilization as observed when the dominant DRG1 mutants were used in the *in vitro* assays. DRG1 was described before to have an intrinsic GTPase activity that does not require a GAP (Francis et al., 2012; O'Connell et al., 2009; Perez-Arellano et al., 2013). Thus, it seems likely that DRG1 needs its GTP hydrolysis activity in a different context, for instance in chromatin decondensation but not for its microtubule-associated functions. Although not using its GTPase activity in this context, it is surprising and unusual that the GTPase DRG1 regulates other GTPases, namely the tubulins.

DRG1 could perform its microtubule-associated functions independently of each other for instance regulated by the oligomeric state as described above, but it is more conceivable that the functions are connected and influence each other: the bundling might stabilize microtubules preventing microtubule disassembly after a cold shock, respectively; the observed stabilization could also be a consequence of highly accelerated polymerization; the bundling could also increase the microtubule density around DRG1 and thus increase the polymerization in a

specific location; the diffusion could increase the targeting of DRG1 to the microtubule ends where it functions as polymerase. Different scenarios are conceivable.

Certain observed characteristics of DRG1 were also described for motor proteins. Kinesin-1 is a plus end directed motor protein which binds microtubules not only via its N-terminal motor domain but also has a C-terminal microtubule binding site which attaches to a second microtubule. If two antiparallel microtubules are bound by two oppositely arranged kinesins and the kinesin motor domains move towards the plus ends, the two microtubules will slide away from each other. However, if the two microtubules are arranged in parallel, the forces of the two kinesins will balance each other resulting in cross-linking but not sliding of the two microtubules (reviewed in Lu and Gelfand, 2017). DRG1 also bundled and moved on microtubules. Although the TGS domain and the globular assembly of the HTH and S5D2L domains could function equivalent to the two globular heads of molecular motors, it seems rather unlikely. The DRG1 structure and size is most likely to small for “walking” like a typical motor complex. Second, kinesins and dyneins move by conformational changes induced through ATP hydrolysis while the microtubule-associated functions of DRG do not require GTP hydrolysis. Third, while kinesins and dyneins usually show a specificity for one direction, the slow diffusion of DRG1 seemed bidirectional rather resembling the depolymerase MCAK (Helenius et al., 2006). Several microtubule-binding proteins diffuse randomly, one-dimensional on the microtubule driven by thermal energy (reviewed in Cooper and Wordeman, 2009). Next to increasing the chance of reaching the microtubule ends compared to diffusion in solution, it was suggested to facilitate moving around obstacles on the microtubule surface, reaching the microtubule ends more rapidly over short distances and needing no energy compared to directed motility of motor proteins. Interestingly, some kinesins were observed to also have a component of random diffusive movement on top of the directed motor motility.

DRG1 shows GTPase activity over a wide range of pHs and temperatures with an optimum at pH 8 to 9 and 42°C (Perez-Arellano et al., 2013) suggesting that it might be involved in stress response or other situations that are laborious for the cell. Although, concerning the GTPase activity, preferentially active at warm

temperatures, stabilization of microtubules during cold shock might also be an extreme situation that is tolerated better from DRG1 compared to other proteins.

The *in vitro* experiments do not distinguish between mitotic and interphase microtubule dynamics. The cold shock experiments in HeLa cells showed that DRG1 is involved in spindle dynamics during mitosis, though. Furthermore, when DRG1 was knocked-down in HeLa cells, the timing from prophase to anaphase onset and the timing from aster to anaphase spindle formation were extended. Although, the spindle size and intensity measured via the eGFP-tubulin signal were not changed, the prolonged timing of mitotic phases occurred most likely due to a slower formation of the mitotic spindle. This is in agreement with the slower re-growth of the mitotic spindle after a cold shock in cells lacking DRG1. The slower assembly can be explained by the polymerization activity of DRG1 accelerating the assembly directly or by the stabilization and bundling activities of DRG1 that might prevent disassembly of already assembled spindle microtubules. Despite convincing results for a mitotic involvement, it is possible that DRG1 also plays a role in microtubule dynamics during interphase when all the mentioned activities are equally important for instance in transport processes and cell shape establishment and maintenance (reviewed in de Forges et al., 2012).

The fact that it took a long time to identify DRG1 as microtubule-associated protein might be explained, next to other reasons, by the many partially redundant pathways involved in spindle assembly causing individually often only small phenotypes when inhibited. Nevertheless, each missing factor and mis-regulated pathway increases the chance of chromosome segregation errors. Thus, it is not surprising that mis-regulation of microtubule-associated proteins is often observed in different disease contexts (e.g. Alonso et al., 2016; Du et al., 2016; Kumar et al., 2016; Schneider et al., 2017).

8.3 Possible connections of the chromatin- and microtubule-associated functions of DRG1

In this work, DRG1 was identified as chromatin decondensation factor as well as microtubule-associated protein with various functions. Both of these fields of activities are performed during mitosis, spindle assembly in the beginning, chromatin decondensation at the end. It is conceivable that these two pathways and the functions of DRG1 are connected or independent of each other. If the latter holds true, regulation and discrimination of the functions can occur spatially or temporally. Spindle assembly happens prior to chromatin decondensation, DRG1 or its targets could therefore be temporally modified by posttranslational modifications or interaction partners, so that DRG1 can only act in one of the two pathways at a certain time point during the cell cycle or developmental stage. Although the latter, different functions of DRG1 during different developmental stages, seems less likely than cell cycle dependent functions considering the activities of DRG1. Regulation via interaction partners could for instance occur by binding to DFRP1 or by tetramer formation of DRG1, DRG2, DFRP1 and DFRP2. Also the ratio of DRG1 and DRG2 might be important. For chromatin decondensation a complex of these four proteins might be important as they co-depleted together, or at least DRG1 and DRG2 might function redundantly or in association in this case. DFRP2 did not bind to microtubules, even not in HeLa nuclear extract, suggesting that the microtubule-associated functions of DRG1 are not performed in a tetramer complex.

A spatial regulation is also conceivable. Regulations via different localizations in the cell seems thereby much more likely than by different tissue types. If DRG1 performs its microtubule-associated functions in the early steps of spindle assembly, the chromatin might still be excluded from the microtubule-associated DRG1 molecules by the not yet fully disassembled nuclear envelope. Same if DRG1 performs its chromatin-associated functions in the late steps of chromatin decondensation, the chromatin might already (partially) be excluded from the cytosol by the assembling nuclear envelope, protected from microtubules. Thus, in this scenario, DRG1 would perform its microtubule- and chromatin-associated functions not only temporally but also spatially separated.

On the other hand, several scenarios of a connection of spindle assembly and chromatin decondensation are imaginable. The role of microtubules in nuclear envelope reformation is controversial. While on the one hand it seems that microtubules need to be removed before reformation of the nuclear envelope in order to not sterically inhibit membrane closure and also to prevent certain signaling molecules that delay nuclear reformation from reaching the nucleus, microtubules on the other hand deliver membranes and nuclear pore complex components to nascent nuclei. Concomitant with this, nuclei formed upon microtubule depletion show a reduced size while nuclear shape is disturbed upon excessive microtubule polymerization (reviewed in Xue and Funabiki, 2014). Furthermore, nuclei assembled in the presence of the microtubule-depolymerizing drug nocodazole or a kinesin inhibitor lack nuclear pore complexes which is in agreement with the decreased size possibly caused by lacking nuclear import (Ewald et al., 2001).

Either way, even if the majority of microtubules needs to be removed, it is possible that a specific subset of microtubules remains to deliver necessary nuclear building blocks but maybe also to pull the chromatin apart from each other, inducing chromatin decondensation. Microtubules exist in many different isoforms, can be modified by a plethora of posttranslational modifications (reviewed in Gadadhar et al., 2017) and can be covered by specific factors. By this, a certain subset of microtubules that is responsible for pulling chromatin apart might be distinguishable from the bulk microtubules that need to disassemble in order to allow nuclear envelope reassembly. But also if this is not the case and all microtubules need to be removed for chromatin decondensation, DRG1 might connect the two pathways and needs to move from one target to the other, maybe even by physical connections of microtubules to chromatin that then get resolved. Besides DRG1, also RuvBL1/2 are involved in spindle assembly (reviewed in Nano and Houry, 2013) and chromatin decondensation (Magalska et al., 2014), supporting the idea that these processes are connected or at least regulated in dependence of each other, meaning for instance spindle assembly needs to get switched off in order to let chromatin decondensation happen. ISWI is another protein that shows chromatin remodeling (reviewed in Tyagi et al., 2016) but also microtubule-associated functions (Yokoyama et al., 2009).

For interphase it is indeed known that the microtubule cytoskeleton influences chromatin structure even if no polymerized microtubules are present in the nucleus and a direct physical link is not existing (reviewed in Maizels and Gerlitz, 2015). This can happen by factors that are transported via microtubule motors to the centrosome which is in close proximity to the nucleus at that stage and therefore facilitates import to the nucleus. Furthermore, soluble parts of the cytoskeleton like tubulins are found under certain conditions in the nucleus where they might directly influence chromatin structure and last, mechanical forces by the microtubule cytoskeleton can influence chromatin arrangements via nuclear pore and other complexes that bridge these two. In mammalian melanoma cells, heterochromatin accumulates in the nucleus close to the site where the centrosome or microtubule organizing center is. The same was observed for centromeric chromatin in drosophila embryos during cellularization and in *S. pombe*.

During mitosis microtubules and their molecular motor proteins are involved in arranging the chromosomes on the metaphase plate and in pushing the chromosome arms in the right positions to make the kinetochores accessible for bipolar microtubule-end on attachment (reviewed in Heald and Khodjakov, 2015). If the mitotic interaction with microtubules primes the chromosomes also further for chromatin decondensation and the following interphase chromatin arrangement remains open. Similarly, if this is the case, which role DRG1 and RuvBL1/2 play in this context is currently unclear. It was described before that the individual chromatin position in the reforming nucleus is influenced by the timing of sister chromatid separation which is in turn perhaps mediated by the amount of centromeric heterochromatin (Gerlich et al., 2003) and that chromatin decondenses in a radial expansion mechanisms involving little rearrangements which leads to chromosomes with the same neighbouring chromosomes during mitosis and interphase (Manders et al., 2003). This leaves room for various hypotheses about further connections of the mitotic spindle and re-formation of the interphase chromatin state.

DRG1 was previously also described to be involved in translation as it co-fractionates with poly-ribosomes (Daugeron et al., 2011; Francis et al., 2012;

Ishikawa et al., 2009; Wout et al., 2009), although the exact function in this context remains obscure. The ribosomal function of DRG1 seems not to be connected to the microtubule-associated functions as the latter ones were shown in a direct, minimal system not requiring translation and not including more factors besides DRG1, tubulins, GTP and buffer components. The chromatin decondensation function is as well uncoupled from translation as the *in vitro* reconstitution was performed in the presence of the translational inhibitor cycloheximide. Thus, either DRG1 plays an additional role in translation, unconnected to its microtubule- and chromatin-associated functions or it is not really involved in ribosomal functions and rather the ribosome functions as sequestering site and therefore regulation of DRG1. An additional function in translation could be spatiotemporal regulated and separated from the other functions as described before, for instance different cellular localizations, interaction partners or cell cycle stages could determine the function. As all three processes mainly happen at different times of the cell cycle, a regulation in this manner seems conceivable.

Interesting to note, DRG1 does not need its GTPase activity for the microtubule-associated functions while it is important for chromatin decondensation. Although it is possible that the inhibition of chromatin decondensation by addition of the dominant mutants was caused by a similar effect as the wild-type addition and not by the mutations. In this case a second GTPase must be involved in chromatin decondensation which was inhibited by GTP γ S.

Although many open questions remain regarding the mechanistic details and connections of the different pathways, DRG1 was discovered to be involved in chromatin decondensation at the end of mitosis as well as being a microtubule binding, bundling, polymerization and stabilization factor that is involved in spindle assembly dynamics in cells. Being involved in so fundamental pathways essential for the healthiness of the cell, it will be exciting to find out more about the exact functions, targets and interaction partners of DRG1 in the future.

9 References

- Alonso, A.D., C. Beharry, C.P. Corbo, and L.S. Cohen. 2016. Molecular mechanism of prion-like tau-induced neurodegeneration. *Alzheimer's & dementia : the journal of the Alzheimer's Association*. 12:1090-1097.
- Alushin, G.M., G.C. Lander, E.H. Kellogg, R. Zhang, D. Baker, and E. Nogales. 2014. High-resolution microtubule structures reveal the structural transitions in alphabeta-tubulin upon GTP hydrolysis. *Cell*. 157:1117-1129.
- Aumeier, C., L. Schaedel, J. Gaillard, K. John, L. Blanchoin, and M. Thery. 2016. Self-repair promotes microtubule rescue. *Nat Cell Biol*. 18:1054-1064.
- Belmont, A.S. 2006. Mitotic chromosome structure and condensation. *Curr Opin Cell Biol*. 18:632-638.
- Brugues, J., V. Nuzzo, E. Mazur, and D.J. Needleman. 2012. Nucleation and transport organize microtubules in metaphase spindles. *Cell*. 149:554-564.
- Burglin, T.R., I.W. Mattaj, D.D. Newmeyer, R. Zeller, and E.M. De Robertis. 1987. Cloning of nucleoplasmin from *Xenopus laevis* oocytes and analysis of its developmental expression. *Genes Dev*. 1:97-107.
- Carazo-Salas, R.E., G. Guarguaglini, O.J. Gruss, A. Segref, E. Karsenti, and I.W. Mattaj. 1999. Generation of GTP-bound Ran by RCC1 is required for chromatin-induced mitotic spindle formation. *Nature*. 400:178-181.
- Cavazza, T., and I. Vernos. 2015. The RanGTP Pathway: From Nucleo-Cytoplasmic Transport to Spindle Assembly and Beyond. *Frontiers in cell and developmental biology*. 3:82.
- Chen, Y., M.M. Rolls, and W.O. Hancock. 2014. An EB1-kinesin complex is sufficient to steer microtubule growth in vitro. *Curr Biol*. 24:316-321.
- Chretien, D., F. Metoz, F. Verde, E. Karsenti, and R.H. Wade. 1992. Lattice defects in microtubules: protofilament numbers vary within individual microtubules. *J Cell Biol*. 117:1031-1040.
- Cooper, J.R., and L. Wordeman. 2009. The diffusive interaction of microtubule binding proteins. *Curr Opin Cell Biol*. 21:68-73.
- Dasso, M., T. Seki, Y. Azuma, T. Ohba, and T. Nishimoto. 1994. A mutant form of the Ran/TC4 protein disrupts nuclear function in *Xenopus laevis* egg extracts by inhibiting the RCC1 protein, a regulator of chromosome condensation. *EMBO J*. 13:5732-5744.
- Daugeron, M.C., M. Prouteau, F. Lacroute, and B. Seraphin. 2011. The highly conserved eukaryotic DRG factors are required for efficient translation in a manner redundant with the putative RNA helicase Slh1. *Nucleic Acids Res*. 39:2221-2233.
- de Forges, H., A. Bouissou, and F. Perez. 2012. Interplay between microtubule dynamics and intracellular organization. *The international journal of biochemistry & cell biology*. 44:266-274.
- Devitt, M.L., K.J. Maas, and J.P. Stafstrom. 1999. Characterization of DRGs, developmentally regulated GTP-binding proteins, from pea and Arabidopsis. *Plant molecular biology*. 39:75-82.
- Du, Y., L. Liu, C. Wang, B. Kuang, S. Yan, A. Zhou, C. Wen, J. Chen, Y. Wu, X. Yang, G. Feng, B. Liu, A. Iwamoto, M. Zeng, J. Wang, X. Zhang, and H. Liu. 2016. TACC3 promotes colorectal cancer tumorigenesis and correlates with poor prognosis. *Oncotarget*. 7:41885-41897.
- Ewald, A., C. Zunkler, D. Lourim, and M.C. Dabauvalle. 2001. Microtubule-dependent assembly of the nuclear envelope in *Xenopus laevis* egg extract. *Eur J Cell Biol*. 80:678-691.
- Francis, S.M., M.E. Gas, M.C. Daugeron, J. Bravo, and B. Seraphin. 2012. Rbg1-Tma46 dimer structure reveals new functional domains and their role in polysome recruitment. *Nucleic Acids Res*. 40:11100-11114.
- Fygenon, D.K., E. Braun, and A. Libchaber. 1994. Phase diagram of microtubules. *Physical review. E, Statistical physics, plasmas, fluids, and related interdisciplinary topics*. 50:1579-1588.
- Gadadhar, S., S. Bodakuntla, K. Natarajan, and C. Janke. 2017. The tubulin code at a glance. *J Cell Sci*. 130:1347-1353.

- Gant, T.M., and K.L. Wilson. 1997. Nuclear assembly. *Annu Rev Cell Dev Biol.* 13:669-695.
- Gerlich, D., J. Beaudouin, B. Kalbfuss, N. Daigle, R. Eils, and J. Ellenberg. 2003. Global chromosome positions are transmitted through mitosis in mammalian cells. *Cell.* 112:751-764.
- Heald, R., and A. Khodjakov. 2015. Thirty years of search and capture: The complex simplicity of mitotic spindle assembly. *J Cell Biol.* 211:1103-1111.
- Heald, R., R. Tournebize, A. Habermann, E. Karsenti, and A. Hyman. 1997. Spindle assembly in *Xenopus* egg extracts: respective roles of centrosomes and microtubule self-organization. *J Cell Biol.* 138:615-628.
- Helenius, J., G. Brouhard, Y. Kalaidzidis, S. Diez, and J. Howard. 2006. The depolymerizing kinesin MCAK uses lattice diffusion to rapidly target microtubule ends. *Nature.* 441:115-119.
- Helmke, K.J., and R. Heald. 2014. TPX2 levels modulate meiotic spindle size and architecture in *Xenopus* egg extracts. *J Cell Biol.* 206:385-393.
- Henzel, M.J., Y. Wei, M.A. Mancini, A. Van Hooser, T. Ranalli, B.R. Brinkley, D.P. Bazett-Jones, and C.D. Allis. 1997. Mitosis-specific phosphorylation of histone H3 initiates primarily within pericentromeric heterochromatin during G2 and spreads in an ordered fashion coincident with mitotic chromosome condensation. *Chromosoma.* 106:348-360.
- Hsu, J.Y., Z.W. Sun, X. Li, M. Reuben, K. Tatchell, D.K. Bishop, J.M. Grushcow, C.J. Brame, J.A. Caldwell, D.F. Hunt, R. Lin, M.M. Smith, and C.D. Allis. 2000. Mitotic phosphorylation of histone H3 is governed by Ipl1/aurora kinase and Glc7/PP1 phosphatase in budding yeast and nematodes. *Cell.* 102:279-291.
- Hudson, J.D., and P.G. Young. 1993. Sequence of the *Schizosaccharomyces pombe* gtp1 gene and identification of a novel family of putative GTP-binding proteins. *Gene.* 125:191-193.
- Ishikawa, K., T. Akiyama, K. Ito, K. Semba, and J. Inoue. 2009. Independent stabilizations of polysomal Drg1/Dfrp1 complex and non-polysomal Drg2/Dfrp2 complex in mammalian cells. *Biochem Biophys Res Commun.* 390:552-556.
- Ishikawa, K., S. Azuma, S. Ikawa, Y. Morishita, J. Gohda, T. Akiyama, K. Semba, and J. Inoue. 2003. Cloning and characterization of *Xenopus laevis* drg2, a member of the developmentally regulated GTP-binding protein subfamily. *Gene.* 322:105-112.
- Ishikawa, K., S. Azuma, S. Ikawa, K. Semba, and J. Inoue. 2005. Identification of DRG family regulatory proteins (DFRPs): specific regulation of DRG1 and DRG2. *Genes to cells : devoted to molecular & cellular mechanisms.* 10:139-150.
- Kajtez, J., A. Solomatina, M. Novak, B. Polak, K. Vukusic, J. Rudiger, G. Cojoc, A. Milas, I. Sumanovac Sestak, P. Risteski, F. Tavano, A.H. Klemm, E. Roscioli, J. Welburn, D. Cimini, M. Gluncic, N. Pavin, and I.M. Tolic. 2016. Overlap microtubules link sister k-fibres and balance the forces on bi-oriented kinetochores. *Nature communications.* 7:10298.
- Kalab, P., K. Weis, and R. Heald. 2002. Visualization of a Ran-GTP gradient in interphase and mitotic *Xenopus* egg extracts. *Science.* 295:2452-2456.
- Karabay, A., and R.A. Walker. 2003. Identification of Ncd tail domain-binding sites on the tubulin dimer. *Biochem Biophys Res Commun.* 305:523-528.
- Kirschner, M., and T. Mitchison. 1986. Beyond self-assembly: from microtubules to morphogenesis. *Cell.* 45:329-342.
- Kollman, J.M., A. Merdes, L. Mourey, and D.A. Agard. 2011. Microtubule nucleation by gamma-tubulin complexes. *Nat Rev Mol Cell Biol.* 12:709-721.
- Kumar, M., S. Mehra, A. Thakar, N.K. Shukla, A. Roychoudhary, M.C. Sharma, R. Ralhan, and S.S. Chauhan. 2016. End Binding 1 (EB1) overexpression in oral lesions and cancer: A biomarker of tumor progression and poor prognosis. *Clinica chimica acta; international journal of clinical chemistry.* 459:45-52.
- Kumar, S., M. Iwao, T. Yamagishi, M. Noda, and M. Asashima. 1993. Expression of GTP-binding protein gene drg during *Xenopus laevis* development. *The International journal of developmental biology.* 37:539-546.

- Lee, E.H., H.J. Kim, J.J. Park, J.Y. Choi, W.J. Cho, S.J. Cha, C.H. Moon, J.M. Park, W.J. Yoon, B.J. Lee, D.H. Lee, H.S. Kang, M.A. Yoo, H.D. Kim, and J.W. Park. 1998. Molecular cloning of a novel GTP-binding protein induced in fish cells by rhabdovirus infection. *FEBS Lett.* 429:407-411.
- Leipe, D.D., Y.I. Wolf, E.V. Koonin, and L. Aravind. 2002. Classification and evolution of P-loop GTPases and related ATPases. *J Mol Biol.* 317:41-72.
- Li, B., and B. Trueb. 2000. DRG represents a family of two closely related GTP-binding proteins. *Biochim Biophys Acta.* 1491:196-204.
- Lu, L., Y. Lv, J. Dong, S. Hu, and R. Peng. 2016. DRG1 is a potential oncogene in lung adenocarcinoma and promotes tumor progression via spindle checkpoint signaling regulation. *Oncotarget.* 7:72795-72806.
- Lu, W., and V.I. Gelfand. 2017. Moonlighting Motors: Kinesin, Dynein, and Cell Polarity. *Trends Cell Biol.*
- MacCallum, D.E., A. Losada, R. Kobayashi, and T. Hirano. 2002. ISWI remodeling complexes in *Xenopus* egg extracts: identification as major chromosomal components that are regulated by INCENP-aurora B. *Mol Biol Cell.* 13:25-39.
- Magalska, A., A.K. Schellhaus, D. Moreno-Andres, F. Zanini, A. Schooley, R. Sachdev, H. Schwarz, J. Madlung, and W. Antonin. 2014. RuvB-like ATPases function in chromatin decondensation at the end of mitosis. *Dev Cell.* 31:305-318.
- Maizels, Y., and G. Gerlitz. 2015. Shaping of interphase chromosomes by the microtubule network. *The FEBS journal.* 282:3500-3524.
- Manders, E.M., A.E. Visser, A. Koppen, W.C. de Leeuw, R. van Liere, G.J. Brakenhoff, and R. van Driel. 2003. Four-dimensional imaging of chromatin dynamics during the assembly of the interphase nucleus. *Chromosome Res.* 11:537-547.
- Mastronarde, D.N., K.L. McDonald, R. Ding, and J.R. McIntosh. 1993. Interpolar spindle microtubules in PTK cells. *J Cell Biol.* 123:1475-1489.
- McDonald, K.L., E.T. O'Toole, D.N. Mastronarde, and J.R. McIntosh. 1992. Kinetochore microtubules in PTK cells. *J Cell Biol.* 118:369-383.
- Mitchison, T., and M. Kirschner. 1984. Dynamic instability of microtubule growth. *Nature.* 312:237-242.
- Murnion, M.E., R.R. Adams, D.M. Callister, C.D. Allis, W.C. Earnshaw, and J.R. Swedlow. 2001. Chromatin-associated protein phosphatase 1 regulates aurora-B and histone H3 phosphorylation. *J Biol Chem.* 276:26656-26665.
- Murray, A.W. 1991. Cell cycle extracts. *Methods Cell Biol.* 36:581-605.
- Nano, N., and W.A. Houry. 2013. Chaperone-like activity of the AAA+ proteins Rvb1 and Rvb2 in the assembly of various complexes. *Philos Trans R Soc Lond B Biol Sci.* 368:20110399.
- Newmeyer, D.D., and K.L. Wilson. 1991. Egg extracts for nuclear import and nuclear assembly reactions. *Methods Cell Biol.* 36:607-634.
- Nogales, E., M. Whittaker, R.A. Milligan, and K.H. Downing. 1999. High-resolution model of the microtubule. *Cell.* 96:79-88.
- O'Connell, A., G. Robin, B. Kobe, and J.R. Botella. 2009. Biochemical characterization of Arabidopsis developmentally regulated G-proteins (DRGs). *Protein expression and purification.* 67:88-95.
- Okamoto, S., and K. Ochi. 1998. An essential GTP-binding protein functions as a regulator for differentiation in *Streptomyces coelicolor*. *Molecular microbiology.* 30:107-119.
- Perez-Arellano, I., M. Spinola-Amilibia, and J. Bravo. 2013. Human Drg1 is a potassium-dependent GTPase enhanced by Lerepo4. *The FEBS journal.* 280:3647-3657.
- Petry, S. 2016. Mechanisms of Mitotic Spindle Assembly. *Annu Rev Biochem.* 85:659-683.
- Philpott, A., and G.H. Leno. 1992. Nucleoplasmin remodels sperm chromatin in *Xenopus* egg extracts. *Cell.* 69:759-767.
- Philpott, A., G.H. Leno, and R.A. Laskey. 1991. Sperm decondensation in *Xenopus* egg cytoplasm is mediated by nucleoplasmin. *Cell.* 65:569-578.

- Polak, B., P. Risteski, S. Lesjak, and I.M. Tolic. 2017. PRC1-labeled microtubule bundles and kinetochore pairs show one-to-one association in metaphase. *EMBO Rep.* 18:217-230.
- Powers, M., E.K. Evans, J. Yang, and S. Kornbluth. 2001. Preparation and use of interphase Xenopus egg extracts. *Current protocols in cell biology*. Chapter 11:Unit 11 10.
- Prosser, S.L., and L. Pelletier. 2017. Mitotic spindle assembly in animal cells: a fine balancing act. *Nat Rev Mol Cell Biol.* 18:187-201.
- Ramadan, K., R. Bruderer, F.M. Spiga, O. Popp, T. Baur, M. Gotta, and H.H. Meyer. 2007. Cdc48/p97 promotes reformation of the nucleus by extracting the kinase Aurora B from chromatin. *Nature.* 450:1258-1262.
- Redeker, V., R. Melki, D. Prome, J.P. Le Caer, and J. Rossier. 1992. Structure of tubulin C-terminal domain obtained by subtilisin treatment. The major alpha and beta tubulin isoforms from pig brain are glutamylated. *FEBS Lett.* 313:185-192.
- Redemann, S., J. Baumgart, N. Lindow, M. Shelley, E. Nazockdast, A. Kratz, S. Prohaska, J. Bragues, S. Furthauer, and T. Muller-Reichert. 2017. C. elegans chromosomes connect to centrosomes by anchoring into the spindle network. *Nature communications.* 8:15288.
- Sazuka, T., Y. Tomooka, Y. Ikawa, M. Noda, and S. Kumar. 1992. DRG: a novel developmentally regulated GTP-binding protein. *Biochem Biophys Res Commun.* 189:363-370.
- Schellhaus, A.K., P. De Magistris, and W. Antonin. 2016. Nuclear Reformation at the End of Mitosis. *J Mol Biol.* 428:1962-1985.
- Schellhaus, A.K., A. Magalska, A. Schooley, and W. Antonin. 2015. A Cell Free Assay to Study Chromatin Decondensation at the End of Mitosis. *Journal of visualized experiments : JoVE*:e53407.
- Schellhaus, A.K., D. Moreno-Andrés, M. Chugh, H. Yokoyama, A. Moschopoulou, S. De, F. Bono, K. Hipp, E. Schäffer, and W. Antonin. *In revision*. Developmentally Regulated GTP binding protein 1 (DRG1) controls microtubule dynamics. *Scientific Reports*.
- Schenker, T., C. Lach, B. Kessler, S. Calderara, and B. Trueb. 1994. A novel GTP-binding protein which is selectively repressed in SV40 transformed fibroblasts. *J Biol Chem.* 269:25447-25453.
- Schneider, M.A., P. Christopoulos, T. Muley, A. Warth, U. Klingmueller, M. Thomas, F.J. Herth, H. Dienemann, N.S. Mueller, F. Theis, and M. Meister. 2017. AURKA, DLGAP5, TPX2, KIF11 and CKAP5: Five specific mitosis-associated genes correlate with poor prognosis for non-small cell lung cancer patients. *International journal of oncology.* 50:365-372.
- Shimmin, L.C., and P.P. Dennis. 1989. Characterization of the L11, L1, L10 and L12 equivalent ribosomal protein gene cluster of the halophilic archaebacterium Halobacterium cutirubrum. *EMBO J.* 8:1225-1235.
- Sommer, K.A., G. Petersen, and E.K. Bautz. 1994. The gene upstream of DmRP128 codes for a novel GTP-binding protein of Drosophila melanogaster. *Mol Gen Genet.* 242:391-398.
- Subramanian, R., and T.M. Kapoor. 2012. Building complexity: insights into self-organized assembly of microtubule-based architectures. *Dev Cell.* 23:874-885.
- Tilney, L.G., J. Bryan, D.J. Bush, K. Fujiwara, M.S. Mooseker, D.B. Murphy, and D.H. Snyder. 1973. Microtubules: evidence for 13 protofilaments. *J Cell Biol.* 59:267-275.
- Tyagi, M., N. Imam, K. Verma, and A.K. Patel. 2016. Chromatin remodelers: We are the drivers!! *Nucleus.* 7:388-404.
- Vagnarelli, P. 2012. Mitotic chromosome condensation in vertebrates. *Exp Cell Res.* 318:1435-1441.
- Voelzmann, A., I. Hahn, S.P. Pearce, N. Sanchez-Soriano, and A. Prokop. 2016. A conceptual view at microtubule plus end dynamics in neuronal axons. *Brain research bulletin.* 126:226-237.
- Walther, T.C., P. Askjaer, M. Gentzel, A. Habermann, G. Griffiths, M. Wilm, I.W. Mattaj, and M. Hetzer. 2003. RanGTP mediates nuclear pore complex assembly. *Nature.* 424:689-694.

- Wilkins, B.J., N.A. Rall, Y. Ostwal, T. Kruitwagen, K. Hiragami-Hamada, M. Winkler, Y. Barral, W. Fischle, and H. Neumann. 2014. A cascade of histone modifications induces chromatin condensation in mitosis. *Science*. 343:77-80.
- Wout, P.K., E. Sattlegger, S.M. Sullivan, and J.R. Maddock. 2009. *Saccharomyces cerevisiae* Rbg1 protein and its binding partner Gir2 interact on Polyribosomes with Gcn1. *Eukaryotic cell*. 8:1061-1071.
- Xue, J.Z., and H. Funabiki. 2014. Nuclear assembly shaped by microtubule dynamics. *Nucleus*. 5:40-46.
- Yokoyama, H., S. Rybina, R. Santarella-Mellwig, I.W. Mattaj, and E. Karsenti. 2009. ISWI is a RanGTP-dependent MAP required for chromosome segregation. *J Cell Biol*. 187:813-829.

10 Appendix

Original published articles and submitted manuscripts included in this thesis.

RuvB-like ATPases Function in Chromatin Decondensation at the End of Mitosis

Adriana Magalska,^{1,4} Anna Katharina Schellhaus,¹ Daniel Moreno-Andrés,¹ Fabio Zanini,² Allana Schooley,¹ Ruchika Sachdev,¹ Heinz Schwarz,² Johannes Madlung,³ and Wolfram Antonin^{1,*}

¹Friedrich Miescher Laboratory of the Max Planck Society, Spemannstrasse 39, 72076 Tübingen, Germany

²Max Planck Institute for Developmental Biology, Spemannstrasse 35, 72076 Tübingen, Germany

³Proteome Center Tübingen, University of Tübingen, 72076 Tübingen, Germany

⁴Present address: Nencki Institute of Experimental Biology, Polish Academy of Sciences, 3 Pasteur Street, 02-093 Warsaw, Poland

*Correspondence: wolfram.antonin@tuebingen.mpg.de

<http://dx.doi.org/10.1016/j.devcel.2014.09.001>

SUMMARY

Chromatin undergoes extensive structural changes during the cell cycle. Upon mitotic entry, metazoan chromatin undergoes tremendous condensation, creating mitotic chromosomes with 50-fold greater compaction relative to interphase chromosomes. At the end of mitosis, chromosomes reestablish functional interphase chromatin competent for replication and transcription through a decondensation process that is cytologically well described. However, the underlying molecular events and factors remain unidentified. We describe a cell-free system that recapitulates chromatin decondensation based on purified mitotic chromatin and *Xenopus* egg extracts. Using biochemical fractionation, we identify RuvB-like ATPases as chromatin decondensation factors and demonstrate that their ATPase activity is essential for decondensation. Our results show that decompaction of metaphase chromosomes is not merely an inactivation of known chromatin condensation factors but rather an active process requiring specific molecular machinery. Our cell-free system provides an important tool for further molecular characterization of chromatin decondensation and its coordination with concomitant processes.

INTRODUCTION

Cells have evolved highly elaborate mechanisms to transmit genetic information accurately to their offspring. These mechanisms often involve major cellular reorganization. In metazoa, the nucleus entirely disintegrates during each round of cell division (for a review, see [Kutay and Hetzer, 2008](#)). At the beginning of mitosis, the nuclear envelope breaks down and the chromatin condenses to rod-shaped chromosomes, which are captured by the mitotic spindle and segregated to the emerging daughter cells. The two resulting cells and their nuclei must therefore reestablish the functional interphase state. This reestablishment during mitotic exit requires the complete reversal of events that occurred at the onset of mitosis. The chromosomes decondense, and the nuclear envelope and other nuclear structures reform.

Whereas mitotic entry and the processes leading to successful spindle formation and chromatin segregation are comparatively well studied ([Walczak et al., 2010](#); [Walczak and Heald, 2008](#)) much less is known about the important processes at the end of mitosis. In animal cells, mitotic exit is driven by the inactivation of mitotic kinases ([Peters, 2006](#)), the extraction of ubiquitylated Aurora B from chromosomes by the AAA+ (ATPases associated with diverse cellular activities) ATPase p97 ([Ramadan et al., 2007](#)), and the activation of several protein phosphatases, most prominently, PP1 ([Landsverk et al., 2005](#); [Steen et al., 2000](#); [Thompson et al., 1997](#)) and PP2A ([Schmitz et al., 2010](#)). These events collectively result in the reversal of mitotic phosphorylation on a broad range of substrates ([Dephoure et al., 2008](#); [Olsen et al., 2010](#)), yet little is known about the actual machineries that mediate specific mitotic exit events ([Wurzenberger and Gerlich, 2011](#)). This is especially evident for chromatin decondensation, a prerequisite for the formation of interphase nuclear structures. Metaphase chromosomes are highly condensed—DNA compaction is up to 50-fold higher than in interphase ([Belmont, 2006](#))—but how this condensation is achieved is still ill defined (for a review, see [Hansen, 2012](#); [Ohta et al., 2011](#)). However, the process that reorganizes the genome into a structure competent for transcription and replication is largely uncharted territory. We are ignorant about the proteins that mediate chromatin decondensation, the distinct steps in this most likely multistep procedure, and its regulation.

To date, chromatin decondensation has mainly been examined in the context of sperm chromatin remodeling after fertilization. Highly compacted sperm DNA undergoes reorganization due to the presence of nucleoplamin (NPM2) stored in oocyte cytoplasm ([Philpott et al., 1991](#)). This process has been intensively studied using *Xenopus laevis* egg extracts. *Xenopus* sperm chromatin consists of a complex mixture of sperm-specific basic proteins and histones H3 and H4. NPM2 replaces these basic proteins from the male pronucleus with histones H2A and H2B stored in the egg, relaxing the tightly wound sperm chromatin structure ([Philpott and Leno, 1992](#)). However, as mitotic chromatin is already structured around H2A and H2B and does not contain these sperm-specific proteins, chromatin decondensation at the end of mitosis is likely to proceed by another yet-unknown mechanism.

Here, we describe a cell-free assay that faithfully recapitulates decondensation of mitotic chromatin. Using this assay, we show that chromatin decondensation requires ATP and GTP hydrolysis and is, thus, an active process. We identify RuvB-like

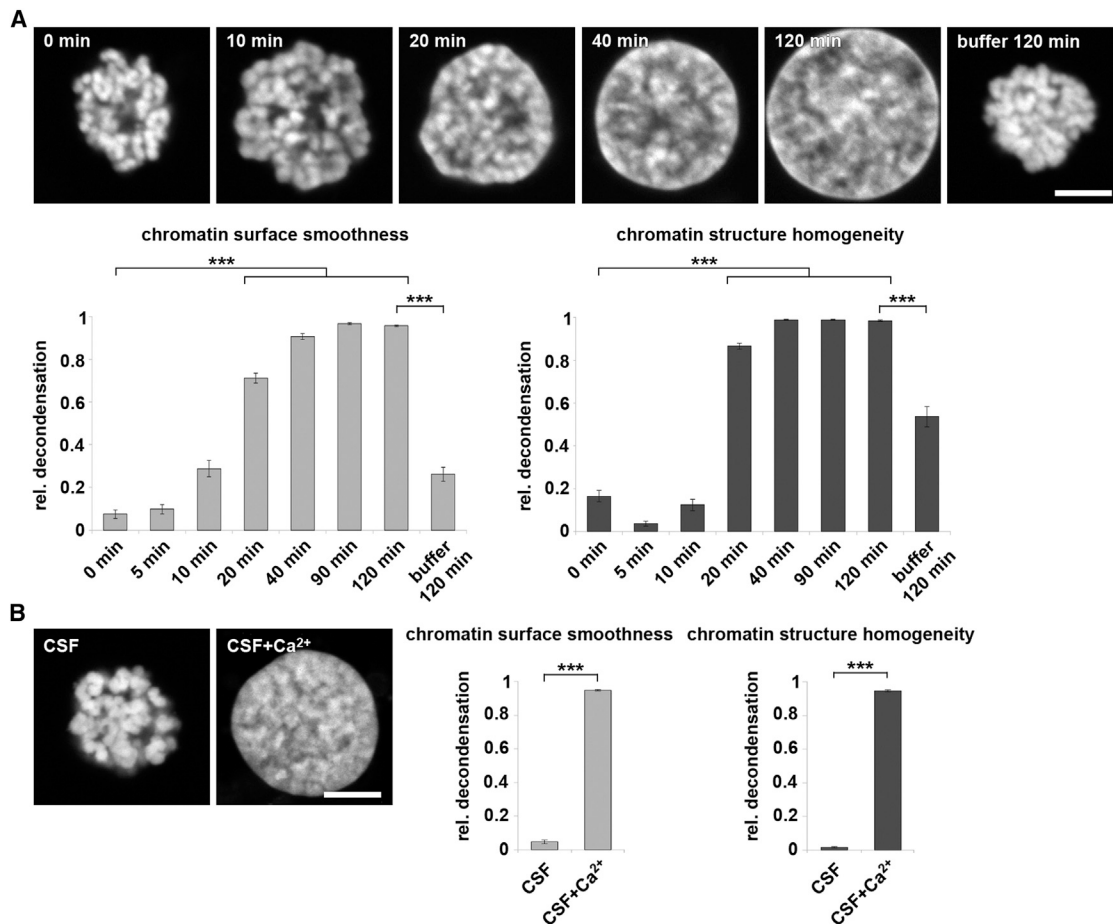


Figure 1. Reconstitution of Chromatin Decondensation in *Xenopus* Egg Extracts

(A) Time course of the in vitro decondensation reaction. Mitotic chromatin clusters from HeLa cells were incubated with postmitotic *Xenopus* egg extracts for the indicated time. Samples were fixed with 4% PFA and 0.5% glutaraldehyde, stained with DAPI, and analyzed by confocal microscopy. For quantification of the decondensation reaction, the smoothness of the boundary of the chromatin (light gray) and the homogeneity of DAPI staining (dark gray) were analyzed. The means (\pm SEM) of three independent experiments are shown, each including at least ten chromatin substrates for each time point, *** $p < 0.001$ by one-way ANOVA, Dunnett's C post hoc test. rel, relative.

(B) Mitotic chromatin clusters from HeLa cells were incubated for 120 min with CSF-arrested *Xenopus* egg extracts in the absence or presence of 1 mM CaCl₂, which induces mitotic exit. Samples were fixed, and the decondensation reaction was quantified as in (A). The means (\pm SEM) of three independent experiments are shown, each including at least ten chromatin substrates, *** $p < 0.001$ by Mann-Whitney test.

Scale bars, 5 μ m. See also Figure S1.

ATPases as crucial chromatin decondensation factors and show that their ATPase activity is essential for decondensation. Intriguingly, both metazoan RuvB-like proteins, RuvBL1 and RuvBL2 can function alone in chromatin decondensation in contrast to many other RuvBL1/RuvBL2-mediated processes, which require both components.

RESULTS

A Cell-free Assay to Monitor Mitotic Chromatin Decondensation

Chromatin decondensation at the end of mitosis is underinvestigated due to a lack of appropriate assays to monitor the process. To overcome this limitation, we have developed a cell-free assay that recapitulates chromatin decondensation in vitro. We incubated highly condensed chromosome clusters isolated from

mitotic HeLa cells with cytosol and purified membranes derived from *Xenopus* egg extracts mimicking the postmitotic state. Using DAPI staining and confocal microscopy, we observed sequential morphological changes of chromatin structure (Figure 1A) that resembled chromosome decondensation in cells exiting mitosis (see Figure S1A available online). Highly compacted distinguishable metazoan chromosomes decondensed in a time-dependent manner. After 10–20 min, the individual chromosomes merged to an apparently single corpus, which became progressively spherical and finally adopted an interphasic nuclear appearance. Chromatin decondensation was not induced by the incubation of chromatin substrates with buffer alone, indicating the presence of an essential decondensation activity in egg extracts. Mitotic (cytostatic factor [CSF]-arrested) egg extracts did not support the decondensation of the chromatin substrate (Figure 1B). However, addition of 1 mM Ca²⁺ ions to

mitotic extracts, which causes mitotic exit (Murray, 1991), did induce chromatin decondensation, indicating that postmitotic conditions are required for the process. An equal progressive decondensation was observed when, instead of HeLa cell chromatin, mitotic chromatin generated from *Xenopus* sperm DNA was used (Figure S1B) demonstrating the universality of the process.

We quantified mitotic HeLa chromatin decondensation based on the homogeneity of DAPI staining and the smoothness of the chromatin boundary (Figure 1A; see [Experimental Procedures](#) for details). These features were chosen with the following rationale: when chromatin is completely decondensed, the nuclear shape is spherical and bulk chromatin appears to be distributed rather homogeneously; when chromatin is condensed, the surface appears rough and bulk chromatin is clustered in distinct chromosomes. Both parameters increased over the time course of HeLa chromosome decondensation and reliably built up the process, indicating a highly reproducible progression of chromatin decondensation in our assay system.

In addition to chromatin decondensation, our *in vitro* system recapitulates several other mitotic exit events. Histone H3 phosphorylation at serine 10, a marker of the mitotic state of chromatin (Hendzel et al., 1997), was rapidly diminished on incubation with postmitotic *Xenopus* egg extract (Figure 2A, upper panel). Dephosphorylation of this site also occurred when mitotic chromatin was incubated with buffer alone, indicating that the relevant phosphatase activity is present on mitotic chromatin. However, mitotic chromatin incubated with buffer remained condensed (Figures 1A and 2A), consistent with previous findings that this modification is not essential for the establishment or maintenance of condensed mitotic chromatin in yeast or vertebrates (Hsu et al., 2000; MacCallum et al., 2002).

The decondensing chromatin in our assay system was enclosed by membranes, which eventually formed a smooth nuclear envelope (Figures 2B and 2C). The nuclear envelope contained nuclear pore complexes, gatekeepers of the nucleus that mediate nuclear import and export. Nuclear pore complex formation was analyzed by immunofluorescence with mAB414 (Davis and Blobel, 1986), an antibody that recognizes four different nuclear pore complex proteins (Figure 2A, middle panel). Nuclear pore complex proteins labeled by this antibody were first detected approximately 20 min after initiation of decondensation. After a 60–120 min incubation in postmitotic *Xenopus* extracts, the nuclei were capable of nuclear import and export (Figure 2D). Taken together, these results show that our cell-free system recapitulates chromatin decondensation as well as nuclear envelope and pore reformation and is, thus, an invaluable tool for studying mitotic exit events. Notably, in the absence of added membranes, chromatin decondensation similarly occurred, although nuclear envelopes and pore complexes, as expected, did not reform (data not shown). This indicates that chromatin decondensation does not require a reforming nuclear envelope and functional pore complexes, but it is possible that this is a peculiarity of the cell-free assay.

Chromatin Decondensation Requires ATP and GTP Hydrolysis

Having established the versatility of the assay, we first investigated the basic requirements of chromatin decondensation.

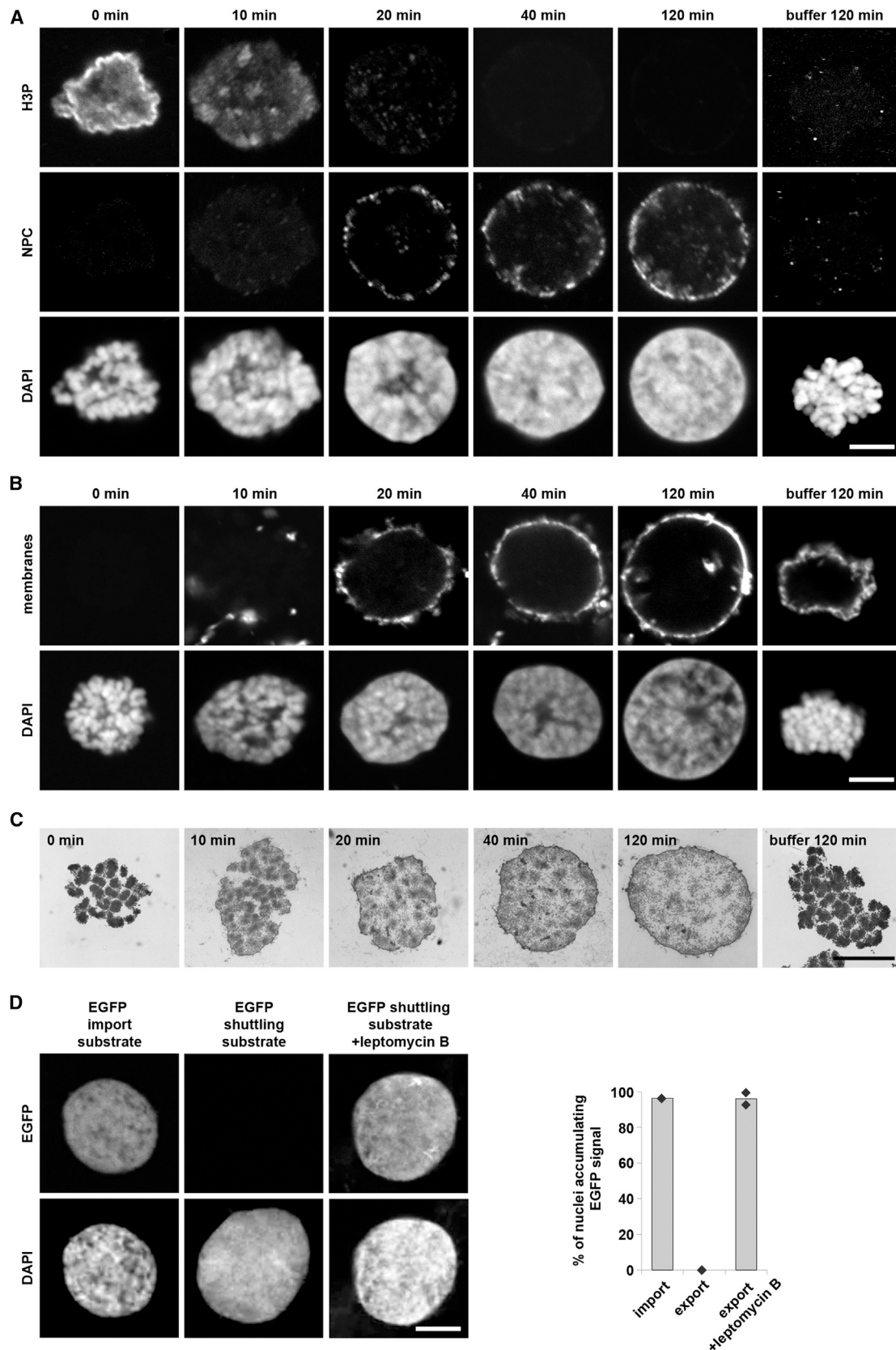
The removal of endogenous nucleoside triphosphates from the extracts by hexokinase treatment blocked chromatin decondensation (Figure S2A), indicating that some energy-consuming step is required. Nonhydrolyzable ATP or GTP analogs inhibited chromatin decondensation, suggesting that both ATP- and GTP-dependent activities are involved in chromatin decondensation (Figure 3). ATP dependence might be explained by a requirement for the ATPase p97, which removes Aurora kinase B from chromatin during decondensation (Ramadan et al., 2007). However, inhibition of Aurora kinase B by hesperadin, which bypasses the need for p97 in this process (Ramadan et al., 2007), did not restore chromatin decondensation in the presence of nonhydrolyzable ATP analogs, suggesting that at least one other ATPase is involved (data not shown).

Although DNA transcription is thought to be absent in *Xenopus* egg extracts (Newport and Kirschner, 1982), we wanted to exclude that transcriptional activity is required for chromatin decondensation in our assay system. As expected, addition of the transcription inhibitors actinomycin D or 5,6-dichloro-1- β -D-ribofuranosylbenzimidazole did not affect chromatin decondensation (Figure S2B).

RuvBL1 and RuvBL2 Can Function Individually as ATPases in Chromatin Decondensation

To identify essential chromatin decondensation factors, we fractionated the cytosol derived from postmitotic *Xenopus* egg extracts and assayed for chromatin decondensation activity. Differential ammonium sulfate precipitation yielded two fractions that individually had severely reduced decondensation activity but were highly active when combined (Figure 4A; Figure S3A). We further purified the first of these ammonium sulfate fractions by ion exchange and size exclusion chromatography (see [Experimental Procedures](#) for detailed information) and assayed the activities of the obtained fractions in combination with the second ammonium sulfate fraction. By mass spectrometry analysis of the gel filtration fractions with highest decondensation activity (G13–G15), we identified several candidate chromatin decondensation factors, including the ATPase RuvBL2. RuvBL2 is known to form a double hexameric ring complex with a second ATPase, RuvBL1 (Jha and Dutta, 2009; Puri et al., 2007). Indeed, western blot analysis confirmed the presence of RuvBL1 and RuvBL2 in the active fractions throughout the purification procedure and enrichment in the most active gel filtration fractions (Figure 4A), which makes these proteins possible candidates for the decondensation activity. RuvBL1/RuvBL2 (also known as RVB1/RVB2, pontin/reptin, and TIP49/TIP48) are two highly conserved members of the AAA+ superfamily. They associate with diverse chromatin remodeling complexes, which are implicated in a variety of nuclear processes, including transcriptional regulation, DNA damage response, and small nuclear ribonucleoprotein particle (snRNP) assembly (for a review, see Jha and Dutta, 2009; Nano and Houry, 2013; Tosi et al., 2013).

To assess the relevance of RuvBL1 and RuvBL2 for chromatin decondensation, we performed antibody inhibition experiments in the decondensation assay. The addition of purified anti-RuvBL1 or anti-RuvBL2 immunoglobulin G (IgG) to the reactions significantly impaired chromatin decondensation compared to the addition of control IgG (Figures 4B and S3B).



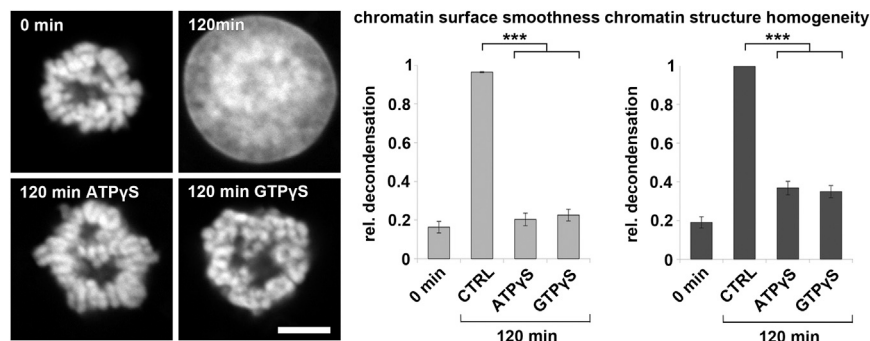


Figure 3. Chromatin Decondensation Requires ATP and GTP Hydrolysis

HeLa mitotic chromatin was decondensed in the presence of 10 mM ATP γ S, 10 mM GTP γ S, or buffer control (CTRL). Samples were fixed with 4% PFA and 0.5% glutaraldehyde at indicated time points, analyzed, and quantified. The means (\pm SEM) of three independent experiments are shown, each including at least ten chromatin substrates for each time point, *** $p < 0.001$ by one-way ANOVA, Dunnett's C post hoc test. rel, relative. Scale bar, 5 μ m. See also Figure S2.

Immunodepletion using antibodies against either RuvBL1 or RuvBL2, respectively, removed both proteins efficiently from the extracts (Figure 4C), indicating that, in *Xenopus* egg extracts, RuvBL1 and RuvBL2 occur mostly together in heteromeric complexes. Both immunodepletion procedures rendered egg extracts incompetent for chromatin decondensation in contrast to control depletions (Figure 4D). The addition of purified recombinant RuvBL1-RuvBL2 complexes to a final concentration of 0.04 μ g/ μ l, which matches the endogenous concentration (Figure S3C), was sufficient to rescue the depletion phenotype (Figure 4D), indicating on-target specificity of the immunodepletion. These experiments demonstrate that RuvBL1/2 indeed function in chromatin decondensation and are crucial for this process.

RuvBL1 and RuvBL2 Can Function Individually as ATPases in Chromatin Decondensation

In many cellular processes, RuvBL1 and RuvBL2 operate together by forming heteromeric complexes (Jha and Dutta, 2009; Nano and Houry, 2013; Nguyen et al., 2013; Tosi et al., 2013; Venteicher et al., 2008); however, in some instances, these proteins act antagonistically (Bauer et al., 2000; Rottbauer et al., 2002). Surprisingly, the addition of either purified homohexameric RuvBL1 or RuvBL2 complexes to depleted extracts restored decondensation activity as efficiently as the addition of the heteromeric RuvBL1-RuvBL2 complex (Figure 5A). This indicates that both proteins can function redundantly and independently of each other in this process.

The addition of recombinant ATPase-deficient RuvBL1/2 mutants, either individually or in a heteromeric complex (RuvBL1 D302N/RuvBL2 D298N) (Matias et al., 2006; Mézard et al., 1997) (Figure S4C), did not rescue the depletion phenotype, indi-

cating that the ATPase function of either proteins is required for its role in chromatin decondensation (Figure 5B). The addition of excess RuvBL1 D302N, RuvBL2 D298N, or the RuvBL1 D302N/RuvBL2 D298N complex to untreated extracts inhibited chromatin decondensation, while the wild-type proteins and complexes had no effect (Figures 5C and S4A). RuvB-like ATPases perform their different cellular functions in conjunction with a variety of cofactors (for a review, see Jha and Dutta, 2009; Nano and Houry, 2013), and this is most likely also the case for chromatin decondensation (see Discussion). Thus, the dominant-negative effect of ATPase-deficient RuvBL1/2 mutants is likely to be caused by a sequestration of these cofactors. Together, these experiments using ATPase-deficient RuvBL1/2 versions demonstrate that chromatin decondensation depends on ATPase-proficient RuvB-like proteins.

Although RuvB-like proteins are required for chromatin decondensation, they are not sufficient. When purified recombinant RuvBL1, RuvBL2, or the heteromeric RuvBL1/2 complex were added to HeLa mitotic chromatin in buffer in the presence of ATP, no chromatin decondensation was detected (Figure S4B), indicating that other factors are also crucially required (see Discussion).

RuvBL1 and RuvBL2 Localize on the Decondensing Chromatin

We next analyzed the localization of RuvBL1 and RuvBL2 during mitotic exit. Consistent with their role in chromatin decondensation, RuvBL1 and RuvBL2 localize and enrich on postmitotic decondensing chromatin, both in the *in vitro* assay (Figure 6A) and in HeLa cells (Figure S5A). Both RuvB-like proteins are excluded from chromatin during earlier stages of mitosis, including

Figure 2. Decondensing Chromatin Assembles into Functional Nuclei

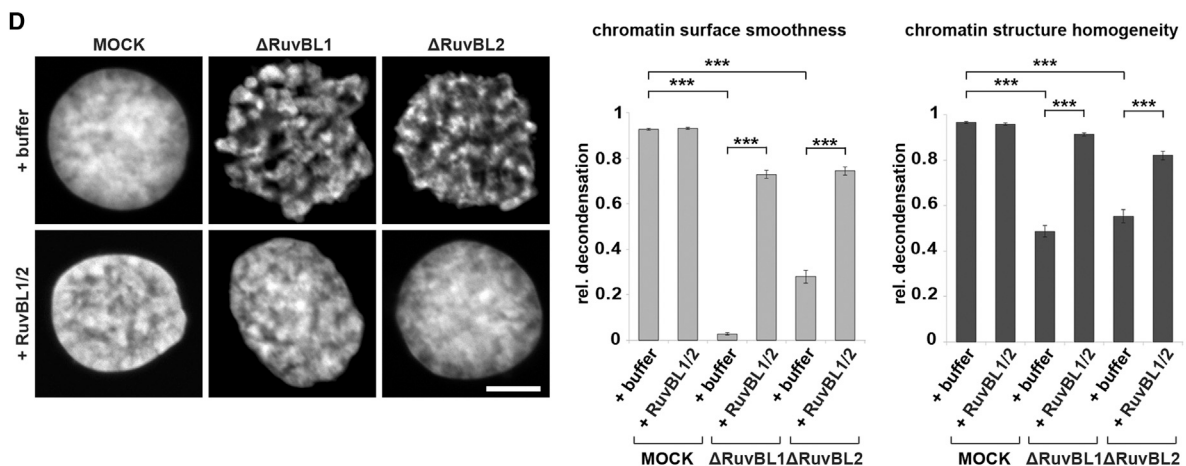
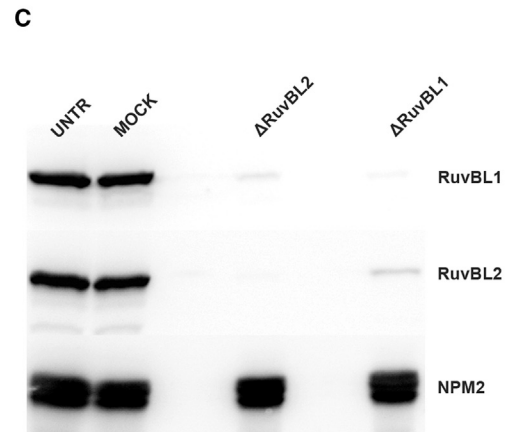
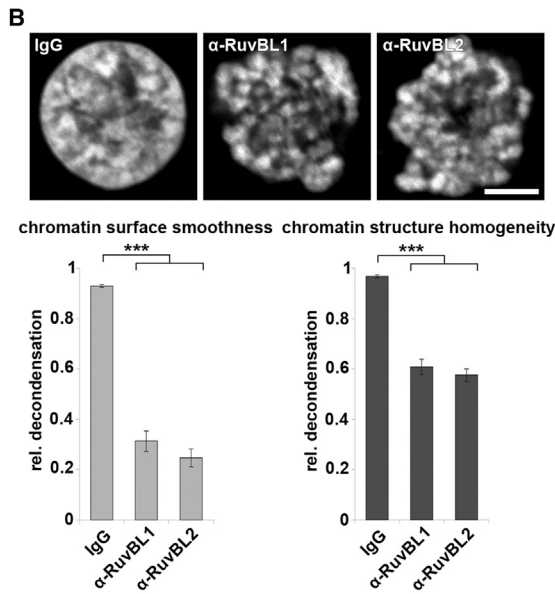
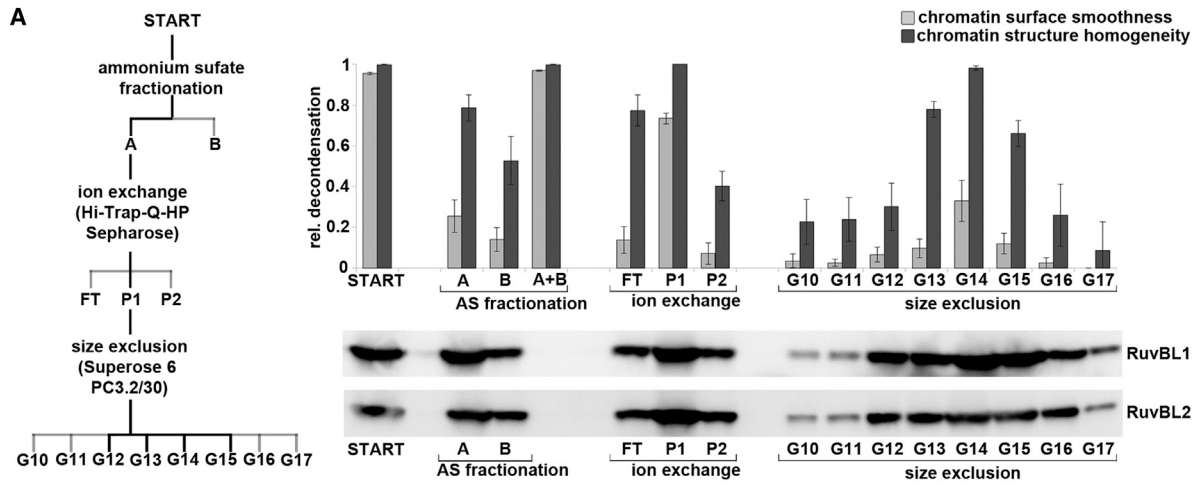
(A) Mitotic chromatin clusters from HeLa cells were incubated with *Xenopus* egg extracts for the indicated time and fixed with 4% PFA. Immunofluorescence shows histone H3 serine 10 phosphorylation (H3P, upper panel), nuclear pore complexes (NPC, middle panel), and chromatin (DAPI).

(B) For visualization of nuclear envelope reformation, HeLa mitotic chromatin substrates and DiIc18 (1,1'-dioctadecyl-3,3,3',3'-tetramethylindocarbocyanine perchlorate)-labeled membranes (upper panel) were added to the egg extracts or the buffer control. Samples were fixed at indicated time points with 4% PFA and 0.5% glutaraldehyde, stained with DAPI (lower panel), and analyzed by confocal microscopy.

(C) Chromatin decondensation using HeLa mitotic chromatin was analyzed by transmission electron microscopy. Samples were fixed at indicated time points with 4% PFA and 2.5% glutaraldehyde, postfixed in 1% OsO₄, and stained with 1% uranyl acetate. After embedding in Epon, ultrathin sections (50–70 nm) were stained with uranyl acetate and lead citrate and viewed with a Philips CM10 microscope.

(D) HeLa mitotic chromatin was decondensed for 120 min. An enhanced green fluorescent protein (EGFP)-fused import substrate (left column) or a shuttling substrate containing a nuclear localization signal and a nuclear export signal (middle and right column) was added. Nuclear export was inhibited by the addition of 300 nM leptomycin B. Samples were stained with DAPI and analyzed by confocal microscopy. The weighted average percentage of two independent experiments, each including at least 100 randomly chosen chromatin substrates, is shown. Diamonds indicate data points of the individual experiments.

Scale bars, 5 μ m.



(legend on next page)

metaphase in agreement with previous reports (Gartner et al., 2003; Sigala et al., 2005).

When depleting the endogenous RuvBL1/2 complex, both recombinant RuvBL1 and RuvBL2 could be detected on the chromatin template (Figure 6A), indicating that both proteins can independently localize to chromatin. This observation is consistent with the finding that either homomeric complex can substitute the heteromeric complex to support chromatin decondensation (Figure 5A). The ATPase-deficient mutants similarly localized to chromatin, indicating that the ATPase function is not required for chromatin localization.

Having identified RuvBL1/2 as chromatin decondensation factors, we analyzed the fate of known chromatin condensation factors on the chromatin on depletion of RuvB-like proteins. Topoisomerase II, KIF4A, and the condensin II complex were detected on the chromatin at all stages of the decondensation reaction (Figures 6B and S5B), as expected (Gerlich et al., 2006; Mazumdar et al., 2004; Tavormina et al., 2002). A similar pattern was observed for Repo-Man, also known as CDCA2, which recruits the protein phosphatase PP1 to chromatin during mitotic exit and was shown to coordinate chromatin decondensation and nuclear envelope reformation (Vagnarelli et al., 2011); and for Mel28 (also referred to as ELYS), a chromatin-binding protein that acts as a seeding point for nuclear pore complex formation (Franz et al., 2007). The condensin I complex is lost from the chromatin in the course of decondensation (Gerlich et al., 2006). In all instances, depletion of RuvBL1/2 did not affect the spatiotemporal localization of these proteins on decondensing chromatin, indicating that RuvB-like ATPases act independently of these factors during decondensation.

RuvB-like ATPases Are Not Required for Nuclear Envelope and Pore Complex Formation

Our data show that the RuvB-like ATPases function as key decondensation factors of mitotic chromatin. In organisms undergoing open mitosis, the nuclear envelope and nuclear pore complexes break down at the beginning of mitosis and reform on the decondensing chromatin in telophase (for a review, see Kutay and Hetzer, 2008; Schooley et al., 2012). On depletion of RuvBL1/2 in the decondensation assay, we did not observe formation of a closed nuclear envelope and nuclear pore complex reassembly (data not shown). This could indicate that RuvB-like ATPases are also involved in these processes. Alternatively, chromatin decondensation might be a prerequisite for nuclear envelope and pore complex assembly. To distinguish

these two possibilities, we sought to bypass the need of RuvBL1/2 for chromatin decondensation by using an already decompacted chromatin template. For this, *Xenopus* sperm heads were incubated in postmitotic egg extracts. In this assay, which recapitulates the processes naturally occurring after entry of sperm DNA into an egg, pronuclei with intact nuclear envelopes and pore complexes are formed, and this system has been widely used to study these assembly processes (Gant and Wilson, 1997). Notably, sperm DNA is, in this experimental setup, decompacted by the NPM2-mediated exchange of protamines to histones H2A and H2B (Philpott and Leno, 1992). When sperm heads were incubated with control or RuvBL1/2-depleted postmitotic extracts, pronuclei with closed nuclear envelopes and intact nuclear pore complexes were formed (Figure 7). These experiments demonstrate that, as expected, RuvB-like proteins are not required for sperm DNA decompaction. Notably, they are also not crucial for nuclear envelope and pore complex formation. In this experimental system, the pronuclei undergo nuclear expansion after initial NPM2-dependent sperm DNA decompaction. This process, which is also referred to as nuclear swelling/expansion or secondary decondensation, requires nuclear import and, thus, a functional nuclear envelope including pore complexes (Philpott et al., 1991; Wright, 1999). The DAPI staining of the pronuclei assembled in the absence of RuvBL1/2 indicates that this nuclear swelling does not require RuvB-like ATPases. These data also show that distinct mitotic exit events such as chromatin decondensation and nuclear envelope/pore complex reformation can be uncoupled in vitro.

Mitotic chromatin decondensation does not require NPM2, which, in turn, is needed for sperm DNA decompaction (Figure S6). This supports the view that sperm DNA and mitotic chromatin decondensation are mechanistically fundamentally different.

DISCUSSION

Here, we show that chromatin decondensation can be faithfully reconstituted in a cell-free assay. Using this system, we demonstrate that the process requires ATP and GTP hydrolysis. It is not merely an inactivation of known chromatin condensation factors but an active process involving specific molecular machinery. We identify a defined requirement for the RuvB-like ATPases in chromatin decondensation, but not for nuclear envelope and pore complex formation. Our assay system is, therefore, a valuable tool for the dissection of the cellular processes

Figure 4. Chromatin Decondensation Requires RuvB-like ATPases

(A) *Xenopus* egg extracts were fractionated by differential ammonium sulfate precipitation, ion exchange, and size exclusion chromatography (see fractionation scheme on the left with the fractions showing decondensation activity in black) and were tested for the state of chromatin decondensation on HeLa mitotic chromatin after 120 min. For ion exchange and size exclusion fractions, reactions were performed in the presence of fraction B of the ammonium sulfate precipitation. The lower panels show the distribution of RuvBL1 and RuvBL2 in fractions analyzed by western blotting. Representative quantification and western blot analysis of one fractionation experiment is shown. FT, flowthrough. rel, relative.

(B) Chromatin decondensation on HeLa mitotic chromatin was performed for 120 min in the presence of 4 mg/ml affinity-purified IgG against RuvBL1, RuvBL2, or control IgGs.

(C) Western blot of untreated (UNTR), mock, and RuvBL1/2-depleted extracts, the latter two generated by two passages over control IgG- or anti-RuvBL1 or anti-RuvBL2 IgG-bound beads, respectively. NPM2 serves as a control protein unaffected by this treatment.

(D) Mock or RuvBL1/2-depleted extracts supplemented with buffer or purified recombinant RuvBL1-RuvBL2 complex (0.04 $\mu\text{g}/\mu\text{l}$ to match the endogenous concentration) were tested for chromatin decondensation on HeLa mitotic chromatin (120 min time point).

In (B) and (D), the means (\pm SEM) of three independent experiments are shown, each including at least 20 chromatin substrates. *** $p < 0.001$ by one-way ANOVA, Dunnett's C post hoc test. Scale bars, 5 μm . See also Figure S3.

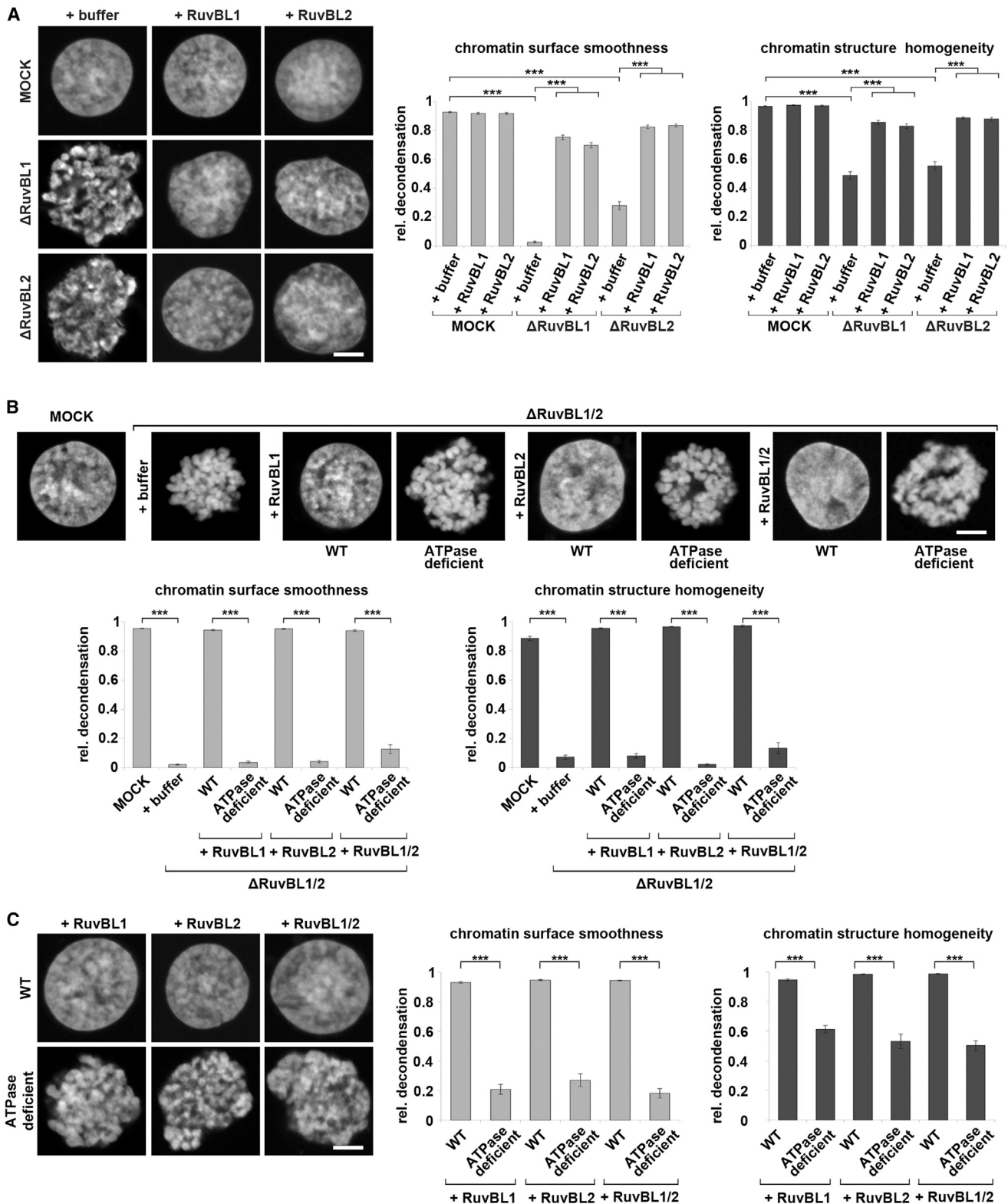


Figure 5. RuvBL1 or RuvBL2 Alone Is Sufficient to Support Chromatin Decondensation and Require ATPase Activity

(A) RuvBL1/2-depleted extracts (generated by two passages over anti-RuvBL1 or anti-RuvBL2 IgG-bound beads, respectively) were supplemented with purified recombinant RuvBL1 or RuvBL2 (0.02 μ g/ μ l to match the endogenous concentration) and tested for chromatin decondensation on HeLa mitotic chromatin. rel. relative.

(legend continued on next page)

that lead to the assembly of functional interphase chromatin after mitosis.

Cell-free extracts derived from frog eggs, especially from *Xenopus laevis*, have been widely used to study cell cycle regulation as well as many mitotic and nuclear processes since their development and first use 30 years ago (Lohka and Masui, 1983). These extracts recapitulate complex cellular reactions such as chromatin condensation, spindle assembly, and nuclear envelope breakdown (Galy et al., 2008; Maresca and Heald, 2006). Nuclear envelope and pore complex formation has been intensively studied in pronucleus formation using sperm DNA as a chromatin template (for a review, see Gant and Wilson, 1997). Here, we use mitotic chromatin to study chromatin decondensation and nuclear reformation during mitotic exit. We show that the nuclei formed on the decondensing chromatin contain a closed nuclear envelope with two membranes and nuclear pore complexes (Figure 2). These nuclei are competent for nuclear import and export and DNA replication (Figure 2D; A.M. and W.A., unpublished data), showing that they represent a functional interphasic status.

So far, chromatin decondensation has been mainly investigated in the context of male pronucleus formation around sperm DNA. However, it is unlikely that this involves the same machinery as chromatin decondensation at the end of mitosis. Indeed, our data show that sperm DNA decompacts in the absence of the RuvB-like ATPases (Figure 7), which are required for mitotic chromatin decondensation. In contrast, sperm DNA decondensation depends on the histone chaperone NPM2 (Philpott and Leno, 1992; Philpott et al., 1991), which conversely is not necessary for mitotic chromatin decondensation (Figure S6), consistent with the fact that NPM2 is absent in somatic cells (Burns et al., 2003).

In contrast to sperm DNA decompaction, which is an energy-independent process (Philpott et al., 1991), mitotic chromatin decondensation requires cellular energy (Figure S2). The inhibition of mitotic chromatin decondensation observed in the presence of nonhydrolyzable ATP (Figure 3) suggests that ATPases are involved in the process. Indeed, we show that RuvB-like ATPases and, specifically, their ATPase functions are compulsory in addition to p97, the only protein previously implicated in the postmitotic decondensation of chromatin (Ramadan et al., 2007).

We envision chromatin decondensation as a multistep procedure involving several activities. Indeed, each fraction of our ammonium sulfate fractionation is largely inactive on its own, and only when they are recombined is decondensation activity restored (Figures 4A and S3A). Consistent with the notion of multiple necessary decondensation factors, RuvB-like ATPases are not sufficient to promote chromatin decondensation if added alone to the mitotic chromatin template (Figure S4B). Most likely,

yet-unidentified RuvBL1/2 interacting factors are crucially required for the RuvBL1/2-mediated step in chromatin decondensation as in other processes mediated by these ATPases (for a review, see Jha and Dutta, 2009; Nano and Houry, 2013). In addition, chromatin decondensation most likely involves other RuvBL1/2-independent steps. The inhibition by nonhydrolyzable GTP (Figure 3) suggests that at least one GTPase is involved. The nature of the GTPases is currently unknown but an interesting avenue for future research.

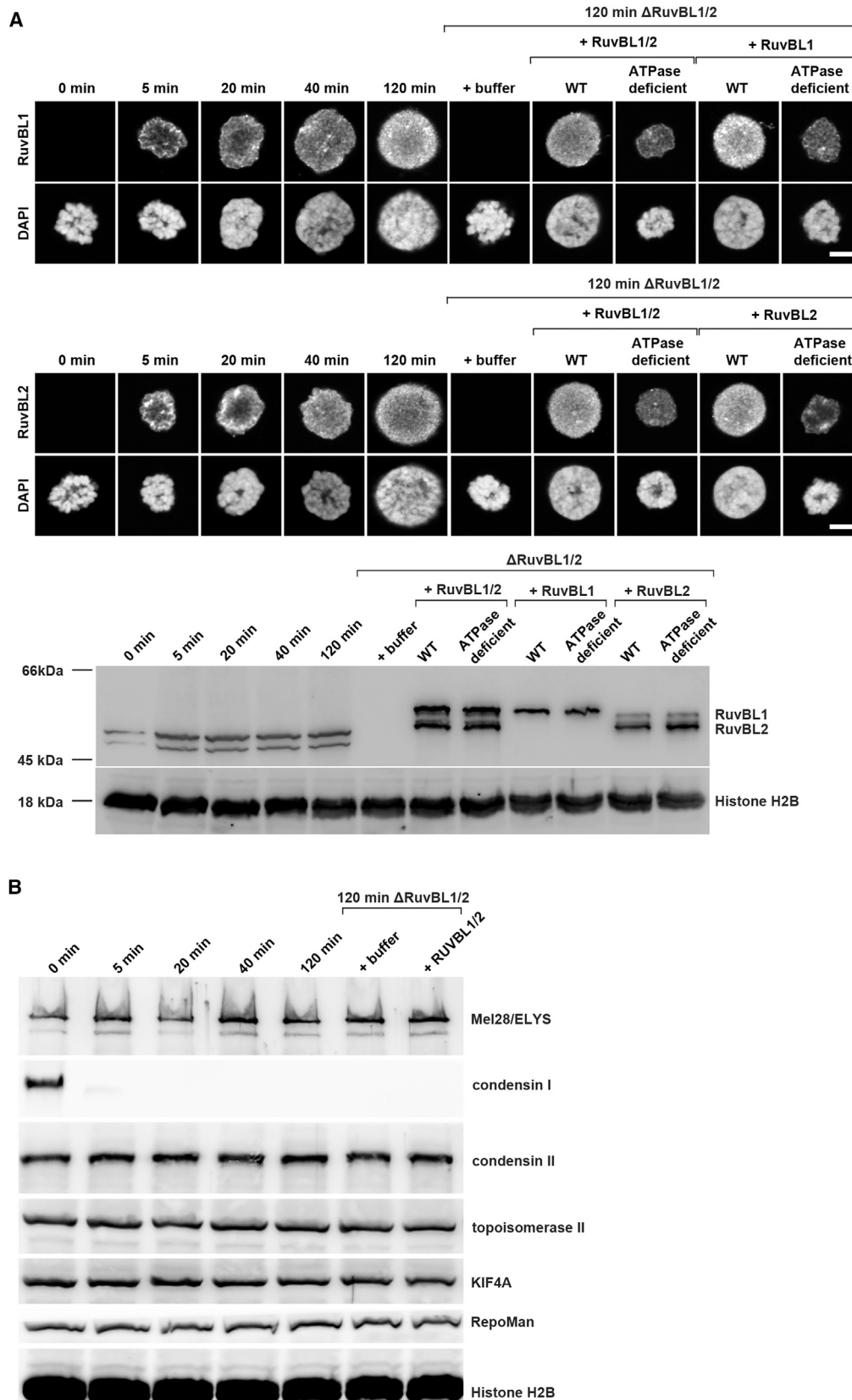
RuvB-like proteins are highly conserved and essential eukaryotic AAA+ ATPases involved in a wide range of cellular reactions as components of large protein complexes (for a review, see Jha and Dutta, 2009; Nano and Houry, 2013). These include many chromatin-related, but also other, processes such as chromatin remodeling, transcriptional regulation, and DNA damage response, as well as snoRNP, telomere, and spindle assembly (Ducat et al., 2008; Ikura et al., 2000; Jónsson et al., 2001; Krogan et al., 2003; Lim et al., 2000; Newman et al., 2000; Shen et al., 2000; Venteicher et al., 2008; Wood et al., 2000; Zhao et al., 2005). RuvB-like ATPases show similarity to prokaryotic RuvB proteins but, because of an insertion into the ATPase domain, lack the helicase activity found in the bacterial proteins (Ikura et al., 2000; Matias et al., 2006). Currently, the precise function of RuvB-like ATPases in the different chromatin remodeling and other complexes is unclear (Jha and Dutta, 2009; Rosenbaum et al., 2013). Here, we add chromatin decondensation, a yet-ill-defined but nevertheless essential process during mitosis, to the list of RuvBL1/2-dependent processes. We show that the ATPase activity of RuvBL1/2 is mandatory for chromatin decondensation (Figure 5), in contrast to other RuvBL1/2-dependent processes such as transcriptional regulation (Jónsson et al., 2001). Because RuvB-like ATPases are part of several chromatin remodeling complexes (for a review, see Jha and Dutta, 2009; Rosenbaum et al., 2013), it is tempting to speculate that chromatin decondensation at the end of mitosis functionally requires histone rearrangements, a hypothesis that needs to be addressed in the future.

Many RuvBL1/2-dependent processes rely on a heterododecameric complex formed by both proteins (Nguyen et al., 2013; Tosi et al., 2013; Venteicher et al., 2008; Zhao et al., 2005), and our results confirm that, also in *Xenopus* eggs, these proteins are found to a large extent in heteromeric complexes. In other processes, such as Polycomb or NF- κ B-mediated gene repression and β -catenin signaling, RuvBL1 and RuvBL2 act antagonistically (Baek et al., 2002; Bauer et al., 2000; Diop et al., 2008; Kim et al., 2005; Rottbauer et al., 2002). Our readdition experiments suggest that RuvBL1 or RuvBL2 alone can fulfill the RuvB-like dependent functions in chromatin decondensation and thus, in this context, are redundant (Figure 5). Whether this feature is also seen in other RuvB-like-dependent processes

(B) Chromatin decondensation was analyzed in RuvBL1/2-depleted extracts (generated by consecutive passage over anti-RuvBL1 and anti-RuvBL2 IgG-bound beads) supplemented with ATPase-deficient mutant versions of the RuvBL1, RuvBL2, or the RuvBL1-RuvBL2 complex (RuvBL1 D302N and RuvBL2 D298N) matching the endogenous concentration. WT, wild-type.

(C) Chromatin decondensation in the presence of 40-fold excess compared to endogenous concentrations of recombinant wild-type RuvBL1, RuvBL2, or the RuvBL1-RuvBL2 complex or ATPase-deficient mutants of the respective proteins.

Samples were analyzed after 120 min. The means (\pm SEM) of three independent experiments are shown, each including at least 20 chromatin substrates. *** $p < 0.001$ by two-way ANOVA, Sidlak post hoc test for (A) and (B) and by one-way ANOVA, Dunnett's C post hoc test for (C). WT, wild-type. Scale bars, 5 μ m. See also Figure S4.



(legend on next page)

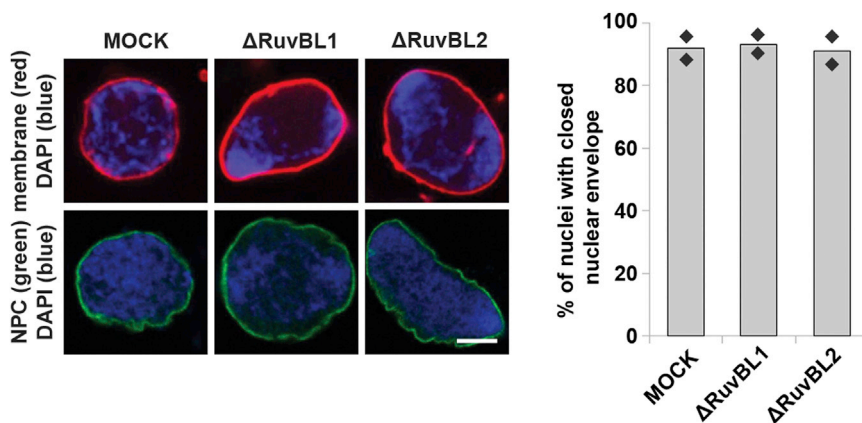


Figure 7. RuvB-like ATPases Are Specifically Required for Chromatin Decondensation during Mitotic Exit

Pronuclei were assembled on *Xenopus* sperm chromatin in mock-treated or RuvBL1/2-depleted extracts (using anti-RuvBL1 or anti-RuvBL2 antibodies). After 120 min, samples were fixed with 4% PFA and 0.5% glutaraldehyde and analyzed for membrane staining (DiIC18, upper panel) or for nuclear pore complexes (NPC, lower panel) by immunofluorescence with the antibody mAB414. Chromatin was stained with DAPI. Right panel shows the quantitation of chromatin substrates with closed nuclear envelopes as weighted average percentage of two independent experiments, each including at least 100 chromatin substrates. Diamonds indicate data points of the individual experiments. Scale bar, 5 μ m. See also Figure S6.

remains to be investigated. It is also possible that chromatin decondensation constitutes a unique and probably archetypal process where RuvBL1 and RuvBL2 can substitute for each other.

Interestingly, RuvB-like ATPases have been implicated in various human cancers and have been speculated to be a promising therapeutic target (for a review, see Huber et al., 2008; Nano and Houry, 2013). Often, the precise function of RuvBL1 and RuvBL2 in pathogenesis is not defined. Whether their role in chromatin decondensation is relevant for this will be an exciting and promising avenue for future research.

EXPERIMENTAL PROCEDURES

Cell-free Decondensation of Mitotic Chromatin

Cytosol was prepared by crushing activated *Xenopus laevis* eggs by a low-speed centrifugation (20 min at 21,000 \times g) to obtain egg extracts, followed by high-speed centrifugations (twice, 12 min at 360,000 \times g). Activation of the eggs—which are naturally arrested in the second meiotic metaphase—by treatment with a Ca^{2+} ionophore induces meiotic exit. Thus, extracts prepared from these eggs represent a postmitotic/interphasic state and are competent to induce late mitotic/interphasic events such as nuclear reformation or DNA replication. The protocol including the preparation of flotation purified membranes is described in detail in Eisenhardt et al. (2014). Mitotic chromatin was isolated as in Gasser and Laemmli (1987). In vitro chromatin decondensation was induced by incubating approximately 1,000 mitotic chromatin clusters in 18 μ l of cytosol from *Xenopus* egg extracts and 2 μ l of flotation purified membranes supplemented with 3 μ M 6-dimethylaminopurine, 10 mM ATP, 10 mM creatine phosphate, 0.2 mg/ml creatine kinase, and 0.4 mg/ml glycogen at 20°C. As a negative control, sucrose buffer (250 mM sucrose, 50 mM KCl, 2.5 mM MgCl_2 , and 10 mM HEPES [pH 7.5]) was used instead of cytosol. At the end of the incubation time, samples were fixed in 0.5 ml 4% paraformaldehyde (PFA) and 0.5% glutaraldehyde in 80 mM PIPES [pH 6.8], 1 mM MgCl_2 , 150 mM sucrose, and 10 μ g/ml DAPI for 30 min on ice. Chromatin was reisolated by centrifugation through a 30% sucrose cushion in PBS

(15 min at 2,500 \times g) on poly-L-lysine-coated coverslips and mounted in Vectashield (Vector Laboratories). Samples were analyzed using a confocal microscope (FV1000; Olympus; equipped with a photomultiplier [model R7862; Hamamatsu]) with 405, 488, and 559 nm laser lines and a 60 \times numerical aperture 1.35 oil immersion objective lens using the FluoView software (Olympus) at room temperature. Immunofluorescence and transmission electron microscopy was performed as in Theerthagiri et al. (2010).

For western blot analysis of reisolated chromatin (modified from Hayashihara et al. (2008)), the decondensation reaction was increased by a factor of ten. At the end of the reaction, samples were immediately layered on top of 1 ml wash buffer—10 mM HEPES [pH 7.5], 50 mM KCl, 14% (v/v) Optiprep (Sigma), 1 mM dithiothreitol, 2.5 mM MgCl_2 , 0.2 mM spermine, 0.5 mM spermidine, 1 mM ATP, 10 μ g/ml 4-(2-aminoethyl)-benzenesulfonylfluoride, 0.2 μ g/ml leupeptin, 0.1 μ g/ml pepstatin, 0.2 μ g/ml aprotinin—and the chromatin was pelleted (30 min at 10,000 \times g in a swing-out rotor) and analyzed.

In depletion experiments, cytosol was incubated twice with antibody-coated beads at a 1.2:1 beads-to-cytosol ratio for 20 min. CSF-arrested extracts were prepared as in Murray (1991) and released into interphase by the addition of 1 mM CaCl_2 .

Quantification of In Vitro Chromatin Decondensation

Chromatin boundaries were defined by an intensity threshold, and the total chromatin area was calculated. For the smoothness analysis, the perimeter of the boundary was used to estimate the surface roughness as a ratio of the perimeter squared over area. To analyze chromatin homogeneity, chromosomes were defined using an edge-finding algorithm (the largest eigenvalue of the structure tensor; ImageJ plugin FeatureJ, <http://www.imagescience.org/meijering/>), and the sum of the chromosomes' areas was computed and normalized to the total area within the boundary. To minimize the statistical effects of very irregularly shaped (highly condensed) chromatin, a maximum of 20% (in roughness/relative area) above the fully decondensed state was adopted for both analyses. Surface smoothness and internal homogeneity were defined as the differences from the maximal roughness and maximal relative area, respectively. The fully condensed state was set to zero, and the maximal decondensed state to one and all other values were normalized accordingly.

Figure 6. RuvBL1 and RuvBL2 Localize to the Decondensing Chromatin

(A) HeLa mitotic chromatin was incubated with extracts for the indicated time. RuvBL1/2-depleted extracts (generated by consecutive passage over anti-RuvBL1 and anti-RuvBL2 IgG-bound beads) were supplemented with buffer, recombinant RuvBL1-RuvBL2 complex, RuvBL1, or RuvBL2 or ATPase-deficient versions of the proteins (matching the endogenous concentrations) and used in the decondensation reaction for 120 min. Samples were fixed with 4% PFA and processed for immunofluorescence, or chromatin was reisolated and analyzed by western blot (histone H2B shows equal chromatin loading). Scale bars, 5 μ m.

(B) HeLa mitotic chromatin incubated as in (A) was reisolated and probed for the presence of Mel28/ELYS, the condensin I and II complex (CAP-G or CAP-D3 antibodies, respectively), topoisomerase II α , the chromokinesin KIF4A, and Repo-MAN. Please note that during the reisolation procedure, rapid rebinding of *Xenopus* proteins to chromatin and/or their exchange with the HeLa proteins occurs so that they can be detected already at t = 0.

See also Figure S5.

Fractionation of *Xenopus* Egg Extracts

Xenopus egg cytosol was subjected to sequential fractionation to allow the identification of factors involved in chromatin decondensation. The fractions obtained were then tested in the *in vitro* assay described earlier for decondensation activity. First, cytosolic egg extract was fractionated by ammonium sulfate precipitation. Proteins that precipitated in 20% ammonium sulfate (fraction A) and those that did not precipitate (fraction B) were separated. Fraction B was then precipitated by increasing the ammonium sulfate concentration to 50%. Both fractions were resuspended in sucrose buffer. Fraction A was then applied to a Hi-Trap-Q-HP-Sepharose column (GE Healthcare) and eluted using a step gradient of 500 mM KCl. The decondensation-active fraction (P1) was further separated on a Superose 6 PC3.2/30 column (GE Healthcare) in sucrose buffer. Fractions were eluted at a 1.5–2.0 ml retention volume. For the decondensation assay, fractions A and B obtained from ammonium sulfate precipitation—as well as the flowthrough, P1, and P2 from the ion exchange—were dialyzed against sucrose buffer. The decondensation assay was always performed in the presence of fraction B in a 1:4 volume ratio. Active fractions eluted from the size exclusion column (G13–G15) were analyzed by mass spectrometry (described in the [Supplemental Information](#)).

Pronuclear Assembly Assay

For pronuclear assembly, cytosol from *Xenopus* egg was incubated with 1,000 sperm heads prepared from *Xenopus* testis (Gurdon, 1976) for 10 min at 20°C to allow for sperm chromatin decondensation. To start the reaction, floated DiIc18 (1,1'-dioctadecyl-3,3',3'-tetramethylindocarbocyanine perchlorate)-labeled membranes (Antonin et al., 2005), 10 mM ATP, 10 mM creatine phosphate, 0.2 mg/ml creatine kinase, and 0.4 mg/ml glycogen were added. For depletions, cytosol was incubated twice with antibody-coated beads at a 1.2:1 bead-to-cytosol ratio for 20 min.

Miscellaneous

Statistical analysis was performed with the IBM-SPSS Statistics 21 software. Live cell imaging, nuclear import and ATPase assays, production of recombinant proteins, and a description of the antibodies used can be found in the [Supplemental Experimental Procedures](#).

SUPPLEMENTAL INFORMATION

Supplemental Information includes Supplemental Experimental Procedures and six figures and can be found with this article online at <http://dx.doi.org/10.1016/j.devcel.2014.09.001>.

AUTHOR CONTRIBUTIONS

A.M. and W.A. designed the experiments. A.M., A.K.S., A.S., and W.A. performed decondensation experiments; A.M. and D.M.-A. performed live-cell imaging; F.Z. designed and wrote the image analysis software for the decondensation measurements; R.S. purified recombinant RuvBL1/2 complexes; H.S. performed electron microscopy; J.M. performed mass spectrometry; and W.A. wrote the manuscript.

ACKNOWLEDGMENTS

This work was supported by the German Research Foundation and the European Research Council (AN377/3-1 and 309528 CHROMDECON to W.A.) and by a PhD Fellowship of the Boehringer Ingelheim Fonds to A.K.S. We are grateful to A. Konopka (Nencki Institute of Experimental Biology) for help with the statistical analysis; K. Feldmeier for advice on the ATPase activity measurements (Max Planck Institute [MPI] for Developmental Biology); C. Liebig (Light Microscopy Facility of the MPI for Developmental Biology) for suggestions on image acquisition and analysis; and I. Poser in the lab of A. Hyman (MPI of Molecular Cell Biology and Genetics) for providing stable HeLa BAC cell lines (funded by the MitoSys project, European Community's Seventh Framework Programme [FP7/2007-2013], grant agreement 241548). A.M. is especially thankful for continuous support by G. Wilczyński (Nencki Institute of Experimental Biology).

Received: May 5, 2014

Revised: July 22, 2014

Accepted: September 3, 2014

Published: October 23, 2014

REFERENCES

- Antonin, W., Franz, C., Haselmann, U., Antony, C., and Mattaj, I.W. (2005). The integral membrane nucleoporin pom121 functionally links nuclear pore complex assembly and nuclear envelope formation. *Mol. Cell* *17*, 83–92.
- Baek, S.H., Ohgi, K.A., Rose, D.W., Koo, E.H., Glass, C.K., and Rosenfeld, M.G. (2002). Exchange of N-CoR corepressor and Tip60 coactivator complexes links gene expression by NF- κ B and beta-amyloid precursor protein. *Cell* *110*, 55–67.
- Bauer, A., Chauvet, S., Huber, O., Usseglio, F., Rothbächer, U., Aragnol, D., Kemler, R., and Pradel, J. (2000). Pontin52 and reptin52 function as antagonistic regulators of beta-catenin signalling activity. *EMBO J.* *19*, 6121–6130.
- Belmont, A.S. (2006). Mitotic chromosome structure and condensation. *Curr. Opin. Cell Biol.* *18*, 632–638.
- Burns, K.H., Viveiros, M.M., Ren, Y., Wang, P., DeMayo, F.J., Frail, D.E., Eppig, J.J., and Matzuk, M.M. (2003). Roles of NPM2 in chromatin and nucleolar organization in oocytes and embryos. *Science* *300*, 633–636.
- Davis, L.I., and Blobel, G. (1986). Identification and characterization of a nuclear pore complex protein. *Cell* *45*, 699–709.
- Dephoure, N., Zhou, C., Villén, J., Beausoleil, S.A., Bakalarski, C.E., Elledge, S.J., and Gygi, S.P. (2008). A quantitative atlas of mitotic phosphorylation. *Proc. Natl. Acad. Sci. USA* *105*, 10762–10767.
- Diop, S.B., Bertaux, K., Vasanthi, D., Sarkeshik, A., Goirand, B., Aragnol, D., Tolwinski, N.S., Cole, M.D., Pradel, J., Yates, J.R., 3rd, et al. (2008). Reptin and Pontin function antagonistically with PcG and TrxG complexes to mediate Hox gene control. *EMBO Rep.* *9*, 260–266.
- Ducat, D., Kawaguchi, S., Liu, H., Yates, J.R., 3rd, and Zheng, Y. (2008). Regulation of microtubule assembly and organization in mitosis by the AAA+ ATPase Pontin. *Mol. Biol. Cell* *19*, 3097–3110.
- Eisenhardt, N., Schooley, A., and Antonin, W. (2014). *Xenopus* *in vitro* assays to analyze the function of transmembrane nucleoporins and targeting of inner nuclear membrane proteins. *Methods Cell Biol.* *122*, 193–218.
- Franz, C., Walczak, R., Yavuz, S., Santarella, R., Gentzel, M., Askjaer, P., Galy, V., Hetzer, M., Mattaj, I.W., and Antonin, W. (2007). MEL-28/ELYS is required for the recruitment of nucleoporins to chromatin and postmitotic nuclear pore complex assembly. *EMBO Rep.* *8*, 165–172.
- Galy, V., Antonin, W., Jaedicke, A., Sachse, M., Santarella, R., Haselmann, U., and Mattaj, I. (2008). A role for gp210 in mitotic nuclear-envelope breakdown. *J. Cell Sci.* *121*, 317–328.
- Gant, T.M., and Wilson, K.L. (1997). Nuclear assembly. *Annu. Rev. Cell Dev. Biol.* *13*, 669–695.
- Gartner, W., Rossbacher, J., Zierhut, B., Daneva, T., Base, W., Weissel, M., Waldhäusl, W., Pasternack, M.S., and Wagner, L. (2003). The ATP-dependent helicase RUVBL1/TIP49a associates with tubulin during mitosis. *Cell Motil. Cytoskeleton* *56*, 79–93.
- Gasser, S.M., and Laemmli, U.K. (1987). Improved methods for the isolation of individual and clustered mitotic chromosomes. *Exp. Cell Res.* *173*, 85–98.
- Gerlich, D., Hirota, T., Koch, B., Peters, J.M., and Ellenberg, J. (2006). Condensin I stabilizes chromosomes mechanically through a dynamic interaction in live cells. *Curr. Biol.* *16*, 333–344.
- Gurdon, J.B. (1976). Injected nuclei in frog oocytes: fate, enlargement, and chromatin dispersal. *J. Embryol. Exp. Morphol.* *36*, 523–540.
- Hansen, J.C. (2012). Human mitotic chromosome structure: what happened to the 30-nm fibre? *EMBO J.* *31*, 1621–1623.
- Hayashihara, K., Uchiyama, S., Kobayashi, S., Yanagisawa, M., Matsunaga, S., and Fukui, K. (2008). Isolation method for human metaphase chromosomes. *Protocol Exchange*. Published online August 13, 2008. <http://dx.doi.org/10.1038/nprot.2008.166>.

- Hendzel, M.J., Wei, Y., Mancini, M.A., Van Hooser, A., Ranalli, T., Brinkley, B.R., Bazett-Jones, D.P., and Allis, C.D. (1997). Mitosis-specific phosphorylation of histone H3 initiates primarily within pericentromeric heterochromatin during G2 and spreads in an ordered fashion coincident with mitotic chromosome condensation. *Chromosoma* 106, 348–360.
- Hsu, J.Y., Sun, Z.W., Li, X., Reuben, M., Tatchell, K., Bishop, D.K., Grushcow, J.M., Brame, C.J., Caldwell, J.A., Hunt, D.F., et al. (2000). Mitotic phosphorylation of histone H3 is governed by Ipl1/aurora kinase and Glc7/PP1 phosphatase in budding yeast and nematodes. *Cell* 102, 279–291.
- Huber, O., Ménard, L., Haurie, V., Nicou, A., Taras, D., and Rosenbaum, J. (2008). Pontin and reptin, two related ATPases with multiple roles in cancer. *Cancer Res.* 68, 6873–6876.
- Ikura, T., Ogryzko, V.V., Grigoriev, M., Groisman, R., Wang, J., Horikoshi, M., Scully, R., Qin, J., and Nakatani, Y. (2000). Involvement of the TIP60 histone acetylase complex in DNA repair and apoptosis. *Cell* 102, 463–473.
- Jha, S., and Dutta, A. (2009). Rvb1/Rvb2: running rings around molecular biology. *Mol. Cell* 34, 521–533.
- Jónsson, Z.O., Dhar, S.K., Narlikar, G.J., Auty, R., Wagle, N., Pellman, D., Pratt, R.E., Kingston, R., and Dutta, A. (2001). Rvb1p and Rvb2p are essential components of a chromatin remodeling complex that regulates transcription of over 5% of yeast genes. *J. Biol. Chem.* 276, 16279–16288.
- Kim, J.H., Kim, B., Cai, L., Choi, H.J., Ohgi, K.A., Tran, C., Chen, C., Chung, C.H., Huber, O., Rose, D.W., et al. (2005). Transcriptional regulation of a metastasis suppressor gene by Tip60 and beta-catenin complexes. *Nature* 434, 921–926.
- Krogan, N.J., Keogh, M.C., Datta, N., Sawa, C., Ryan, O.W., Ding, H., Haw, R.A., Pootoolal, J., Tong, A., Canadien, V., et al. (2003). A Snf2 family ATPase complex required for recruitment of the histone H2A variant Htz1. *Mol. Cell* 12, 1565–1576.
- Kutay, U., and Hetzer, M.W. (2008). Reorganization of the nuclear envelope during open mitosis. *Curr. Opin. Cell Biol.* 20, 669–677.
- Landsverk, H.B., Kirkhus, M., Bollen, M., Küntziger, T., and Collas, P. (2005). PNUts enhances in vitro chromosome decondensation in a PP1-dependent manner. *Biochem. J.* 390, 709–717.
- Lim, C.R., Kimata, Y., Ohdate, H., Kokubo, T., Kikuchi, N., Horigome, T., and Kohno, K. (2000). The *Saccharomyces cerevisiae* RuvB-like protein, Tih2p, is required for cell cycle progression and RNA polymerase II-directed transcription. *J. Biol. Chem.* 275, 22409–22417.
- Lohka, M.J., and Masui, Y. (1983). Formation in vitro of sperm pronuclei and mitotic chromosomes induced by amphibian ooplasmic components. *Science* 220, 719–721.
- MacCallum, D.E., Losada, A., Kobayashi, R., and Hirano, T. (2002). ISWI remodeling complexes in *Xenopus* egg extracts: identification as major chromosomal components that are regulated by INCENP-aurora B. *Mol. Biol. Cell* 13, 25–39.
- Maresca, T.J., and Heald, R. (2006). Methods for studying spindle assembly and chromosome condensation in *Xenopus* egg extracts. *Methods Mol. Biol.* 322, 459–474.
- Matias, P.M., Gorynia, S., Donner, P., and Carrondo, M.A. (2006). Crystal structure of the human AAA+ protein RuvBL1. *J. Biol. Chem.* 281, 38918–38929.
- Mazumdar, M., Sundareshan, S., and Misteli, T. (2004). Human chromokinesin KIF4A functions in chromosome condensation and segregation. *J. Cell Biol.* 166, 613–620.
- Mézard, C., Davies, A.A., Stasiak, A., and West, S.C. (1997). Biochemical properties of RuvBD113N: a mutation in helicase motif II of the RuvB hexamer affects DNA binding and ATPase activities. *J. Mol. Biol.* 271, 704–717.
- Murray, A.W. (1991). Cell cycle extracts. *Methods Cell Biol.* 36, 581–605.
- Nano, N., and Houry, W.A. (2013). Chaperone-like activity of the AAA+ proteins Rvb1 and Rvb2 in the assembly of various complexes. *Philos. Trans. R. Soc. Lond. B Biol. Sci.* 368, 20110399.
- Newman, D.R., Kuhn, J.F., Shanab, G.M., and Maxwell, E.S. (2000). Box C/D snoRNA-associated proteins: two pairs of evolutionarily ancient proteins and possible links to replication and transcription. *RNA* 6, 861–879.
- Newport, J., and Kirschner, M. (1982). A major developmental transition in early *Xenopus* embryos: I. characterization and timing of cellular changes at the midblastula stage. *Cell* 30, 675–686.
- Nguyen, V.Q., Ranjan, A., Stengel, F., Wei, D., Aebersold, R., Wu, C., and Leschziner, A.E. (2013). Molecular architecture of the ATP-dependent chromatin-remodeling complex SWR1. *Cell* 154, 1220–1231.
- Ohta, S., Wood, L., Bukowski-Wills, J.C., Rappsilber, J., and Earnshaw, W.C. (2011). Building mitotic chromosomes. *Curr. Opin. Cell Biol.* 23, 114–121.
- Olsen, J.V., Vermeulen, M., Santamaria, A., Kumar, C., Miller, M.L., Jensen, L.J., Gnäd, F., Cox, J., Jensen, T.S., Nigg, E.A., et al. (2010). Quantitative phosphoproteomics reveals widespread full phosphorylation site occupancy during mitosis. *Sci. Signal.* 3, ra3.
- Peters, J.M. (2006). The anaphase promoting complex/cyclosome: a machine designed to destroy. *Nat. Rev. Mol. Cell Biol.* 7, 644–656.
- Philpott, A., and Leno, G.H. (1992). Nucleoplasmin remodels sperm chromatin in *Xenopus* egg extracts. *Cell* 69, 759–767.
- Philpott, A., Leno, G.H., and Laskey, R.A. (1991). Sperm decondensation in *Xenopus* egg cytoplasm is mediated by nucleoplasmin. *Cell* 65, 569–578.
- Puri, T., Wendler, P., Sigala, B., Saibil, H., and Tsaneva, I.R. (2007). Dodecameric structure and ATPase activity of the human TIP48/TIP49 complex. *J. Mol. Biol.* 366, 179–192.
- Ramadan, K., Bruderer, R., Spiga, F.M., Popp, O., Baur, T., Gotta, M., and Meyer, H.H. (2007). Cdc48/p97 promotes reformation of the nucleus by extracting the kinase Aurora B from chromatin. *Nature* 450, 1258–1262.
- Rosenbaum, J., Baek, S.H., Dutta, A., Houry, W.A., Huber, O., Hupp, T.R., and Matias, P.M. (2013). The emergence of the conserved AAA+ ATPases Pontin and Reptin on the signaling landscape. *Sci. Signal.* 6, mr1.
- Rottbauer, W., Saurin, A.J., Lickert, H., Shen, X., Burns, C.G., Wo, Z.G., Kemler, R., Kingston, R., Wu, C., and Fishman, M. (2002). Reptin and pontin antagonistically regulate heart growth in zebrafish embryos. *Cell* 111, 661–672.
- Schmitz, M.H., Held, M., Janssens, V., Hutchins, J.R., Hudecz, O., Ivanova, E., Goris, J., Trinkle-Mulcahy, L., Lamond, A.I., Poser, I., et al. (2010). Live-cell imaging RNAi screen identifies PP2A-B55alpha and importin-beta1 as key mitotic exit regulators in human cells. *Nat. Cell Biol.* 12, 886–893.
- Schooley, A., Vollmer, B., and Antonin, W. (2012). Building a nuclear envelope at the end of mitosis: coordinating membrane reorganization, nuclear pore complex assembly, and chromatin de-condensation. *Chromosoma* 121, 539–554.
- Shen, X., Mizuguchi, G., Hamiche, A., and Wu, C. (2000). A chromatin remodeling complex involved in transcription and DNA processing. *Nature* 406, 541–544.
- Sigala, B., Edwards, M., Puri, T., and Tsaneva, I.R. (2005). Relocalization of human chromatin remodeling cofactor TIP48 in mitosis. *Exp. Cell Res.* 310, 357–369.
- Steen, R.L., Martins, S.B., Taskén, K., and Collas, P. (2000). Recruitment of protein phosphatase 1 to the nuclear envelope by A-kinase anchoring protein AKAP149 is a prerequisite for nuclear lamina assembly. *J. Cell Biol.* 150, 1251–1262.
- Tavormina, P.A., Côme, M.G., Hudson, J.R., Mo, Y.Y., Beck, W.T., and Gorbisky, G.J. (2002). Rapid exchange of mammalian topoisomerase II alpha at kinetochores and chromosome arms in mitosis. *J. Cell Biol.* 158, 23–29.
- Theerthagiri, G., Eisenhardt, N., Schwarz, H., and Antonin, W. (2010). The nucleoporin Nup188 controls passage of membrane proteins across the nuclear pore complex. *J. Cell Biol.* 189, 1129–1142.
- Thompson, L.J., Bollen, M., and Fields, A.P. (1997). Identification of protein phosphatase 1 as a mitotic lamin phosphatase. *J. Biol. Chem.* 272, 29693–29697.
- Tosi, A., Haas, C., Herzog, F., Gilmozzi, A., Berninghausen, O., Ungewickell, C., Gerhold, C.B., Lakomek, K., Aebersold, R., Beckmann, R., and Hopfner, K.P. (2013). Structure and subunit topology of the INO80 chromatin remodeler and its nucleosome complex. *Cell* 154, 1207–1219.

- Vagnarelli, P., Ribeiro, S., Sennels, L., Sanchez-Pulido, L., de Lima Alves, F., Verheyen, T., Kelly, D.A., Ponting, C.P., Rappsilber, J., and Earnshaw, W.C. (2011). Repo-Man coordinates chromosomal reorganization with nuclear envelope reassembly during mitotic exit. *Dev. Cell* *21*, 328–342.
- Venteicher, A.S., Meng, Z., Mason, P.J., Veenstra, T.D., and Artandi, S.E. (2008). Identification of ATPases pontin and reptin as telomerase components essential for holoenzyme assembly. *Cell* *132*, 945–957.
- Walczak, C.E., and Heald, R. (2008). Mechanisms of mitotic spindle assembly and function. *Int. Rev. Cytol.* *265*, 111–158.
- Walczak, C.E., Cai, S., and Khodjakov, A. (2010). Mechanisms of chromosome behaviour during mitosis. *Nat. Rev. Mol. Cell Biol.* *11*, 91–102.
- Wood, M.A., McMahon, S.B., and Cole, M.D. (2000). An ATPase/helicase complex is an essential cofactor for oncogenic transformation by c-Myc. *Mol. Cell* *5*, 321–330.
- Wright, S.J. (1999). Sperm nuclear activation during fertilization. *Curr. Top. Dev. Biol.* *46*, 133–178.
- Wurzenberger, C., and Gerlich, D.W. (2011). Phosphatases: providing safe passage through mitotic exit. *Nat. Rev. Mol. Cell Biol.* *12*, 469–482.
- Zhao, R., Davey, M., Hsu, Y.C., Kaplanek, P., Tong, A., Parsons, A.B., Krogan, N., Cagney, G., Mai, D., Greenblatt, J., et al. (2005). Navigating the chaperone network: an integrative map of physical and genetic interactions mediated by the hsp90 chaperone. *Cell* *120*, 715–727.

Developmental Cell, Volume 31

Supplemental Information

RuvB-like ATPases Function in Chromatin

Decondensation at the End of Mitosis

**Adriana Magalska, Anna Katharina Schellhaus, Daniel Moreno-Andrés, Fabio Zanini,
Allana Schooley, Ruchika Sachdev, Heinz Schwarz, Johannes Madlung, and Wolfram
Antonin**

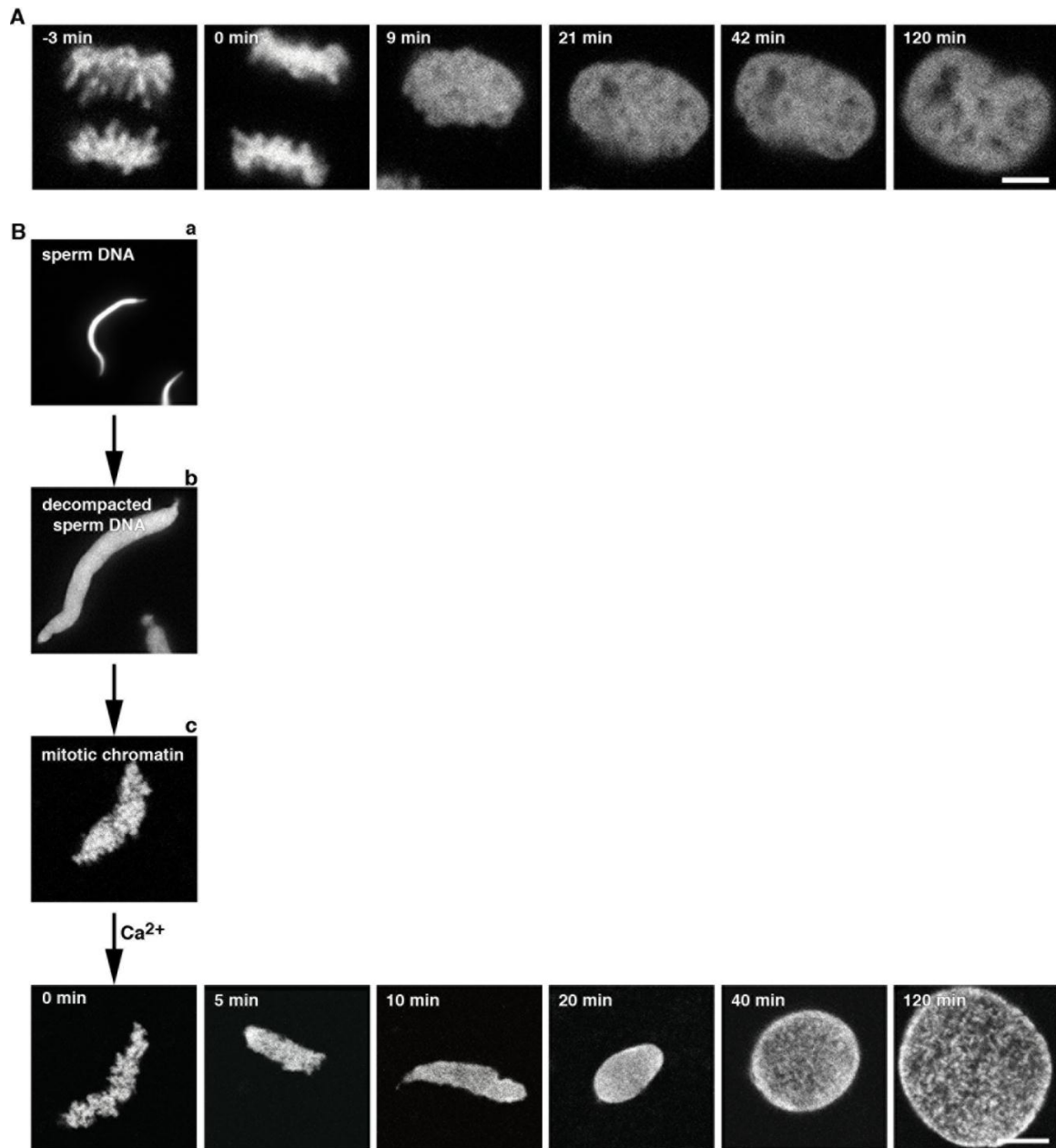


Figure S1, related to Figure 1

- A) Time course of chromatin decondensation in HeLa cells recorded with time-lapse confocal microscopy. Chromatin is visualized as mCherry-tagged histone H2B. Time is normalized to telophase onset.
- B) *Xenopus* sperm heads were incubated in CSF-arrested *Xenopus* egg extracts for 60 min to generate mitotic chromatin. Please note that during this treatment the highly condensed crescent shaped sperm DNA (a) is de-compacted in CSF extracts in a nucleoplasmin (NPM2) dependent exchange of protamines to histones (b), which is not occurring during post-mitotic chromatin decondensation, and then condensed to mitotic chromatin (c). For a more extensive documentation of these steps see e.g. (de

la Barre et al., 1999). The transition to interphase was induced by addition of 1 mM CaCl_2 , which initiates post-mitotic chromatin decondensation. Samples were fixed at indicated time points after Ca^{2+} addition with 4% PFA and 0.5% glutaraldehyde, stained with DAPI, and analyzed by confocal microscopy.

Scale bars are 5 μm .

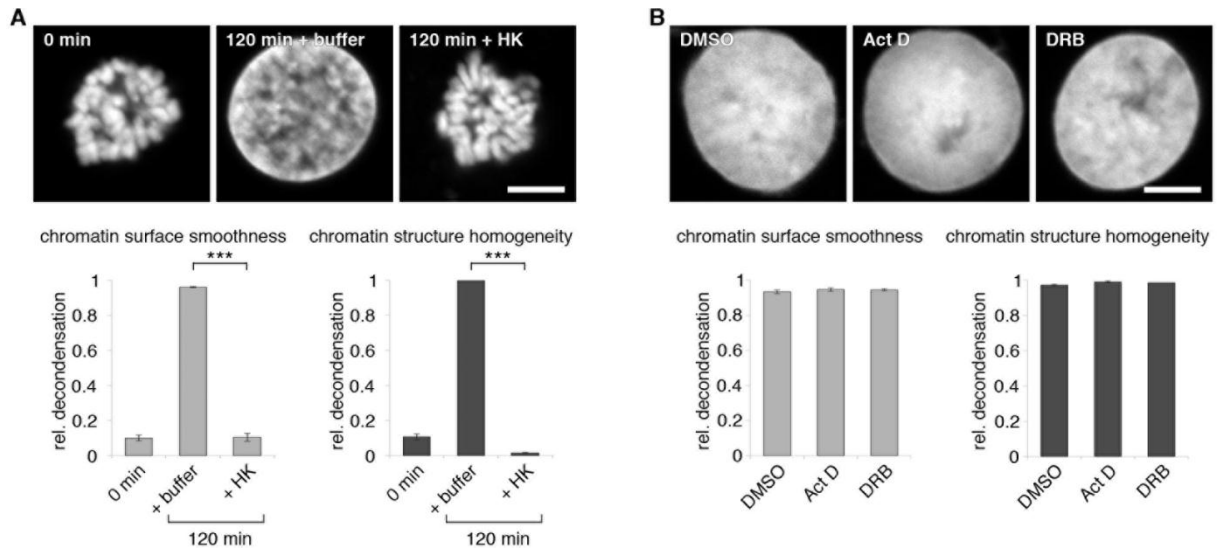


Figure S2, related to Figure 3

A) The decondensation reaction using HeLa mitotic clusters was incubated with 100 U of hexokinase (HK) to eliminate endogenous ATP. Samples were fixed at indicated time points with 4% PFA and 0.5% glutaraldehyde, stained with DAPI, analyzed by confocal microscopy.

B) The decondensation reaction using HeLa mitotic clusters was supplemented with 12 μ M actinomycin D (Act D), a concentration sufficient to inhibit class I, II and III gene transcription (Bensaude, 2011), or 1 mM 5,6-dichloro-1-beta-D-ribofuranosylbenzimidazole (DRB, both dissolved in DMSO), which inhibits class II gene transcription, or the same volume of DMSO. Samples were fixed after 120 min with 4% PFA and 0.5% glutaraldehyde, stained with DAPI, analyzed by confocal microscopy.

Decondensation was quantified as in Figure 1A. The mean of three independent experiments each including at least ten chromatin substrates are shown. Error bars represent the SEM, *** represents $P < 0.001$ by Mann Whitney test for A. For B no statistical significant difference ($P > 0.05$) was detected by one-way ANOVA test. Scale bars are 5 μ m.

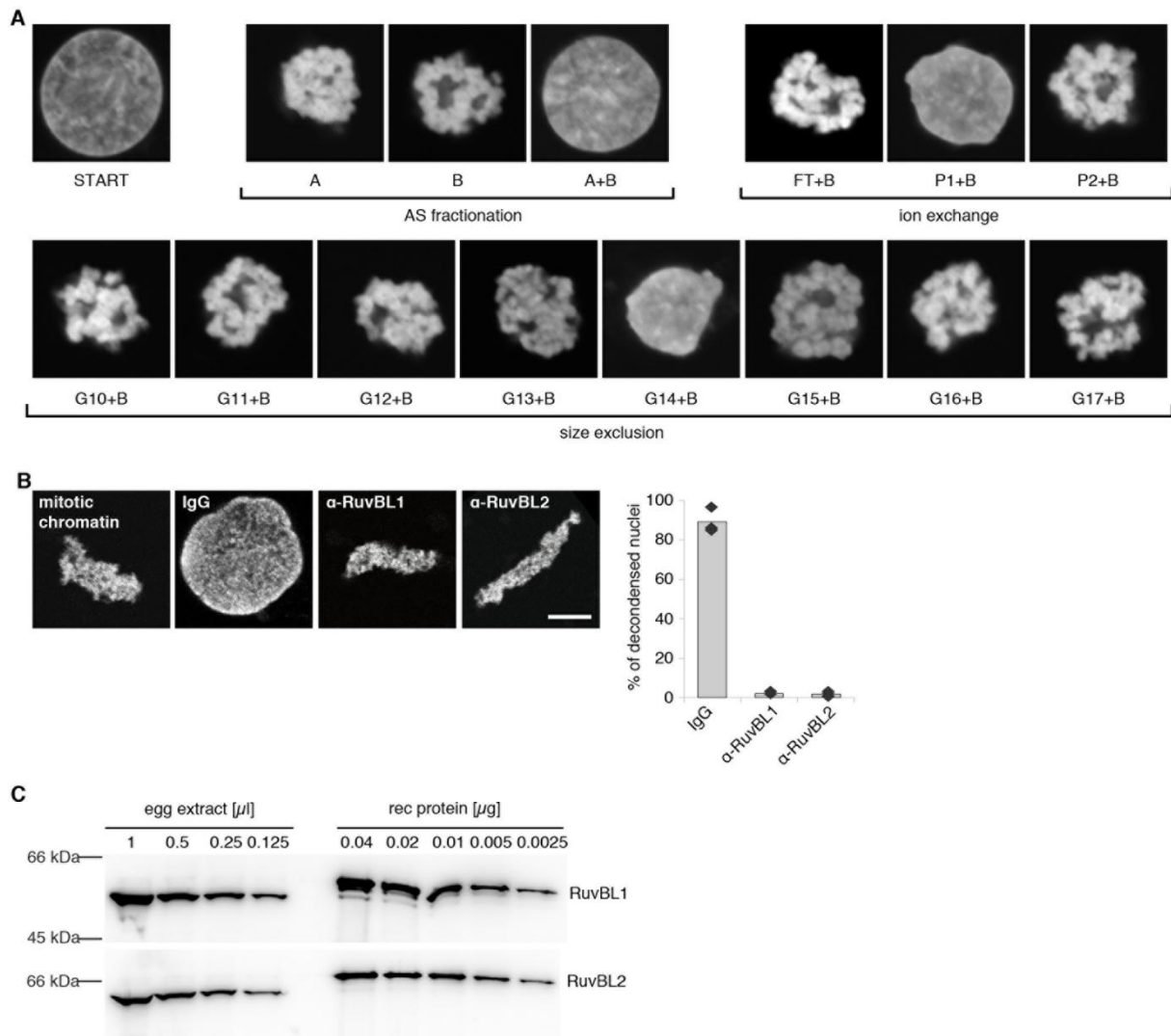


Figure S3, related to Figure 4

- A)** Representative confocal images of DAPI stained HeLa mitotic chromatin incubated with the different fractions according to the fractionation procedure as presented in Figure 4A. Please note that as in Figure 4A the fractions of the ion exchange and size exclusion chromatography are only shown in combination with fraction B.
- B)** *Xenopus* sperm heads were incubated in CSF-arrested *Xenopus* egg extracts for 60 min to generate mitotic chromatin and pre-incubated for 5 min with 4 mg/ml affinity purified IgG against RuvBL1, RuvBL2 or control IgGs. Transition to interphase was induced by addition of 1 mM CaCl₂. Samples were fixed 120 min after Ca²⁺ addition with 4% PFA and 0.5% glutaraldehyde, stained with DAPI and the fraction of decondensed chromatin templates was quantified. The weighted average percentage of three independent experiments, each including at least 100

randomly chosen chromatin substrates is shown, diamonds indicate individual data points.

- C) Dilution series of *Xenopus* egg extracts and purified recombinant RuvBL1 or RuvBL2 were analyzed by western blot and quantified. Based on the quantitation the endogenous RuvBL1 and RuvBL2 concentrations are estimated both to 0.02 $\mu\text{g}/\mu\text{l}$ which corresponds to a 0.4 μM concentration of the monomers. The equal concentration of RuvBL1 and RuvBL2 is in agreement with the notion that these proteins are mostly found in a heteromeric complex in *Xenopus* egg extracts (see Figure 4D).

Scale bars are 5 μm .

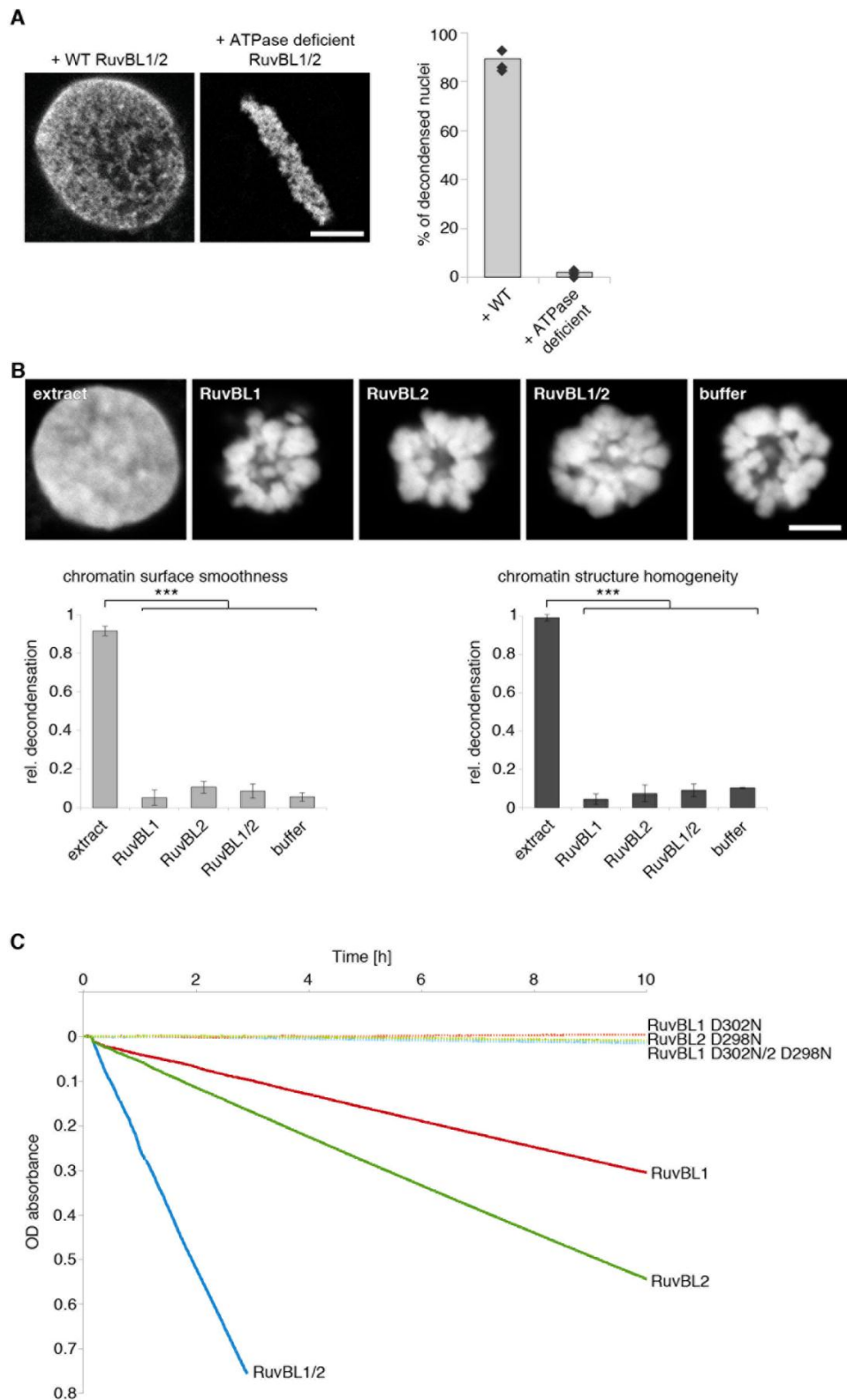


Figure S4, related to Figure 5

A) *Xenopus* sperm heads were incubated in CSF-arrested *Xenopus* egg extracts for 60 min to generate mitotic chromatin and pre-incubated for 5 min with recombinant wild type or ATPase deficient RuvBL1-RuvBL2 complex. The transition to interphase was

induced by addition of 1 mM CaCl₂. Samples were fixed 120 min after Ca²⁺ addition with 4% PFA and 0.5% glutaraldehyde, stained with DAPI and the fraction of decondensed chromatin templates quantified. The weighted average percentage of three independent experiments, each including at least 100 randomly chosen chromatin substrates is shown, diamonds indicate individual data points.

B) Mitotic chromatin clusters from HeLa cells were incubated at 20°C with post-mitotic *Xenopus* egg extracts or 0.4 μM recombinant purified RuvBL1, RuvBL1 or the heteromeric RuvBL1/2 complex in sucrose buffer supplemented with 3 μM 6-Dimethylaminopurine, 10 mM ATP, 10 mM creatine phosphate, 0.2 mg/ml creatine kinase, and 0.4 mg/ml glycogen. Samples were fixed after 120 min with 4% PFA and 0.5% glutaraldehyde, stained with DAPI, analyzed by confocal microscopy and decondensation was quantified as in Figure 1A. The mean of three independent experiments each including at least ten chromatin substrates are shown. Error bars represent the SEM, *** represents $P < 0.001$ by one-way ANOVA, Sidlak post-hoc test. No statistical significant difference was detected within the RuvB-like ATPase and buffer samples ($P = 1$). Scale bars are 5 μm.

C) The ATPase activity of the RuvBL1, RuvBL2 and the heteromeric RuvBL1/2 complexes as well as the ATPase deficient versions (RuvBL1 D302N, RuvBL2 D298N or the RuvBL1 D302N/RuvBL2 D298N) was analyzed at a protein concentration of 2 μg/ml for RuvBL1 and RuvBL2 complexes and 4 μg/ml for RuvBL1/2 complexes. The rather low ATPase activity with a generation rate of 18 mol Pi/(min x mol RuvBL1/2), 2 mol Pi/(min x mol RuvBL1) and 3.5 mol Pi/(min x mol RuvBL2) is in agreement with reported values (e.g. (Puri et al., 2007)). Similarly, an elevated ATPase activity for the heteromeric complex has been reported before (e.g. (Puri et al., 2007), see also <http://www.gref-bordeaux.fr/en/node/303> for a comprehensive summary of ATPase activity measurements of RuvB-like ATPases). Please note that no ATPase activity can be detected for the ATPase deficient versions.

Scale bars are 5 μm.

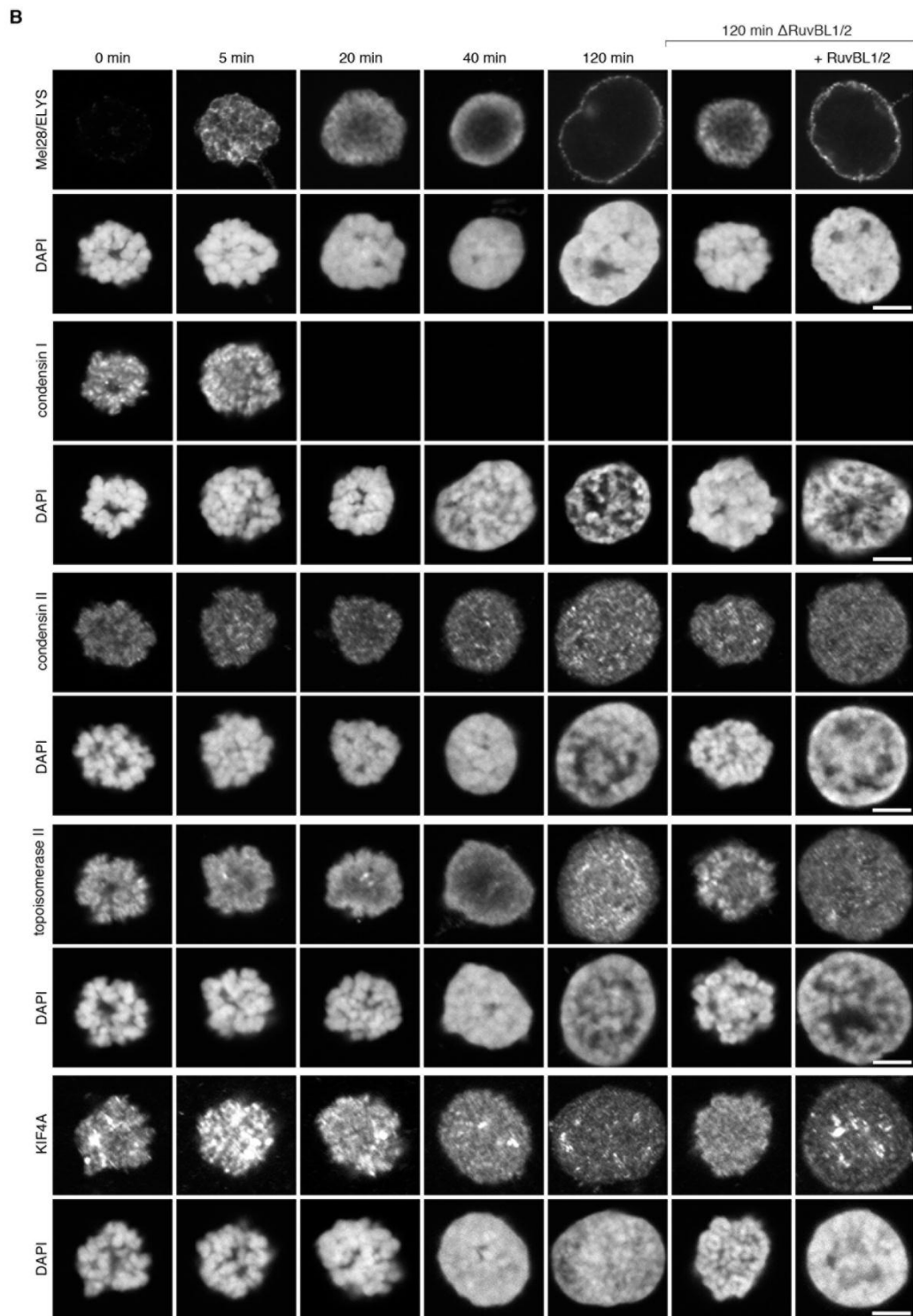
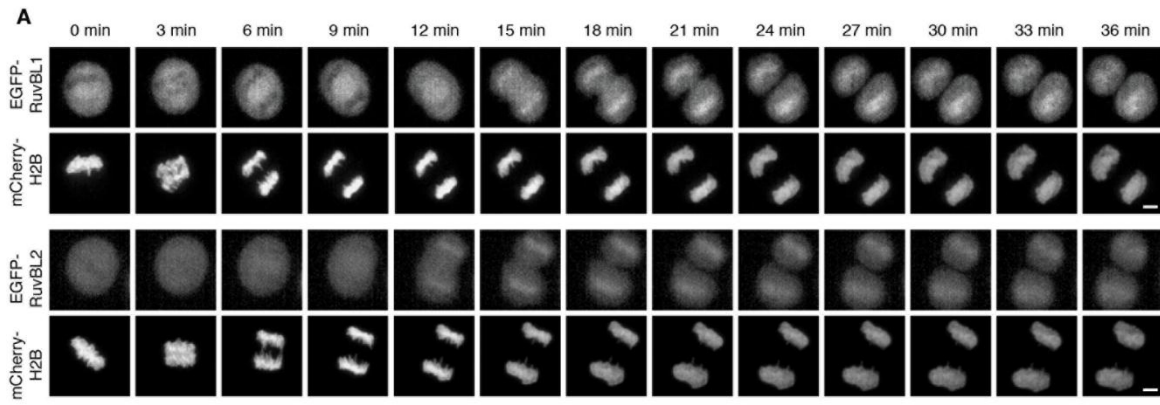


Figure S5, related to Figure 6

- A)** Time course of mitotic exit in HeLa cells stably expressing mCherry-tagged histone H2B and EGFP-RuvBL1 (upper panel) or EGFP-RuvBL2 (lower panel) recorded by time-lapse confocal microscopy. Time is normalized to the last metaphase frame before anaphase onset.
- B)** Mitotic chromatin clusters from HeLa cells were incubated with post-mitotic *Xenopus* egg extracts for the indicated time to induce chromatin decondensation. RuvBL1/2 depleted extracts (generated by consecutive passage over anti-RuvBL1 and anti-RuvBL2 IgG bound beads) were supplemented with buffer or recombinant RuvBL1-RuvBL2 complex for 120 min. Samples were fixed with 4% PFA and stained using antibodies against the nuclear pore complex protein Mel28/ELYS, the condensin I and II complex (using CAP-G or CAP-D3 antibodies, respectively), topoisomerase II α and the chromokinesin KIF4A.

Scale bars are 5 μ m.

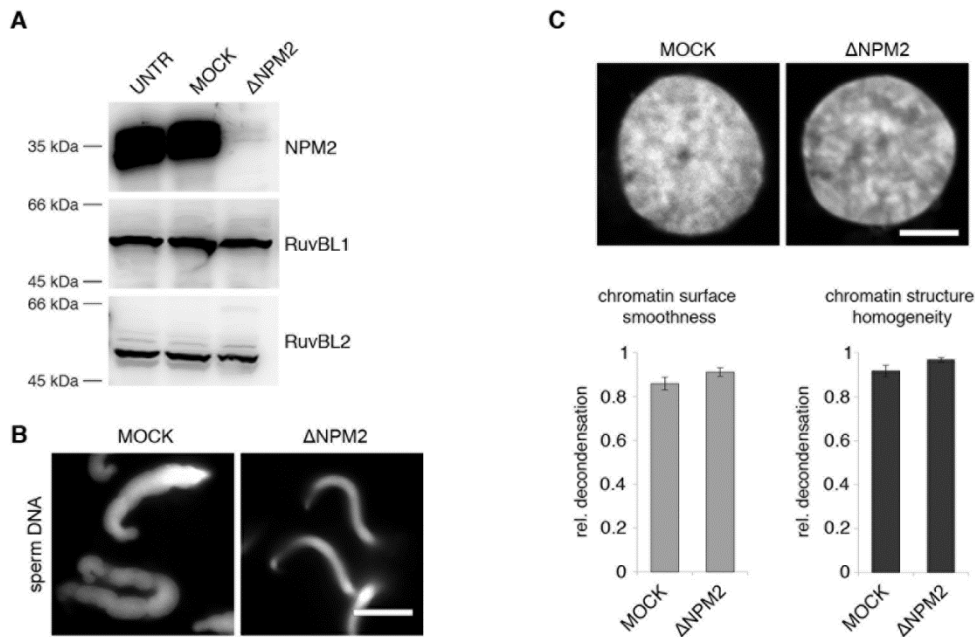


Figure S6, related to Figure 7

- A)** Western blot of untreated, mock or nucleoplasmin (NPM2) depleted *Xenopus laevis* egg extracts. The quantities of RuvBL1 and RuvBL2 in extracts are not affected by this treatment.
- B)** *Xenopus laevis* sperm heads were incubated with mock or nucleoplasmin (NPM2) depleted extracts for 10 min, fixed with 4% PFA and 0.5% glutaraldehyde, stained with DAPI and analyzed on a Axiovert 200 M fluorescence wide field microscope (Zeiss). Please note the block in sperm chromatin de-compaction in the absence of nucleoplasmin as previously reported (Philpott et al., 1991).
- C)** Mock or nucleoplasmin (NPM2) depleted extracts were tested for chromatin decondensation on HeLa mitotic chromatin (120 min time point). The mean (\pm SEM) of three independent experiments each including at least 20 chromatin substrates are shown. Mann-Whitney test showed no statistical significant difference between the samples ($P > 0.05$)
- Scale bars are 5 μ m.

Supplemental Experimental Procedures

Antibodies and recombinant proteins

Antibodies against Ser10 phosphorylated Histone H3 were from Cell Signaling, mAb414 from Babco, topoisomerase IIa (Ki-S1) from Millipore, RepoMan (R11611) from Sigma and Kif4A (H00024137-B01) from Abnova. Antibodies against Mel28/ELYS were described in (Franz et al., 2007). Antibodies against *Xenopus* CAP-D3 and CAP-G were generated as described (Kimura and Hirano, 2000; Ono et al., 2003). Full-length *Xenopus* nucleoplasmin (NPM2) was expressed from a pET28a construct and used for antibody production in rabbits. *Xenopus* RuvBL1 and RuvBL2 were expressed from pET30a constructs (Ducat et al., 2008), purified in the presence of 1 mM ATP and 0.1 mM MgCl₂ by Ni-affinity chromatography and used for antibody production in rabbits. For biochemical experiments RuvBL1 and RuvBL2 were further purified by size exclusion chromatography on a Superose 6 10/300GL column (GE-Healthcare). Purified hexameric RuvBL1 and RuvBL2 complexes were incubated overnight in an equimolar ratio and isolated as hetero-dodecameric complexes by size exclusion chromatography on a Superose 6 10/300GL column. ATPase-dead RuvBL1 and RuvBL2 mutants were generated by *in vitro* mutagenesis and purified as above.

Cell culture and live-cell imaging

HeLa cells stably expressing either EGFP-mouse RuvBL1 or EGFP-mouse RuvBL2 generated from EGFP-tagged BACs (Poser et al., 2008) were transfected with pIRES-puro-mCherryH2B (Steigemann et al., 2009) using FUGENE 6 (Promega) and selected in complete DMEM medium supplemented with 2.5 µg/ml puromycin and 500 µg/ml G418. Positive clones with adequate expression levels of both fluorophores were amplified in complete DMEM medium with 0.5 µg/ml puromycin and 500 µg/ml G418. The cells were seeded 24 hours before live-cell imaging in µ-slide 8 well chamber (Ibidi) with complete DMEM medium. Live-cell confocal microscopy was conducted using an LSM 5 live microscope (Zeiss) equipped with a heating and CO₂ incubation system (Ibidi). Images were acquired under the control of the ZEN software (Zeiss) as time and Z-series. A LD-Apocromant 40x/1.1 W objective was used for image acquisition. EGFP was excited with a 488-nm diode laser and mCherry was excited with a 561-nm diode laser. Images were projected in Z using the maximum intensity projection tool of ZEN software.

Liquid Chromatography-Mass Spectrometry (MS) Analysis

Proteins were subjected to tryptic in-gel digestion (Borchert et al., 2010), and the peptide mixtures were desalted with C18 Stage Tips (Rappsilber et al., 2007). LC-MS analyses were performed on a nanoLC (Easy-nLC, Thermo Fisher Scientific) coupled to a 4000QTrap (Applied Biosystems/MDS Sciex) mass spectrometer equipped with a nanoelectrospray ion source. Chromatographic separation of the peptides was performed on a 15-cm fused silica emitter of 75- μ m inner diameter (New Objective), packed in-house with reversed-phase ReproSil-Pur C18-AQ 3- μ m resin (Dr. Maisch GmbH). The peptide mixtures were injected onto the column in HPLC solvent A (0.5% acetic acid) at a flow rate of 500 nl/min and subsequently eluted with a 43-min segmented gradient of 5%–80% HPLC solvent B (80% ACN in 0.5% acetic acid) at a flow rate of 200 nl/min. MS data acquisition was conducted in the positive ion mode. The mass spectrometer was operated in data-dependent mode to automatically switch between MS and MS/MS acquisition. One MS was followed by three MS/MS events. MS data were searched using the Mascot search engine (Matrix Science, London, UK) against a target-decoy database (Elias and Gygi, 2007) consisting of the *X. laevis* database (Xenbase 20100129) plus 262 commonly observed contaminants.

All MS data were combined into a single peak list and processed in a combined database search using the MS Quant software package. In the database search, carbamidomethylation (Cys) was set as fixed modification, whereas oxidation (Met) and acetylation (protein N termini) were set as variable modifications. The mass tolerances for precursor and fragment ions were set to 1.5 Daltons and 0.5 Daltons, respectively. The identified peptides were classified based on their mascot ion scores; protein identification was defined as valid if at least two peptides with mascot scores better than $P < 0.1$ were identified and at least one of them had a score of $P < 0.05$. RuvBL2 was identified with two peptides covering 4.6% of the protein sequence, GLGLDDALEPR (peptide score 55, mass deviation 0.07945Da) and VYSLFLDESR (peptide score 75, mass deviation 0.03565Da). The peptide scores of both peptides correspond to mascot scores better than $P < 0.01$.

In vitro nuclear transport assay

Nuclear import and export were tested using modified Nplc-M9-M10 or Nplc-M9-NES reporters, respectively, from (Englmeier et al., 1999). Reporters were fused to an N-terminal EGFP, cloned into pET28a and purified via an N-terminal Hexa-Histidine tag and size exclusion chromatography on a Superose 6 10/300 GL column (GE-Healthcare). A 0.1 mg/ml aliquot of the purified protein was added to nuclei assembled in the decondensation reaction

and supplemented with an energy regenerating system (10 mM ATP, 10 mM creatine phosphate, 0.2 mg/ml creatine kinase, and 0.4 mg/ml glycogen; final concentrations). Samples were incubated for another 30 min, fixed and processed for microscopy. Leptomycin B (300 nM) was added to block nuclear export.

ATPase assay

ATPase activity was measured in sucrose buffer supplemented with 2 mM phosphoenolpyruvate, 1mM ATP, 0.2 mM NADH, 0.1 mg/ml BSA 2 µg/ml lactate dehydrogenase (Roche), 2 µg/ml pyruvate kinase (Sigma) at 25°C on a Cary 50 spectrophotometer (Varian) following the rational described in (Huang and Hackney, 1994). In short, the ADP generated by the RuvB-like ATPases is reconverted by the pyruvate kinase to ATP. The resulting pyruvate is processed to lactate by the lactate dehydrogenase under consumption of NADH, the loss of which is monitored at 340 nm.

Supplemental References

- Bensaude, O. (2011). Inhibiting eukaryotic transcription: Which compound to choose? How to evaluate its activity? *Transcr* 2, 103-108.
- Borchert, N., Dieterich, C., Krug, K., Schutz, W., Jung, S., Nordheim, A., Sommer, R.J., and Macek, B. (2010). Proteogenomics of *Pristionchus pacificus* reveals distinct proteome structure of nematode models. *Genome Res* 20, 837-846.
- de la Barre, A.E., Robert-Nicoud, M., and Dimitrov, S. (1999). Assembly of mitotic chromosomes in *Xenopus* egg extract. *Methods Mol Biol* 119, 219-229.
- Ducat, D., Kawaguchi, S., Liu, H., Yates, J.R., 3rd, and Zheng, Y. (2008). Regulation of microtubule assembly and organization in mitosis by the AAA+ ATPase Pontin. *Molecular biology of the cell* 19, 3097-3110.
- Elias, J.E., and Gygi, S.P. (2007). Target-decoy search strategy for increased confidence in large-scale protein identifications by mass spectrometry. *Nat Methods* 4, 207-214.
- Englmeier, L., Olivo, J.C., and Mattaj, I.W. (1999). Receptor-mediated substrate translocation through the nuclear pore complex without nucleotide triphosphate hydrolysis. *Curr Biol* 9, 30-41.
- Franz, C., Walczak, R., Yavuz, S., Santarella, R., Gentzel, M., Askjaer, P., Galy, V., Hetzer, M., Mattaj, I.W., and Antonin, W. (2007). MEL-28/ELYS is required for the recruitment of nucleoporins to chromatin and postmitotic nuclear pore complex assembly. *EMBO Rep* 8, 165-172.
- Huang, T.G., and Hackney, D.D. (1994). *Drosophila* kinesin minimal motor domain expressed in *Escherichia coli*. Purification and kinetic characterization. *J Biol Chem* 269, 16493-16501.
- Kimura, K., and Hirano, T. (2000). Dual roles of the 11S regulatory subcomplex in condensin functions. *Proceedings of the National Academy of Sciences of the United States of America* 97, 11972-11977.
- Ono, T., Losada, A., Hirano, M., Myers, M.P., Neuwald, A.F., and Hirano, T. (2003). Differential contributions of condensin I and condensin II to mitotic chromosome architecture in vertebrate cells. *Cell* 115, 109-121.
- Philpott, A., Leno, G.H., and Laskey, R.A. (1991). Sperm decondensation in *Xenopus* egg cytoplasm is mediated by nucleoplasmin. *Cell* 65, 569-578.
- Poser, I., Sarov, M., Hutchins, J.R., Heriche, J.K., Toyoda, Y., Pozniakovsky, A., Weigl, D., Nitzsche, A., Hegemann, B., Bird, A.W., *et al.* (2008). BAC TransgeneOmics: a high-throughput method for exploration of protein function in mammals. *Nat Methods* 5, 409-415.
- Puri, T., Wendler, P., Sigala, B., Saibil, H., and Tsaneva, I.R. (2007). Dodecameric structure and ATPase activity of the human TIP48/TIP49 complex. *J Mol Biol* 366, 179-192.
- Rappsilber, J., Mann, M., and Ishihama, Y. (2007). Protocol for micro-purification, enrichment, pre-fractionation and storage of peptides for proteomics using StageTips. *Nat Protoc* 2, 1896-1906.
- Steigemann, P., Wurzenberger, C., Schmitz, M.H., Held, M., Guizetti, J., Maar, S., and Gerlich, D.W. (2009). Aurora B-mediated abscission checkpoint protects against tetraploidization. *Cell* 136, 473-484.

Video Article

A Cell Free Assay to Study Chromatin Decondensation at the End of Mitosis

Anna K. Schellhaus¹, Adriana Magalska², Allana Schooley¹, Wolfram Antonin¹¹Friedrich Miescher Laboratory, Max Planck Society²Nencki Institute of Experimental Biology, Polish Academy of Sciences

*These authors contributed equally

Correspondence to: Wolfram Antonin at wolfram.antonin@tuebingen.mpg.deURL: <http://www.jove.com/video/53407>DOI: [doi:10.3791/53407](https://doi.org/10.3791/53407)Keywords: Molecular Biology, Issue 106, Cell-free assay, mitotic exit, chromatin isolation, *Xenopus* egg extract, chromatin decondensation, nuclear reformation, chromatin condensation

Date Published: 12/19/2015

Citation: Schellhaus, A.K., Magalska, A., Schooley, A., Antonin, W. A Cell Free Assay to Study Chromatin Decondensation at the End of Mitosis. *J. Vis. Exp.* (106), e53407, doi:10.3791/53407 (2015).

Abstract

During the vertebrate cell cycle chromatin undergoes extensive structural and functional changes. Upon mitotic entry, it massively condenses into rod shaped chromosomes which are moved individually by the mitotic spindle apparatus. Mitotic chromatin condensation yields chromosomes compacted fifty-fold denser as in interphase. During exit from mitosis, chromosomes have to re-establish their functional interphase state, which is enclosed by a nuclear envelope and is competent for replication and transcription. The decondensation process is morphologically well described, but in molecular terms poorly understood: We lack knowledge about the underlying molecular events and to a large extent the factors involved as well as their regulation. We describe here a cell-free system that faithfully recapitulates chromatin decondensation *in vitro*, based on mitotic chromatin clusters purified from synchronized HeLa cells and *X. laevis* egg extract. Our cell-free system provides an important tool for further molecular characterization of chromatin decondensation and its co-ordination with processes simultaneously occurring during mitotic exit such as nuclear envelope and pore complex re-assembly.

Video Link

The video component of this article can be found at <http://www.jove.com/video/53407/>

Introduction

Xenopus laevis egg extract is a powerful and widely applied tool to study complicated cellular events in the simplicity of a cell-free assay. Since their first description by Lohka & Masui¹ they have been extensively used to study mitotic processes such as chromatin condensation², spindle assembly³, nuclear envelope breakdown⁴, but also nucleocytoplasmic transport⁵ or DNA replication⁶. The events taking place at the end of mitosis, necessary for reformation of the interphasic nucleus such as nuclear envelope reformation and nuclear pore complex reassembly are much less understood compared to the early mitotic events but can be similarly studied using *Xenopus* egg extract⁷. We have recently established an assay based on *Xenopus* egg extract to study chromatin decondensation at the end of mitosis⁸, an under-investigated process that awaits its detailed characterization.

In metazoans, chromatin is highly condensed at mitotic entry in order to perform faithfully segregation of the genetic material. To ensure that the chromatin is accessible for gene expression and DNA replication during interphase, it needs to be de-compacted at the end of mitosis. In vertebrates, chromatin is up to fifty-fold more compacted during mitosis compared to interphase⁹, in contrast to yeasts where the mitotic compaction is usually much lower, e.g., only two-fold in *S. cerevisiae*¹⁰. Vertebrate chromatin decondensation has been mostly studied in the context of sperm DNA reorganization after egg fertilization. A molecular mechanism, in which nucleoplasmin, an abundant oocyte protein, exchanges sperm-specific protamines to histones H2A and H2B stored in the egg. This process was also elucidated using *Xenopus* egg extract^{11,12}. However, the expression of nucleoplasmin is limited to oocytes¹³ and mitotic chromatin does not contain these sperm-specific protamines. Therefore chromatin decondensation at the end of mitosis is nucleoplasmin independent⁸.

For the *in vitro* decondensation reaction we employ extract generated from activated *X.laevis* eggs and chromatin clusters isolated from synchronized HeLa cells. Treatment of eggs with a calcium ionophore mimics the calcium release into the oocyte generated by sperm entry during fertilization. The calcium wave triggers the cell cycle resumption and the egg, arrested in the second metaphase of meiosis, progresses to the first interphase¹⁴. Therefore, egg extracts prepared from activated eggs represent the mitotic exit/interphase state and are competent to induce events specific for mitotic exit like chromatin decondensation, nuclear envelope and pore complex reformation. For the isolation of mitotic chromatin clusters we used a slightly modified version of the protocol published by Gasser & Laemmli¹⁵, where chromosome clusters are released by lysis from HeLa cells synchronized in mitosis and isolated in polyamine containing buffers by gradient centrifugations.

Protocol

Mitotic Chromatin Cluster Isolation from HeLa Cells

1. Preparations

1. Cell Culture Solutions

1. Prepare complete Dulbecco's modified Eagle's medium (DMEM) by adding 10% fetal calf serum, 100 units/ml penicillin, 100 µg/ml streptomycin and 2 mM glutamine to the DMEM. Prepare Phosphate buffer saline (PBS) containing 2.7 mM KCl, 137 mM NaCl, 10 mM Na₂HPO₄·2H₂O and 2 mM KH₂PO₄ in deionized water, and adjust pH to 7.4 with 10 N NaOH.

NOTE: PBS can be kept as 10x stock solution over time at RT. Dilute it with deionized water to 1x before use. Filter the 1x solution again if it will be used in cell culture.

2. Prepare a 40 mM stock of thymidine solution (cell culture suitable) in DMEM medium. Dissolve 0.97 g thymidine in 90 ml of DMEM medium. Adjust final volume to 100 ml. Store stock solution at -20 °C. Dissolve (**CAUTION!** work under chemical hood, wear gloves and mouth protection) nocodazole to a 5 mg/ml stock solution in DMSO.

2. Mitotic Clusters Isolation Solutions

NOTE: All solutions described in 1.2 need to be kept on ice after preparation/thawing throughout the whole experiment.

1. Autoclave deionized water for 105 min at 121 °C. Dissolve spermine tetrahydrochloride in autoclaved, deionized water to a final concentration of 200 mM (69.6 mg/ml). Store stock solution at -20 °C. Dissolve spermidine trihydrochloride in autoclaved, deionized water to a final concentration of 200 mM (50.8 mg/ml). Store stock solution at -20 °C.
2. Prepare 5 % (w/v) digitonin (**CAUTION!** work under chemical hood, wear gloves and mouth protection) in hot, deionized water. Filter and store aliquots at -20 °C. Dissolve phenylmethylsulfonyl fluoride (PMSF) (**CAUTION!** work under chemical hood, wear gloves and mouth protection) to a final concentration of 200 mM (35 mg/ml) in 100% ethanol. Store stock solution at -20 °C.
3. Dissolve dithiothreitol (DTT) with deionized water to a final concentration of 1 M (154 mg/ml) (**CAUTION!** work under chemical hood, wear gloves). Filter and store stock solution at -20 °C.
4. Prepare a 100-fold protease inhibitor mix (**CAUTION!** work under chemical hood, wear gloves) by dissolving 10 mg/ml AEBSF (4-(2-Aminoethyl-)-benzylsulfonamide), 0.2 mg/ml leupeptin, 0.1 mg/ml pepstatin and 0.2 mg/ml aprotinin in deionized water. Store stock solution at -20 °C.
5. Prepare a 10x stock solution of buffer A containing 150 mM Tris-Cl (pH 7.4), 800 mM KCl, 20 mM EDTA-KOH (pH 7.4), 2 mM spermine tetrahydrochloride and 5 mM spermidine trihydrochloride. Store buffer A at 4 °C without spermine tetrahydrochloride and spermidine trihydrochloride, which should be added freshly just before use.
NOTE: EDTA only dissolves at pHs higher than 8, therefore, to prepare a high concentrated EDTA-KOH stock solution (0.5 M recommended), add 5 N KOH to pH just above 8 to dissolve it. Afterwards titrate down to pH 7.4.
6. Prepare a 20x stock solution of buffer As containing 100 mM Tris-HCl (pH 7.4), 400 mM KCl, 400 mM EDTA-KOH (pH 7.4) and 5 mM spermidine trihydrochloride. Buffer As can be stored under same conditions as buffer A.
NOTE: Prepare the working solutions I to IV (see in the following steps), the glycerol gradient and the colloidal silica particles solutions containing silica particles (15 to 30 nm diameter) coated with non-dialyzable polyvinylpyrrolidone (PVP) freshly just before the isolation procedure (PMSF and digitonin should be added directly before use as PMSF is labile in aqueous solutions and digitonin tends to precipitate upon long term storage on ice).
7. Prepare 100 ml of solution I by adding 0.5x buffer A, 1 mM DTT, 1:100 of the protease inhibitor mix and 0.1 mM PMSF into autoclaved, deionized water. Prepare 50 ml of solution II (for cell lysis) by adding 1x buffer A, 1 mM DTT, 1:100 of the protease inhibitor mix, 0.1 mM PMSF, 0.1 % digitonin and 10 % glycerol into autoclaved, deionized water.
8. Prepare 200 ml of solution III containing 0.25x buffer A, 1 mM DTT, 1:100 of the protease inhibitor mix, 0.1 mM PMSF and 0.05 % digitonin in autoclaved, deionized water. Prepare 40 ml of solution IV containing 1x buffer As, 1 mM DTT, 1:100 of the protease inhibitor mix, 0.1 mM PMSF and 0.1 % digitonin in autoclaved, deionized water.
9. Prepare 120 ml of glycerol gradient solution by adding 25% glycerol and 0.1 % digitonin to solution I.
10. Prepare 150 ml of colloidal silica particles solution containing 60 % v/v (volume per volume) of a suspension containing silica particles (15 to 30 nm diameter) coated with non-dialyzable polyvinylpyrrolidone (PVP), 15% glycerol, 2 mM spermidine trihydrochloride and 0.8 mM spermine tetrahydrochloride in solution IV.
11. Prepare cluster storage buffer containing 250 mM sucrose, 15 mM Hepes (pH 7.4), 0.5 mM spermidine trihydrochloride, 0.2 mM spermine tetrahydrochloride, 1:100 of the protease inhibitor mix, 0.3% BSA and 30% glycerol. The cluster storage buffer can be kept at -20 °C.
12. Prepare squash fix solution containing 10% formaldehyde (**CAUTION!** work under chemical hood, wear gloves), 50% glycerol, twofold Mark's Modified Ringers buffer (MMR see 4.5.) and 0.2 µg/ml DAPI (**CAUTION!** wear gloves). Store at 4 °C in light protected reaction tubes. It is not crucial for the experiment to use this squash fix recipe, alternative recipes will also work.

2. Synchronization of Cells

1. On Day 1: Seed HeLa cells in five 75 cm² (250 ml) flasks with media and incubate it at 37 °C in 5% CO₂.
NOTE: This will yield in approximately 18 x 10⁶ cells at the day of chromatin cluster isolation.
2. On Day 2: When cells are at least 50% confluent (roughly half of the surface is covered by cells and there is still room for cells to grow), add thymidine to a final concentration of 2 mM (thymidine block) and culture cells for 24 hr at 37 °C in 5% CO₂.

NOTE: This will arrest the cells at the G1/S phase border.

3. On Day 3: Aspirate medium containing thymidine and add sterile PBS. Wash cells by delicate rinsing with sterile PBS. Aspirate PBS and gently add 15-20 ml of fresh, warm complete DMEM medium and culture cells for 3 to 4 hr at 37 °C in 5% CO₂ to release them from the G1/S-phase block.
4. On day 3 (continuation): After releasing the cells from the G1/S-phase block, add nocodazole to a final concentration of 100 ng/ml. Dilute nocodazole by adding 2 µl of stock solution (5 mg/ml) to 98 µl of fresh DMEM medium, and add 1 µl of diluted nocodazole per each ml of cell culture. Culture cells for approximately 12 hr at 37 °C in 5% CO₂. This will block the cells in mitosis.

3. Mitotic Clusters Isolation

1. On day 4: Isolate mitotic clusters. Using a bright field microscopy, check if the majority of cells are mitotic. If less than 50% of the cells are mitotic wait until more cells reach mitosis. Collect mitotic cells by tapping vigorously at the side of the flask (or by gently spraying with the pipette), this will detach remaining mitotic cells. Transfer the cell suspension to 50 ml conical centrifuge tubes.
NOTE: Mitotic cells become round and can be easily detached from the flask bottom (just like cells after trypsinization), unlike cells in other cell cycle stages, which are flat and firmly attached to the flask.
2. Harvest mitotic cells by spinning the tubes at 1,500 x g for 10 min (4 °C or RT) and removing the supernatant afterwards. Resuspend the cell pellet in 8 ml PBS, pool into one 50 ml conical centrifuge tube, fill the tube completely with PBS and spin again for 10 min at 1,500 x g. Repeat this washing procedure three times in total.
3. From now on perform all steps on ice with cold solutions. Vigorously resuspend the pellet in 37 ml of cold solution II. Transfer the suspension to a cold 40 ml glass-glass homogenizer using a 25 ml pipette and lyse cells on ice by douncing with a tight pestle until mitotic clusters are free of cytoplasmic material. The number of strokes is highly dependent on the digitonin stock and can vary from 3 to 20 times.
NOTE: Homogenization can be fairly vigorous, but should be considered complete when nearly all mitotic cells are lysed and the clusters are seen to be free of cytoplasmic material (see 3.4).
4. After a couple of strokes mix 5-10 µl of the cell suspension 1:2 with Trypan blue and check by microscopy in a Neubauer chamber. When the cells are lysed chromatin is stained blue and free of cell membranes (NOTE: possible cytoplasmic remnants will be accumulate around the blue stained chromatin and will be easy to distinguish).
NOTE: Mitotic cells will lyse before interphasic cells but nevertheless be careful not to overdo homogenization in order to avoid contamination with interphasic nuclei and mangled chromatin.
5. Immediately layer the whole cell lysate over cold step gradients (with 5 ml of 60% colloidal silica particles solution at the bottom, overlaid with 19.5 ml of glycerol gradient solution each) in five polycarbonate centrifugation tubes (28.8 x 107.0 mm, it is recommended to place the tubes on ice before to cool them down) using a 10 ml pipette. Do not keep cells in solution II for a long time, thus it is recommended to prepare the tubes and the gradient beforehand (e.g., during the washing steps).
6. Centrifuge the gradients for 30 min at 1,000 x g at 4 °C in a fixed angle rotor.
NOTE: Nuclei, unlysed cells and clusters are recovered together at the interface of the glycerol and the colloidal silica particles layers.
7. Remove the liquid above the interphase using a pipette and transfer the rest to the cold homogenizer. Re-homogenize mixture by 3-15 strokes (again depending on the digitonin stock) with the tight pestle to eliminate aggregates and to remove cytoskeletal fibers from the clusters. After every couple of strokes check the efficiency of homogenization. Mix 1 µl of the sample with 1 µl of squash fix supplemented with DAPI and examine under the fluorescent microscope.
NOTE: The number of strokes is crucial, the presence of cluster aggregates means, that the number of strokes is insufficient, while mangled chromatin and nuclei debris indicate that the homogenization was too strong.
8. Distribute the solution among four new polycarbonate centrifugation tubes (28.8 x 107.0 mm) (approx. 10 ml solution per tube) and fill them completely up with 60 % colloidal silica particles solution (approx. 30 ml colloidal silica particles solution per tube).
NOTE: Avoid overloading the colloidal silica particles gradient since clusters can easily be trapped if there is too much cytoplasmic debris in the gradient.
9. Spin for 5 min at 3,000 x g, followed by 30 min at 45,440 x g at 4 °C in a fixed angle rotor.
NOTE: As before, interphasic nuclei will be kept from entering the gradient (if homogenization was not done too heavily which releases nuclei from cytoplasmic debris) but the clusters will accumulate around 1.5 cm from the bottom of the tube, often as a loose ball.
10. Remove the liquid above the clusters using a pipette, pool the rest into one tube, resuspend well and redistribute to two polycarbonate centrifugation tubes (28.8 x 107.0 mm). Dilute the cluster suspension 1:4 with solution III in each tube and mix well. Mark the site where the pellet will be and spin 1,000 x g for 15 min at 4 °C in a fixed angle rotor.
11. Resuspend the pellets in Solution III, pool into one 50 ml conical centrifuge tube and fill up with Solution III. Centrifuge at only 300 x g for approximately 10 min. Do not centrifuge at higher velocity - it might cause irreversible aggregation of clusters.
12. Wash again with Solution III in 1.5 or 2 ml reaction tubes (resuspend the pellets and fill the tubes completely up) and centrifuge at 300 x g. Remove the supernatant carefully with a pipette. Resuspend pellet carefully in 250 µl cluster storage buffer (if you have several pellets use 250 µl for all together and pool them). Dilute 5-10 µl of the sample 1:2 with Trypan blue and count in the Neubauer chamber. If applicable dilute more to obtain an approximate concentration of 500 clusters/µl.
13. Push the suspension through a 100 µm cell strainer to make sure to remove cluster aggregations resulting from improper resuspension. The clusters can be stored for months in -80 °C. To avoid multiple refreezing make appropriate aliquots and snap freeze in liquid nitrogen.

4. Preparations of Buffer for Interphasic *Xenopus laevis* Egg Extract

NOTE: *Xenopus laevis* frogs are maintained and treated in accordance with the guidelines and regulations set forth by the Convention of the council of Europe on the protection of vertebrate animals used for experimental and other purposes (EU ratified in 1998) and the German law pertaining to the use of vertebrate animals in research.

1. Prepare DTT and a 100-fold protease inhibitor mix according to 1.2.3 and 1.2.4. Dissolve cytochalasin B to a final concentration of 10 mg/ml in DMSO, aliquot (10 or 20 µl recommended) and store at -20 °C.
2. Dissolve cycloheximide to a final concentration of 20 mg/ml in ethanol, aliquot (500 µl recommended) and store at -20 °C. Dissolve the calcium ionophore A23187 to a final concentration of 2 mg/ml in ethanol, aliquot and store at -20 °C.

NOTE: PI, DTT, cytochalasin B, cycloheximide and A23187 can be repeatedly frozen and thawed.

3. Prepare 20x Mark's Modified Ringers buffer (MMR) containing 2 M NaCl, 40 mM KCl, 20 mM MgCl₂, 40 mM CaCl₂, 2 mM EDTA and 100 mM Hepes, adjust pH to 8.0 with 5 N KOH.

NOTE: The 20x MMR can be kept over long time at RT. Depending on the amounts of eggs, for one preparation of interphasic egg extract 1 L of 1x MMR per injected frog and an additional 5-10 liters for the washing steps are necessary. Re-adjust the pH of 1x MMR to 8.0 with 5 N KOH. 1x MMR prepared to keep the frogs in O/N x 1 should be at RT. 1x MMR prepared for the extract preparation should be kept cold until it is used, however it is not crucial for the experiment that the 1x MMR is really cold.

4. Prepare 1 L of sucrose buffer containing 250 mM sucrose, 50 mM KCl, 2.5 mM MgCl₂ and 10 mM Hepes pH 7.5. Sucrose buffer should be prepared the day before using sterile water and should be kept at 4 °C.
5. Prepare the dejelling solution freshly on the morning of the experiment by dissolving 2% L-cystein in 0.25x MMR. Adjust pH to 7.8 with 5 N KOH. Keep at 4 °C until it is used.

5. Protocol for Interphasic *Xenopus laevis* Egg Extract

1. Inject 120 I.E. pregnant mare's serum gonadotropin (PMSG) into the dorsal lymph sac of each frog 3-10 days before the experiment (5 ml syringes, 27 G 3/4" needles).

NOTE: This injection will induce ovulation. The amount of eggs one frog lays varies a lot. A well laying frog might produce eggs occupying a volume of up to 7 ml after being de-jellynated which corresponds to up to 3.5 ml of crude extract. However, consider that some frogs might not lay or will lay bad eggs.

2. Inject 500 I.E. human chorionic gonadotropin (hCG) per frog the evening before the experiment (5 ml syringes, 27G 3/4" needles). This will induce the release of the eggs. Keep the frogs for 13-17 hr at 18 °C in individual tanks containing 1.2 l 1x MMR (pH 8).
3. Collect the eggs by pouring them into 600-1,000 ml glass beakers.
4. Wash eggs intensively, approximately 4 times, with 1x MMR by decanting the supernatant when the eggs have settled down and refilling the beaker with fresh buffer afterwards.

NOTE: The eggs are stable before they are dejellynated and the washing buffer can be directly applied on the eggs.

5. Dejellynate the eggs by incubation in the 2% cystein solution. Change buffer once after 2-4 min by decanting the buffer and carefully filling the beaker with fresh buffer. Consider dejellynating complete when the volume of the eggs drastically decreases and the eggs become more densely packed.

NOTE: The dejellyning needs approximately 5-7 min and should be stopped when visible but latest after 10 min.

6. Wash eggs approximately 4 times with 1x MMR by decanting and refilling the buffer supernatant.
7. Activate eggs in 100 ml 1x MMR by adding 8 µl of the calcium ionophore (2 mg/ml in ethanol). Stop activation when animal cap contraction becomes visible or after 10 min.

NOTE: The animal cap contraction can be identified by the compaction of the black half of the egg.

8. Wash carefully 4 times with 1x MMR by decanting and refilling the buffer supernatant.
9. Incubate eggs for 20 min in 1x MMR at RT.
10. Prepare the centrifugation tubes during the incubation time: Place 50 µl sucrose buffer, 50 µl 100-fold protease inhibitor mix, 5 µl 1 M DTT, 12.5 µl cycloheximide (to prevent translation, especially of cyclin B) and 2.5 µl cytochalasin B (to prevent actin polymerization) in 5 ml centrifugation tubes (13 x 51 mm). Alternatively, for more than 30 ml of eggs, 14 ml tubes (14 x 95 mm) can be used, in this case increase volumes by 2.4 times.
11. Wash the eggs twice with cold sucrose buffer (decant and refill buffer in the glass beaker) and transfer them into centrifugation tubes using a plastic Pasteur pipette with wide opening (cut off the narrow end).
12. Pack eggs by spinning for 1 min at 130 x g. Put the tubes in 15 ml conical centrifuge tubes for this purpose (put the 14 ml tubes in 50 ml conical centrifuge tubes, respectively). The goal is to remove as much buffer as possible to prevent dilution of the extract. After centrifugation, remove excess of buffer using a plastic Pasteur pipette and eventually fill more eggs on top.
13. Spin in a 6 x 5 ml swing rotor for 20 min at 21,000 x g at 4 °C.
14. Remove low speed extract using a 5 ml syringe with a 16 G 1 1/2" needle, between yellow yolk on top and dark broken egg debris in the bottom. For this purpose, push the syringe needle through the wall of the centrifuge tube just above the layer of broken egg debris in the bottom. Hold the tube against a resistance when pushing with the needle.
15. Per 1 ml of extract add 10 µl 100-fold protease inhibitor mix, 1 µl of 1 M DTT, 2.5 µl cycloheximide (20 mg/ml) and 0.5 µl cytochalasin B (10 mg/ml). Keep the extract on ice.

NOTE: The extract can be either used directly for the experiment or aliquoted, snap frozen and stored in liquid nitrogen for several months. Freezing the extract will decrease its activity. For delicate experiments like immunodepletion it is highly recommended to use fresh extract immediately.

6. Preparation of Buffers for *In Vitro* Reconstitution of Chromatin Decondensation

1. Prepare the energy mix stock solution containing 25 mM ATP, 25 mM GTP, 127.5 mg/ml creatine phosphate and 2.5 mg/ml creatine kinase in buffer containing 250 mM sucrose, 1.2 mM Hepes, 5.9 mM KCl and 0.3 mM MgCl₂. Aliquot and store at -80 °C. Use freshly after thawing, do not refreeze.
2. Dissolve 0.2 g/ml glycogen in deionized water. Store at -20 °C. Dissolve 6-dimethyl aminopurine (DMAP) to a final concentration of 0.25 M in DMSO. Aliquot and store at -20 °C. Use freshly after thawing, do not refreeze.

3. Prepare 30 % (w/v) sucrose in PBS, filter and store at 4 °C. Prepare 4 % VikiFix solution containing 80 mM PIPES pH 6.8, 1 mM MgCl₂, 150 mM sucrose and 4 % paraformaldehyde (PFA) (**CAUTION!** work under chemical hood, wear gloves and mouth protection).
NOTE: The PFA is difficult to dissolve therefore it is recommended to do it as following: For 1 l Viki-Fix dissolve 24.2 g PIPES and 40 g PFA in separate beakers, both in hot (almost boiling) deionized water. Both will dissolve through addition of 10 N NaOH but be careful to not add too much. Add 51.4 g sucrose and 1 ml 1 M MgCl₂ to the PFA solution. Add the PIPES solution to the other mix. Fill up to 1 l final volume and adjust pH to neutral by adding NaOH.
4. Dissolve 10 mg/ml 4',6-diamidino-2-phenylindole (DAPI) in water (**CAUTION!** wear gloves). Store in the dark at -20 °C.

7. Protocol for *In Vitro* Reconstitution of Chromatin Decondensation

1. Spin low speed interphasic extract for 12 min at 386,000 x g in a fixed angle 20 x 0.2 ml or at 355 000 x g in a 10 x 2.0 ml rotor.
2. Gently remove the lipid layer on top using a vacuum pump or pipette and take the supernatant (thereafter called high speed extract) avoiding membrane contamination from the bottom layer and discard the pellet.
NOTE: To reduce possible membrane contamination it is advisable to spin the extract twice or to dilute the extract with 20 % of the volume with sucrose buffer before the centrifugation. However, dilution and additional centrifugation steps can reduce the extract activity.
3. Pipet 18 µl of high speed extract into a 1.5 ml reaction tube, add 0.7 µl mitotic cluster (amount can be slightly varied according to chromatin stock concentration), 0.5 µl glycogen, 0.5 µl energy mix and 0.3 µl DMAP. Use tips with wide opening to mix the reaction as soon as the chromatin is added to prevent shearing of the decondensing chromatin.
NOTE: The reaction can be performed in the presence or absence of membranes (see **Figure 3**). To decondense chromatin in the presence of membranes, add 2 µl of floated membranes prepared according to the protocol described by Eisenhardt *et al.*¹⁶
4. Incubate the reaction mixture for up to 2 hr (or less to study earlier time points of the decondensation process) at 20 °C.
5. Fix the sample by adding ice cold 0.5 ml Viki-Fix containing 0.5% glutaraldehyde and 0.1 mg/ml DAPI and incubation for 20-30 min on ice.
NOTE: If the samples will be further processed for immunofluorescence, the fixation should be done without glutaraldehyde as this often interferes with the antibody staining. However if only the DAPI staining will be analyzed, the addition of glutaraldehyde will preserve a nicer chromatin structure.
6. Incubate round coverslips (diameter 12 mm) for 5 min with poly-L-lysine solution to increase the affinity of the coverslips to chromatin. Dry the coverslips on filter paper afterwards.
7. Assemble flat-bottom centrifugation tubes (6 ml, 16/55 mm) by putting the coverslips with the coated site to the top on the bottom of the centrifugation tube. Add 800 µl of the 30 % sucrose cushion and layer the fixed sample on top.
8. Spin for 15 min at 2,500 x g at 4 °C.
NOTE: The flat-bottom centrifugation tubes fit to rotors that adopt 15 ml conical centrifuge tubes.
9. Decant the supernatant, then remove the coverslips from the tubes by poking carefully the bottom of the centrifugation tube with a 16 G 1 ½" syringe needle. For this purpose tape the lid of the needle and the needle itself together at their bottoms and cut the front end of the lid so that the needle sticks about 3 mm out. When the coverslip is lifted by the needle on one site, use tweezers to remove the coverslip.
10. Wash the coverslip quickly by dipping it in deionized water, dry it gently by touching its side to a filter paper and place it on the microscope slide on a drop of mounting media. Seal it with nail polish, dry and keep in dark.
NOTE: Samples fixed without glutaraldehyde can be stored in PBS in a 24-well plate and used further for immunofluorescence staining. If stored for several days, add 0.05 % sodium azide (**CAUTION!** wear gloves) to the PBS to avoid contamination with bacteria.
11. Analyze the samples by fluorescence microscopy of the DAPI signal (using *e.g.*, a confocal microscope with a 405 nm laser).

8. Preparation of Buffer for Immunofluorescence Staining of *In Vitro* Reconstituted Chromatin Decondensation Samples

1. Prepare PBS according to 1.1.1. Dissolve NH₄Cl to a final concentration of 50 mM in PBS. Keep this solution at 4 °C. Dissolve 5 µg/ml DAPI in PBS (prepare freshly). Add 0.1 % Triton X-100 to PBS. Keep at 4 °C. Prepare blocking buffer freshly before use by diluting 3 % bovine serum albumin (BSA) in PBS + 0.1 % Triton X-100.

9. Protocol for Immunofluorescence Staining of *In Vitro* Reconstituted Chromatin Decondensation Samples

NOTE: All following incubations of the coverslips are made in a 24-well plate with at least 250 µl solution per well, if not stated otherwise. *In vitro* decondensed chromatin samples are more sensitive than fixed cells therefore be careful when adding or removing solutions. It is recommended to use plastic Pasteur pipettes cut angular. For washing steps and secondary antibody incubation place the plate at RT on rocking or rotating platform, moving not faster than 100 rpm.

1. Quench samples by incubating coverslips with 1 ml NH₄Cl in PBS for 5 min. Block samples by incubating them with 1ml blocking buffer for at least 30 min.
2. Assemble a humidity chamber for the incubation with the primary antibody: Put a wet tissue on the bottom of a closable box and the lid of the 24-well plate upside down on top of the wet tissue. Place parafilm into the lid and add 70 µl of the antibody solution per sample on the parafilm. For the antibody solution, dilute antiserum or affinity purified antibodies 1:100 in blocking buffer.
3. Place the coverslips upside down on top of the antibody solution and incubate them for 1 to 2 hr. Place the coverslips back to the 24-well plate with the sample side facing up and wash samples three times for 10 min with 1 ml 0.1 % Triton X-100 in PBS.
4. Incubate coverslips for 1 hr at RT in 250 µl secondary fluorescently-tagged antibody diluted in blocking buffer to a concentration recommended by the manufacturer. Protect from light. Wash three times for 10 min with 1 ml 0.1 % Triton X-100 in PBS.
5. Incubate the samples for 10 min with 1ml of 5 µg/ml DAPI in PBS. Wash three times for 5 min with 1 ml 0.1 % Triton X-100 in PBS.

6. Wash the coverslip quickly by dipping it in deionized water, dry it gently by touching its side to a filter paper and place it on the microscope slide on top of a drop of mounting media. Seal it with nail polish, dry and keep at 4 °C in the dark until used. Analyze the samples by fluorescence microscopy.

Representative Results

Time dependence of the decondensation reaction

Figure 1 shows a typical time course of the decondensation assay. The cluster of chromosomes visible at the beginning of the reaction decondenses and merges into a single, round and smooth nucleus. When the egg extract is replaced by sucrose buffer the chromosome cluster remains condensed, which suggest that decondensation activity is present in the egg extract.

Chromatin decondensation is an energy dependent process

The *in vitro* decondensation reaction can be conveniently manipulated *e.g.*, by addition of inhibitors. In the experiment shown on **Figure 2**, the non-hydrolyzable ATP or GTP analogs, ATP γ S or GTP γ S, were added to the reaction. Both inhibit the decondensation showing, that it is an ATP and GTP dependent, active process (**Figure 2**).

Chromatin decondensation and nuclear envelope reformation can be separated

The decondensation assay was performed in the presence or absence of membranes (**Figure 3**). Please note that in both conditions chromatin undergoes decondensation, however addition of membranes results in bigger nuclei. Most probably, reformation of the nuclear envelope induces a secondary decondensation step by yet another mechanism dependent on nuclear transport.

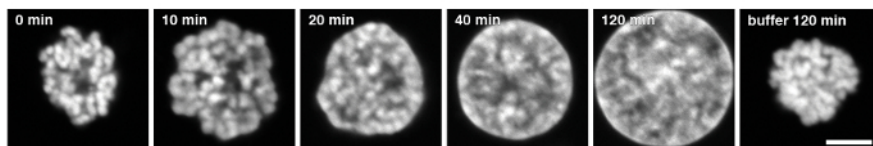


Figure 1. Time course of the *in vitro* decondensation reaction. Mitotic chromatin clusters from HeLa cells were incubated with interphasic *Xenopus* egg extract. Samples were fixed at indicated time points with 4% PFA and 0.5% glutaraldehyde, stained with DAPI and analyzed by confocal microscopy. Re-printed from Magalska *et al.*⁸. Scale bar is 5 μ m. [Please click here to view a larger version of this figure.](#)

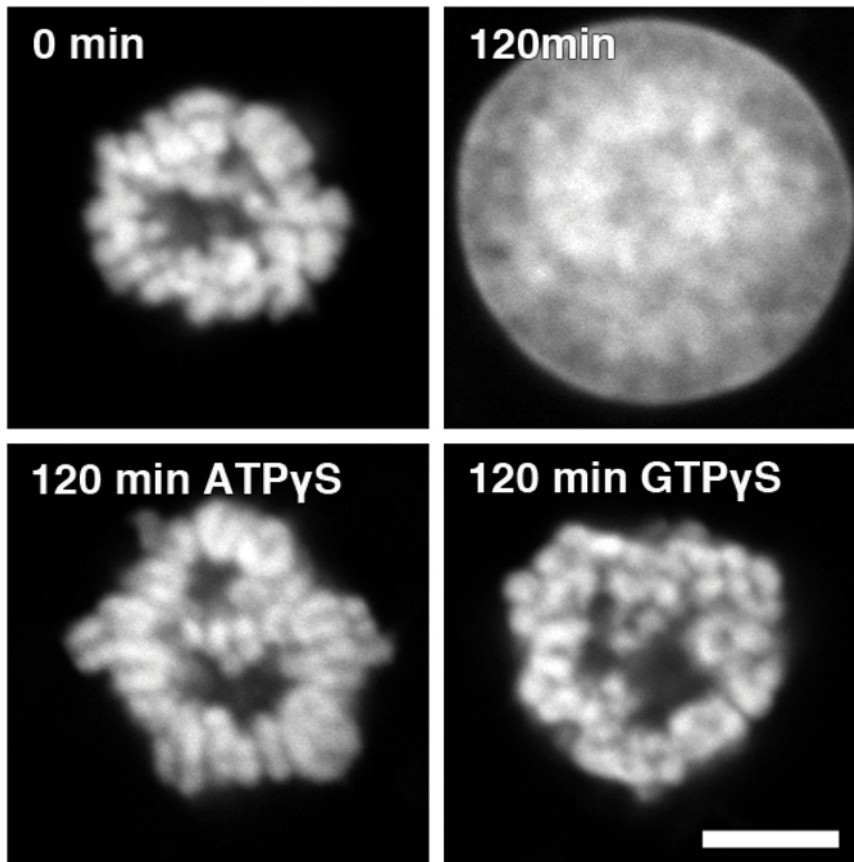


Figure 2. Chromatin decondensation requires ATP and GTP hydrolysis. Chromatin decondensation was performed in the presence of 10 mM ATP γ S, 10 mM GTP γ S or control buffer. Samples were fixed with 4% PFA and 0.5% glutaraldehyde at indicated time points and analyzed by confocal microscopy. Re-printed from Magalska *et al.*⁸. Scale bar is 5 μ m. [Please click here to view a larger version of this figure.](#)

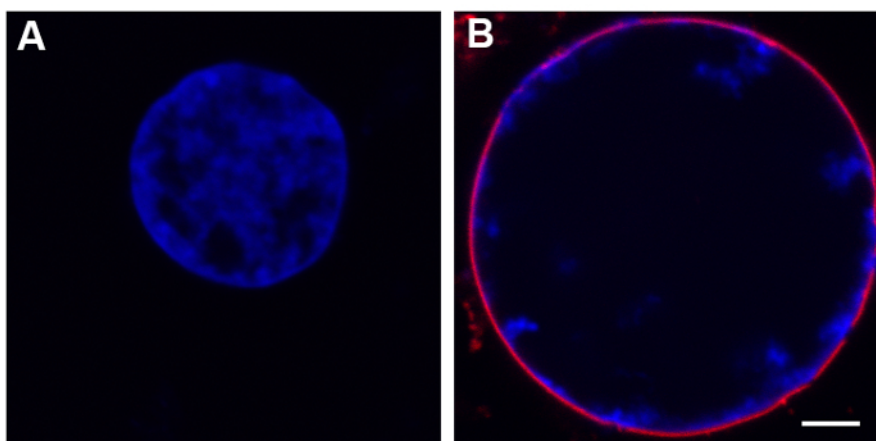


Figure 3. Chromatin decondensation in the presence and absence of membranes. Chromatin decondensation was performed in the absence (A) or presence (B) of floatation purified membranes for 120 min. Samples were fixed with 4% PFA and 0.5 % glutaraldehyde and analyzed by confocal microscopy. Chromatin is stained with DAPI, membranes with DiI_{C18} (1,1'-Dioctadecyl-3,3,3',3'-tetramethylindocarbocyanine perchlorate). Scale bar is 5 μ m. [Please click here to view a larger version of this figure.](#)

Discussion

Xenopus laevis egg extracts are a very useful tool to faithfully reproduce cellular processes *in vitro*, and this system was successfully used in the characterization of cell cycle and cell division events^{2,3,5,6,17}. Due to large stores of nuclear components sequestered in the egg during oogenesis, egg extracts are an excellent source of cellular components. Compared to other approaches like RNAi on mammalian tissue cell lines or genetic manipulation, it offers several advantages: The cell-free system allows studying cellular processes in which cellular viability would

be otherwise a limitation. Moreover single steps of complex processes can be analyzed in simple assays. The here presented decondensation assay allows studying molecular mechanisms of postmitotic decondensation with no interference from other mitotic events, respectively. *Xenopus* egg extracts are easy to manipulate by depletion of specific proteins and addition of inhibitors or mutated proteins⁸. For example, **Figure 2** shows the result of adding the non-hydrolyzable ATP or GTP analogs, ATP γ S and GTP γ S to the decondensation assay. By dilution and differential centrifugation of *Xenopus* eggs components like membranes and cytosol can be separated¹⁶. **Figure 3** shows the decondensation assay performed in the presence or absence of membranes. Finally, the cell-free assay can also be used to identify novel factors *e.g.*, by a fractionation approach. Using such a strategy we have identified the AAA⁺-ATPases RuvBL1/RuvBL2 as crucial decondensation factors⁸.

In vitro systems based on *X. laevis* eggs have been employed with different DNA templates: Forbes *et al.* showed that injection of phage λ DNA into unfertilized *X. laevis* eggs induced the assembly of chromatin on naked phage λ DNA. As injection of viral DNA activated the egg, the assembly of chromatin was followed by formation of a nucleus-like structure¹⁸ and similarly λ -phage DNA can be used in combination with egg extracts to generate nucleus like structures *in vitro*¹⁹. Magnetic beads coated with DNA have been used to study chromatinization of DNA²⁰ and recruitment of nuclear membranes²¹ as well as assembly of a nuclear envelope and pore complexes²², although it remains open to which extent this resembled a bona fide nuclear re-assembly process. The protocol presented here allows decondensation of isolated mitotic chromatin clusters from HeLa cells using extract generated from activated *Xenopus* eggs. It thoroughly reconstructs events leading to a reformation of an interphasic nucleus⁸. Compared to the widely applied nuclear assembly reaction used to study the formation of the nuclear envelope and the nuclear pore complexes at the end of mitosis, in the decondensation assay HeLa mitotic chromatin clusters instead of sperm DNA are used. Sperm DNA can be assembled into mitotic chromatin or even individual chromosomes upon incubation with extract prepared from unfertilized and non-activated eggs³. We decided to use mitotic clusters as chromatin source to simplify the procedure and avoid interference from chromatin condensation. In addition, the preparation of the egg extract is slightly modified: For the chromatin decondensation low speed extract cleared by two high speed centrifugation steps in fixed angle rotors are used. Low speed extract can be stored for up to 6 month in liquid nitrogen without losing its activity. In contrast, in the nuclear assembly reactions, cytosol and floated membranes are generated from low speed extracts by dilution and differential high-speed centrifugation before possible freezing (see Eisenhardt *et al.*¹⁶ for a detailed protocol). In our assay system, addition of membranes allows the formation of a closed nuclear envelope including nuclear pore complexes. The resulting nuclei are competent for nuclear import and export⁸. Thus, this system supports both chromatin decondensation and nuclear envelope reformation. Interestingly, chromatin decondensation is also possible in the absence of membranes (**Figure 3**). However addition of membranes results in slightly bigger nuclei. Most likely, the reformation of the nuclear envelope induces a secondary decondensation step by yet undefined mechanisms, which depends on nuclear import.

For the isolation of mitotic chromatin clusters from HeLa cells, a modified version of the protocol established by Gasser and Laemmli¹⁵ was used. Synchronized mitotic cells are lysed in a buffer containing the non-ionic detergent digitonin and by mechanic forces. The chromatin is isolated as clusters that contain all chromosomes from one nucleus. The crucial difference compared to single chromosome isolation protocols is the fact that the cells are not hypotonically swollen but cooled down to 4 °C before lysis. This prevents the disconnection of the individual chromosomes^{15,23}. Compared to the protocol published by J.R. Paulson²³ who recognized the advantage of the isolation of whole chromatin clusters, Gasser & Laemmli used EDTA-containing polyamine buffers instead of Mg²⁺ based buffers to reduce the activity of kinases, nucleases, proteases and phosphatases and by this decrease the amount of protein and DNA modifications occurring during the isolation process¹⁵. Additionally, using a colloidal silica particles gradient during differential centrifugation highly reduces cytoplasmic contamination. The protocol can also be used to isolate mitotic chromatin clusters from Chinese hamster ovary and mouse cells¹⁵.

Altogether, our protocol faithfully reconstitutes chromatin decondensation as it happens at the end of mitosis. The ATP dependence of the *in vitro* chromatin decondensation can be at least in part explained by the involvement of RuvBL1/2 but also another AAA⁺-ATPase, p97, which removes the mitotic kinase Aurora B from the chromatin during mitotic exit²⁴. Why the process requires GTP hydrolysis is one of the open questions that we intend to answer using this setup.

Disclosures

The authors have nothing to disclose.

Acknowledgements

This work was supported by the German Research Foundation and the ERC (AN377/3-2 and 309528 CHROMDECON to W.A.) and a PhD Fellowship of the Boehringer Ingelheim Fonds to A.K.S. Figure 1 & 2 are reprinted from *Developmental Cell* **31**(3), Magalska *et al.*, RuvB-like ATPases function in chromatin decondensation at the end of mitosis, 305-318, 2014, with kind permission from Elsevier.

References

1. Lohka, M. J., & Masui, Y. Formation *in vitro* of sperm pronuclei and mitotic chromosomes induced by amphibian ooplasmic components. *Science*. **220**, 719-721. (1983).
2. de la Barre, A. E., Robert-Nicoud, M., & Dimitrov, S. Assembly of mitotic chromosomes in *Xenopus* egg extract. *Methods Mol Biol.* **119**, 219-229, (1999).
3. Maresca, T. J., & Heald, R. Methods for studying spindle assembly and chromosome condensation in *Xenopus* egg extracts. *Methods Mol Biol.* **322**, 459-474, (2006).
4. Galy, V. *et al.* A role for gp210 in mitotic nuclear-envelope breakdown. *J Cell Sci.* **121**, 317-328, (2008).
5. Chan, R. C., & Forbes, D. I. *In vitro* study of nuclear assembly and nuclear import using *Xenopus* egg extracts. *Methods Mol Biol.* **322**, 289-300 (2006).
6. Gillespie, P. J., Gambus, A., & Blow, J. J. Preparation and use of *Xenopus* egg extracts to study DNA replication and chromatin associated proteins. *Methods.* **57**, 203-213, (2012).

7. Gant, T. M., & Wilson, K. L. Nuclear assembly. *Annu Rev Cell Dev Biol.* **13**, 669-695, (1997).
8. Magalska, A. *et al.* RuvB-like ATPases function in chromatin decondensation at the end of mitosis. *Developmental Cell.* **31**, 305-318, (2014).
9. Belmont, A. S. Mitotic chromosome structure and condensation. *Curr Opin Cell Biol.* **18**, 632-638, (2006).
10. Lavoie, B. D., Tuffo, K. M., Oh, S., Koshland, D., & Holm, C. Mitotic chromosome condensation requires Brn1p, the yeast homologue of Barren. *Mol Biol Cell.* **11**, 1293-1304, (2000).
11. Philpott, A., & Leno, G. H. Nucleoplasmin remodels sperm chromatin in *Xenopus* egg extracts. *Cell.* **69**, 759-767, (1992).
12. Philpott, A., Leno, G. H., & Laskey, R. A. Sperm decondensation in *Xenopus* egg cytoplasm is mediated by nucleoplasmin. *Cell.* **65**, 569-578, (1991).
13. Burglin, T. R., Mattaj, I. W., Newmeyer, D. D., Zeller, R., & De Robertis, E. M. Cloning of nucleoplasmin from *Xenopus laevis* oocytes and analysis of its developmental expression. *Genes Dev.* **1**, 97-107, (1987).
14. Whitaker, M. Calcium at fertilization and in early development. *Physiological reviews.* **86**, 25-88, (2006).
15. Gasser, S. M., & Laemmli, U. K. Improved methods for the isolation of individual and clustered mitotic chromosomes. *Exp Cell Res.* **173**, 85-98, (1987).
16. Eisenhardt, N., Schooley, A., & Antonin, W. *Xenopus in vitro* assays to analyze the function of transmembrane nucleoporins and targeting of inner nuclear membrane proteins. *Methods Cell Biol.* **122**, 193-218, (2014).
17. Wignall, S. M., Deehan, R., Maresca, T. J., & Heald, R. The condensin complex is required for proper spindle assembly and chromosome segregation in *Xenopus* egg extracts. *J Cell Biol.* **161**, 1041-1051, (2003).
18. Forbes, D. J., Kirschner, M. W., & Newport, J. W. Spontaneous formation of nucleus-like structures around bacteriophage DNA microinjected into *Xenopus* eggs. *Cell.* **34**, 13-23, (1983).
19. Hartl, P., Olson, E., Dang, T., & Forbes, D. J. Nuclear assembly with lambda DNA in fractionated *Xenopus* egg extracts: an unexpected role for glycogen in formation of a higher order chromatin intermediate. *J Cell Biol.* **124**, 235-248 (1994).
20. Sandaltzopoulos, R., Blank, T., & Becker, P. B. Transcriptional repression by nucleosomes but not H1 in reconstituted preblastoderm *Drosophila* chromatin. *EMBO J.* **13**, 373-379 (1994).
21. Ulbert, S., Platani, M., Boue, S., & Mattaj, I. W. Direct membrane protein-DNA interactions required early in nuclear envelope assembly. *J Cell Biol.* **173**, 469-476, (2006).
22. Zhang, C., & Clarke, P. R. Chromatin-independent nuclear envelope assembly induced by Ran GTPase in *Xenopus* egg extracts. *Science.* **288**, 1429-1432, (2000).
23. Paulson, J. R. Isolation of chromosome clusters from metaphase-arrested HeLa cells. *Chromosoma.* **85**, 571-581, (1982).
24. Ramadan, K. *et al.* Cdc48/p97 promotes reformation of the nucleus by extracting the kinase Aurora B from chromatin. *Nature.* **450**, 1258-1262, (2007).



Nuclear Reformation at the End of Mitosis

Anna Katharina Schellhaus[†], Paola De Magistris[†] and Wolfram Antonin

Friedrich Miescher Laboratory of the Max Planck Society, Spemannstrasse 39, 72076 Tübingen, Germany

Correspondence to Wolfram Antonin: wolfram.antonin@tuebingen.mpg.de

<http://dx.doi.org/10.1016/j.jmb.2015.09.016>

Edited by R. W. Kriwacki

Abstract

Cells have developed highly sophisticated ways to accurately pass on their genetic information to the daughter cells. In animal cells, which undergo open mitosis, the nuclear envelope breaks down at the beginning of mitosis and the chromatin massively condenses to be captured and segregated by the mitotic spindle. These events have to be reverted in order to allow the reformation of a nucleus competent for DNA transcription and replication, as well as all other nuclear processes occurring in interphase. Here, we summarize our current knowledge of how, in animal cells, the highly compacted mitotic chromosomes are decondensed at the end of mitosis and how a nuclear envelope, including functional nuclear pore complexes, reassembles around these decondensing chromosomes.

Crown Copyright © 2015 Published by Elsevier Ltd. All rights reserved.

Introduction

The defining feature of the eukaryotic cell is the compartmentalization of genetic material inside the nucleus. The spatial and temporal separation of transcription and translation has enabled eukaryotes to achieve a level of regulatory complexity that is unprecedented in prokaryotes. This is accomplished by the nuclear envelope (NE), which serves as the physical barrier between the cytoplasm and the nucleoplasm (Fig. 1). Nuclear pore complexes (NPCs) are the gateways of the NE allowing diffusion of small substances and regulated trafficking of macromolecules up to a size of 50 nm (for review, see Ref. [1]). The NE consists of two membranes that are separated by the perinuclear space. The inner nuclear membrane (INM) is connected to the outer nuclear membrane (ONM) via the pore membrane, points of fusion where NPCs reside. In addition, the ONM is connected to the membrane network of the endoplasmic reticulum (ER) (Fig. 1). Thus, INM and ONM form a continuum with the ER and can be considered as subcompartments of the latter. However, the INM is additionally characterized by a distinct protein composition. Integral membrane proteins of the INM interact at multiple sites with chromatin and the nuclear lamina, which forms a

tight proteinous network underlying and stabilizing the NE.

For cell division, the genetic material needs to be passed on to the two emerging daughter cells. After the DNA is replicated in S-phase, it must be physically separated by the mitotic spindle, a microtubule-based structure assembled from predominantly cytoplasmic components. In order to allow microtubule contact to chromosomes, different strategies have evolved (for review, see Ref. [2]): many eukaryotes, including yeasts, employ closed or semiclosed mitosis, during which tubulin and microtubule-associated proteins are imported into the nucleus and an intranuclear spindle assembles. In contrast, metazoan cells divide by open or semiopen mitosis (Fig. 2). In this mode, the NE is at least partially disassembled during prophase to allow microtubules access to the chromatin. Concomitantly, the chromatin becomes increasingly condensed and individualized. During metaphase, chromosomes align at the metaphase plate. Once the spindle assembly checkpoint is satisfied due to proper kinetochore–microtubule attachment and tension, chromosomes are segregated in anaphase to the two emerging daughter cells by the mitotic spindle. In late anaphase and telophase, the nucleus starts to reform. We will discuss here nuclear

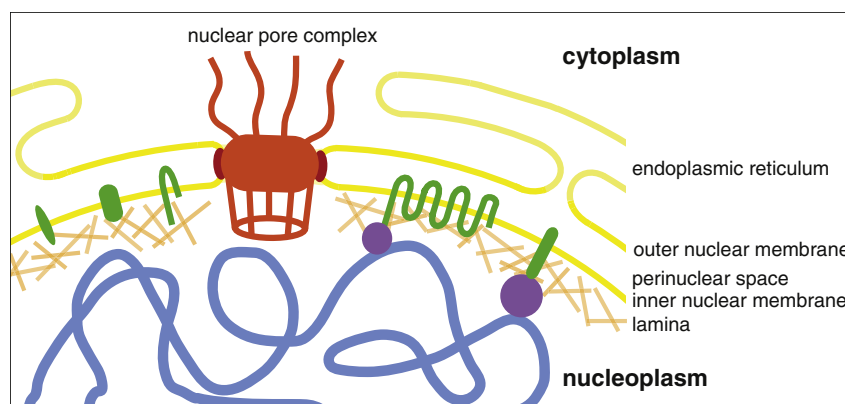


Fig. 1. The metazoan interphase nuclear envelope. The nuclear envelope is formed by two membranes, the inner and outer nuclear membranes that enclose the perinuclear space and that are continuous with the lumen of the ER. Embedded in the nuclear envelope are nuclear pore complexes (red) that shape the two nuclear membranes to a pore. The is defined by a specific set of integral membrane proteins (green) that interact with chromatin (blue), chromatin-associated proteins (violet) and the lamina (beige), a protein meshwork of lamins stabilizing the nuclear envelope.

reformation at the end of mitosis in animal cells, with an emphasis on chromatin decondensation and the reassembly of a functional NE and pore complexes. Comprehensive overviews on how other nuclear structures including nucleoli reform are given in other recent reviews (e.g., see Ref. [3]).

In the last years, progress in answering the relevant questions concerning nuclear reformation has been made both by life cell imaging, mostly in mammalian tissue culture cells (e.g., see Refs. [4–6]) but also in *Caenorhabditis elegans* (for review, see Ref. [7]), and by detailed biochemical analysis. The latter often relies on the use of egg extracts from *Xenopus laevis* that have been extremely instrumental to reconstitute and functionally dissect complicated cellular reactions in a test tube. Often, sperm DNA is used as a chromatin template, around which, after its decompaction, a closed NE including pore complexes is formed. This process occurs naturally when a sperm enters the egg. Although nuclear reassembly in dividing cells has, as far as we know, much in common with this pronuclear assembly, especially, for example, in terms of NPC assembly, some aspects might be adapted to the specific needs of early embryogenesis. In addition, some peculiarities of the cell-free system are attributed to the preparation method. For example, during breakage of the eggs, the ER network fragments and forms vesicles. These vesicles bind to chromatin and fuse to a closed NE upon chromatin incubation in egg extracts, which has been misinterpreted as proof for the existence of membrane vesicles as source of the NE during nuclear reformation at the end of mitosis (for discussion, see Ref. [8]). In this review, we will also attempt to point out where results from *in vitro* experiments should be taken with a grain of skepticism and would benefit from confirmation in living cells.

Mitotic Exit Regulation

Processes initiating the entry of mitosis (Fig. 2) such as NE breakdown, spindle assembly and chromosome alignment are driven by various mitotic kinases, most importantly the cyclin-dependent kinase 1 (CDK1)/cyclin B complex and members of the Aurora and Polo-like kinase (PLK) families (reviewed in Ref. [9]). In addition to its regulation via phosphorylation and dephosphorylation, CDK activation requires binding of cyclins (reviewed in Ref. [10]). In contrast, PLK1 is mainly regulated by its targeting to diverse proteins at different cellular sites throughout the cell cycle that have been primed before by phosphorylation (reviewed in Ref. [11]). Similarly, the localization of Aurora B kinase is tightly regulated during mitotic progression (reviewed in Refs. [12] and [13]). Aurora B is the catalytic subunit of the chromosomal passenger complex (CPC) that additionally consists of the targeting subunits Borealin and Survivin, as well as the bridging subunit INCENP (inner centromere protein). The targeting subunits regulate CPC's localization and translocate the complex from the chromosome arms to the inner centromeric chromatin in early mitosis, where it controls proper attachment of the spindle to the kinetochores. Subsequently, in anaphase, the CPC localizes to the spindle midzone, where it is involved in its stabilization and in cytokinesis.

Mitotic kinases phosphorylate various substrates including nucleoporins (i.e., NPC proteins, Nups), lamins and histones, and they cause a global hyperphosphorylated mitotic state in the cell (e.g., see Ref. [14]). Once the spindle is properly bipolarly attached to the kinetochores, the spindle assembly checkpoint is satisfied and in turn stops inhibiting the anaphase promoting complex (APC) activity (reviewed in Ref. [15]). The active APC, in a complex

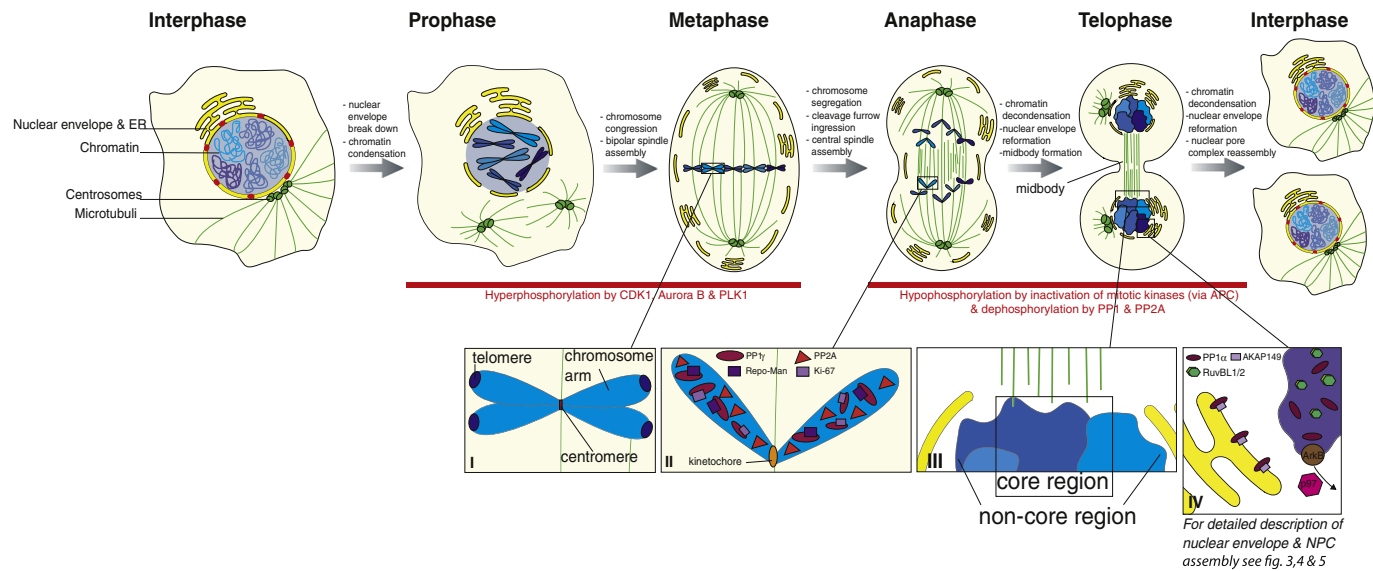


Fig. 2. Mitosis and nuclear reorganization. In interphase, the nuclear envelope encloses the chromatin. When cells enter mitosis, the nuclear envelope breaks down, characterized by nuclear pore complex (red) disassembly and absorption of the nuclear membrane into the ER, microtubule rearrangement and chromatin condensation. In the further mitotic progression, a bipolar spindle assembles and the condensed chromosomes congress to the metaphase plate. All these processes are driven by high activity of mitotic kinases characteristic for the first half of mitosis. The second half of mitosis is characterized by a global decrease in phosphorylation activity both by inactivation of mitotic kinases and by activation of phosphatases. This is required for chromatin decondensation, nuclear envelope and nuclear pore complex reassembly.

with its cofactor CDC20, ubiquitinylates cyclin B and securin and primes them for their proteasomal degradation. The degradation of securin releases the protease separase that is now free to cleave a subunit of the cohesin complex allowing sister chromatid separation. Cyclin B degradation, on the other hand, causes an inactivation of CDK1 that results in the transition from metaphase to anaphase, which is a point of no return. Later in anaphase, the decreased CDK1 activity allows APC to assemble with a different cofactor, CDH1 (CDC20 homolog 1), which broadens its substrate specificity to, for example, Aurora B, PLK1 and its earlier cofactor CDC20. The inactivation and/or degradation of mitotic kinases are necessary but not sufficient to induce mitotic exit. The manifold phosphorylations, previously introduced by mitotic kinases, need to be reversed from their targets to allow for mitotic progression including chromosome segregation, spindle elongation, cytokinesis and reestablishment of the interphasic nucleus. Thus, the ratio of kinase to phosphatase activity defines the shift from early to late mitotic events.

Budding yeast employs a well-studied mitotic exit regulation mechanism, mainly driven by the phosphatase CDC14 (reviewed in Ref. [16]). CDC14 is activated by its release from the nucleolus in early anaphase, induced by the signaling cascade network FEAR (CDC fourteen early anaphase release network) and later sustained by the signaling cascade network MEN (mitotic exit network). However, whereas mitotic entry regulation by the different mitotic kinases is generally conserved in all eukaryotes, CDC14 does not play the prevalent role in mitotic exit regulation in metazoans. Although homologs are found in a large variety of organisms, they seem to have functions unrelated to mitotic exit—however, a role in mitotic exit cannot be excluded either (reviewed in Ref. [17]). Instead, members of the PP1 and PP2A protein phosphatase families seem to be the key players in regulating mitotic exit in metazoans.

The number of catalytic protein phosphatase subunits encoded by the human genome is much smaller as compared to the number of protein kinases. An increased substrate specificity and regulation spectrum is achieved by a large number of regulatory subunits that associate with the catalytic subunits and change their substrate binding capability and localization. PP1 typically forms a heterodimer consisting of one of the four almost identical catalytic subunits, PP1 α , PP1 β/δ , PP1 γ 1 or PP1 γ 2 in mammals and one of several regulatory subunits. PP2A usually forms a heterotrimeric complex consisting of the catalytic subunit PP2A α or PP2A β , the scaffolding subunit PR65 (protein phosphatase 2 regulatory subunit) α or β and one of at least 15 different isoforms of regulatory subunits that belong to the B55, B56, B'' or B''' families.

Although it is controversial whether PP1 and PP2A are direct or indirect antagonists of CDK phosphorylation, both certainly play important roles during mitotic exit.

So far, four different regulatory subunits have been described to be involved in late mitotic functions of PP1: Repo-Man, PNUTS (phosphatase 1 nuclear targeting subunit), Ki-67 and AKAP149 (A-kinase anchoring protein). Repo-Man targets PP1 γ to anaphase chromosomes (Fig. 2, inset II) [18] resulting in dephosphorylation of histone H3 at T3, S10 and S28 [5]. Loss of Repo-Man impairs the reversal of these mitotic H3 phosphorylations and causes abnormally shaped nuclei with irregular NEs and cytoplasmic NPC formation [5]. These observations point to a regulatory role of Repo-Man in NPC reassembly in the reforming NE at the end of mitosis, as cytoplasmic NPC formation, so-called *annulate lamellae*, is often seen upon interfering with this process [19,20]. Repo-Man binds and recruits importin β , a key regulator of NE/NPC reassembly (see sections “Establishing a Nuclear Envelope Membrane Domain” and “Regulating NPC Assembly at the End of Mitosis”), to anaphase chromosomes but the molecular details and mechanisms of the nuclear reformation defects seen upon Repo-Man depletion remain to be elucidated.

Another factor that targets PP1 γ to anaphase chromosomes, only recently identified, is Ki-67 (Fig. 2, inset II). Ki-67 is part of the perichromosomal layer, a coat of mainly nucleolar proteins and RNAs assembling around mitotic chromatin forming an intersection to the surrounding cytoplasm (reviewed in Ref. [21]). Depletion of Ki-67 reduces PP1 γ targeting in anaphase but does not detectably affect NE reformation [22,23]. It remains to be seen whether Ki-67 function is at least in part redundant with Repo-Man and whether codepletion of both targeting subunits aggravates mitotic exit defects.

The targeting subunit PNUTS recruits PP1 α to the reforming nucleus—probably via reviving nuclear import—during mitotic exit but later than chromatin recruitment of PP1 γ by Repo-Man [18,24]. PNUTS accumulates at the nuclear periphery just before the sealing of the NE and has been suggested to regulate chromatin decondensation [24] but the precise targets of PP1 α -mediated dephosphorylation important for this remain to be identified.

The transmembrane-domain-containing protein AKAP149 targets PP1 in a phosphorylation-regulated manner to the reforming NE at the end of mitosis (Fig. 2, inset IV) [25–28]. The PP1 anchoring by AKAP149 is necessary for the dephosphorylation of lamin B resulting in the reformation of the nuclear lamina.

In addition to the recruitment of PP1 catalytic subunits at a specific time point to their site of action, PP1 activity is further controlled via modifications of its regulatory subunit. For example, phosphorylation

of Repo-Man by CDK1/cyclin B prevents PP1 binding, as well as stable chromatin targeting [5,29]. In addition, the catalytic subunit can also be directly regulated. In *Xenopus* egg extracts, protein kinase A phosphorylates the inhibitor 1 upon mitotic entry that, in turn, binds and blocks PP1 [30]. The catalytic subunit of PP1 is further inhibited through direct phosphorylation by CDK1. Low CDK1 levels during mitotic exit are proposed to trigger PP1 to dephosphorylate itself, as well as inhibitor 1 in order to obtain full phosphatase activity. It remains to be seen how conserved this regulation is. Nevertheless, it is conceivable that regulation of PP1 occurs in time, by controlling the activity of the catalytic subunits, and in space, by defining the localization of the complex via its targeting subunits.

In addition to PP1 phosphatases, PP2A complexes have been implicated in mitotic exit regulation. A genome-wide RNAi screen against phosphatases identified the PP2A–B55 α complex as key mitotic exit phosphatase [31]. Downregulation of the regulatory subunit B55 α delayed exclusively mitotic exit, while the catalytic and scaffolding subunits retarded also mitotic entry, hinting to additional early mitotic functions of these PP2A subunits. The assembly of the holoenzyme is prevented by mitotic phosphorylation of B55 α [31] but might be in addition controlled by phosphorylation and methylation of the catalytic subunit [32]. Furthermore, importin β interaction with the PP2A–B55 α is suggested to regulate mitotic exit function of the complex via nucleoplasmic/cytoplasmic transport or via importin β 's function as a molecular chaperone [31]. In contrast to the latter study in human cells, another PP2A regulatory subunit, B55 δ , was implicated in mitotic exit regulation using *Xenopus* egg extracts [33]. Immunodepletion of PP2A–B55 δ leads to premature mitotic entry and blocks exit from mitosis. The experiments suggest that this effect is due to direct or indirect dephosphorylation of CDK substrates.

One of the crucial targets for PP2A dephosphorylation might be the small chromatin binding protein BAF (barrier-to-autointegration factor). BAF functions as a bridge between chromatin, lamins and INM proteins (reviewed in Ref. [34]) and is involved in late nuclear mitotic events, for example, the reformation of the NE, further discussed in later paragraphs (see section “Establishing a Nuclear Envelope Membrane Domain”). Aside from its manifold other interaction partners, BAF binds to the INM protein LEM4 (LEM domain containing 4) [35]. Upon mitotic entry, BAF is phosphorylated by VRK1 (the vaccinia-related kinase 1) that leads to its dissociation from chromatin, LEM4 and other INM proteins. This occurs simultaneously with NE breakdown [36,37]. Upon mitotic exit, LEM4 inhibits VRK1 and recruits PP2A. PP2A dephosphorylates BAF and enables its chromatin and INM protein binding

capability that is necessary for the nuclear reformation [35] (Fig. 3). Thus, it is conceivable that LEM4 acts as a PP2A regulatory subunit in this case. This, however, is a matter of controversy, as a different study suggests that PP4 is the major BAF phosphatase [38] and thus additional features of BAF regulation during mitotic exit might be involved. Nevertheless, the LEM4–BAF pathway shows that further possibilities of tuning protein phosphatase activities and new regulatory subunits might be involved in mitotic exit control, awaiting their identification and characterization.

In summary, PP1 and PP2A phosphatases have each been independently linked to mitotic exit control (Fig. 2, insets II and IV). However, the relative contributions and respective importance of the two phosphatase families remain controversial. As both are controlled by phosphorylation, it is conceivable that PP1 and PP2A activities interdepend from each other by cross-dephosphorylation or inhibiting the corresponding inactivating kinases. Indeed, a mitotic phosphatase relay system was recently described in fission yeast, where PP1 activation is required for the reactivation of PP2A to coordinate mitotic progression and exit [39]. It will be interesting to see whether similar principles also account for mitotic exit regulation in metazoans.

Chromatin Decondensation

Chromatin structure in the interphase nucleus is not random: instead, chromosomes assemble in specific territories, which are often cell type specific and maintain a relative radial position with respect to the nuclear periphery (reviewed in Refs. [40] and [41]). Within the last years, it has become increasingly clear that this three-dimensional organization plays an important role in regulation of gene expression (reviewed in Ref. [42]). Also, on smaller scales, many local and long-range contacts among genes and other sequence elements that organize the genome exist. A number of controversial models of the interphasic chromatin structure aim explaining genome organization, each based on different microscopy techniques, as well as genomic approaches such as 3-C, 4-C, 5-C and Hi-C (reviewed in Ref. [43]). The first level of compaction is achieved by wrapping the DNA around nucleosomes—consisting of core histone octamers—to form a 10-nm chromatin fiber (referring to the diameter of the fiber). Already the next layer of compaction is disputed: recent results question the existence of the 30-nm fiber for which different models have been proposed based on electron microscopy and *in vitro* assembly studies, and these rather suggest a more dynamic, disordered folding accompanied by nucleosome fluctuations influencing the chromatin accessibility (reviewed in Ref. [44]). The mechanism of formation

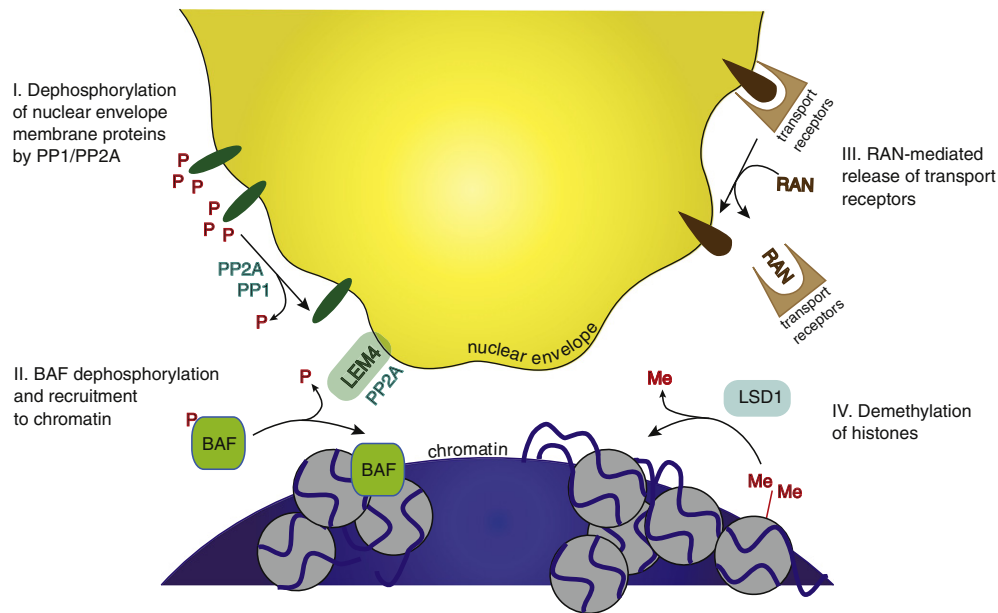


Fig. 3. Regulation of nuclear membrane recruitment to chromatin. Nuclear membrane recruitment to chromatin at the end of mitosis is regulated by dephosphorylation of INM proteins (I) and chromatin proteins (II) such as the LEM4/PP2A-mediated dephosphorylation of BAF. Not only RAN-mediated release of transport receptors (III) but also changes on the chromatin landscape (IV) such as LSD1-mediated histone demethylation might contribute.

of any higher-order organization, although clearly evident from a variety of experiments, remains similarly controversial.

Equally unsecured is our knowledge about the structural organization of mitotic chromosomes, a topic that has been fascinating biologists for decades. Although it was apparent from early days of mitosis research that mitotic chromatin is condensed, estimates about the compaction grade of mitotic chromatin in animal cells compared to its interphase state differ considerably, from 2-fold to 50-fold [45,46]. As for the interphasic chromatin structure, microscopic, biophysical and recently chromosome conformation capture methods led to various models attempting to explain how these structures are organized. These models fall mainly into two broad categories: one class of models proposes that the DNA hierarchically folds into increasingly higher-order structures (e.g., see Refs. [47] and [48]). The second class suggests that mitotic chromatin forms series of loops that are attached to a central chromosome scaffold axis (e.g., see Ref. [49]). Interestingly, recent chromosome conformation capture results suggest that mitotic chromatin indeed consists of loops of various sizes [50]. According to this study, compartmentalization and specific domains of interphasic chromatin are lost during formation of mitotic chromosomes, leading to homogenous mitotic chromosome structures independent of the cell type. In contrast, another recent study suggests that the DNase I sensitivity profile of mitotic and interphasic chromatin

is not changed globally [51]. This indicates that the accessibility of chromatin is not altered during the cell cycle, with a few local exceptions such as hypersensitive regions in interphase that indeed lose accessibility to a larger extent than other regions.

Although many potential chromatin condensation factors have been identified, their exact functions often remain controversial. This might be attributed to the fact that mitotic chromatin condensation, in preparation for sister chromatid separation, most likely requires several distinct activities that are due to their contemporaneous and probably interdependent nature hard to distinguish in molecular terms: this includes disentanglement of sister chromatid DNA molecules, compaction of chromatin into the thread-like structure and probably the formation of a longitudinal scaffold axis with a certain rigidity. Condensins and topoisomerase II, both major chromosomal components, are often regarded as key factors in establishing the mitotic chromosome structure. Because of its decatenation activity [52], topoisomerase II is certainly involved in DNA disentanglement [53]. Whether it is in addition required for chromatin compaction is controversial: experiments in fission yeast and *Xenopus* egg extracts have implicated a requirement for topoisomerase II α in chromatin condensation [54,55], in agreement with pioneering work from the Laemmli laboratory, where the protein was identified as a major nonhistone component of the scaffold axis [56,57] involved in chromatin condensation [58,59]. However, knockdowns of topoisomerase II α in fly

and human cell lines impair chromosome segregation but do not result in prominent condensation defects [60,61]. Condensins have been identified as chromatin condensation factors in *Xenopus* egg extracts [62,63]. In most eukaryotes, two condensin complexes exist, condensin I and condensin II, which form a ring-like structure including an ATPase subunit. There is universal agreement that condensins are involved in sister chromatid disentanglement [53,64]. Whether these protein complexes actually drive mitotic chromatin compaction has always been controversial (reviewed in Ref. [65]). RNAi data from various organisms suggest that cells lacking condensins are defective in chromosome segregation rather than chromatin condensation [66–68]. Alternatively, a so-far unknown regulator of chromosome architecture was suggested to induce mitotic chromatin formation, later inhibited by the Repo-Man–PP1 complex and replaced by condensins in their possible function of stabilizing mitotic chromosomes [29]. This model results from the observation that conditional knockout of the shared condensins I and II subunit SMC2 causes anaphase chromatin bridges and loss of compact chromosome architecture, which can be rescued by the inhibition of Repo-Man-guided PP1 recruitment to anaphase chromosomes. However, recent experiments show that, at least in meiotic cell divisions in mice, condensins have a crucial role in chromatin thread formation [69] and indicate that condensins might be indeed functioning in both DNA disentanglement and compaction.

Two condensin interacting proteins have been implicated in mitotic chromatin condensation, MCPH1 (microcephalin 1) and KIF4A (kinesin family member 4A) [70,71]. MCPH1 is thought to regulate loading of condensin II on chromatin [70]. MCPH1 mutations lead to premature condensation, delayed decondensation and disturbed metaphase chromatin structure [72]. This seemingly counterintuitive phenotype for a condensation factor loading protein might be explained by an altered ratio of condensins I and II on the chromatin. In line with this, shifting the ratio of condensin I to condensin II complexes affects mitotic chromatin structure in *Xenopus* egg extracts [73], pointing to the possibility of counteracting or at least nonredundant functions of condensins I and II, which also target to chromatin at different time points during mitotic entry [74]. In the case of KIF4A, its depletion was suggested to cause hypercondensation [71]. However, recent results indicate that KIF4A depletion rather affects structural integrity of mitotic chromosomes [75]. Therefore, it was proposed that KIF4A and condensins promote lateral chromosome compaction by loop formation, while topoisomerase II promotes axial compaction upon decatenation of the loops.

Histone modifications are crucial regulators of chromatin structure and function, most prominently

in remodeling interphasic chromatin in order to stimulate or repress gene expression. Whether changes in chromatin structure induced by histone modifications also play a role in mitotic chromatin compaction and decompaction is arguable. Some posttranslational histone modification patterns depend on the developmental or cell cycle stage (reviewed in Ref. [76]). For example, H3K27 trimethylation shows a different pattern in interphase compared to mitosis, hinting to partial remodeling of the epigenome during mitosis [77]. Striking mitotic marks are phosphorylations of threonine 3 and serine 10 of histone H3. The former is involved in recruiting CPC to the centromere in early mitosis (reviewed in Ref. [13]). The second, widely used as a convenient mitotic mark, was due to its correlation with the compacted chromatin state thought to be involved in or even cause chromatin condensation and conversely dephosphorylation of H3S10 in chromatin decondensation (e.g., see Ref. [78]). However, H3S10 phosphorylation and chromatin condensation can be uncoupled and are thus not essential for each other [79–82]. Thus, H3S10 phosphorylation might be part of another mitotic function, unrelated to chromatin condensation. It is, for example, required for the release of the heterochromatin protein HP1 from chromatin [83] and it is conceivable that it is similarly involved in the detachment and/or recruitment of other chromatin binding factors during mitosis. Newer results obtained by cross-linking experiments in yeast argue again for an involvement of H3S10 phosphorylation in chromatin condensation by recruiting the histone deacetylase Hst2p to this modified site. Hst2p deacetylates H4K16, enabling the interaction of the H4 tail with the neighboring nucleosome leading ultimately to chromatin condensation [84]. However, it remains open whether this mechanism also contributes to mitotic chromatin condensation in metazoans. Yeasts undergo closed mitosis and compact their chromatin to a much smaller extent [85] and thus might use a different, less sophisticated, mechanism. Additionally, the decrease of the distance of two loci on a single chromosome as analyzed by Wilkins *et al.* [84] does not necessarily reflect the condensation of the whole genome.

The highly condensed mitotic chromatin is segregated to the two emerging daughter cells once the spindle assembly checkpoint is satisfied. Maximal compaction of mitotic chromosomes is, however, not attained at metaphase but rather at late anaphase when segregation is almost complete [86]. This compaction is achieved by axial shortening of the chromosome arms in a condensin-independent manner, regulated by Aurora B kinase activity. The late maximal compaction could be necessary to resolve anaphase chromatin bridges by a “pulling-apart” mechanism, or it could serve as a security mechanism shortly before NE reformation to ensure

that all chromosomes are integrated into the reconstituted nucleus. The chromokinesin KIF22 is involved in this maximal axial compaction in late anaphase, although the exact function still needs to be uncovered [87]. Later on, the compacted chromatin decondenses in a yet-ill-defined process.

Chromatin decondensation has been mostly investigated on sperm chromatin after fertilization. The highly compacted sperm DNA decondenses by exchanging the protamines X and Y—sperm-specific histones—to the canonical core histone proteins H2A and H2B. This exchange is executed by the oocyte protein nucleoplasmin in an ATP-independent manner [88,89]. This process differs from decondensation of somatic chromatin at the end of mitosis, as the latter does not involve protamine to histone exchange. Indeed, chromatin decondensation at the end of mitosis does not require nucleoplasmin [82], consistent with the fact that nucleoplasmin is absent from somatic cells [90]. Using a cell-free assay based on *Xenopus* egg extracts and isolated mitotic chromatin from somatic cells, it was shown that mitotic chromatin decondensation requires cellular energy in the form of ATP and GTP [82]. This suggests that chromatin decondensation is an active process and not simply chromatin relaxation caused by the dissociation of chromatin condensation factors. Consistently, in this assay, chromatin decondensation depends on the presence of egg extracts, in contrast to earlier observations where a basal decondensation activity of mitotic chromatin was observed in the presence of only buffer and an ATP-regenerating system [24]. This discrepancy might be explained by a less harsh chromatin isolation procedure used in Landsverk *et al.* [24] that might retain more proteins on the chromatin.

The ATP dependence is, at least in part, explained by the dependence of chromatin decondensation on the AAA⁺-ATPase p97 (also known as valosin-containing protein (VCP) in vertebrates and CDC48 in yeast) [91]. p97, in a complex with its cofactors UFD1 (ubiquitin fusion degradation 1) and NPL4 (nuclear protein localization 4), is required for the removal of ubiquitylated Aurora B kinase from chromatin (Fig. 2, inset IV). It is currently unclear whether Aurora B needs to be removed from chromosomes in order to inhibit its kinase activity toward chromosomal substrates. Alternatively, removal might be necessary in order to function at a different location at this late mitotic state or simply to increase chromatin accessibility for chromatin decondensation factors at specific sites. In HeLa cells, p97-UFD1-NPL4 seems to be directly antagonizing Aurora B activity already at early mitotic stages, which is required for faithful chromosome segregation [92]. Also in this case, the relevant Aurora B targets, whose phosphorylations need to be prevented, are unidentified.

A second ATPase complex formed by RuvBL1 and RuvBL2 (RuvB-like 1/2, also known as Pontin/Tip49 and Reptin/Tip48) is involved in chromatin decondensation at the end of mitosis [82]. RuvBL1 and RuvBL2 are AAA⁺-ATPases that form together a mixed dodecameric complex. They are involved in a variety of cellular processes including snoRNP, telomerase complex and spindle assembly, chromatin remodeling, transcriptional regulation and signal transduction (reviewed in Ref. [93]). The precise function of RuvBL1/2 in chromatin decondensation, like in many other processes, still needs to be uncovered. However, their chromatin enrichment during mitotic exit [82] and their known function as components of different chromatin remodeling complexes in interphase implicate that they might similarly act by restructuring chromatin at the end of mitosis. Certainly, it is also possible that RuvBL1/2 recruits and activates, or removes and inactivates, relevant chromatin decondensation or condensation factors, respectively, to their site of action. Although the recombinant RuvBL1/2 complex rescues the depletion phenotype of these ATPases from *Xenopus* egg extracts regarding chromatin decondensation, the complex alone is not sufficient to drive chromatin decondensation, indicating that other, yet-unknown crucial factors are required [82]. The fact that chromatin decondensation depends on GTP hydrolysis [82] suggests that a GTPase is involved in the process. Although being involved in many mitotic processes [94] including NE and pore complex reformation at the end of mitosis (see sections “Establishing a Nuclear Envelope Membrane Domain” and “Regulating NPC Assembly at the End of Mitosis”), RAN (Ras-related nuclear protein) seems not to be involved, as excess of RAN mutants does not block chromatin decondensation (our unpublished data). Therefore, future studies are needed to identify the GTPase involved in chromatin decondensation and its precise function.

To establish a fully functional interphase nucleus, not only the chromatin needs to decondense but also an NE needs to reform (discussed in detail in section “The Nuclear Envelope Emerges from the Mitotic ER”). Formation of the NE was suggested to contribute to chromatin decondensation, via involvement of the INM proteins SUN1 (Sad1 and UNC84 domain containing 1) and the lamin B receptor (LBR). In the case of LBR, a truncated version of the protein, missing the domain necessary for the chromatin interaction, causes failure of NE assembly and inhibition of chromatin decondensation [95]. However, cells expressing truncated LBR undergo apoptosis in early G1 phase of these daughter cells and the observed condensed phenotype might be attributed to apoptosis that is also characterized by hypercondensed chromatin. SUN1, a member of the LINC (linker of nucleoskeleton and cytoskeleton)

complex, which in interphase connects the cytoplasmic and nuclear cytoskeleton, accumulates in anaphase on the chromosome periphery concomitantly with the initiation of the NE reformation. SUN1 is suggested to target the histone acetylase hALP, which acetylates histones H2B and H4 on several sites, to the NE [96]. siRNA-mediated downregulation of SUN1 leads to delayed decondensation, often accompanied by apoptosis, while a fusion protein consisting of the N-terminus of SUN1 lacking the transmembrane region and full-length hALP induces premature decondensation, even before chromatin segregation. Although it is not clear to which extent the N-terminus of SUN1 enhances hALP chromatin localization, these results suggest that histone modifications are involved in the chromatin condensation–decondensation cycle. To which extent the NE contributes to this remains unclear. *In vitro*, chromatin decondensation and formation of a closed NE can be functionally separated [82]. Here, chromatin can decondense in the absence of NE formation. However, the presence of membranes leads to a further enlargement of the volume occupied by chromatin [82,97]. This is most likely due to the fact that formation of a functional NE including NPCs allows for nuclear import. This increase in nuclear volume is referred to as nuclear swelling or nuclear expansion [89,98]. Whether it only reflects an increase of nuclear volume due to the presence of more nucleoplasmic proteins or indeed a further decompaction of the chromatin remains to be seen.

We still are largely ignorant about the factors involved in chromatin decondensation, as well as their regulation or the exact structural rearrangements occurring, but it is important to consider that mitotic chromatin consists of different structural and functional compartments: one can, at least, distinguish the chromosome arms, the centromeres involved in mitotic spindle attachment via the kinetochores and telomeres that protect the chromosome ends (Fig. 2, inset I). It is most likely too simple to imagine that all these domains decondense via the same mechanism—however, we are far from understanding the differences yet. Chromatin regions that are more densely packed during interphase undergo less compaction/decompaction during mitosis compared to less densely packed areas—although both undergo obvious condensation/decondensation [99]. This is in line with the formation of homogenous mitotic chromosomes [50]. Also, decompaction of the chromatin is not the only requirement for the formation of a properly functional nucleus. The chromatin needs to acquire a highly elaborated structure consisting of different territories and domains with different grades of compaction—often correlating with the transcriptional activity (reviewed in Ref. [40]). Additionally, nuclear bodies—most prominent thereby nucleoli—need to

reform, each enriching different protein and RNA factors usually at specific gene loci to fulfill their individual functions in the interphase nucleus (reviewed in Refs. [3] and [100]).

The global interphase chromatin pattern is similar between the mother and daughter cells [101]. Life cell imaging of chromatin decondensation revealed a radial expansion mechanism with little relative rearrangements, meaning that “mitotic chromatin neighbors” also become “interphasic neighbors” [99]. Thus, the interphasic genome structure is already established before NE reformation. How can the cell inherit this specific structure if all mitotic chromosomes show a similar, homogenous structure? The timing of sister chromatid separation—probably defined by the individual amount of centromeric heterochromatin—defines the position of single chromosomes in the reforming nucleus [101]; sister chromatids positioned close to the spindle poles separate earlier than the ones close to the cleavage furrow. It is unlikely that sister chromatid separation timing is the only mechanism to transfer the information necessary to reestablish such a subtle interphasic nuclear structure. Epigenetic memory cannot only be retained by chromatin localization but it is conceivable that chromatin modification scenarios are involved. Among these, retention of transcription factors and other chromatin binding proteins on the chromatin during mitosis—although globally removed as transcription is inhibited during mitosis - or maintenance of some specific posttranslational histone modifications could contribute (reviewed in Ref. [102]). How these events are coordinated with overall chromatin decompaction and NE reformation remains to be seen.

The Nuclear Envelope Emerges from the Mitotic ER

The NE reforms on the decondensing chromatin and reestablishes the barrier between the nucleoplasm and the cytoplasm. The nuclear membranes are continuous with the ER membranes; therefore, the NE can be regarded as a subdomain of the ER. This becomes especially obvious during metazoan mitosis, when the NE breaks down and its membranes merge into, and are, at least on a light-microscopical level, undistinguishable from the bulk ER [103–105]. The morphology of the mitotic ER and thus the starting point for ER restructuring leading to NE reestablishment at the end of mitosis is a matter of debate. Some studies suggest that ER sheets convert into fenestrated sheets and tubules [106–108] whereas others propose that tubules transform into sheets [109–112]. Depending on the model of mitotic ER structure, NE reformation at the end of mitosis is differently envisioned: ER tubules are thought to extend from the ER network, contact the decondensing chromatin, become immobilized and flatten and expand to give rise to INM and ONM

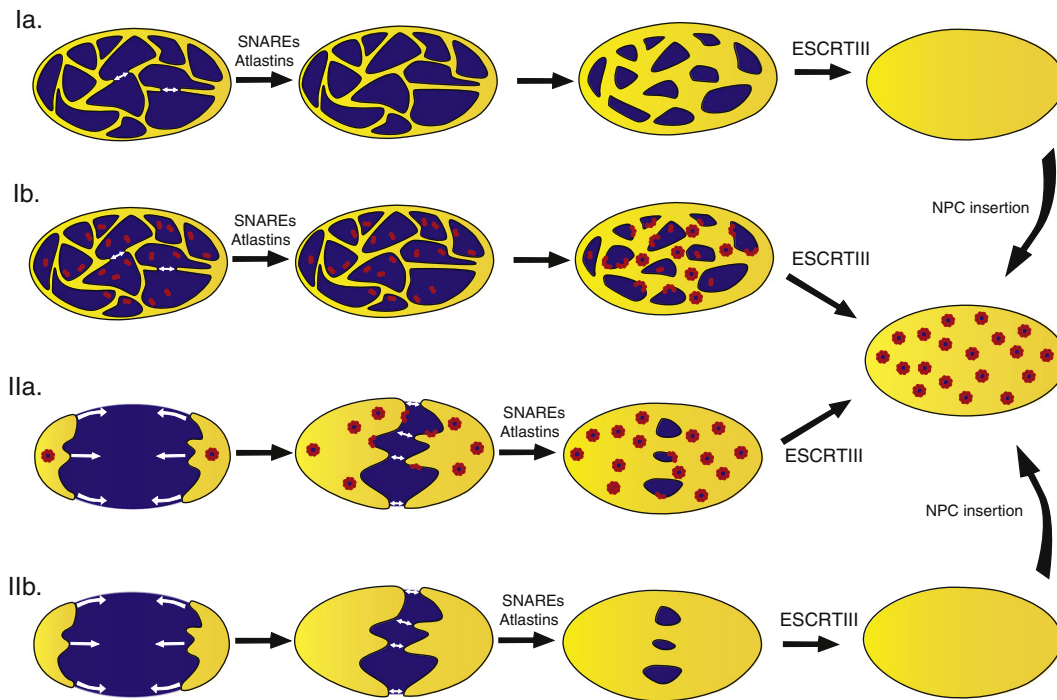


Fig. 4. Nuclear envelope reformation by ER restructuring. The nuclear envelope is formed by reorganization of the mitotic ER. Tubular ER structures are suggested to contact the chromatin, form a network on the surface, flatten and close the remaining holes to form a closed nuclear envelope (Ia and Ib). Alternative models propose that ER membrane sheets contact the chromatin, spread on its surface and enclose it (IIa and IIb). Necessary membrane fusion and sealing events are indicated. Both types of models are compatible with a simultaneous formation of a closed nuclear envelope and NPCs (enclosure models, Ib and IIa) or integration of NPCs in the already sealed nuclear envelope (insertion models, Ia and IIb).

sheets [106] (Fig. 4, Ia and Ib). Alternatively, flat ER membrane sheets would contact and subsequently enclose the chromatin to form the NE [111] (Fig. 4, IIa and IIb). As both interphasic and mitotic ER network morphologies vary considerably between cell types [107,113], it is conceivable that both modes of NE formation exist, depending on the cell type.

The ER interacts with microtubules in interphase and this interconnection undergoes important remodeling during mitosis. The mitotic ER is excluded from the central spindle area and from the chromosomes until the onset of NE reformation in late anaphase [108,114]. In mitosis, the association of ER membranes with microtubules is strongly reduced, and it is very likely that this contributes to ER exclusion from the spindle [112,115,116]. Indeed, mitotic phosphorylation of the integral ER membrane protein STIM1 (stromal interaction molecule 1) abolishes its interaction with microtubules and a STIM1 phosphorylation mutant causes aberrant accumulation of ER membranes within the mitotic spindle in HeLa cells [116]. Microtubule binding of another ER membrane protein, CLIMP-63 (cytoskeleton-linking membrane protein 63), is similarly negatively regulated by mitotic phosphorylation

[117,118] and it is conceivable that this modification similarly helps to exclude the ER from the spindle area. In addition, an active mechanism contributes to the clearance of the ER from the central spindle area: the ER membrane proteins REEP3 and REEP4 (receptor expression-enhancing proteins 3 and 4) function as linkers between the ER and microtubules and transport the ER that has entered the spindle area to the spindle poles [4]. Depletion of REEP3/REEP4 causes cytokinesis and chromosome segregation defects, as well as aberrant shaped nuclei in interphase. This highlights the importance of correct mitotic ER morphology and distribution.

Microtubules *per se* seem not to be required for NE reformation [112,119,120] and microtubule formation rather needs to be inhibited close to chromatin [121]. Depletion of DPPA2 (developmental pluripotency associated 2), a chromatin binding and microtubule destabilizing protein, from *Xenopus* egg extracts or the addition of the microtubule stabilizing drug taxol, prevents NE formation. Interestingly, nuclear expansion is inhibited by pervasively depolymerizing microtubules when DPPA2 is delocalized from chromatin and thus ectopically active or when microtubule depolymerizing agents

such as colcemid or nocodazol are added [121,122]. This effect could be due to a reduction of ER membranes around the reassembled nuclei, as ER membranes are required for nuclear membrane expansion to allow nuclear growth [122–124]. Notably, the NE formed *in vitro* in the presence of colcemid and nocodazol reportedly does not contain NPCs [120] and hence the subsequent, expected lack of nuclear import could explain, at least in part, the nuclear growth defect. Consistently, long-term exposure of sublethal concentrations of the microtubule inhibitor colchicine or vinblastine induces formation of *annulate lamellae* in tissue culture cells [125] that also indicates, as previously mentioned, a malfunction in NPC reassembly into the reforming NE at the end of mitosis [19,20]. The lack of NPCs could indicate that microtubules contribute to the proper segregation of nuclear membrane domains from the ER membrane continuum at the end of mitosis, including transmembrane nucleoporins crucially required for NPC formation [126,127]. It remains to be seen whether an NE reformed in the absence of functional microtubules contains typical INM proteins at a comparable level.

Establishing a Nuclear Envelope Membrane Domain

In late anaphase, nuclear membranes start approaching chromatin [103,104,128]. It is thought that integral membrane proteins of the INM and their chromatin binding affinity are the driving force for this process [123,129]. Many INM proteins including LBR [130–132] and the LEM-domain-containing proteins LAP2 β (lamin-associated polypeptide 2 β) [133,134], MAN1/LEMD3 [135] and emerin [136] associate with chromatin, in the case of LBR by interacting with HP1 [137]. LEM-domain-containing proteins interact with the previously introduced chromatin-associated protein BAF (see section “Mitotic Exit Regulation”). BAF recruits LEM-domain-containing proteins to chromatin during mitotic exit, and the LEM proteins reciprocally modulate the distribution of BAF during interphase [138–140]. In addition to BAF-mediated recruitment, binding of several INM proteins to chromatin, including transmembrane nucleoporin NDC1 (nuclear division cycle 1) and POM121 (pore membrane protein), can occur by a direct DNA binding capability that relies on the presence of basic domains [129]. The rapid recruitment of membranes to chromatin at the onset of anaphase might therefore be explained by the existence of more than one chromatin interaction strategy of INM proteins. These multiple interactions might also explain why individual INM proteins are nonessential for nuclear reassembly *in vivo*, with the exception of LBR, for which opposing results have been reported [95,123].

Binding of both, soluble and membrane proteins, to the chromatin surface at the end of mitosis does not occur uniformly but can be referred to two zones on the chromatin area, called core and noncore chromatin regions (Fig. 2, inset III). The core (or central) region is established on the surfaces proximal and distal to the mitotic spindle, and the noncore region is established on the surfaces lateral to the mitotic spindle. The core region is enriched in A-type lamins but also with emerin and LAP2 β , which are recruited locally by BAF [138,141]. Other factors such as lamin B, LBR and nucleoporins localize preferentially on the peripheral noncore region [138,142,143]. Interestingly, the initial steps of NPC formation, that is, the binding of chromatin by the nucleoporin MEL28/ELYS (maternal effect lethal/embryonic large molecule derived from yolk sac) and the recruitment of Nup107-160 complex on the noncore region, control the formation of chromatin subdomains [144], linking NPC assembly to the establishment of chromatin reorganization at the end of mitosis. It is currently unclear which specific features of noncore chromatin render it competent for MEL28/ELYS binding and subsequent NPC assembly.

The reassociation of nuclear membranes with chromatin and the reestablishment of the NE are tightly regulated in time and space. Different mechanisms are involved, including phosphorylation/dephosphorylation cycles on INM proteins, regulation of the chromatin proteins BAF and HP1, presumably the RAN system and potentially also histone modifications (summarized in Fig. 3). Chromatin binding of nuclear membranes is controlled *in vitro* by the counteracting activities of CDK1/cyclin B [145–147], which blocks chromatin association, and protein phosphatases, namely PP1 [146,148], which promote membrane recruitment. A variety of integral NE proteins, including GP210, LBR, LAP2 β , emerin, MAN1, NDC1 and POM121 are phosphorylated at the onset of mitosis, which is thought to prevent their association with chromatin and contribute to the disassembly of the NE [14,127,149–151]. Conversely, one would expect that dephosphorylation of these proteins during mitotic exit triggers their chromatin recruitment. Although this is conceivable, in most instances, evidence for a direct contribution of phosphorylation/dephosphorylation cycles in the regulation of chromatin binding and NE dynamics of these proteins is lacking. The best-characterized example is the recruitment of LBR to chromatin at the end of mitosis, which also points out that the regulation might be more complex. LBR binding to chromatin is prevented *in vitro* by phosphorylation of a specific serine residue in an arginine/serine repeat domain [148,152,153]. The timing of ER membrane recruitment of LBR to anaphase chromosomes is controlled by LBR dephosphorylation in human cells [154]. In addition to dephosphorylation in its arginine/serine repeat domain, phosphorylation of LBR by the

serine/arginine-rich protein-specific kinase SRPK1 [152,153,155] is required for its association with chromatin *in vitro*.

Two chromatin-associated proteins, HP1 and BAF, link chromosome decondensation and NE formation. Chromatin recruitment of HP1 requires the dephosphorylation of histone H3 at S10 and is promoted by H3K9 methylation, a characteristic histone modification of heterochromatin [83,156–158]. HP1 chromatin recruitment in anaphase [159] could cooperate in the association of LBR with chromatin during mitotic exit, in addition to the fact that LBR can also interact directly with DNA, histones and other chromatin-associated proteins [160]. The presence of Aurora B on mitotic chromosomes prevents the recruitment of nuclear membranes and by that ensures that the NE does not assemble before successful segregation of the chromatin [91,161]. The putative phosphorylation targets of Aurora B in this process are unknown, but it is possible that serine 10 phosphorylation of histone H3 is involved: this particular phosphorylation, in fact, would prevent HP1 chromatin localization [83]. Chromatin recruitment of BAF during anaphase is crucial for NE reassembly and is regulated by its phosphorylation. BAF phosphorylation by the kinase VRK1 reduces its affinity for chromatin [37], and loss of the BAF-mediated link between chromatin and nuclear membranes contributes to NE disassembly [36]. As discussed above (see section “Mitotic Exit Regulation”), the INM LEM4 is required for BAF dephosphorylation during mitotic exit by recruiting PP2A and by inhibiting VRK1 [35]. Thus, the NE/chromatin interaction via LEM proteins is at least in part regulated by cell-cycle-dependent phosphorylation/dephosphorylation cycles of BAF (Fig. 3).

Cell-cycle-dependent waves of phosphorylation and dephosphorylation can account for the temporal coregulation of mitotic chromosome decondensation, NE formation and NPC assembly. However, NE assembly, as well as NPC assembly, must be restricted to the chromatin. This regulation is thought to be provided by the small GTPase RAN, which in interphase functions in nucleoplasmic/cytoplasmic transport of cargos across the NPC. RAN, in its GTP-bound state that is locally generated in the nucleus, stimulates the release of importin-bound cargo in the nucleoplasm, but it is also required for many mitotic processes. Despite the absence of an NE, chromatin is demarcated by a high concentration of the GTP-bound RAN throughout the cell cycle [162] and GTP-bound RAN-mediated release of importins from a variety of target proteins controls a range of processes, varying from spindle assembly and chromatin segregation to assembly of the nuclear membranes and nuclear pores around chromatin, in later stages of mitosis (for review, see Ref. [94]). It is conceivable that the RAN/importin

system, used by the cell to target integral membrane proteins to the NE in interphase [20,163], also regulates the recruitment of INM proteins to post-mitotic chromatin in a similar way (Fig. 3) [164]. Importin β binds LBR during mitosis [95,165] and this inhibitory complex dissociates in the presence of GTP-bound RAN [165]. The importin family might prevent undesired interactions between the positively charged DNA binding domains of INM proteins and chromatin during mitosis. In the case of LBR, the importin β and chromatin binding sites overlap. Indeed, a functional RAN cycle is essential for nuclear assembly *in vitro* [166,167] but whether this is directly via regulation of NE/chromatin interactions remains to be seen.

In parallel with RAN as a spatial marker for chromatin, chromatin modifications during mitotic exit might also contribute to the regulation of nuclear membrane recruitment. In addition to the possible involvement of H3 Ser10 dephosphorylation in regulation of HP1 chromatin localization, the lysine-specific demethylase LSD1 has been implicated in regulation of NE reformation. LSD1 catalyzes the demethylation of monomethylated and dimethylated lysines K4 and K9 of histone H3 tails [168]. Downregulation in HeLa cells extends telophase and affects NE reassembly [97]. *In vitro* experiments suggest that nuclear membrane recruitment to chromatin is impaired upon inhibition or removal of LSD1. Although nonhistone protein targets of LSD1 demethylase activity cannot be excluded, the identification of the histone demethylase LSD1 as an essential regulator of nuclear assembly indicates that cell cycle regulated chromatin state and more precisely histone modifications play a role in controlling nuclear membrane binding on the decondensing chromatin (Fig. 3).

In summary, the reversal of mitosis-specific phosphorylations on nuclear membrane proteins regulates the timing of nuclear membrane recruitment to chromatin; nonetheless, the precise sites of modification have yet to be identified and it is currently not clear how prevalent this mode of regulation is. Changes on the chromatin landscape at the end of mitosis contribute similarly; these include binding of chromatin-associated factors such as BAF and HP1 and probably also changes in the histone modification patterns. Spatial organization by the RAN system might facilitate the binding of nuclear membrane proteins to chromatin by exposing their DNA binding domains proximally to chromatin, but the contribution of such a mechanism has not been proved yet.

Nuclear Envelope Sealing

Complete fusion of the membranes at the newly forming nucleus is required for reestablishment of

nuclear compartmentalization. As the NE and the ER are connected and share similar mechanics, it is possible that NE fusion employs the same machinery and factors as the bulk ER. In *Xenopus* egg extracts, NSF (NEM-sensitive factor) and α -SNAP (soluble NSF adaptor protein), factors of the SNAP receptor (SNARE) activation, are critically required for formation of a closed NE [112,169], suggesting that SNARE-mediated membrane fusion is needed. However, the specific SNARE proteins involved in NE formation still await identification. Formation and maintenance of an ER network additionally requires integral membrane GTPases, atlastins, which mediate fusion between ER tubules [170,171]. *In vitro*, formation of a closed NE is blocked by a dominant negative version of atlastin [112], suggesting an involvement of this GTPase, most likely because the NE formation is initiated in this experimental setup by an ER network formed on the chromatin surface [166]. Given the controversy whether ER sheets or tubules are the membrane structure initiating NE formation, it remains to be seen whether and to which extent atlastins also directly contribute to closed NE formation *in vivo*.

Two recent studies indicate components of the ESCRT-III (endosomal sorting complex required for transport) complex as involved in NE reformation, as depletion of ESCRT-III constituents results in failure to seal the NE and, therefore, in leaky nuclei [172,173]. ESCRT-III is known to participate in constricting the neck of membrane buds or even entire cells, during vesicle formation into multivesicular bodies, HIV virus egress and cytokinesis. During NE reformation, it is suggested to function in a topologically similar event: the closure of final gaps that remain open when NE encloses the chromatin. These gaps might be holes in the NE that remain after membrane flattening and expansion of an ER network [106] if not filled by NPCs (Fig. 4, insets Ia and Ib, see below). Alternatively, the holes could be the ones remaining when sheet-like membranes enclosing the chromatin merge (Fig. 4, insets IIa and IIb) [111].

Although the studies in Refs. [172] and [173] agree on the crucial role of the ESCRT-III complex in NE closure, each adds distinctive insights into ESCRT-III function in nuclear sealing. Vietri and collaborators show that the ESCRT-III complex recruits the microtubule severing ATPase spastin [173]. Spastin is suggested to disassemble spindle microtubules, which would otherwise prevent NE sealing. Olmos and colleagues show that the ATPase p97 recruits the ESCRT-III complex via its adaptor protein UFD1 to function in NE sealing [172]. Interestingly, earlier *in vitro* data suggested that p97 is required for NE reassembly together with UFD1 and another cofactor, NPL4 [174]. p97 depletion impairs formation of a closed NE, although membrane vesicles still bind but fail to fuse to an ER-like network on the chromatin

template. This phenotype is difficult to reconcile with sealing of small holes in the reforming NE mediated by the ESCRT-III complex. It rather suggests that p97 is also involved in additional, yet-uncharacterized steps in NE reformation. As sperm chromatin was directly incubated with interphasic extracts in these experiments [174], it is unlikely that the extraction of Aurora B from chromatin mediated by p97, observed on mitotic chromatin [91], accounts for the crucial p97 function also in this experimental system.

During vesicle formation in multivesicular body formation, the ESCRT machinery recognizes ubiquitinated membrane proteins [175]. The fact that p97, which recognizes ubiquitinated proteins via its adaptors UFD1 and NPL4, is involved in the pore sealing process [176] points into the same direction. If so, it remains to be seen which NE membrane proteins are crucial ubiquitinated targets for the ESCRT-III function in NE sealing.

Building NPCs into the Nuclear Envelope

The coordinated reassembly of NPCs begins concomitantly with the reformation of the NE. NPCs form large pores in the envelope with a diameter of approximately 130 nm at the sites where the ONM and INM fuse [177]. Only a few of the roughly 30 different nucleoporins are integral membrane proteins residing in the ER during mitosis. Most nucleoporins are soluble during open mitosis in animals and are recruited from the cytosol to reassemble NPCs during mitotic exit. Two profoundly different modes for NPC reassembly at the end of mitosis have been proposed, insertion or enclosure (see Fig. 4, discussed in Ref. [178]). According to insertion models, NPCs assemble and integrate into the two juxtaposed membrane sheets of an intact NE [111,179,180]. NPC formation would thus follow the formation of a closed NE and requires the fusion of the ONM and INM across the NE lumen. Alternatively, enclosure models propose that NPC reassembly does not occur by insertion into the sealed NE, but it is rather accomplished by the contact and envelopment of the assembling NPCs on the chromatin surface by the outgrowing ER-derived membranes [178,181–183]. Both suggested modes of NE formation (an ER network that forms and flattens on the chromatin surface or outgrowing ER membrane sheets; discussed earlier in the text) are compatible not only with enclosure but also with insertion models (Fig. 4).

The general NPC structure can be regarded as a stack of three rings with cytoplasmic and nucleoplasmic extensions: the outer or cytoplasmic ring is connected to the cytoplasmic filaments whereas the nuclear ring is connected to the nuclear basket. Sandwiched between those two peripheral rings and

located in the midplane of the NE lays the so-called spoke or inner ring. The inner ring is laterally linked to the pore membrane and connected to the central transport channel formed mostly by the FG-repeat-containing nucleoporins. Although NPC dimensions and masses vary among organisms, this general structural arrangement, including the 8-fold symmetry, is conserved (for review, see Ref. [184]). Understanding the assembly pathway of these huge structures lastly embedded in the two membranes of the NE remains a formidable task. *Xenopus* egg extracts have been extensively employed for delineating the assembly pathway, as individual steps such as initiation, membrane association, termination of the NPC scaffold assembly and establishment of the transport channel can be disconnected and studied separately in this system.

Despite the differences in the models for NPC reassembly at the end of mitosis, it is commonly agreed that the process is initiated on chromatin (Fig. 5) by the nucleoporin MEL28/ELYS [19,185–187]. MEL28/ELYS can bind DNA directly, but recent elegant reconstitution experiments show that its binding to histone-containing chromatin is crucial for NPC assembly [188,189]. MEL28/ELYS acts as a seeding point for NPC formation and recruits the Nup107-160 complex to assembly sites [19]. The Nup107-160 complex is an essential scaffolding component of NPCs and forms the largest part of the cytoplasmic and nucleoplasmic rings [177,190]. *In vitro*, MEL28/ELYS and the Nup107-160 complex can bind to chromatin in the absence of membranes [19,183,186,191]. The first connection between the assembling NPC and nuclear membranes is achieved by the subsequent association of the transmembrane nucleoporin POM121 with the newly forming pores [126], a process likely mediated by binding of POM121 to the Nup107-160 complex [192,193]. It is also likely that NDC1, another transmembrane nucleoporin that is found at forming pores at the same time [127], also contributes to the connection of NPCs to membranes, but the mechanism remains to be established.

The following steps can be ordered starting from the membrane sites of the pore and proceeding toward the center of the pore. First, nucleoporins of the second major structural complex within NPCs, the Nup93 complex, join the assembling pore, presumably forming the majority of the inner ring [6]. The Nup93 complex contains the nucleoporins Nup93, Nup53 and Nup155 and the two orthologues Nup188 and Nup205. In contrast to the Nup107-160 complex, which is recruited as a preassembled complex, the Nup93 complex builds from individual components [124,194–196]. In assembled NPCs, the different components of the complex are present in different numbers ranging from 16 to 48 [197]. The precise arrangement of these nucleoporins, with respect to each other and within the inner ring,

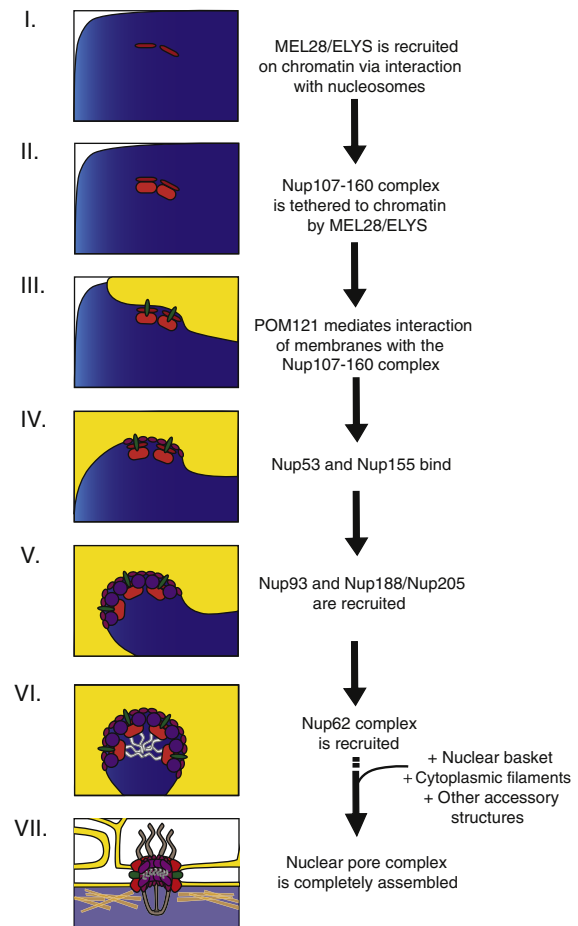


Fig. 5. Ordered NPC assembly at the end of mitosis. The chromatin binding nucleoporin MEL28/ELYS initiates NPC assembly on the chromatin (I) by recruiting the Nup107-160 complex (II), which in turn associates with the nuclear envelope membranes via the transmembrane nucleoporin POM121 (III). The recruitment of the Nup93 complex is mediated by its membrane-associated nucleoporins, Nup53 and Nup155, which interact with integral membrane proteins at the nascent pore membrane (IV) and promote the incorporation of Nup93, Nup188 and Nup205 to complete the structural backbone of the NPC (V). The subsequent recruitment of FG-repeat-containing nucleoporins of the Nup62 complex (VI) combined with the previous association Nup98 (data not shown) establishes the central channel, a hydrophobic meshwork that confers the transport properties of the NPC. The fully assembled NPC (VII) consists of multiple copies of the component nucleoporins, which are arranged in octagonal symmetry to create a cylindrical channel. Peripheral structures include the cytoplasmic filaments and the nuclear basket, protruding from opposite faces of the NPC.

remains to be defined. In the assembly process of the Nup93 complex, Nup53 is the first to associate with the nascent pore, followed by Nup155 [198,199]. Both proteins can directly bind membranes [194,200] and both also interact with the transmembrane nucleoporins NDC1 and POM121

[127,192,193] and therefore constitute a second connection between the NPC and membranes at the pore. Interaction of Nup53 with NDC1 also modulates Nup53's membrane bending activity, which is crucial for successful NPC assembly [198]. This indicates that protein–protein and protein–membrane interactions are not only required for timely recruitment of the different NPC components but also involved in a more sophisticated interplay that we just begin to unravel. Nup93 interacts with Nup53 and is subsequently incorporated [196], together with its binding partners Nup188 and Nup205 [124], to complete the structural backbone of the pore. Nup93, probably together with interactions via Nup205/Nup188, recruits the FG-repeat-containing nucleoporins of the Nup62 complex [196,201]. The Nup62 complex members Nup62, Nup58 and Nup54/45, together with the FG-containing nucleoporin Nup98, form a large part of the hydrophobic meshwork localized in the center of the pore. Nup98 is recruited at the same time as the Nup93 complex [6] by a still-ill-defined mechanism. It is possible that its interaction to the Nup107-160 [202] takes part in Nup98 recruitment.

The formation of peripheral NPC structures, such as the nuclear basket on the nucleoplasmic side and the cytoplasmic filaments, follows the establishment of the structural pore and central channel [6]. On the nuclear side, Nup153 is required for the recruitment of Nup50 and TPR [203–205]. It is likely that Nup153 itself is recruited via its interaction with the Nup107-160 complex [202]. If so, it remains to be seen why Nup153 only interacts with Nup107-160 complexes located in the nuclear ring structure. The order of events in the assembly of the cytoplasmic filaments is less defined, but Nup358 is required for this [206].

Despite significant progresses in delineating the assembly pathway of NPCs, a number of important questions remain. Many nucleoporins are symmetrically distributed within the nucleoplasmic and cytoplasmic rings of the NPC, including the Nup107-160 complex [177], but the timing and details of the mechanism by which the cytoplasmic portion of the NPC assembles remain elusive. Within the nucleoplasmic and cytoplasmic rings, 16 Nup107-160 complexes arrange into two concentric rings of eight units [177]. It is unclear whether these rings assemble simultaneously or whether these are distinguishable events. The Nup107-160 complex interacts with different nucleoporins in the nucleoplasmic and cytoplasmic rings, for example, with MEL28/ELYS in the nucleoplasmic ring and Nup358 in the cytoplasmic ring. What defines these different interaction patterns remains to be elucidated. The same questions apply for Nup98, which is present in 48 copies within the vertebrate NPC [197]. Finally, despite the known octagonal symmetry of the pore, further work is needed to establish whether the

numerous copies of each subcomplex are recruited simultaneously around the pore circumference.

Once a closed NE with functional NPCs has reassembled, the nuclei further expand, and they assemble and accommodate more NPCs, a process that continues during all interphase and that is hence referred to as interphase or *de novo* NPC assembly. It is a matter of debate whether NPC reformation at the end of mitosis and interphase NPC assembly follow the overall same pathway. In all likelihood, at least in interphase, NPC assembly follows an insertion pathway as NPC integrates into the already intact NE. Whereas NPC reformation at the end of mitosis critically requires MEL28/ELYS [19,185], it is dispensable for NPC formation occurring in interphase [20]. New evidences suggest that the function of MEL28/ELYS as initiating assembly point is taken over by Nup153 in interphase NPC assembly. Nup153 would then direct the Nup107-160 complex to the INM and pore assembly sites [207]. This functional difference in initiation, on the chromatin at the end of mitosis and on the nuclear membranes during interphase, might be an indication that, in contrast to interphase NPC assembly, NPC reassembly at the end of mitosis follows an enclosure pathway. The need for membrane deforming and/or membrane deformation sensing modules required in some nucleoporins specifically for interphase NPC assembly [20,194,207] is in agreement with this hypothesis. However, a step toward a definitive answer will be made when the fusion machinery required for the fusion of ONM and INM is identified. The prediction for the enclosure model is that NPC reassembly does not depend on this machinery, in contrast to interphase NPC assembly. On the other hand, the insertion model forecasts that both assembly modes depend, in all likelihood, on the same fusion machinery.

Regulating NPC Assembly at the End of Mitosis

As the NE breaks down at the beginning of mitosis, NPCs disassemble into their building blocks, which are, with the exception of the few transmembrane nucleoporins, largely dispersed in the mitotic cytosol as single proteins or in some cases as subcomplexes and do not reassemble into NPCs until mitotic exit. Some nucleoporins have additional functions during mitosis outside of NPC formation, including centrosome positioning, spindle assembly, kinetochore organization, the spindle assembly checkpoint, chromosome segregation and cytokinesis (for review, see Ref. [94]). Several nucleoporins, including members of the Nup107-160 complex, Nup98, Tpr and Nup53, are hyperphosphorylated during mitosis [127,150,208–212] and it has been suggested that this phosphorylation cascade acts as a

general mechanism to keep nucleoporins dissociated, preventing premature NPC reassembly and at the same time allowing for their diverse mitotic functions. For instance, hyperphosphorylation of Nup98 initiates the NPC disassembly at the beginning of mitosis [209]. Conversely, interactions between nucleoporins could be promoted by late mitotic dephosphorylations. However, the fact that the kinases and phosphatases involved perform a variety of functions in mitotic entry, progression and exit (see section “Mitotic Exit Regulation”) results in the lack of direct evidence for such a mechanism. Moreover, identifying causative phosphorylation events is complicated by a high degree of redundancy, as exemplified by the Nup98 case: Nup98 is phosphorylated by CDK1 and members of the NIMA-related kinase family at 13 different sites to allow for its dissociation from NPC at the entry of mitosis [209]. In addition, it remains to be seen whether other posttranslational changes on nucleoporins regulate NPC disassembly and reassembly.

NPC reassembly is initiated on, and thus directed to, the chromatin surface by RAN. As discussed for NE reassembly, high concentrations of RAN-GTP generated in the vicinity of the chromatin are supposed to release transport receptors from nucleoporins that, in turn, can interact and assemble to NPCs. Good evidence for this model is the aberrant formation of NPCs in ER membrane stacks distal from the NE, *annulate lamellae*, when the RAN-GTP gradient is disturbed [213]. MEL28/ELYS and the Nup107-160 complex are likely candidates for such a RAN-dependent regulation because they bind transport receptors and associate with chromatin in the early stages of NPC assembly [19,186,191,213]. However, many nucleoporins bind transport receptors to facilitate nuclear transport, and these events are not restricted to FG-repeat-containing regions, as in Nup50 and Nup153 for example [214,215]. In addition, nucleoporins also bind transport receptors to allow their import to the nucleoplasmic side of the pore, where they function in *de novo* NPC assembly during the entire interphase [20,207,216]. Notably, Nup153 membrane interaction capability, which is required for initiating interphase NPC assembly, is regulated *in vitro* by the transport receptor transportin [207]. This opens the possibility that both initiating steps, MEL28/ELYS chromatin recruitment after mitosis and Nup153 INM binding in interphase, are regulated by RAN, consistent with the proposal that interphase NPC assembly is also regulated by this GTPase [217]. However, definitive proof for this model is lacking.

As similarly discussed for the regulation of NE reformation, changes on the chromatin landscape during mitotic exit might regulate NPC reassembly. Despite its DNA binding activity, MEL28/ELYS requires nucleosomes for its proper recruitment to

initiate NPC reassembly on the chromatin [188,189]. It is tempting to speculate that histone modifications might contribute to this, especially as MEL28/ELYS distribution is nonhomogenous on the chromatin during mitotic exit, but it first accumulates at the chromosomal noncore region [144]. Furthermore, downregulation of the lysine demethylase LSD1 affects NPC reformation indicated by a high presence of *annulate lamellae* [97], and *in vitro*, MEL28/ELYS chromatin interaction is reduced upon LSD1 depletion. Whether a corresponding increase in methylated histone H3 is causative for the effects and whether the phenotype is primarily an NE defect or an NPC assembly defect remain to be established.

Lamina and LINC Complex Reassembly

In addition to proper NE and NPC formation, nuclear assembly at the end of mitosis must include reestablishment of additional structures. The nuclear lamina is a fibrous structure formed by lamins and located underneath the NE. It is connected to the NE via interactions of lamins with INM proteins and members of the LINC complex. The lamina is depolymerized at the onset of mitosis [218] by the CDK1-mediated phosphorylations of lamins [219,220]. Conversely, lamins are dephosphorylated at the end of mitosis to allow reassembly of this structure. PP1, which is recruited to the NE by AKAP149, removes mitotic phosphorylations from lamin B in telophase [25,221]. Although some association of nuclear lamins is observed during early stages of NE reformation [103], the bulk of nuclear lamins are reassembled into the lamina only after the nuclei have regained competence for nuclear import [26,222]. Arrangements of lamins into the lamina during interphase have been studied intensively, but we still miss a clear picture of how the assembly process occurs (reviewed in Ref. [223]). Similarly, we do not know when the interactions to NPCs are established [103,224], occurring most likely via the lamin-interacting nucleoporin Nup153 [225,226].

The LINC complexes provide physical connection between the backbone scaffold of the intranuclear and extranuclear compartments and play pivotal roles in a vast series of evolutionally divergent tasks, from yeast to mammals (reviewed in Ref. [227]). Since nuclear integrity is lost at the onset of mitosis, it is conceivable that the LINC complexes lose connection with both sides of the NE. Indeed, the LINC complex component SUN1 is phosphorylated by CDK1 at the onset of mitosis that disrupts its lamina interaction [228], whereas binding to KASH domains on the luminal side is not affected. As the LINC complexes provide mechanical stability to the nucleus, it is possible that torsional stress that tears the nucleus during prophase contributes to release

the LINC. Whether LINC complexes themselves remain intact during mitosis as suggested previously [228] for SUN1 and Nesprin 2 remains to be seen under nonoverexpression conditions and for other LINC complex pairs. Independent of this, at the end of mitosis, the LINC complex needs to reestablish its interaction to the nucleoskeleton and probably also to the cytoskeleton. If the LINC complex disassembles during mitosis, it also needs to reassemble and all these pathways remain to be established.

Conclusion

At the end of the open mitosis in metazoans, the interphase nucleus competent for DNA transcription and replication, pre-RNA processing and many other nuclear functions such as biogenesis of ribosomal subunits need to reestablish. For some processes including NE and pore complex reassembly, we have a detailed knowledge about the steps and factors involved despite the fact that a number of open questions remain. For others such as chromatin decondensation, we are just beginning to identify the factors involved and we are largely ignorant about the molecular mechanisms. In addition, the regulation in time and space of the different processes occurring at the end of mitosis is far from being understood and especially how they are coordinated with each other. It is similarly often unclear but conceivable that malfunctions in the different pathways or their coordination would have implications for human diseases. For example, lamina assembly faults are linked to a variety of human diseases, summarized as laminopathies (for review, see Ref. [229]). It remains to be seen whether this applies also to other processes and will be an interesting avenue for future research.

Acknowledgements

We are thankful to Daniel Moreno-Andrés, Marion Weberruss and Hideki Yokoyama for critical comments on the manuscript. This work was supported by the German Research Foundation and the European Research Council (AN377/3-2 and 309528 CHROMDECON to W.A.), a PhD Fellowship of the Boehringer Ingelheim Fonds to A.K.S. and a PhD Fellowship of the International Max Planck Research School "From Molecules to Organisms" to P.D.M.

Received 31 July 2015;

Received in revised form 17 September 2015;

Accepted 19 September 2015

Available online 28 September 2015

Keywords:

nuclear envelope;
nuclear pore complex;
chromatin decondensation;
mitotic exit

†A.K.S. and P.D.M. contributed equally to this work.

Abbreviations used:

NPC, nuclear pore complex; INM, inner nuclear membrane; ONM, outer nuclear membrane; ER, endoplasmic reticulum; CPC, chromosomal passenger complex; APC, anaphase promoting complex.

References

- [1] S.R. Wentz, M.P. Rout, The nuclear pore complex and nuclear transport, *Cold Spring Harbor Perspect. Biol.* 2 (2010) a000562.
- [2] C.J. Smoyer, S.L. Jaspersen, Breaking down the wall: The nuclear envelope during mitosis, *Curr. Opin. Cell Biol.* 26 (2014) 1–9.
- [3] D. Hernandez-Verdun, Assembly and disassembly of the nucleolus during the cell cycle, *Nucleus* 2 (2011) 189–194.
- [4] A.L. Schlaitz, J. Thompson, C.C. Wong, J.R. Yates III, R. Heald, REEP3/4 ensure endoplasmic reticulum clearance from metaphase chromatin and proper nuclear envelope architecture, *Dev. Cell* 26 (2013) 315–323.
- [5] P. Vagnarelli, S. Ribeiro, L. Sennels, L. Sanchez-Pulido, F. de Lima Alves, T. Verheyen, D.A. Kelly, C.P. Ponting, J. Rappsilber, W.C. Earnshaw, Repo-Man coordinates chromosomal reorganization with nuclear envelope reassembly during mitotic exit, *Dev. Cell* 21 (2011) 328–342.
- [6] E. Dultz, E. Zanin, C. Wurzenberger, M. Braun, G. Rabut, L. Sironi, J. Ellenberg, Systematic kinetic analysis of mitotic dis- and reassembly of the nuclear pore in living cells, *J. Cell Biol.* 180 (2008) 857–865.
- [7] M. Gorjanacz, A. Jaedicke, I.W. Mattaj, What can *Caenorhabditis elegans* tell us about the nuclear envelope? *FEBS Lett.* 581 (2007) 2794–2801.
- [8] P. Collas, J.C. Courvalin, Sorting nuclear membrane proteins at mitosis, *Trends Cell Biol.* 10 (2000) 5–8.
- [9] E.A. Nigg, Mitotic kinases as regulators of cell division and its checkpoints, *Nat. Rev. Mol. Cell Biol.* 2 (2001) 21–32.
- [10] M. Malumbres, Cyclin-dependent kinases, *Genome Biol.* 15 (2014) 122.
- [11] M. Petronczki, P. Lenart, J.M. Peters, Polo on the rise—From mitotic entry to cytokinesis with Plk1, *Dev. Cell* 14 (2008) 646–659.
- [12] M. Kitagawa, S.H. Lee, The chromosomal passenger complex (CPC) as a key orchestrator of orderly mitotic exit and cytokinesis, *Front. Cell Dev. Biol.* 3 (2015) 14.
- [13] M. Carmena, M. Wheelock, H. Funabiki, W.C. Earnshaw, The chromosomal passenger complex (CPC): From easy rider to the godfather of mitosis, *Nat. Rev. Mol. Cell Biol.* 13 (2012) 789–803.
- [14] N. Dephoure, C. Zhou, J. Villen, S.A. Beausoleil, C.E. Bakalarski, S.J. Elledge, S.P. Gygi, A quantitative atlas of mitotic phosphorylation, *Proc. Natl. Acad. Sci. U. S. A.* 105 (2008) 10762–10767.

- [15] S. Sivakumar, G.J. Gorbsky, Spatiotemporal regulation of the anaphase-promoting complex in mitosis, *Nat. Rev. Mol. Cell Biol.* 16 (2015) 82–94.
- [16] F. Stegmeier, A. Amon, Closing mitosis: The functions of the Cdc14 phosphatase and its regulation, *Annu. Rev. Genet.* 38 (2004) 203–232.
- [17] A. Mocchiari, E. Schiebel, Cdc14: A highly conserved family of phosphatases with non-conserved functions? *J. Cell Sci.* 123 (2010) 2867–2876.
- [18] L. Trinkle-Mulcahy, J. Andersen, Y.W. Lam, G. Moorhead, M. Mann, A.I. Lamond, Repo-Man recruits PP1 gamma to chromatin and is essential for cell viability, *J. Cell Biol.* 172 (2006) 679–692.
- [19] C. Franz, R. Walczak, S. Yavuz, R. Santarella, M. Gentzel, P. Askjaer, V. Galy, M. Hetzer, I.W. Mattaj, W. Antonin, MEL-28/ELYS is required for the recruitment of nucleoporins to chromatin and postmitotic nuclear pore complex assembly, *EMBO Rep.* 8 (2007) 165–172.
- [20] C.M. Doucet, J.A. Talamas, M.W. Hetzer, Cell cycle-dependent differences in nuclear pore complex assembly in metazoa, *Cell* 141 (2010) 1030–1041.
- [21] A.A. Van Hooser, P. Yuh, R. Heald, The perichromosomal layer, *Chromosoma* 114 (2005) 377–388.
- [22] M. Takagi, Y. Nishiyama, A. Taguchi, N. Imamoto, Ki67 antigen contributes to the timely accumulation of protein phosphatase 1gamma on anaphase chromosomes, *Int. J. Biol. Chem.* 289 (2014) 22877–22887.
- [23] D.G. Booth, M. Takagi, L. Sanchez-Pulido, E. Petfalski, G. Vargiu, K. Samejima, N. Imamoto, C.P. Ponting, D. Tollervey, W.C. Earnshaw, P. Vagnarelli, Ki-67 is a PP1-interacting protein that organises the mitotic chromosome periphery, *Elife* 3 (2014) e01641.
- [24] H.B. Landsverk, M. Kirkhus, M. Bollen, T. Kuntziger, P. Collas, PNUITS enhances *in vitro* chromosome decondensation in a PP1-dependent manner, *Biochem. J.* 390 (2005) 709–717.
- [25] R.L. Steen, S.B. Martins, K. Tasken, P. Collas, Recruitment of protein phosphatase 1 to the nuclear envelope by A-kinase anchoring protein AKAP149 is a prerequisite for nuclear lamina assembly, *J. Cell Biol.* 150 (2000) 1251–1262.
- [26] R.L. Steen, P. Collas, Mistargeting of B-type lamins at the end of mitosis: Implications on cell survival and regulation of lamins A/C expression, *J. Cell Biol.* 153 (2001) 621–626.
- [27] R.L. Steen, M. Beullens, H.B. Landsverk, M. Bollen, P. Collas, AKAP149 is a novel PP1 specifier required to maintain nuclear envelope integrity in G1 phase, *J. Cell Sci.* 116 (2003) 2237–2246.
- [28] T. Kuntziger, M. Rogne, R.L. Folstad, P. Collas, Association of PP1 with its regulatory subunit AKAP149 is regulated by serine phosphorylation flanking the RVXF motif of AKAP149, *Biochemistry* 45 (2006) 5868–5877.
- [29] P. Vagnarelli, D.F. Hudson, S.A. Ribeiro, L. Trinkle-Mulcahy, J.M. Spence, F. Lai, C.J. Farr, A.I. Lamond, W.C. Earnshaw, Condensin and Repo-Man-PP1 cooperate in the regulation of chromosome architecture during mitosis, *Nat. Cell Biol.* 8 (2006) 1133–1142.
- [30] J.Q. Wu, J.Y. Guo, W. Tang, C.S. Yang, C.D. Freil, C. Chen, A.C. Nairn, S. Kornbluth, PP1-mediated dephosphorylation of phosphoproteins at mitotic exit is controlled by inhibitor-1 and PP1 phosphorylation, *Nat. Cell Biol.* 11 (2009) 644–651.
- [31] M.H. Schmitz, M. Held, V. Janssens, J.R. Hutchins, O. Hudecz, E. Ivanova, J. Goris, L. Trinkle-Mulcahy, A.I. Lamond, I. Poser, A.A. Hyman, K. Mechtler, J.M. Peters, D.W. Gerlich, Live-cell imaging RNAi screen identifies PP2A-B55alpha and importin-beta1 as key mitotic exit regulators in human cells, *Nat. Cell Biol.* 12 (2010) 886–893.
- [32] S. Longin, K. Zwaenepoel, J.V. Louis, S. Dilworth, J. Goris, V. Janssens, Selection of protein phosphatase 2A regulatory subunits is mediated by the C terminus of the catalytic subunit, *J. Biol. Chem.* 282 (2007) 26971–26980.
- [33] S. Mochida, S. Ikeo, J. Gannon, T. Hunt, Regulated activity of PP2A-B55 delta is crucial for controlling entry into and exit from mitosis in *Xenopus* egg extracts, *EMBO J.* 28 (2009) 2777–2785.
- [34] A. Margalit, A. Brachner, J. Gotzmann, R. Foisner, Y. Gruenbaum, Barrier-to-autointegration factor—A BAFling little protein, *Trends Cell Biol.* 17 (2007) 202–208.
- [35] C. Asencio, I.F. Davidson, R. Santarella-Mellwig, T.B. Ly-Hartig, M. Mall, M.R. Wallenfang, I.W. Mattaj, M. Gorjanacz, Coordination of kinase and phosphatase activities by Lem4 enables nuclear envelope reassembly during mitosis, *Cell* 150 (2012) 122–135.
- [36] M. Gorjanacz, E.P. Klerkx, V. Galy, R. Santarella, C. Lopez-Iglesias, P. Askjaer, I.W. Mattaj, *Caenorhabditis elegans* BAF-1 and its kinase VRK-1 participate directly in post-mitotic nuclear envelope assembly, *EMBO J.* 26 (2007) 132–143.
- [37] R.J. Nichols, M.S. Wiebe, P. Traktman, The vaccinia-related kinases phosphorylate the N' terminus of BAF, regulating its interaction with DNA and its retention in the nucleus, *Mol. Biol. Cell* 17 (2006) 2451–2464.
- [38] X. Zhuang, E. Semenova, D. Maric, R. Craigie, Dephosphorylation of barrier-to-autointegration factor by protein phosphatase 4 and its role in cell mitosis, *J. Biol. Chem.* 289 (2014) 1119–1127.
- [39] A. Grallert, E. Boke, A. Hagting, B. Hodgson, Y. Connolly, J.R. Griffiths, D.L. Smith, J. Pines, I.M. Hagan, A PP1-PP2A phosphatase relay controls mitotic progression, *Nature* 517 (2015) 94–98.
- [40] T. Cremer, M. Cremer, S. Dietzel, S. Muller, I. Solovei, S. Fakan, Chromosome territories—A functional nuclear landscape, *Curr. Opin. Cell Biol.* 18 (2006) 307–316.
- [41] T. Misteli, Beyond the sequence: Cellular organization of genome function, *Cell* 128 (2007) 787–800.
- [42] W.A. Bickmore, The spatial organization of the human genome, *Annu. Rev. Genomics Hum. Genet.* 14 (2013) 67–84.
- [43] A.S. Belmont, Large-scale chromatin organization: The good, the surprising, and the still perplexing, *Curr. Opin. Cell Biol.* 26 (2014) 69–78.
- [44] K. Maeshima, R. Imai, S. Tamura, T. Nozaki, Chromatin as dynamic 10-nm fibers, *Chromosoma* 123 (2014) 225–237.
- [45] P. Vagnarelli, Mitotic chromosome condensation in vertebrates, *Exp. Cell Res.* 318 (2012) 1435–1441.
- [46] A.S. Belmont, Mitotic chromosome structure and condensation, *Curr. Opin. Cell Biol.* 18 (2006) 632–638.
- [47] J.C. Hansen, Conformational dynamics of the chromatin fiber in solution: Determinants, mechanisms, and functions, *Annu. Rev. Biophys. Biomol. Struct.* 31 (2002) 361–392.
- [48] K. Maeshima, M. Eltsov, Packaging the genome: The structure of mitotic chromosomes, *J. Biochem.* 143 (2008) 145–153.
- [49] J.R. Paulson, U.K. Laemmli, The structure of histone-depleted metaphase chromosomes, *Cell* 12 (1977) 817–828.
- [50] N. Naumova, M. Imakaev, G. Fudenberg, Y. Zhan, B.R. Lajoie, L.A. Mirny, J. Dekker, Organization of the mitotic chromosome, *Science* 342 (2013) 948–953.
- [51] C.C. Hsiung, C.S. Morrissey, M. Udugama, C.L. Frank, C.A. Keller, S. Baek, B. Giardine, G.E. Crawford, M.H. Sung, R.C.

- Hardison, G.A. Blobel, Genome accessibility is widely preserved and locally modulated during mitosis, *Genome Res.* 25 (2015) 213–225.
- [52] J.C. Wang, Cellular roles of DNA topoisomerases: A molecular perspective, *Nat. Rev. Mol. Cell Biol.* 3 (2002) 430–440.
- [53] J. Baxter, N. Sen, V.L. Martinez, M.E. De Carandini, J.B. Schwartzman, J.F. Diffley, L. Aragon, Positive supercoiling of mitotic DNA drives decatenation by topoisomerase II in eukaryotes, *Science* 331 (2011) 1328–1332.
- [54] T. Uemura, H. Ohkura, Y. Adachi, K. Morino, K. Shiozaki, M. Yanagida, DNA topoisomerase II is required for condensation and separation of mitotic chromosomes in *S. pombe*, *Cell* 50 (1987) 917–925.
- [55] T. Hirano, T.J. Mitchison, Topoisomerase II does not play a scaffolding role in the organization of mitotic chromosomes assembled in *Xenopus* egg extracts, *J. Cell Biol.* 120 (1993) 601–612.
- [56] W.C. Earnshaw, B. Halligan, C.A. Cooke, M.M. Heck, L.F. Liu, Topoisomerase II is a structural component of mitotic chromosome scaffolds, *J. Cell Biol.* 100 (1985) 1706–1715.
- [57] C.D. Lewis, U.K. Laemmli, Higher order metaphase chromosome structure: Evidence for metalloprotein interactions, *Cell* 29 (1982) 171–181.
- [58] Y. Adachi, M. Luke, U.K. Laemmli, Chromosome assembly *in vitro*: Topoisomerase II is required for condensation, *Cell* 64 (1991) 137–148.
- [59] S.M. Gasser, T. Laroche, J. Falquet, E. Boy de la Tour, U.K. Laemmli, Metaphase chromosome structure. Involvement of topoisomerase II, *J. Mol. Biol.* 188 (1986) 613–629.
- [60] A.J. Carpenter, A.C. Porter, Construction, characterization, and complementation of a conditional-lethal DNA topoisomerase IIalpha mutant human cell line, *Mol. Biol. Cell* 15 (2004) 5700–5711.
- [61] C.J. Chang, S. Goulding, W.C. Earnshaw, M. Carmena, RNAi analysis reveals an unexpected role for topoisomerase II in chromosome arm congression to a metaphase plate, *J. Cell Sci.* 116 (2003) 4715–4726.
- [62] T. Hirano, R. Kobayashi, M. Hirano, Condensins, chromosome condensation protein complexes containing XCAP-C, XCAP-E and a *Xenopus* homolog of the *Drosophila* Barren protein, *Cell* 89 (1997) 511–521.
- [63] T. Hirano, T.J. Mitchison, A heterodimeric coiled-coil protein required for mitotic chromosome condensation *in vitro*, *Cell* 79 (1994) 449–458.
- [64] A. Charbin, C. Bouchoux, F. Uhlmann, Condensin aids sister chromatid decatenation by topoisomerase II, *Nucleic Acids Res.* 42 (2014) 340–348.
- [65] R. Gassmann, P. Vagnarelli, D. Hudson, W.C. Earnshaw, Mitotic chromosome formation and the condensin paradox, *Exp. Cell Res.* 296 (2004) 35–42.
- [66] K.A. Hagstrom, V.F. Holmes, N.R. Cozzarelli, B.J. Meyer, C. elegans condensin promotes mitotic chromosome architecture, centromere organization, and sister chromatid segregation during mitosis and meiosis, *Genes Dev.* 16 (2002) 729–742.
- [67] D.F. Hudson, P. Vagnarelli, R. Gassmann, W.C. Earnshaw, Condensin is required for nonhistone protein assembly and structural integrity of vertebrate mitotic chromosomes, *Dev. Cell* 5 (2003) 323–336.
- [68] S. Steffensen, P.A. Coelho, N. Cobbe, S. Vass, M. Costa, B. Hassan, S.N. Prokopenko, H. Bellen, M.M. Heck, C.E. Sunkel, A role for *Drosophila* SMC4 in the resolution of sister chromatids in mitosis, *Curr. Biol.* 11 (2001) 295–307.
- [69] M. Houlard, J. Godwin, J. Metson, J. Lee, T. Hirano, K. Nasmyth, Condensin confers the longitudinal rigidity of chromosomes, *Nat. Cell Biol.* 17 (2015) 771–781.
- [70] D. Yamashita, K. Shintomi, T. Ono, I. Gavvovidis, D. Schindler, H. Neitzel, M. Trimborn, T. Hirano, MCPH1 regulates chromosome condensation and shaping as a composite modulator of condensin II, *J. Cell Biol.* 194 (2011) 841–854.
- [71] M. Mazumdar, S. Sundareshan, T. Misteli, Human chromokinesin KIF4A functions in chromosome condensation and segregation, *J. Cell Biol.* 166 (2004) 613–620.
- [72] M. Arroyo, M. Trimborn, A. Sanchez, T. Hirano, H. Neitzel, J.A. Marchal, Chromosome structure deficiencies in MCPH1 syndrome, *Chromosoma* (2015) Epub ahead of print.
- [73] K. Shintomi, T. Hirano, The relative ratio of condensin I to II determines chromosome shapes, *Genes Dev.* 25 (2011) 1464–1469.
- [74] T. Hirota, D. Gerlich, B. Koch, J. Ellenberg, J.M. Peters, Distinct functions of condensin I and II in mitotic chromosome assembly, *J. Cell Sci.* 117 (2004) 6435–6445.
- [75] K. Samejima, I. Samejima, P. Vagnarelli, H. Ogawa, G. Vargiu, D.A. Kelly, F. de Lima Alves, A. Kerr, L.C. Green, D.F. Hudson, S. Ohta, C.A. Cooke, C.J. Farr, J. Rappsilber, W.C. Earnshaw, Mitotic chromosomes are compacted laterally by KIF4 and condensin and axially by topoisomerase IIalpha, *J. Cell Biol.* 199 (2012) 755–770.
- [76] J.C. Black, C. Van Rechem, J.R. Whetstone, Histone lysine methylation dynamics: Establishment, regulation, and biological impact, *Mol. Cell* 48 (2012) 491–507.
- [77] E. Terrenoire, F. McDonald, J.A. Halsall, P. Page, R.S. Ilingworth, A.M. Taylor, V. Davison, L.P. O'Neill, B.M. Turner, Immunostaining of modified histones defines high-level features of the human metaphase epigenome, *Genome Biol.* 11 (2010) R110.
- [78] M.J. Hendzel, Y. Wei, M.A. Mancini, A. Van Hooser, T. Ranalli, B.R. Brinkley, D.P. Bazett-Jones, C.D. Allis, Mitosis-specific phosphorylation of histone H3 initiates primarily within pericentromeric heterochromatin during G2 and spreads in an ordered fashion coincident with mitotic chromosome condensation, *Chromosoma* 106 (1997) 348–360.
- [79] J.Y. Hsu, Z.W. Sun, X. Li, M. Reuben, K. Tatchell, D.K. Bishop, J.M. Grushcow, C.J. Brame, J.A. Caldwell, D.F. Hunt, R. Lin, M.M. Smith, C.D. Allis, Mitotic phosphorylation of histone H3 is governed by Ipl1/aurora kinase and Glc7/PP1 phosphatase in budding yeast and nematodes, *Cell* 102 (2000) 279–291.
- [80] M.E. Murnion, R.R. Adams, D.M. Callister, C.D. Allis, W.C. Earnshaw, J.R. Swedlow, Chromatin-associated protein phosphatase 1 regulates aurora-B and histone H3 phosphorylation, *J. Biol. Chem.* 276 (2001) 26656–26665.
- [81] D.E. MacCallum, A. Losada, R. Kobayashi, T. Hirano, ISWI remodeling complexes in *Xenopus* egg extracts: Identification as major chromosomal components that are regulated by INCENP-aurora B, *Mol. Biol. Cell* 13 (2002) 25–39.
- [82] A. Magalska, A.K. Schellhaus, D. Moreno-Andres, F. Zanini, A. Schooley, R. Sachdev, H. Schwarz, J. Madlung, W. Antonin, RuvB-like ATPases function in chromatin decondensation at the end of mitosis, *Dev. Cell* 31 (2014) 305–318.
- [83] T. Hirota, J.J. Lipp, B.H. Toh, J.M. Peters, Histone H3 serine 10 phosphorylation by Aurora B causes HP1 dissociation from heterochromatin, *Nature* 438 (2005) 1176–1180.
- [84] B.J. Wilkins, N.A. Rall, Y. Ostwal, T. Kruitwagen, K. Hiragami-Hamada, M. Winkler, Y. Barral, W. Fischle, H. Neumann, A cascade of histone modifications induces chromatin condensation in mitosis, *Science* 343 (2014) 77–80.

- [85] B.D. Lavoie, K.M. Tuffo, S. Oh, D. Koshland, C. Holm, Mitotic chromosome condensation requires Bm1p, the yeast homologue of Barren, *Mol. Biol. Cell* 11 (2000) 1293–1304.
- [86] F. Mora-Bermudez, D. Gerlich, J. Ellenberg, Maximal chromosome compaction occurs by axial shortening in anaphase and depends on Aurora kinase, *Nat. Cell Biol.* 9 (2007) 822–831.
- [87] M. Ohsugi, K. Adachi, R. Horai, S. Kakuta, K. Sudo, H. Kotaki, N. Tokai-Nishizumi, H. Sagara, Y. Iwakura, T. Yamamoto, Kid-mediated chromosome compaction ensures proper nuclear envelope formation, *Cell* 132 (2008) 771–782.
- [88] A. Philpott, G.H. Leno, Nucleoplasmin remodels sperm chromatin in *Xenopus* egg extracts, *Cell* 69 (1992) 759–767.
- [89] A. Philpott, G.H. Leno, R.A. Laskey, Sperm decondensation in *Xenopus* egg cytoplasm is mediated by nucleoplasmin, *Cell* 65 (1991) 569–578.
- [90] T.R. Burglin, I.W. Mattaj, D.D. Newmeyer, R. Zeller, E.M. De Robertis, Cloning of nucleoplasmin from *Xenopus laevis* oocytes and analysis of its developmental expression, *Genes Dev.* 1 (1987) 97–107.
- [91] K. Ramadan, R. Bruderer, F.M. Spiga, O. Popp, T. Baur, M. Gotta, H.H. Meyer, Cdc48/p97 promotes reformation of the nucleus by extracting the kinase Aurora B from chromatin, *Nature* 450 (2007) 1258–1262.
- [92] G. Dobrynin, O. Popp, T. Romer, S. Bremer, M.H. Schmitz, D.W. Gerlich, H. Meyer, Cdc48/p97-Ufd1-Npl4 antagonizes Aurora B during chromosome segregation in HeLa cells, *J. Cell Sci.* 124 (2011) 1571–1580.
- [93] N. Nano, W.A. Houry, Chaperone-like activity of the AAA+ proteins Rvb1 and Rvb2 in the assembly of various complexes, *Philos. Trans. R. Soc. Lond. Ser. B Biol. Sci.* 368 (2013) 20110399.
- [94] D.J. Forbes, A. Travesa, M.S. Nord, C. Bernis, Nuclear transport factors: Global regulation of mitosis, *Curr. Opin. Cell Biol.* 35 (2015) 78–90.
- [95] X. Lu, Y. Shi, Q. Lu, Y. Ma, J. Luo, Q. Wang, J. Ji, Q. Jiang, C. Zhang, Requirement for lamin B receptor and its regulation by importin {beta} and phosphorylation in nuclear envelope assembly during mitotic exit, *J. Biol. Chem.* 285 (2010) 33281–33293.
- [96] Y.H. Chi, K. Haller, J.M. Peloponese Jr., K.T. Jeang, Histone acetyltransferase hALP and nuclear membrane protein hSUN1 function in de-condensation of mitotic chromosomes, *J. Biol. Chem.* 282 (2007) 27447–27458.
- [97] A. Schooley, D. Moreno-Andres, P. DeMagistis, B. Vollmer, W. Antonin, The lysine demethylase LSD1 is required for nuclear envelope reformation at the end of mitosis, *J. Cell Sci.* 128 (2015) 3466–3477, <http://dx.doi.org/10.1242/jcs.173013>.
- [98] S.J. Wright, Sperm nuclear activation during fertilization, *Curr. Top. Dev. Biol.* 46 (1999) 133–178.
- [99] E.M. Manders, A.E. Visser, A. Koppen, W.C. de Leeuw, R. van Liere, G.J. Brakenhoff, R. van Driel, Four-dimensional imaging of chromatin dynamics during the assembly of the interphase nucleus, *Chromosome Res.* 11 (2003) 537–547.
- [100] J.E. Sleeman, L. Trinkle-Mulcahy, Nuclear bodies: New insights into assembly/dynamics and disease relevance, *Curr. Opin. Cell Biol.* 28 (2014) 76–83.
- [101] D. Gerlich, J. Beaudouin, B. Kalbfuss, N. Daigle, R. Eils, J. Ellenberg, Global chromosome positions are transmitted through mitosis in mammalian cells, *Cell* 112 (2003) 751–764.
- [102] F. Wang, J.M. Higgins, Histone modifications and mitosis: Countermarks, landmarks, and bookmarks, *Trends Cell Biol.* 23 (2013) 175–184.
- [103] N. Daigle, J. Beaudouin, L. Hartnell, G. Imreh, E. Hallberg, J. Lippincott-Schwartz, J. Ellenberg, Nuclear pore complexes form immobile networks and have a very low turnover in live mammalian cells, *J. Cell Biol.* 154 (2001) 71–84.
- [104] J. Ellenberg, E.D. Siggia, J.E. Moreira, C.L. Smith, J.F. Presley, H.J. Worman, J. Lippincott-Schwartz, Nuclear membrane dynamics and reassembly in living cells: Targeting of an inner nuclear membrane protein in interphase and mitosis, *J. Cell Biol.* 138 (1997) 1193–1206.
- [105] L. Yang, T. Guan, L. Gerace, Integral membrane proteins of the nuclear envelope are dispersed throughout the endoplasmic reticulum during mitosis, *J. Cell Biol.* 137 (1997) 1199–1210.
- [106] D.J. Anderson, M.W. Hetzer, Nuclear envelope formation by chromatin-mediated reorganization of the endoplasmic reticulum, *Nat. Cell Biol.* 9 (2007) 1160–1166.
- [107] M. Puhka, M. Joensuu, H. Vihinen, I. Belevich, E. Jokitalo, Progressive sheet-to-tubule transformation is a general mechanism for endoplasmic reticulum partitioning in dividing mammalian cells, *Mol. Biol. Cell* 23 (2012) 2424–2432.
- [108] M. Puhka, H. Vihinen, M. Joensuu, E. Jokitalo, Endoplasmic reticulum remains continuous and undergoes sheet-to-tubule transformation during cell division in mammalian cells, *J. Cell Biol.* 179 (2007) 895–909.
- [109] D. Poteryaev, J.M. Squirrell, J.M. Campbell, J.G. White, A. Spang, Involvement of the actin cytoskeleton and homotypic membrane fusion in ER dynamics in *Caenorhabditis elegans*, *Mol. Biol. Cell* 16 (2005) 2139–2153.
- [110] L. Lu, M.S. Ladinsky, T. Kirchhausen, Cisternal organization of the endoplasmic reticulum during mitosis, *Mol. Biol. Cell* 20 (2009) 3471–3480.
- [111] L. Lu, M.S. Ladinsky, T. Kirchhausen, Formation of the postmitotic nuclear envelope from extended ER cisternae precedes nuclear pore assembly, *J. Cell Biol.* 194 (2011) 425–440.
- [112] S. Wang, F.B. Romano, C.M. Field, T.J. Mitchison, T.A. Rapoport, Multiple mechanisms determine ER network morphology during the cell cycle in *Xenopus* egg extracts, *J. Cell Biol.* 203 (2013) 801–814.
- [113] L.M. Westrate, J.E. Lee, W.A. Prinz, G.K. Voeltz, Form follows function: The importance of endoplasmic reticulum shape, *Annu. Rev. Biochem.* 84 (2015) 791–811, <http://dx.doi.org/10.1146/annurev-biochem-072711-163501>.
- [114] D.J. Anderson, M.W. Hetzer, Reshaping of the endoplasmic reticulum limits the rate for nuclear envelope formation, *J. Cell Biol.* 182 (2008) 911–924.
- [115] J. Niclas, V.J. Allan, R.D. Vale, Cell cycle regulation of dynein association with membranes modulates microtubule-based organelle transport, *J. Cell Biol.* 133 (1996) 585–593.
- [116] J.T. Smyth, A.M. Beg, S. Wu, J.W. Putney Jr., N.M. Rusan, Phosphoregulation of STIM1 leads to exclusion of the endoplasmic reticulum from the mitotic spindle, *Curr. Biol.* 22 (2012) 1487–1493.
- [117] D.R. Klopfenstein, F. Kappeler, H.P. Hauri, A novel direct interaction of endoplasmic reticulum with microtubules, *EMBO J.* 17 (1998) 6168–6177.
- [118] C. Vedrenne, D.R. Klopfenstein, H.P. Hauri, Phosphorylation controls CLIMP-63-mediated anchoring of the endoplasmic reticulum to microtubules, *Mol. Biol. Cell* 16 (2005) 1928–1937.
- [119] L. Dreier, T.A. Rapoport, *In vitro* formation of the endoplasmic reticulum occurs independently of microtubules by a controlled fusion reaction, *J. Cell Biol.* 148 (2000) 883–898.
- [120] A. Ewald, C. Zunkler, D. Lourim, M.C. Dabauvalle, Microtubule-dependent assembly of the nuclear envelope in *Xenopus laevis* egg extract, *Eur. J. Cell Biol.* 80 (2001) 678–691.
- [121] J.Z. Xue, E.M. Woo, L. Postow, B.T. Chait, H. Funabiki, Chromatin-bound *Xenopus* Dppa2 shapes the nucleus by

- locally inhibiting microtubule assembly, *Dev. Cell* 27 (2013) 47–59.
- [122] Y. Hara, C.A. Merten, Dynein-based accumulation of membranes regulates nuclear expansion in *Xenopus laevis* egg extracts, *Dev. Cell* 33 (2015) 562–575.
- [123] D.J. Anderson, J.D. Vargas, J.P. Hsiao, M.W. Hetzer, Recruitment of functionally distinct membrane proteins to chromatin mediates nuclear envelope formation *in vivo*, *J. Cell Biol.* 186 (2009) 183–191.
- [124] G. Theerthagiri, N. Eisenhardt, H. Schwarz, W. Antonin, The nucleoporin Nup188 controls passage of membrane proteins across the nuclear pore complex, *J. Cell Biol.* 189 (2010) 1129–1142.
- [125] R.G. Kessel, H. Katow, Effects of prolonged antitubulin culture on annulate lamellae in mouse alpha L929 fibroblasts, *J. Morphol.* 179 (1984) 291–304.
- [126] W. Antonin, C. Franz, U. Haselmann, C. Antony, I.W. Mattaj, The integral membrane nucleoporin pom121 functionally links nuclear pore complex assembly and nuclear envelope formation, *Mol. Cell* 17 (2005) 83–92.
- [127] J. Mansfeld, S. Guttinger, L.A. Hawryluk-Gara, N. Pante, M. Mall, V. Galy, U. Haselmann, P. Muhlhäusser, R.W. Wozniak, I.W. Mattaj, U. Kutay, W. Antonin, The conserved transmembrane nucleoporin NDC1 is required for nuclear pore complex assembly in vertebrate cells, *Mol. Cell* 22 (2006) 93–103.
- [128] E. Robbins, N.K. Gonatas, The ultrastructure of a mammalian cell during the mitotic cycle, *J. Cell Biol.* 21 (1964) 429–463.
- [129] S. Ulbert, M. Platani, S. Boue, I.W. Mattaj, Direct membrane protein–DNA interactions required early in nuclear envelope assembly, *J. Cell Biol.* 173 (2006) 469–476.
- [130] P. Collas, J.C. Courvalin, D. Poccia, Targeting of membranes to sea urchin sperm chromatin is mediated by a lamin B receptor-like integral membrane protein, *J. Cell Biol.* 135 (1996) 1715–1725.
- [131] A. Pypasopoulou, J. Meier, C. Maison, G. Simos, S.D. Georgatos, The lamin B receptor (LBR) provides essential chromatin docking sites at the nuclear envelope, *EMBO J.* 15 (1996) 7108–7119.
- [132] Q. Ye, H.J. Worman, Primary structure analysis and lamin B and DNA binding of human LBR, an integral protein of the nuclear envelope inner membrane, *J. Biol. Chem.* 269 (1994) 11306–11311.
- [133] R. Foisner, L. Gerace, Integral membrane proteins of the nuclear envelope interact with lamins and chromosomes, and binding is modulated by mitotic phosphorylation, *Cell* 73 (1993) 1267–1279.
- [134] K. Furukawa, C. Glass, T. Kondo, Characterization of the chromatin binding activity of lamina-associated polypeptide (LAP) 2, *Biochem. Biophys. Res. Commun.* 238 (1997) 240–246.
- [135] J. Liu, K.K. Lee, M. Segura-Totten, E. Neufeld, K.L. Wilson, Y. Gruenbaum, MAN1 and emerlin have overlapping function(s) essential for chromosome segregation and cell division in *Caenorhabditis elegans*, *Proc. Natl. Acad. Sci. U. S. A.* 100 (2003) 4598–4603.
- [136] Y. Hirano, M. Segawa, F.S. Ouchi, Y. Yamakawa, K. Furukawa, K. Takeyasu, T. Horigome, Dissociation of emerlin from barrier-to-autointegration factor is regulated through mitotic phosphorylation of emerlin in a *Xenopus* egg cell-free system, *J. Biol. Chem.* 280 (2005) 39925–39933.
- [137] Q. Ye, I. Callebaut, A. Pezhman, J.C. Courvalin, H.J. Worman, Domain-specific interactions of human HP1-type chromodomain proteins and inner nuclear membrane protein LBR, *J. Biol. Chem.* 272 (1997) 14983–14989.
- [138] T. Haraguchi, T. Kojidani, T. Koujin, T. Shimi, H. Osakada, C. Mori, A. Yamamoto, Y. Hiraoka, Live cell imaging and electron microscopy reveal dynamic processes of BAF-directed nuclear envelope assembly, *J. Cell Sci.* 121 (2008) 2540–2554.
- [139] A. Margalit, E. Neufeld, N. Feinstein, K.L. Wilson, B. Podbilewicz, Y. Gruenbaum, Barrier to autointegration factor blocks premature cell fusion and maintains adult muscle integrity in *C. elegans*, *J. Cell Biol.* 178 (2007) 661–673.
- [140] S. Ulbert, W. Antonin, M. Platani, I.W. Mattaj, The inner nuclear membrane protein Lem2 is critical for normal nuclear envelope morphology, *FEBS Lett.* 580 (2006) 6435–6441.
- [141] M.C. Dabauvalle, E. Muller, A. Ewald, W. Kress, G. Krohne, C.R. Muller, Distribution of emerlin during the cell cycle, *Eur. J. Cell Biol.* 78 (1999) 749–756.
- [142] T. Haraguchi, T. Koujin, T. Hayakawa, T. Kaneda, C. Tsutsumi, N. Imamoto, C. Akazawa, J. Sukegawa, Y. Yoneda, Y. Hiraoka, Live fluorescence imaging reveals early recruitment of emerlin, LBR, RanBP2, and Nup153 to reforming functional nuclear envelopes, *J. Cell Sci.* 113 (2000) 779–794.
- [143] N. Chaudhary, J.C. Courvalin, Stepwise reassembly of the nuclear envelope at the end of mitosis, *J. Cell Biol.* 122 (1993) 295–306.
- [144] M. Clever, T. Funakoshi, Y. Mimura, M. Takagi, N. Imamoto, The nucleoporin ELYS/Mel28 regulates nuclear envelope subdomain formation in HeLa cells, *Nucleus* 3 (2012) 187–199.
- [145] J. Newport, W. Dunphy, Characterization of the membrane binding and fusion events during nuclear envelope assembly using purified components, *J. Cell Biol.* 116 (1992) 295–306.
- [146] R. Pfaller, C. Smythe, J.W. Newport, Assembly/disassembly of the nuclear envelope membrane: Cell cycle-dependent binding of nuclear membrane vesicles to chromatin *in vitro*, *Cell* 65 (1991) 209–217.
- [147] G.P. Vigers, M.J. Lohka, Regulation of nuclear envelope precursor functions during cell division, *J. Cell Sci.* 102 (1992) 273–284.
- [148] H. Ito, Y. Koyama, M. Takano, K. Ishii, M. Maeno, K. Furukawa, T. Horigome, Nuclear envelope precursor vesicle targeting to chromatin is stimulated by protein phosphatase 1 in *Xenopus* egg extracts, *Exp. Cell Res.* 313 (2007) 1897–1910.
- [149] J.A. Ellis, M. Craxton, J.R. Yates, J. Kendrick-Jones, Aberrant intracellular targeting and cell cycle-dependent phosphorylation of emerlin contribute to the Emery-Dreifuss muscular dystrophy phenotype, *J. Cell Sci.* 111 (1998) 781–792.
- [150] C. Favreau, H.J. Worman, R.W. Wozniak, T. Frappier, J.C. Courvalin, Cell cycle-dependent phosphorylation of nucleoporins and nuclear pore membrane protein Gp210, *Biochemistry* 35 (1996) 8035–8044.
- [151] V. Galy, W. Antonin, A. Jaedicke, M. Sachse, R. Santarella, U. Haselmann, I. Mattaj, A role for gp210 in mitotic nuclear-envelope breakdown, *J. Cell Sci.* 121 (2008) 317–328.
- [152] E. Nikolakaki, J. Meier, G. Simos, S.D. Georgatos, T. Giannakouros, Mitotic phosphorylation of the lamin B receptor by a serine/arginine kinase and p34(cdc2), *J. Biol. Chem.* 272 (1997) 6208–6213.
- [153] M. Takano, Y. Koyama, H. Ito, S. Hoshino, H. Onogi, M. Hagiwara, K. Furukawa, T. Horigome, Regulation of binding of lamin B receptor to chromatin by SR protein kinase and cdc2 kinase in *Xenopus* egg extracts, *J. Biol. Chem.* 279 (2004) 13265–13271.
- [154] L.C. Tseng, R.H. Chen, Temporal control of nuclear envelope assembly by phosphorylation of lamin B receptor, *Mol. Biol. Cell* 22 (2011) 3306–3317.

- [155] M. Dreger, H. Otto, G. Neubauer, M. Mann, F. Hucho, Identification of phosphorylation sites in native lamina-associated polypeptide 2 beta, *Biochemistry* 38 (1999) 9426–9434.
- [156] W. Fischle, B.S. Tseng, H.L. Dormann, B.M. Ueberheide, B.A. Garcia, J. Shabanowitz, D.F. Hunt, H. Funabiki, C.D. Allis, Regulation of HP1-chromatin binding by histone H3 methylation and phosphorylation, *Nature* 438 (2005) 1116–1122.
- [157] A.J. Bannister, P. Zegerman, J.F. Partridge, E.A. Miska, J.O. Thomas, R.C. Allshire, T. Kouzarides, Selective recognition of methylated lysine 9 on histone H3 by the HP1 chromo domain, *Nature* 410 (2001) 120–124.
- [158] M. Lachner, D. O'Carroll, S. Rea, K. Mechtler, T. Jenuwein, Methylation of histone H3 lysine 9 creates a binding site for HP1 proteins, *Nature* 410 (2001) 116–120.
- [159] K. Sugimoto, H. Tasaka, M. Dotsu, Molecular behavior in living mitotic cells of human centromere heterochromatin protein HPLalpha ectopically expressed as a fusion to red fluorescent protein, *Cell Struct. Funct.* 26 (2001) 705–718.
- [160] A.L. Olins, G. Rhodes, D.B. Welch, M. Zwerger, D.E. Olins, Lamin B receptor: Multi-tasking at the nuclear envelope, *Nucleus* 1 (2010) 53–70.
- [161] T. Karg, B. Warecki, W. Sullivan, Aurora B-mediated localized delays in nuclear envelope formation facilitate inclusion of late-segregating chromosome fragments, *Mol. Biol. Cell* 26 (2015) 2227–2241.
- [162] P. Kalab, K. Weis, R. Heald, Visualization of a Ran-GTP gradient in interphase and mitotic *Xenopus* egg extracts, *Science* 295 (2002) 2452–2456.
- [163] Y. Turgay, R. Ungricht, A. Rothballer, A. Kiss, G. Csucs, P. Horvath, U. Kutay, A classical NLS and the SUN domain contribute to the targeting of SUN2 to the inner nuclear membrane, *EMBO J.* 29 (2010) 2262–2275.
- [164] W. Antonin, R. Ungricht, U. Kutay, Traversing the NPC along the pore membrane: Targeting of membrane proteins to the INM, *Nucleus* 2 (2011) 87–91.
- [165] Y. Ma, S. Cai, Q. Lv, Q. Jiang, Q. Zhang, Zhai Sodmergen, Z. & Zhang, C., Lamin B receptor plays a role in stimulating nuclear envelope production and targeting membrane vesicles to chromatin during nuclear envelope assembly through direct interaction with importin beta, *J. Cell Sci.* 120 (2007) 520–530.
- [166] M. Hetzer, D. Bilbao-Cortes, T.C. Walther, O.J. Gruss, I.W. Mattaj, GTP hydrolysis by Ran is required for nuclear envelope assembly, *Mol. Cell* 5 (2000) 1013–1024.
- [167] C. Zhang, P.R. Clarke, Chromatin-independent nuclear envelope assembly induced by Ran GTPase in *Xenopus* egg extracts, *Science* 288 (2000) 1429–1432.
- [168] Y. Shi, F. Lan, C. Matson, P. Mulligan, J.R. Whetstone, P.A. Cole, R.A. Casero, Histone demethylation mediated by the nuclear amine oxidase homolog LSD1, *Cell* 119 (2004) 941–953.
- [169] T. Baur, K. Ramadan, A. Schlundt, J. Kartenbeck, H.H. Meyer, NSF- and SNARE-mediated membrane fusion is required for nuclear envelope formation and completion of nuclear pore complex assembly in *Xenopus laevis* egg extracts, *J. Cell Sci.* 120 (2007) 2895–2903.
- [170] J. Hu, Y. Shibata, P.P. Zhu, C. Voss, N. Rismanchi, W.A. Prinz, T.A. Rapoport, C. Blackstone, A class of dynamin-like GTPases involved in the generation of the tubular ER network, *Cell* 138 (2009) 549–561.
- [171] G. Orso, D. Pendin, S. Liu, J. Tosetto, T.J. Moss, J.E. Faust, M. Micaroni, A. Egorova, A. Martinuzzi, J.A. McNew, A. Daga, Homotypic fusion of ER membranes requires the dynamin-like GTPase atlastin, *Nature* 460 (2009) 978–983.
- [172] Y. Olmos, L. Hodgson, J. Mantell, P. Verkade, J.G. Carlton, ESCRT-III controls nuclear envelope reformation, *Nature* 522 (2015) 236–239.
- [173] M. Vietri, K.O. Schink, C. Campsteijn, C.S. Wegner, S.W. Schultz, L. Christ, S.B. Thoresen, A. Brech, C. Raiborg, H. Stenmark, Spastin and ESCRT-III coordinate mitotic spindle disassembly and nuclear envelope sealing, *Nature* 522 (2015) 231–235.
- [174] M. Hetzer, H.H. Meyer, T.C. Walther, D. Bilbao-Cortes, G. Warren, I.W. Mattaj, Distinct AAA-ATPase p97 complexes function in discrete steps of nuclear assembly, *Nat. Cell Biol.* 3 (2001) 1086–1091.
- [175] M. Babst, D.J. Katzmman, E.J. Estepa-Sabal, T. Meerloo, S.D. Emr, Escrt-III: An endosome-associated heterooligomeric protein complex required for mvb sorting, *Dev. Cell* 3 (2002) 271–282.
- [176] H. Meyer, M. Bug, S. Bremer, Emerging functions of the VCP/p97 AAA-ATPase in the ubiquitin system, *Nat. Cell Biol.* 14 (2012) 117–123.
- [177] K.H. Bui, A. von Appen, A.L. Digulio, A. Ori, L. Sparks, M.T. Mackmull, T. Bock, W. Hagen, A. Andres-Pons, J.S. Glavy, M. Beck, Integrated structural analysis of the human nuclear pore complex scaffold, *Cell* 155 (2013) 1233–1243.
- [178] A. Schooley, B. Vollmer, W. Antonin, Building a nuclear envelope at the end of mitosis: Coordinating membrane reorganization, nuclear pore complex assembly, and chromatin de-condensation, *Chromosoma* 121 (2012) 539–554.
- [179] B. Fichtman, C. Ramos, B. Rasala, A. Harel, D.J. Forbes, Inner/outer nuclear membrane fusion in nuclear pore assembly: Biochemical demonstration and molecular analysis, *Mol. Biol. Cell* 21 (2010) 4197–4211, <http://dx.doi.org/10.1091/mbc.E10-04-0309>.
- [180] C. Macaulay, D.J. Forbes, Assembly of the nuclear pore: Biochemically distinct steps revealed with NEM, GTP gamma S, and BAPTA, *J. Cell Biol.* 132 (1996) 5–20.
- [181] W. Antonin, J. Ellenberg, E. Dultz, Nuclear pore complex assembly through the cell cycle: Regulation and membrane organization, *FEBS Lett.* 582 (2008) 2004–2016.
- [182] B. Burke, J. Ellenberg, Remodelling the walls of the nucleus, *Nat. Rev. Mol. Cell Biol.* 3 (2002) 487–497.
- [183] T.C. Walther, A. Alves, H. Pickersgill, I. Loidice, M. Hetzer, V. Galy, B.B. Hulsmann, T. Kocher, M. Wilm, T. Allen, I.W. Mattaj, V. Doye, The conserved Nup107-160 complex is critical for nuclear pore complex assembly, *Cell* 113 (2003) 195–206.
- [184] G. Kabachinski, T.U. Schwartz, The nuclear pore complex—Structure and function at a glance, *J. Cell Sci.* 128 (2015) 423–429.
- [185] B.A. Rasala, A.V. Orjalo, Z. Shen, S. Briggs, D.J. Forbes, ELYS is a dual nucleoporin/kinetochore protein required for nuclear pore assembly and proper cell division, *Proc. Natl. Acad. Sci. U. S. A.* 103 (2006) 17801–17806.
- [186] A. Rotem, R. Gruber, H. Shorer, L. Shaulov, E. Klein, A. Harel, Importin beta regulates the seeding of chromatin with initiation sites for nuclear pore assembly, *Mol. Biol. Cell* 20 (2009) 4031–4042.
- [187] P.J. Gillespie, G.A. Khoudoli, G. Stewart, J.R. Swedlow, J.J. Blow, ELYS/MEL-28 chromatin association coordinates nuclear pore complex assembly and replication licensing, *Curr. Biol.* 17 (2007) 1657–1662.
- [188] A. Inoue, Y. Zhang, Nucleosome assembly is required for nuclear pore complex assembly in mouse zygotes, *Nat. Struct. Mol. Biol.* 21 (2014) 609–616.
- [189] C. Zierhut, C. Jenness, H. Kimura, H. Funabiki, Nucleosomal regulation of chromatin composition and nuclear assembly

- revealed by histone depletion, *Nat. Struct. Mol. Biol.* 21 (2014) 617–625.
- [190] A. Szyborska, A. de Marco, N. Daigle, V.C. Cordes, J.A. Briggs, J. Ellenberg, Nuclear pore scaffold structure analyzed by super-resolution microscopy and particle averaging, *Science* 341 (2013) 655–658.
- [191] B.A. Rasala, C. Ramos, A. Harel, D.J. Forbes, Capture of AT-rich chromatin by ELYS recruits POM121 and NDC1 to initiate nuclear pore assembly, *Mol. Biol. Cell* 19 (2008) 3982–3996.
- [192] J.M. Mitchell, J. Mansfeld, J. Capitanio, U. Kutay, R.W. Wozniak, Pom121 links two essential subcomplexes of the nuclear pore complex core to the membrane, *J. Cell Biol.* 191 (2010) 505–521.
- [193] S. Yavuz, R. Santarella-Mellwig, B. Koch, A. Jaedicke, I.W. Mattaj, W. Antonin, NLS-mediated NPC functions of the nucleoporin Pom121, *FEBS Lett.* 584 (2010) 3292–3298.
- [194] B. Vollmer, A. Schooley, R. Sachdev, N. Eisenhardt, A.M. Schneider, C. Sieverding, J. Madlung, U. Gerken, B. Macek, W. Antonin, Dimerization and direct membrane interaction of Nup53 contribute to nuclear pore complex assembly, *EMBO J.* 31 (2012) 4072–4084.
- [195] B. Vollmer, W. Antonin, The diverse roles of the Nup93/Nic96 complex proteins—Structural scaffolds of the nuclear pore complex with additional cellular functions, *Biol. Chem.* 395 (2014) 515–528, <http://dx.doi.org/10.1515/hsz-2013-0285>.
- [196] R. Sachdev, C. Sieverding, M. Flotenmeyer, W. Antonin, The C-terminal domain of Nup93 is essential for assembly of the structural backbone of nuclear pore complexes, *Mol. Biol. Cell* 23 (2012) 740–749.
- [197] A. Ori, N. Banterle, M. Iskar, A. Andres-Pons, C. Escher, H. Khanh Bui, L. Sparks, V. Solis-Mezarino, O. Rinner, P. Bork, E.A. Lemke, M. Beck, Cell type-specific nuclear pores: A case in point for context-dependent stoichiometry of molecular machines, *Mol. Syst. Biol.* 9 (2013) 648.
- [198] N. Eisenhardt, J. Redolfi, W. Antonin, Interaction of Nup53 with Ndc1 and Nup155 is required for nuclear pore complex assembly, *J. Cell Sci.* 127 (2014) 908–921.
- [199] E. Rodenas, E.P. Klerkx, C. Ayuso, A. Audhya, P. Askjaer, Early embryonic requirement for nucleoporin Nup35/NPP-19 in nuclear assembly, *Dev. Biol.* 327 (2009) 399–409.
- [200] A. Von Appen, J. Kosinski, L. Sparks, A. Ori, A. Di Giulio, B. Vollmer, M.T. Mackmull, L. Parca, K. Buczak, W. Hagen, A. Andres-Pons, P. Bork, W. Antonin, J.S. Glavy, K.H. Bui, M. Beck, In situ structural analysis of the human nuclear pore complex, *Nature* (2015 Sep 23), <http://dx.doi.org/10.1038/nature15381>, In press.
- [201] B.R. Miller, M. Powers, M. Park, W. Fischer, D.J. Forbes, Identification of a new vertebrate nucleoporin, Nup188, with the use of a novel organelle trap assay, *Mol. Biol. Cell* 11 (2000) 3381–3396.
- [202] S. Vasu, S. Shah, A. Orjalo, M. Park, W.H. Fischer, D.J. Forbes, Novel vertebrate nucleoporins Nup133 and Nup160 play a role in mRNA export, *J. Cell Biol.* 155 (2001) 339–354.
- [203] M.E. Hase, V.C. Cordes, Direct interaction with nup153 mediates binding of Tpr to the periphery of the nuclear pore complex, *Mol. Biol. Cell* 14 (2003) 1923–1940.
- [204] T.C. Walther, M. Fomerod, H. Pickersgill, M. Goldberg, T.D. Allen, I.W. Mattaj, The nucleoporin Nup153 is required for nuclear pore basket formation, nuclear pore complex anchoring and import of a subset of nuclear proteins, *EMBO J.* 20 (2001) 5703–5714.
- [205] S. Krull, J. Thyberg, B. Bjorkroth, H.R. Rackwitz, V.C. Cordes, Nucleoporins as components of the nuclear pore complex core structure and Tpr as the architectural element of the nuclear basket, *Mol. Biol. Cell* 15 (2004) 4261–4277.
- [206] T.C. Walther, H.S. Pickersgill, V.C. Cordes, M.W. Goldberg, T.D. Allen, I.W. Mattaj, M. Fomerod, The cytoplasmic filaments of the nuclear pore complex are dispensable for selective nuclear protein import, *J. Cell Biol.* 158 (2002) 63–77.
- [207] B. Vollmer, M. Lorenz, D. Moreno-Andres, M. Bodenhofer, P. De Magistris, S.A. Astrinidis, A. Schooley, M. Flotenmeyer, S. Leptihn, W. Antonin, Nup153 recruits the Nup107-160 complex to the inner nuclear membrane for interphasic nuclear pore complex assembly, *Dev. Cell* 33 (2015) 717–728.
- [208] J.S. Glavy, A.N. Krutchinsky, I.M. Cristea, I.C. Berke, T. Boehmer, G. Blobel, B.T. Chait, Cell-cycle-dependent phosphorylation of the nuclear pore Nup107-160 subcomplex, *Proc. Natl. Acad. Sci. U. S. A.* 104 (2007) 3811–3816.
- [209] E. Laurell, K. Beck, K. Krupina, G. Theerthagiri, B. Bodenmiller, P. Horvath, R. Aebersold, W. Antonin, U. Kutay, Phosphorylation of Nup98 by multiple kinases is crucial for NPC disassembly during mitotic entry, *Cell* 144 (2011) 539–550.
- [210] C. Macaulay, E. Meier, D.J. Forbes, Differential mitotic phosphorylation of proteins of the nuclear pore complex, *J. Biol. Chem.* 270 (1995) 254–262.
- [211] E.A. Onischenko, N.V. Gubanova, E.V. Kiseleva, E. Hallberg, Cdk1 and okadaic acid-sensitive phosphatases control assembly of nuclear pore complexes in *Drosophila* embryos, *Mol. Biol. Cell* 16 (2005) 5152–5162.
- [212] K. Rajanala, A. Sarkar, G.D. Jhingan, R. Priyadarshini, M. Jalan, S. Sengupta, V.K. Nandicoori, Phosphorylation of nucleoporin Tpr governs its differential localization and is required for its mitotic function, *J. Cell Sci.* 127 (2014) 3505–3520.
- [213] T.C. Walther, P. Askjaer, M. Gentzel, A. Habermann, G. Griffiths, M. Wilm, I.W. Mattaj, M. Hetzer, RanGTP mediates nuclear pore complex assembly, *Nature* 424 (2003) 689–694.
- [214] J. Moroianu, M. Hijikata, G. Blobel, A. Radu, Mammalian karyopherin alpha 1 beta and alpha 2 beta heterodimers: Alpha 1 or alpha 2 subunit binds nuclear localization signal and beta subunit interacts with peptide repeat-containing nucleoporins, *Proc. Natl. Acad. Sci. U. S. A.* 92 (1995) 6532–6536.
- [215] M.E. Lindsay, K. Plafker, A.E. Smith, B.E. Clurman, I.G. Macara, Nup60/Nup50 is a tri-stable switch that stimulates importin-alpha:beta-mediated nuclear protein import, *Cell* 110 (2002) 349–360.
- [216] T. Funakoshi, M. Clever, A. Watanabe, N. Imamoto, Localization of Pom121 to the inner nuclear membrane is required for an early step of interphase nuclear pore complex assembly, *Mol. Biol. Cell* 22 (2011) 1058–1069.
- [217] M.A. D'Angelo, D.J. Anderson, E. Richard, M.W. Hetzer, Nuclear pores form *de novo* from both sides of the nuclear envelope, *Science* 312 (2006) 440–443.
- [218] L. Gerace, G. Blobel, The nuclear envelope lamina is reversibly depolymerized during mitosis, *Cell* 19 (1980) 277–287.
- [219] M. Peter, J. Nakagawa, M. Doree, J.C. Labbe, E.A. Nigg, *In vitro* disassembly of the nuclear lamina and M phase-specific phosphorylation of lamins by cdc2 kinase, *Cell* 61 (1990) 591–602.
- [220] R. Heald, F. McKeon, Mutations of phosphorylation sites in lamin A that prevent nuclear lamina disassembly in mitosis, *Cell* 61 (1990) 579–589.
- [221] L.J. Thompson, M. Bollen, A.P. Fields, Identification of protein phosphatase 1 as a mitotic lamin phosphatase, *J. Biol. Chem.* 272 (1997) 29693–29697.

- [222] J.W. Newport, K.L. Wilson, W.G. Dunphy, A lamin-independent pathway for nuclear envelope assembly, *J. Cell Biol.* 111 (1990) 2247–2259.
- [223] Y. Gruenbaum, O. Medalia, Lamins: The structure and protein complexes, *Curr. Opin. Cell Biol.* 32 (2015) 7–12.
- [224] Y. Guo, Y. Kim, T. Shimi, R.D. Goldman, Y. Zheng, Concentration-dependent lamin assembly and its roles in the localization of other nuclear proteins, *Mol. Biol. Cell* 25 (2014) 1287–1297.
- [225] C. Smythe, H.E. Jenkins, C.J. Hutchison, Incorporation of the nuclear pore basket protein nup153 into nuclear pore structures is dependent upon lamina assembly: Evidence from cell-free extracts of *Xenopus* eggs, *EMBO J.* 19 (2000) 3918–3931.
- [226] T. Al-Haboubi, D.K. Shumaker, J. Koser, M. Wehnert, B. Fahrenkrog, Distinct association of the nuclear pore protein Nup153 with A- and B-type lamins, *Nucleus* 2 (2011) 500–509.
- [227] D.I. Kim, K.C. Birendra, K.J. Roux, Making the LINC: SUN and KASH protein interactions, *Biol. Chem.* 396 (2015) 295–310.
- [228] J.T. Patel, A. Bottrill, S.L. Prosser, S. Jayaraman, K. Straatman, A.M. Fry, S. Shackleton, Mitotic phosphorylation of SUN1 loosens its connection with the nuclear lamina while the LINC complex remains intact, *Nucleus* 5 (2014) 462–473.
- [229] P.M. Davidson, J. Lammerding, Broken nuclei—Lamins, nuclear mechanics, and disease, *Trends Cell Biol.* 24 (2014) 247–256.

Developmentally Regulated GTP binding protein 1 (DRG1) controls microtubule dynamics

Anna Katharina Schellhaus (1, 2), Daniel Moreno-Andrés (1, 2), Mayank Chugh (3), Hideki Yokoyama (1, 2), Athina Moschopoulou (1), Suman De (3), Fulvia Bono (4), Katharina Hipp (4), Erik Schäffer (3), Wolfram Antonin* (1, 2)

*corresponding author

(1) Friedrich Miescher Laboratory of the Max Planck Society, Spemannstraße 39, 72076 Tübingen, Germany

(2) Institute of Biochemistry and Molecular Cell Biology, Medical School, RWTH Aachen University, 52074 Aachen, Germany

(3) Cellular Nanoscience, Center for Plant Molecular Biology (ZMBP), University of Tübingen, 72076 Tübingen, Germany

(4) Max Planck Institute for Developmental Biology, Spemannstraße 35, 72076 Tübingen, Germany

Author for correspondence: wantonin@ukaachen.de

Abbreviations used: DRG1: Developmentally Regulated GTP binding protein 1, DFRP: DRG family regulatory protein, MT: microtubule, NE: nuclear extract, S: supernatant, P: pellet, Rbg1: Ribosome binding GTPase 1, CSF: cyostatic factor arrested, TIRF: total-internal-reflection-fluorescence, HTH: helix-turn-helix

Abstract

The mitotic spindle, essential for segregating the sister chromatids into the two evolving daughter cells, is composed of highly dynamic cytoskeletal filaments, the microtubules. The dynamics of microtubules are regulated by numerous microtubule associated proteins. We identify here Developmentally regulated GTP binding protein 1 (DRG1) as a microtubule binding protein with diverse microtubule-associated functions. DRG1 can diffuse on, promotes polymerization of, bundles, and stabilizes microtubules *in vitro*. HeLa cells with reduced DRG1 levels show prolonged progression from pro- to anaphase because spindle formation is slowed down. To perform its microtubule-associated functions, DRG1, although being a GTPase, does not require GTP hydrolysis. Yet, all domains are required as truncated versions show none of the mentioned activities beside microtubule binding.

Introduction

Microtubules are key cytoskeletal structures that play a vital role in a variety of cellular processes such as intracellular trafficking, regulation of cell polarity, cell shape maintenance, and chromatid segregation during cell division. Microtubules are polar assemblies built from α -/ β -tubulin heterodimers, both of which are GTPases. The most prominent aspect of microtubules is their dynamic instability: Microtubules can shift rapidly between growth and shrinkage especially at the plus tip. This instability is more pronounced during mitosis when the mitotic spindle forms.

Several types of microtubules are found in the mitotic spindle. The kinetochore microtubules connect the centrosome at the minus end with the kinetochore at the plus end, a protein complex assembled on centromeric chromatin. Usually 20-30 kinetochore microtubules are bundled into stable K-fibers, which mediate chromosomal movement. The non-kinetochore microtubules are a part of the spindle body without being attached to the kinetochore. They are important for separating the poles and mitotic spindle stability. Lastly, astral microtubules radiate from the centrosomes toward the cell cortex and, thereby, position the spindle (reviewed in detail in ^{1,2}).

Although pure α / β tubulin dimers are in the presence of GTP sufficient to generate microtubules *in vitro*, in cells nucleating factors are required (reviewed in detail in ¹⁻³). For the mitotic spindle centrosomes are the most prominent nucleation centers but other nucleation pathways exist: microtubules can nucleate around chromosomes which is regulated by the small GTPase Ran. Spindle assembly factors are sequestered by nuclear transport factors like importin α and β and released close to chromosomes by RanGTP. Additionally, microtubules can nucleate from already existing microtubules within the spindle. These other pathways can take over function if no centrosomes are present, e.g. in the second meiotic division of vertebrates, or artificially removed but are also crucial for timely spindle assembly in the presence of centrosomes. The additional nucleation pathways raise the chances that a microtubule finds a kinetochore by increasing microtubule density around chromosomes. In addition, many microtubule associated proteins and mechanics like cell rounding during mitosis are involved in spindle assembly and facilitate the microtubule-kinetochore attachment^{1,2}.

Several classes of microtubule-associated proteins are known: microtubule polymerases and depolymerases, nucleation factors, severing enzymes, microtubule bundling/crosslinking proteins that stabilize microtubule fibers, stabilizing factors that prevent catastrophes, motor proteins that are also essential to establish the bipolar array e.g. by sliding microtubules, microtubule capping/end-binding/tracking factors and many more (reviewed in ³). One difficulty of elucidating unknown pathways and factors or characterizing the function of a newly found factor is that mitotic spindle processes are redundant. However, errors of chromosome segregation increase with missing factors or pathways and can ultimately lead to severe consequences like chromosome mis-segregation. The presence of numerous diverse yet partially redundant factors and pathways most likely represents an inbuilt security mechanism of the cell. Hence, it is crucial as well as challenging to identify such partially redundant factors during spindle assembly and maintenance, which are deregulated in many disease contexts⁴⁻⁶.

Here, we identify Developmentally regulated GTP-binding protein 1 (DRG1) as a microtubule polymerase that also bundles and stabilizes microtubules. DRGs were independently identified in a variety of organisms in the 1990's by several groups⁷⁻¹³ and belong to the subfamily of Obg

GTPases¹⁴. Soon, it was clear that a new GTP-binding protein was found that is highly conserved from archaeobacterial having one DRG to eukaryotes from yeast to human, who contain DRG1 and DRG2¹⁵. Plants even have three DRGs¹⁶. Beside the canonical G-domain they do not share similarities with other known GTPases and their function is still largely unclear. As DRG1 is highly upregulated in mouse embryonic brain it was suggested to act as a developmental factor⁸. However, DRG is also expressed widely in adult tissue^{7,15,17}. Several studies suggested that DRGs are involved in cell growth although the underlying mechanism is still unclear^{18,19}.

DRGs are associated with DRG family regulatory proteins (DFRPs) which stabilize DRGs and prevent their ubiquitination and degradation by the proteasomes^{20,21}. Consistently, DRG1 is substantially downregulated after DFRP1 knock-down. While DRG1 and 2 are highly similar (58 % identity for human proteins), the two DFRPs, DFRP1 and 2 share only similarities in their DFRP domain. This domain is important for DRG interaction but the binding area extends further²². DFRP1 binds specifically to DRG1 while it is under debate if DFRP2 binds exclusively to DRG2 or also to DRG1^{20,21,23}. Like other Obg GTPases DRG1 and its interaction partner DFRP1 might be involved in translation because they co-sediment with polysomes²¹⁻²⁴ and bind RNAs¹⁷. However, the precise role of DRG1 in the process is ambiguous. The crystal structure of the yeast DRG1 homolog, Rbg1 (Ribosome binding GTPase 1), together with a C-terminal fragment of the yeast homolog of DFRP1 (Tma46) shows that the canonical G-domain of the DRGs is interrupted by another domain, the S5D2L domain²². DRG1 seems to have an intrinsic GTPase activity that does not necessarily need a GTPase activating protein as is usually the case for most small GTPases^{16,22,25}. Potassium ions stimulate this activity as well as DFRP1 binding. It is unclear whether DFRP1 functions as GTPase activating protein as it binds opposite to the GTP binding pocket suggesting it stimulates the GTPase activity differently e.g. by improving the affinity to potassium ions.

Despite all these eclectic findings and the high interspecies conservation, the function of DRGs is poorly understood. Using *in vitro* approaches, we show that DRG1 binds to microtubules and bundles them. Furthermore, DRG1 can promote polymerization of microtubules and stabilizes them in the cold. Consistent with this observation, DRG1 is involved in spindle dynamics in human cells.

Results

DRG1 directly interacts with microtubules

DRG1 has been recently shown to localize at the mitotic spindle¹⁹, which raises the question whether the protein can interact with microtubules. To test this, *Xenopus laevis* egg extracts, arrested in a mitotic state, were incubated with polymerized, taxol-stabilized microtubules. After sedimentation of the microtubules by centrifugation, the tubulin-bound fraction was eluted with a high salt buffer (Fig. 1a). Whereas DRG1 and its interaction partner DFRP1 were not pelleted in the absence of microtubules, both proteins were found in the pellet fraction in the presence of microtubules. Both, DRG1 and DFRP1 were eluted with high salt from microtubules indicating that they bind specifically to microtubules. Similar results were obtained from experiments using HeLa nuclear extracts (Fig. 1b, only the eluate is shown). DRG1 and DFRP1 can be pelleted with microtubules and eluted with high salt, similar to two known microtubule-associated proteins MEL28/ELYS and chTOG, the human homolog of XMAP215. In contrast, we did not find the chromatin-associated condensin subunit CAP-G and DFRP2 in the microtubule-bound fraction. A number of microtubule binding proteins are

regulated by nuclear import factors and the Ran-GTP pathway. Similar to MEL28/ELYS²⁶, DRG1 and DFRP1 show a reduced microtubule association in the presence of importin α and β , which is reversed by the dominant positive mutant of Ran, RanQ69L (“RanGTP”).

To test whether DRG1 and DFRP1 bind directly to microtubules we incubated taxol-stabilized microtubules with recombinant DRG1, DFRP1 or DFRP2 (Fig. 1c). Whereas DRG1 and DFRP1 pelleted with microtubules, DFRP2 and a negative control protein remained in the supernatant. Addition of 500 mM NaCl to the incubation buffer prevented DRG1 and DFRP1 microtubule association indicating that the binding is specific and occurs via polar/charge interactions.

DRG1 diffuses on microtubules

To confirm and characterize DRG1 microtubule binding further, we used a total-internal-reflection-fluorescence (TIRF) microscopy-based assay to observe the DRG1 binding and mobility with single-molecule resolution. We observed that DRG1 interacted with microtubules in three different ways (Fig. 2a): DRG1 transiently bound to microtubules either in an immobile (green arrows) or diffusive manner, whereby the diffusion was either fast (magenta arrows) or slow (blue arrows). We analyzed the different proportions of DRG1 binding modes as a function of the DRG1 concentration (Fig. 2b). With decreasing DRG1 concentrations from 40 nM to 80 pM, we observed a decline of the DRG1 fraction showing diffusive microtubule binding and, conversely, an increase in the proportion showing immobile binding. We calculated the interaction times – i.e. the average time that a DRG1 molecule spends on the microtubule lattice – for the different populations. For the lower concentrations of DRG1, the interaction times of the immobile species of DRG1 increased from about 5 s to 12 s, while the interaction time of the slow diffusive DRG1 population decreased with decreasing DRG1 concentrations. The interaction times of the fast diffusive DRG1 population were faster than the image acquisition time of 0.1 s. To test if these three binding modes represent different nucleotide binding states of DRG1, we repeated the experiment in the presence of the non-hydrolysable GTP analogue GTP γ S (Supplementary Figure S1). Although the overall amount of DRG1 bound to microtubules was decreased, DRG1 also bound to microtubules in the presence of GTP γ S. We did not see a significant difference in the proportions of the mobile versus immobile DRG1 populations in comparison to experiments performed in the presence of GTP suggesting that DRG1 binding to microtubules is not determined by the nucleotide state of DRG1. For the lower concentrations of DRG1, the interaction times of the immobile population of DRG1 decreased slightly in the presence of GTP γ S compared to GTP. The slow diffusive movement of DRG1 on the microtubule lattice resembles that of MCAK, a microtubule depolymerase that diffuses on the microtubule to target both ends and performs its function there²⁷. The fast diffusing fraction resembles the behavior of the plus-end tracking protein EB1²⁸. In both cases, the diffusion towards the ends of microtubules facilitates “end-finding” and thus, increases the concentration of the proteins at the microtubule ends as compared to random diffusion in solution. Since microtubule binding did not depend on the nucleotide state, the different behavior might be due to oligomerization of DRG1 or due to different binding domains. Interestingly, different DRG1 intensities visible on the kymograph suggest that DRG1 may bind microtubules not only as a monomer but also as a multimer.

DRG1 binds microtubules via multiple regions

Having observed a direct microtubule interaction of DRG1, we were wondering which domains of the protein are required for microtubule binding. DRG1 consists of an N-terminal helix-turn-helix (HTH) motif, followed by the GTPase domain, which is interrupted by the S5D2L domain; the TGS domain constitutes the C-terminal part of the protein²² (Fig. 3a). As observed in Figure 1, full-length DRG1 pelleted together with taxol-stabilized microtubules in a high salt sensitive manner (Fig. 3b). The truncated proteins lacking the N-terminal HTH or the C-terminal TGS domain were similarly pelleted with microtubules. A varying fraction, depending on the truncation, was also in the supernatant indicating a weaker and differential association with microtubules. Interestingly, both the HTH and the TGS domain individually bound microtubules whereas the isolated S5D2L domain did not show this association. We also detected salt-sensitive microtubule binding for a truncated DRG1 version lacking both the HTH and TGS domain, indicating that the GTPase domain of DRG1 also interacts with microtubules (Fig. 3c). These results show that several domains of DRG1 are able to bind microtubules. We modeled the *Xenopus* DRG1 structure based on the available yeast Rbg1 structure (Fig. 3d). When calculating the electrostatic surface potential, we found an extensive positively charged surface formed by parts of the TGS, the HTH, the S5D2L and the G-domain opposite of the GTP-binding site as previously observed for Rbg1²². As microtubule-associated proteins often interact with microtubules via positively charged domains this whole area might be the microtubule binding site of DRG1.

DRG1 binds to microtubules lacking the negatively charged C-terminus of tubulin

Many microtubule-binding proteins bind tubulin via its acidic, negatively charged, unstructured C-terminus, which is also the site of many posttranslational modifications^{29,30}. This C-terminus can be cleaved off by the protease subtilisin. Repeating the microtubule co-sedimentation assay using subtilisin-digested microtubules showed that DRG1 still bound tubulin lacking the negatively charged C-terminus although the binding affinity might have been reduced (Fig. 3e).

DRG1 bundles microtubules

Since multiple domains of DRG1 were binding microtubules, we tested whether DRG1 could bundle them. To this end, we incubated taxol-stabilized, fluorescently-labeled microtubules with DRG1. Addition of 1 μM recombinant DRG1 induced microtubule bundling as observed by fluorescence microscopy (Fig. 4a). Electron microscopy analysis confirmed microtubule bundling in the presence of DRG1 (Fig. 4b). This bundling activity is consistent with DRG1 having multiple microtubule binding sites.

DRG1 promotes microtubule polymerization

Many microtubule binding proteins regulate microtubule dynamics³. When we added DRG1 to a fluorescently-labeled tubulin solution provided below the critical concentration for spontaneous microtubule growth³¹, we observed microtubule polymerization. A control without DRG1 showed no microtubule growth (Fig. 4c). We confirmed this observation by light scattering experiments: polymerization of tubulin at a relatively low concentration of 2.5 μM was observed when DRG1 was added (Fig. 4d). Thus, DRG1 is a GTPase that induces microtubule polymerization.

DRG1 stabilizes microtubules

The bundling and polymerization activities of DRG1 could indicate that DRG1 might also have a stabilizing effect on microtubules. To test whether DRG1 stabilizes microtubules, we polymerized microtubules from a high concentration of tubulin (12 μ M) in the presence or absence of DRG1 at 37°C for one hour and afterwards placed the sample on ice for 30 minutes. Note that we did not use taxol. Polymerized and stabilized microtubules were pelleted by centrifugation. The microtubules polymerized efficiently under these conditions but disassembled upon placing on ice in the buffer control. In the presence of DRG1, microtubules remained in the polymerized state despite the incubation on ice (Fig. 5a).

This *in vitro* stabilization effect was confirmed in HeLa cells stably expressing histone H2B-mCherry and eGFP-tubulin. For this purpose, DRG1 expression was downregulated by siRNA for 72 hrs (Fig. 5b). Afterwards, the cells were placed for one hour on ice which induced spindle disassembly in the mitotic population. Then, warm medium was added and the re-growth of microtubules was analyzed by fixing and analyzing the samples at different time points. Microtubules re-grew much slower in cells with reduced levels of DRG1 compared to the control cells (Fig. 5c and d). Thus, mitotic spindles recover much faster after a cold shock in cells having endogenous DRG1 levels suggesting that DRG1 either accelerates microtubule re-polymerization once warm medium is added or DRG1 prevents the complete disassembly of the spindle upon cold treatment. Noticeably, remnants of the mitotic spindle are often observed in control cells after 1h on ice (insert Fig. 5d, 0 min) but less frequent in cells lacking DRG1. These remnants might cause a faster re-assembly of the mitotic spindle. Both hypotheses are in agreement with our *in vitro* findings that DRG1 promotes microtubule polymerization and stabilization.

The GTPase activity of DRG1 is not necessary for its microtubule functions

DRG1 is a member of the small GTPase superfamily. To test whether its GTP binding and hydrolyzing activity is required for its microtubule functions, we used a dominant positive *Xenopus* DRG1 mutant, with a P73V exchange in the G1 box of the GTPase domain, which stabilizes the GTP-bound state³², and a dominant negative mutant, DRG1 S78N, which represents the GDP-bound or nucleotide free state of the GTPase^{22,24}. Both mutants were still able to bind microtubules (Fig. 6a), which is consistent with our observation that several domains are able to bind microtubules on their own (Fig. 3b). The mutants are also able to polymerize tubulin (Fig. 6b) and bundle (Fig. 6c) as well as to stabilize microtubules (Fig. 6d). This suggests that DRG1 does not require its GTPase activity for its microtubule-associated functions.

Full-length DRG1 is necessary to bundle, polymerize and stabilize microtubules

As shown above, most truncated versions of DRG1 were capable of binding microtubules. We were curious to see if they are also able to bundle, polymerize and stabilize microtubules. Therefore, we repeated the previously described assays using the recombinant DRG1 fragments. Fragments lacking the HTH, the TGS domain or both, as well as the HTH, the TGS or the S5D2L domain individually were neither able to bundle microtubules (Supplementary Fig. S2a), nor promoted polymerization (Supplementary Fig. S2b) or stabilized them upon cold stress (Supplementary Fig. S2c) under the same conditions used for the wild-type (Fig. 4 and 5). It was observed before in a different context that the full-length protein is necessary for its *in vivo* function²².

DRG1 impacts spindle dynamics in cells

Our results show that DRG1 influences microtubule behavior. To assess its impact on microtubule dynamics in cells, we analyzed HeLa cells stably expressing histone H2B-mCherry and tubulin-eGFP while passing through mitosis. DRG1 expression was down-regulated by siRNA. 24 hours post-transfection, live-cell imaging was carried out for 48 hours (Fig. 7a). Analysis of chromatin features using the software CellCognition³³ showed that the time from prophase to anaphase onset was extended upon DRG1 downregulation as compared to the control conditions (Fig. 7b). Analyzing the spindle features showed that a partial knock-down of DRG1 does not change the size or intensity of the spindle (data not shown), but the time from aster to the anaphase spindle formation was extended (Fig. 7c).

Recently, *Stolz et al.*³⁴ introduced an assay to identify microtubule plus-end regulators: Inhibition of the mitotic kinesin Eg5 by monastrol, which prevents centrosome separation in the beginning of mitosis, causes monoaster formation. *Stolz et al.* observed that these monoasters are asymmetric if microtubule plus-end assembly rates are increased and that this asymmetry can be rescued by low doses of taxol. We knocked down DRG1 by siRNA and treated the cells with monastrol. Indeed, spindles in cells with reduced DRG1 level showed much more asymmetric monoasters when compared to the control (Fig. 8a and b). This phenotype was also rescued by addition of low doses of taxol (Fig. 8c). This phenotype again suggests an involvement of DRG1 in spindle dynamics.

Discussion

The function of DRG1 has been long debated. Considering its high evolutionary conservation, it was suggested that DRG1 has an important function in a fundamental cell biological process. We identify here that DRG1 is involved in spindle assembly. DRG1 binds microtubules and can diffuse on the microtubule lattice *in vitro*. DRG1 promotes microtubule polymerization and bundling and stabilizes them. To perform these latter activities, DRG1 does not require GTP hydrolysis but all its domains as only the full-length protein is functional in these assays. Consistent with these observations DRG1 is also involved in spindle dynamics in HeLa cells: microtubules regrow faster after a cold shock induced disassembly if DRG1 is present; early mitotic progression is extended if DRG1 is downregulated and a high number of asymmetric monoasters forms upon monastrol treatment in cells lacking DRG1.

DRG1 binds directly to microtubules consistent with its previously shown localization at the mitotic spindle¹⁹. Truncated versions of DRG1 lacking the TGS and/or HTH domain as well as the TGS and HTH domain individually are still able to bind microtubules while the S5D2L domain alone is not, although we cannot exclude that the latter is not properly folded. Electrostatic surface potential analysis shows that DRG1 has a highly positively charged surface stretching over the TGS, the HTH, the S5D2L and the G-domain opposite of the GTP-binding site. Many microtubule binding proteins are highly positively charged. Therefore, this positively charged region might be the binding region of DRG1 to microtubules. This would also explain why most of the domains bind microtubules individually. The interaction of positively charged microtubule binding proteins with microtubules usually occurs via the negatively charged C-terminus of tubulin. However, DRG1 still binds to microtubules lacking the C-terminal ends after subtilisin digestion indicating that this is not the major binding site. Similarly, the *drosophila* non-claret disjunctional (Ncd) kinesin-like protein does not strictly depend on the C-terminus of tubulin for microtubule interaction³⁵.

In addition to binding microtubules as an immobile molecule, DRG1 can also diffuse on the microtubule lattice, either fast or slow. This behavior resembles e.g. the microtubule depolymerase MCAK²⁷. MCAK functions at both ends of microtubules. Its random diffusion towards the ends enhances the chances that MCAK binds microtubule ends compared to simple diffusion in solution. It is possible that DRG1 also targets to the microtubule ends to promote microtubule polymerization there. The proportion of the three different binding modes, immobile, slow diffusive and fast diffusive, was depended on the concentration of DRG1. The lower the concentration, the more immobile and the less diffusive DRG1 was. It is unlikely that the three different binding modes represent DRG1 in the three different nucleotide bound states, GTP-bound, GDP-bound and nucleotide free, as we observed similar proportions of the three different binding modes in the presence of the non-hydrolysable GTP analogue GTP γ S. Although the overall binding was decreased in the presence of GTP γ S, the interaction times of the immobile species were extended at low concentrations. The three binding modes might perform three different functions such as polymerization versus bundling, might represent the different binding sites, or different oligomeric states.

While the GTP hydrolysis is not necessary for the microtubule-related functions of DRG1 shown here, the truncated versions of DRG1 have highly reduced or no bundling, polymerization or stabilization activity although mostly still binding microtubules. It was previously shown that the severe growth phenotype caused by triple deletion of the DRG1 and 2 homologs, Rbg1 and 2 together with the ATPase Slh1 in yeast can be rescued by full-length Rbg1 but not by any of the tested truncations²⁴.

The polymerization, bundling and stabilization activities of DRG1 could be completely independent functions or connected to each other: the bundling of microtubules could also stabilize them; the polymerization activity could increase the amount of microtubules in a population that is in the growth phase and thereby stabilize them; the bundling could increase polymerization by increasing the microtubule density close to DRG1. In this respect, it is surprising that tubulins as GTPases are directly regulated by another GTPase, DRG1, although not using its GTP hydrolysis activity in this context.

Consistent with the biochemical assays, in HeLa cells microtubules that depolymerized on ice regrew faster if DRG1 was present. This faster recovery can be either explained by the polymerization activity of DRG1 or by the stabilization activity, which might stabilize small microtubule remnants that regrow faster afterwards when cells were provided with fresh, warm medium. It was observed before that DRG1 shows some thermophilic behavior: DRG1 hydrolyzes GTP over a wide range of temperatures with an optimum at 42°C²⁵. Maybe DRG1 is also more active at cold temperatures compared to other proteins or performs its functions mainly under extreme, stress-situations.

Microtubules have important functions in mitosis and interphase. Our *in vitro* data shows that DRG1 has many functions connected to microtubules but the assays cannot distinguish between mitotic and interphasic functions. The cold shock experiment in HeLa cells suggests that DRG1 performs its function in the mitotic spindle, confirmed by our observation that the timing from prophase to anaphase and from aster formation to anaphase spindles is extended in HeLa cells, in which DRG1 was downregulated by siRNA. Cells treated with monastrol after DRG1 knock down showed a higher proportion of asymmetric spindles compared to the control cells, and this phenotype could be rescued with low doses of taxol. This effect was observed before when negative growth, plus tip regulators were downregulated³⁴. In our biochemical analysis, DRG1 promoted microtubule

polymerization and acted rather as a positive growth factor. It was shown before for XMAP215 that it can act as a microtubule polymerase or de-polymerase depending on the conditions, like a classical metabolic enzyme catalyzing a reaction theoretically in both direction^{36,37}. We cannot exclude that this is also the case for DRG1. However, as we do not understand well the reason for asymmetric aster formation it is more likely that the monastrol assay scores likewise for down-regulating positive and negative regulators.

DRG1 has been suggested to possess a function connected to ribosomes and translation as it co-fractionates with ribosomes. The function in this context is still not fully understood. The probably independent functions of DRG1 concerning microtubules and translation could be spatially or temporally regulated e.g. DRG1 might have different functions during different cell cycle stages or one of the functions could be induced upon stress situations as suggested before¹⁶. Likewise, the function could be regulated by its binding partners.

Together, our analysis shows that DRG1 is a microtubule binding, bundling, polymerization and stabilization factor. It does not need its GTPase activity to perform these functions. Truncated versions bind microtubules but have highly reduced or none of the other activities. Downregulation of DRG1 in HeLa cells indicated that the protein is involved in mitotic spindle assembly. Deregulation of DRG1 was suggested to be involved in cancer formation¹⁹ and it is conceivable that the function of DRG1 in mitotic spindle assembly is connected to this. It is also possible that the microtubule function of DRG1 is not limited to mitosis. How DRG1 potentially affects interphase microtubule function is an interesting question awaiting detailed investigation.

Methods

Protein expression and purification

Constructs for *Xenopus laevis* full-length DFRP1 and DRG1 as well as DRG1 fragments and human full-length DFRP2 were generated from a synthetic DNA optimized for codon usage in *E.coli* (Geneart) and cloned into a pET28a vector or modified pET28a vectors with a SUMO or eGFP-tag. Recombinant protein was expressed in *E.coli* and purified by Ni-affinity chromatography. For fluorescently labeled DRG1, the eGFP-tag was N-terminal. For motility binding assays, the recombinant protein was further purified by ion exchange chromatography (Tricorn High Performance Columns, Mono Q 5/50GL, GE). Proteins were dialyzed against the individual assay buffers.

To gain dominant GTPase mutants, we designed point mutations in the GTPase domain by sequence alignment to other GTPases: to obtain a dominant-negative DRG1 mutant we mutated serine 78 to asparagine, which is a conserved residue that causes a dominant negative mutant e.g. in the small GTPase Ran³⁸ and in Rbg1^{22,24}. To obtain a dominant-positive DRG1 mutant we exchanged proline 73 to valine according to the dominant positive mutant of the *Streptomyces coelicolor* GTPase Obg³². The DRG1 S78N and P73V mutants were generated by mutagenesis using the QuickChange site-directed mutagenesis kit (Agilent). DRG1 fragments used were aa 49-367 (Δ HTH), aa 1-293 (Δ TGS), aa 1-46 (HTH), aa 293-367 (TGS), aa 175-238 (S5D2L) and aa 49-293 (Δ HTH Δ TGS), all based on the *Xenopus laevis* sequence and expressed as His₆-tagged protein from a pET28a vector.

Antibodies

Polyclonal antibodies against full-length *Xenopus* and human His₆-DRG1, *Xenopus* His₆-DFRP1 and *Xenopus* His₆-SUMO-DFRP2A were raised in rabbits and used 1:1,000 in western blotting. Antibodies against MEL28³⁹ and ch-TOG²⁶ as well as CAP-G⁴⁰ have been described previously. The β -actin (A5441), β -tubulin (T7816) and α -tubulin (DM1A) antibodies were obtained from Sigma and the centromere (CREST) antibody (15-234) from Antibodies Incorporated.

Preparation of taxol-stabilized microtubules

To polymerize microtubules for the co-sedimentation assay, porcine brain tubulin (Cytoskeleton, T240) was resuspended in BRB80 (80 mM PIPES, 1 mM MgCl₂, 1 mM EGTA, pH 6.8) to 10 mg/ml. The microtubules were polymerized by adding 2 mM GTP and incubation for 30 minutes at 37 °C. Taxol was added to a final concentration of 20 μ M. After 10 min incubation, the solution was centrifuged for 10 min at 110,000 x g in a TLA120 rotor (Beckman) and 37 °C. The pellet was resuspended in BRB80 + 20 μ M taxol and the concentration was measured using a Bradford assay.

Microtubules for the bundling assay were prepared in a slightly modified way⁴¹: 10 mg/ml unlabeled tubulin, 2 mg/ml Cy3-labeled tubulin and 1 mM GTP were incubated at 37 °C for 30 minutes. The solution was then diluted tenfold with BRB80 + 20 μ M taxol, the microtubules were pelleted by centrifugation for 10 min at maximum speed in a 1.5 ml reaction tube centrifuge at RT and resuspended as above.

Microtubule binding assay with extracts

HeLa nuclear extracts (4C Biotech) were diluted with CSF-XB buffer (100 mM KCl, 0.1 mM CaCl₂, 2 mM MgCl₂, 50 mM sucrose, 10 mM Hepes, 5 mM EGTA, pH 7.7) to 1 mg/ml. CSF-arrested *Xenopus* egg extracts were diluted 1:3 with CSF-XB buffer. After centrifugation at 100,000 g for 10 min at 20°C the supernatant was incubated with 2 μ M taxol-stabilized microtubules (for CSF extracts 4 μ M) at RT for 15 min in the presence of 1mM GTP and 10 μ M taxol. The samples were centrifuged at 100,000 g for 10 min at 20 °C through a cushion of 40 % glycerol in CSF-XB containing 20 μ M taxol. Pellets were resuspended in wash buffer (CSF-XB buffer containing 1 mM DTT, 1 mM GTP, and 20 μ M taxol) and spun for 10 min at 100,000 x g. The washing was repeated one more time. Microtubules binding proteins were eluted with 500 mM NaCl and the pellet and eluate were analyzed by SDS-PAGE and immunoblotting.

Microtubule binding, bundling and polymerization assays with recombinant protein

The microtubule binding, bundling and polymerization assays were done as in ⁴². In short, recombinant protein in CSF-XB buffer was incubated with 2 mM GTP, with or without 12 μ M taxol-stabilized microtubules and with or without 500 mM NaCl in CSF-XB + 20 μ M taxol for 15 min at RT. Afterwards, the solution was spun for 10 min at 100,000 x g in a TLA100 rotor and 20 °C. The supernatant and pellet were analyzed by SDS-PAGE.

For microtubule bundling, 0.1-0.3 μ M Cy3-labeled microtubules⁴¹ were incubated with 1 μ M recombinant protein in 10 μ l BRB80 buffer + 20 μ M taxol for 10 minutes at RT. Samples were squashed between a coverslip and slide without fixation and analyzed by confocal microscopy using a LSM780 Zeiss microscope equipped with a Plan-Apochromat 63x/1.4 Oil DIC objective and 561nm-Diode Lasers. For electron microscopy, the samples were stained in 2 % uranyl acetate. Images were

acquired with a CMOS camera (TemCam-F416, TVIPS, Gauting, Germany) mounted on a Tecnai Spirit (Thermo Fisher Scientific, Eindhoven, The Netherlands) operated at 120 kV.

For microtubule polymerization, 1 μ M recombinant protein was incubated with 4 μ M porcine brain tubulin and 1 μ M Cy3-labeled tubulin and 1 mM GTP for 30 min at 37 °C in BRB80 buffer. The samples were fixed in 400 μ l BRB80 buffer containing 0.25 % glutaraldehyde, 10 % glycerol and 0.1 % TritonX-100 for at least 10 min. Samples were spun through 2 ml 25 % glycerol in BRB80 for 20 min at 4,600 x g in a Sorvall Heraeus 75002027K swing rotor and RT onto a coverslip. The coverslips were post-fixed with methanol at -20 °C for 10 min, washed with PBS and mounted with Mowiol. Samples were imaged by a LSM780 Zeiss equipped with a Plan-Apochromat 63x/1.4 Oil DIC objective and 561nm-Diode Lasers.

To digest the taxol-stabilized microtubules with subtilisin, the protease was added to 0.3 mg/ml for 3 hrs. Another 0.3 mg/ml subtilisin were added after the first 90 minutes. The digestion was stopped by addition of 7 mM PMSF and 1:19 of a protease inhibitor mix (10 mg/ml AEBSF, 0.2 mg/ml leupeptin, 0.1 mg/ml pepstatin, 0.2 mg/ml aprotinin) for 15 min. Another 1:12 of protease inhibitor mix was added followed by 40 min of incubation. The microtubules were pelleted by centrifugation, washed several times and resuspended in BRB80 + 20 μ M taxol. (Concentrations of taxol-stabilized microtubules were decreased in the co-sedimentation assay to reach for the same amount of subtilisin-digested and not digested microtubules.)

Microtubule motility binding assay

For microtubule polymerization 20-30 μ M porcine tubulin were incubated with 5% DMSO, 4 mM MgCl₂, 1 mM ATP in BRB80 (pH 6.9) for 1h at 37°C. Upon finishing, BRB80 supplemented with 10 μ M taxol was added to the reaction tube. Afterwards, the microtubules were spun down at 22psi using a Beckman airfuge. The pellet was re-suspended in BRB80 containing 10 μ M taxol.

The flow cell was constructed as described in ⁴³, but the surface was coated with Chlorotrimethylsilane (MTS, Merck Millipore 102333). The flow channels were washed 4-5 times with sterile filtered BRB80 buffer, followed by incubation with anti- β -tubulin (Sigma Aldrich, T7816) for 15-20 minutes at RT. Afterwards, the channels were washed once with BRB80 and blocked using 1 % Pluronic F-127 (Sigma-Aldrich, P2443) in BRB80 for 20-25 minutes, followed by 5 times washing with BRB80 and incubation with 10 % rhodamine labelled taxol-stabilized microtubules for 15 minutes. The assay buffer (BRB80, 112.5 mM Casein, 1 mM GTP, 20 mM D-Glucose, 250 nM glucose oxidase, 134 nM catalase, 0.5 % β -mercaptoethanol) containing the protein was added after a quick wash of the channel. Samples were imaged at 25°C on a home built total internal reflection fluorescence (TIRF) microscope combined with epifluorescence. The TIRF microscope was equipped with a sCMOS camera (Orca Flash 4.0, Hamamatsu Photonics) and an oil immersion TIRF objective (60x, Nikon). To visualize DRG1 binding, 40 s time-lapse videos were recorded at 10 fps using a continuous image acquisition mode at 100 ms exposure at various concentrations. The fluorophore/protein was excited using 488 laser line (Omicron, LuxX 488-100). Data was primarily processed using FIJI (<http://fiji.sc/Fiji>). The kymographs were generated by a custom written macro and were analyzed for different populations and interaction times at various concentrations. The graphs were plotted using Origin 9.1.

Microtubule polymerization measured by light-scattering

The protocol for the light scattering experiment was adapted from ⁴⁴. 1 μ M recombinant protein was mixed with 2.5 μ M tubulin and 1 mM GTP in polymerization buffer (80 mM PIPES, 2 mM MgCl₂, 0.5 mM EGTA and 10 % glycerol) in a total volume of 200 μ l in a 96-well plate with flat bottom. The absorbance at 340 nm and 37 °C was measured for up to 2:15 hrs in a BioTek Synergy H4 Hybrid Multiplate reader. Data was collected every 38 seconds.

Microtubule stabilization in the cold

The protocol was adapted from ⁴⁴: tubulin (12 μ M) was polymerized in the absence or presence of recombinant protein (5 μ M), GTP (1mM) and DTT (1mM) in BRB80 buffer for 1 h at 37 °C. Afterwards the sample was incubated on ice for 30 min, followed by centrifugation at 312,000 x g for 20 min at 4°C. The supernatant and pellet were analyzed by SDS-PAGE.

Cell Culture and transfection

Cell culture experiments were performed according to ⁴⁵. HeLa cells were maintained in Dulbecco's modified Eagle's medium (DMEM) supplemented with 2mM L-glutamine, 10% fetal bovine serum (FBS) and 500 units/ml penicillin-streptomycin (all from Gibco). The H2B-mCherry and tubulin-eGFP cell line⁴⁶ was a gift from Daniel Gerlich (IMBA, Vienna) and was maintained in DMEM supplemented with 2 mM L-glutamine, 10 % fetal bovine serum (FBS) and additionally with 0.5 μ g/ml puromycin (Gibco) and 500 μ g/ml G-418 (Geneticin; Life Technologies). The knockdown experiments were performed with the following siRNA oligonucleotides: siDRG1-1 (HSS107061), 5'-GAAGGCUUUGGCAUUCGCUUGAACA-3', siDRG1-2 (HSS181476), 5'-CAGCACACCACUUAGGGCUGCUUAA-3', siDRG1-3 (HSS181477), 5'-CCUGUAACUUGAUCUUGAUUGUUCU-3' (ThermoFisher), and AllStars negative control siRNA (from Qiagen). HeLa cell suspensions were transfected with 40 nM siRNA using Lipofectamine RNAiMAX (Invitrogen) according to the manufacturer's instructions.

Live-cell imaging experiments

Live-cell imaging was adapted from ⁴⁵. HeLa H2B-mCherry and tubulin-eGFP cells were transfected with siRNA oligonucleotides in 8-well μ -slide chambers (Ibidi). The cells were imaged for 48 h starting at 24 h post-transfection (approx.), using a Plan-Apochromat 20 \times NA 0.8 objective and a 488-nm and 561-nm diode lasers on a LSM 5 live confocal microscope (Zeiss) equipped with a heating and CO₂ incubation system (Ibidi). ZEN software (Zeiss) was used to acquire images from seven 3.6- μ m-spaced optical z-sections at various positions every 3 min. Then, single position files were generated from the maximum intensity projections in ZEN and converted into image sequences with free licensed AxioVision software (LE64; V4.9.1.0). Segmentation, annotation, classification and tracking of cells progressing through mitosis were performed using the Cecog analyser (<http://www.cellcognition.org/software/cecoganalyser>)³³. The subsequent analysis was performed in Microsoft excel and GraphPad Prism. Three independent experiments were performed.

Cold shock regrowth experiments

HeLa cells expressing H2B-mCherry and tubulin-eGFP were seeded on glass coverslides and transfected with siRNA oligonucleotides in 24-well well plates (Greiner Bio-One). 72 h post-transfection the cells were incubated on ice for 1 h allowing to depolymerize spindle microtubules⁴⁷. Then, cold media was replaced with warm medium and the cells were incubated at 37°C. The cells were fixed at indicated times in 4% PFA after one wash with PBS. Afterwards, Z-Stacks (z-scaling 250nm / Pinhole 26µm) from ten random prometaphase cells per siRNA, time point and experiment (n=2) were acquired using a LSM780 Zeiss equipped with a Plan-Apochromat 63x/1.4 Oil DIC objective and 488nm-Argon and 561nm-Diode lasers. The spindle size quantitation in voxels was obtained using Imaris (Bitplane) by absolute intensity based segmentation of the tubulin-eGFP signal in the spindle. The data was exported as excel files and analyzed using GraphPad Prism.

Evaluation of monoastral mitotic spindles

HeLa cells were seeded on glass coverslides and transfected with siRNA oligonucleotides in 24-well well plates (Greiner Bio-One). 72 h post-transfection the cells were incubated with 70 µM monastrol (Sigma) in the presence or absence of 2 nM taxol for 3 h³⁴, washed with PBS and fixed for immunofluorescence with 4 % PFA. For immunofluorescence staining samples were incubated for 1h in blocking buffer (PBS + 0,1 % Triton-X100 + 3 % BSA). Afterwards the samples were incubated for 2 hrs at RT with anti-α-tubulin (mouse DM1A; Sigma) and anti-human centromere (CREST) (Antibodies Incorporated 15-234) antibodies. As secondary antibodies anti-Alexa-Fluor-488-anti-mouse and anti-Alexa-Fluor-647-anti-human (Life technologies) were used (1 h at RT). After staining with DAPI for 10 min, samples were mounted in mowiol 4-88 (Calbiochem). Z-Stacks (z-scaling 350nm / Pinhole 25um) from five to eight random positions per siRNA and condition were acquired using a LSM780 Zeiss equipped with a Plan-Apochromat 40x/1.3 Oil DIC M27 objective and 405nm-DPSS, 488nm-Argon and 633nm-Diode lasers. The quantification of asymmetric monopolar spindles is based on at least 4 independent experiments with monastrol treatment and on two independent experiments with monastrol and monastrol + taxol treatment. Per condition between 15 and 98 cells with monopolar spindles were analyzed.

Statistical analysis for experiments in HeLa cells

When possible the data was tested for normality by D'Agostino & Pearson omnibus normality test and the variances were compared using an F test (P<0.05). If a Gaussian distribution could be assumed for the data series and they had no significantly different variances, a two-tailed student's t-test was performed. If a Gaussian distribution could be assumed for the data series and they had significantly different variances, a two-tailed student's t-test with Welch's correction was performed. If a Gaussian distribution could not be assumed, a Mann-Whitney test was performed.

References

- 1 Heald, R. & Khodjakov, A. Thirty years of search and capture: The complex simplicity of mitotic spindle assembly. *J Cell Biol* **211**, 1103-1111, doi:10.1083/jcb.201510015 (2015).
- 2 Prosser, S. L. & Pelletier, L. Mitotic spindle assembly in animal cells: a fine balancing act. *Nat Rev Mol Cell Biol* **18**, 187-201, doi:10.1038/nrm.2016.162 (2017).
- 3 Petry, S. Mechanisms of Mitotic Spindle Assembly. *Annu Rev Biochem* **85**, 659-683, doi:10.1146/annurev-biochem-060815-014528 (2016).
- 4 Schneider, M. A. *et al.* AURKA, DLGAP5, TPX2, KIF11 and CKAP5: Five specific mitosis-associated genes correlate with poor prognosis for non-small cell lung cancer patients. *International journal of oncology* **50**, 365-372, doi:10.3892/ijo.2017.3834 (2017).
- 5 Kumar, M. *et al.* End Binding 1 (EB1) overexpression in oral lesions and cancer: A biomarker of tumor progression and poor prognosis. *Clinica chimica acta; international journal of clinical chemistry* **459**, 45-52, doi:10.1016/j.cca.2016.05.012 (2016).
- 6 Du, Y. *et al.* TACC3 promotes colorectal cancer tumourigenesis and correlates with poor prognosis. *Oncotarget* **7**, 41885-41897, doi:10.18632/oncotarget.9628 (2016).
- 7 Lee, E. H. *et al.* Molecular cloning of a novel GTP-binding protein induced in fish cells by rhabdovirus infection. *FEBS Lett* **429**, 407-411 (1998).
- 8 Sazuka, T., Tomooka, Y., Ikawa, Y., Noda, M. & Kumar, S. DRG: a novel developmentally regulated GTP-binding protein. *Biochem Biophys Res Commun* **189**, 363-370 (1992).
- 9 Schenker, T., Lach, C., Kessler, B., Calderara, S. & Trueb, B. A novel GTP-binding protein which is selectively repressed in SV40 transformed fibroblasts. *J Biol Chem* **269**, 25447-25453 (1994).
- 10 Shimmin, L. C. & Dennis, P. P. Characterization of the L11, L1, L10 and L12 equivalent ribosomal protein gene cluster of the halophilic archaeobacterium Halobacterium cutirubrum. *EMBO J* **8**, 1225-1235 (1989).
- 11 Hudson, J. D. & Young, P. G. Sequence of the Schizosaccharomyces pombe gtp1 gene and identification of a novel family of putative GTP-binding proteins. *Gene* **125**, 191-193 (1993).
- 12 Kumar, S., Iwao, M., Yamagishi, T., Noda, M. & Asashima, M. Expression of GTP-binding protein gene drg during Xenopus laevis development. *The International journal of developmental biology* **37**, 539-546 (1993).
- 13 Sommer, K. A., Petersen, G. & Bautz, E. K. The gene upstream of DmRP128 codes for a novel GTP-binding protein of Drosophila melanogaster. *Mol Gen Genet* **242**, 391-398 (1994).
- 14 Leipe, D. D., Wolf, Y. I., Koonin, E. V. & Aravind, L. Classification and evolution of P-loop GTPases and related ATPases. *J Mol Biol* **317**, 41-72, doi:10.1006/jmbi.2001.5378 (2002).
- 15 Li, B. & Trueb, B. DRG represents a family of two closely related GTP-binding proteins. *Biochim Biophys Acta* **1491**, 196-204 (2000).
- 16 O'Connell, A., Robin, G., Kobe, B. & Botella, J. R. Biochemical characterization of Arabidopsis developmentally regulated G-proteins (DRGs). *Protein expression and purification* **67**, 88-95, doi:10.1016/j.pep.2009.05.009 (2009).
- 17 Ishikawa, K. *et al.* Cloning and characterization of Xenopus laevis drg2, a member of the developmentally regulated GTP-binding protein subfamily. *Gene* **322**, 105-112 (2003).
- 18 Devitt, M. L., Maas, K. J. & Stafstrom, J. P. Characterization of DRGs, developmentally regulated GTP-binding proteins, from pea and Arabidopsis. *Plant molecular biology* **39**, 75-82 (1999).
- 19 Lu, L., Lv, Y., Dong, J., Hu, S. & Peng, R. DRG1 is a potential oncogene in lung adenocarcinoma and promotes tumor progression via spindle checkpoint signaling regulation. *Oncotarget* **7**, 72795-72806, doi:10.18632/oncotarget.11973 (2016).
- 20 Ishikawa, K., Azuma, S., Ikawa, S., Semba, K. & Inoue, J. Identification of DRG family regulatory proteins (DFRPs): specific regulation of DRG1 and DRG2. *Genes to cells : devoted to molecular & cellular mechanisms* **10**, 139-150, doi:10.1111/j.1365-2443.2005.00825.x (2005).

- 21 Ishikawa, K., Akiyama, T., Ito, K., Semba, K. & Inoue, J. Independent stabilizations of polysomal Drg1/Dfrp1 complex and non-polysomal Drg2/Dfrp2 complex in mammalian cells. *Biochem Biophys Res Commun* **390**, 552-556, doi:10.1016/j.bbrc.2009.10.003 (2009).
- 22 Francis, S. M., Gas, M. E., Daugeron, M. C., Bravo, J. & Seraphin, B. Rbg1-Tma46 dimer structure reveals new functional domains and their role in polysome recruitment. *Nucleic Acids Res* **40**, 11100-11114, doi:10.1093/nar/gks867 (2012).
- 23 Wout, P. K., Sattlegger, E., Sullivan, S. M. & Maddock, J. R. *Saccharomyces cerevisiae* Rbg1 protein and its binding partner Gir2 interact on Polyribosomes with Gcn1. *Eukaryotic cell* **8**, 1061-1071, doi:10.1128/EC.00356-08 (2009).
- 24 Daugeron, M. C., Prouteau, M., Lacroute, F. & Seraphin, B. The highly conserved eukaryotic DRG factors are required for efficient translation in a manner redundant with the putative RNA helicase Slh1. *Nucleic Acids Res* **39**, 2221-2233, doi:10.1093/nar/gkq898 (2011).
- 25 Perez-Arellano, I., Spinola-Amilibia, M. & Bravo, J. Human Drg1 is a potassium-dependent GTPase enhanced by Lerep4. *The FEBS journal* **280**, 3647-3657, doi:10.1111/febs.12356 (2013).
- 26 Yokoyama, H. *et al.* The nucleoporin MEL-28 promotes RanGTP-dependent gamma-tubulin recruitment and microtubule nucleation in mitotic spindle formation. *Nature communications* **5**, 3270, doi:10.1038/ncomms4270 (2014).
- 27 Helenius, J., Brouhard, G., Kalaidzidis, Y., Diez, S. & Howard, J. The depolymerizing kinesin MCAK uses lattice diffusion to rapidly target microtubule ends. *Nature* **441**, 115-119, doi:10.1038/nature04736 (2006).
- 28 Chen, Y., Rolls, M. M. & Hancock, W. O. An EB1-kinesin complex is sufficient to steer microtubule growth in vitro. *Curr Biol* **24**, 316-321, doi:10.1016/j.cub.2013.11.024 (2014).
- 29 Cooper, J. R. & Wordeman, L. The diffusive interaction of microtubule binding proteins. *Curr Opin Cell Biol* **21**, 68-73, doi:10.1016/j.ceb.2009.01.005 (2009).
- 30 Redeker, V., Melki, R., Prome, D., Le Caer, J. P. & Rossier, J. Structure of tubulin C-terminal domain obtained by subtilisin treatment. The major alpha and beta tubulin isotypes from pig brain are glutamylated. *FEBS Lett* **313**, 185-192 (1992).
- 31 Fygenson, D. K., Braun, E. & Libchaber, A. Phase diagram of microtubules. *Physical review. E, Statistical physics, plasmas, fluids, and related interdisciplinary topics* **50**, 1579-1588 (1994).
- 32 Okamoto, S. & Ochi, K. An essential GTP-binding protein functions as a regulator for differentiation in *Streptomyces coelicolor*. *Molecular microbiology* **30**, 107-119 (1998).
- 33 Held, M. *et al.* CellCognition: time-resolved phenotype annotation in high-throughput live cell imaging. *Nat Methods* **7**, 747-754, doi:10.1038/nmeth.1486 (2010).
- 34 Stolz, A., Ertych, N. & Bastians, H. A phenotypic screen identifies microtubule plus end assembly regulators that can function in mitotic spindle orientation. *Cell Cycle* **14**, 827-837, doi:10.1080/15384101.2014.1000693 (2015).
- 35 Karabay, A. & Walker, R. A. Identification of Ncd tail domain-binding sites on the tubulin dimer. *Biochem Biophys Res Commun* **305**, 523-528 (2003).
- 36 Brouhard, G. J. *et al.* XMAP215 is a processive microtubule polymerase. *Cell* **132**, 79-88, doi:10.1016/j.cell.2007.11.043 (2008).
- 37 Howard, J. & Hyman, A. A. Microtubule polymerases and depolymerases. *Curr Opin Cell Biol* **19**, 31-35, doi:10.1016/j.ceb.2006.12.009 (2007).
- 38 Dasso, M., Seki, T., Azuma, Y., Ohba, T. & Nishimoto, T. A mutant form of the Ran/TC4 protein disrupts nuclear function in *Xenopus laevis* egg extracts by inhibiting the RCC1 protein, a regulator of chromosome condensation. *EMBO J* **13**, 5732-5744 (1994).
- 39 Franz, C. *et al.* MEL-28/ELYS is required for the recruitment of nucleoporins to chromatin and postmitotic nuclear pore complex assembly. *EMBO Rep* **8**, 165-172 (2007).
- 40 Magalska, A. *et al.* RuvB-like ATPases function in chromatin decondensation at the end of mitosis. *Dev Cell* **31**, 305-318, doi:10.1016/j.devcel.2014.09.001 (2014).

- 41 Cahu, J. *et al.* Phosphorylation by Cdk1 increases the binding of Eg5 to microtubules in vitro and in *Xenopus* egg extract spindles. *PLoS One* **3**, e3936, doi:10.1371/journal.pone.0003936 (2008).
- 42 Yokoyama, H., Rybina, S., Santarella-Mellwig, R., Mattaj, I. W. & Karsenti, E. ISWI is a RanGTP-dependent MAP required for chromosome segregation. *J Cell Biol* **187**, 813-829, doi:10.1083/jcb.200906020 (2009).
- 43 Bormuth, V., Varga, V., Howard, J. & Schaffer, E. Protein friction limits diffusive and directed movements of kinesin motors on microtubules. *Science* **325**, 870-873, doi:10.1126/science.1174923 (2009).
- 44 Patel, K., Nogales, E. & Heald, R. Multiple domains of human CLASP contribute to microtubule dynamics and organization in vitro and in *Xenopus* egg extracts. *Cytoskeleton* **69**, 155-165, doi:10.1002/cm.21005 (2012).
- 45 Schooley, A., Moreno-Andres, D., De Magistris, P., Vollmer, B. & Antonin, W. The lysine demethylase LSD1 is required for nuclear envelope formation at the end of mitosis. *J Cell Sci* **128**, 3466-3477, doi:10.1242/jcs.173013 (2015).
- 46 Held, M. *et al.* CellCognition: time-resolved phenotype annotation in high-throughput live cell imaging. *Nat Methods* **7**, 747-754, doi:10.1038/nmeth.1486 (2010).
- 47 Yokoyama, H. *et al.* CHD4 is a RanGTP-dependent MAP that stabilizes microtubules and regulates bipolar spindle formation. *Curr Biol* **23**, 2443-2451, doi:10.1016/j.cub.2013.09.062 (2013).
- 48 Biasini, M. *et al.* SWISS-MODEL: modelling protein tertiary and quaternary structure using evolutionary information. *Nucleic Acids Res* **42**, W252-258, doi:10.1093/nar/gku340 (2014).

Acknowledgments

This work was supported by the German Research Foundation and the ERC (AN377/3-2, AN377/6-1 and 309528 CHROMDECON to W.A.), a PhD Fellowship of the Boehringer Ingelheim Fonds to A.K.S. and PhD Fellowship of the IMPRS "From Molecules to Organisms" to M.C.

The authors have no additional competing financial interests.

Author contributions

A.K.S. and W.A. designed experiments and wrote the manuscript. A.K.S. and A.M. did the cloning of DNA constructs. A.K.S. purified the proteins and performed bundling, polymerization and stabilization experiments. A.K.S. and H.Y. performed MT co-sedimentation assays. M.C. performed TIRF experiments, supervised by E. S. D.M.-A. performed all experiments in HeLa cells. K.H. made the electron microscopy. F.B. performed the structure modelling. S.D. Built the TIRF microscope. All authors discussed the manuscript.

Figure legends

Figure 1: DRG1 and DRFP1 bind microtubules

(a) 4 μM taxol-stabilized microtubules (MTs) were incubated with *Xenopus* cytosolic factor arrested (CSF) extract. Microtubules were co-sedimented together with MT-binding proteins and eluted by 500 mM NaCl in CSF-XB buffer. The pellet and the elution were analyzed by western blotting. **(b)** 2 μM taxol-stabilized microtubules were incubated with HeLa nuclear extract (NE) and sedimented. The eluates (obtained by 500 mM NaCl) were analyzed by western blotting with the indicated antibodies. Importin α and β (α/β) were added to the reaction as well as RanQ69L, which is fixed in the GTP bound state (RanGTP) to test if the binding is regulated by Ran. **(c)** Recombinant *Xenopus laevis* DRG1 and DRFP1 as well as human DRFP2 were incubated with 12 μM taxol-stabilized microtubules to test if the observed binding is direct. RanQ69L served as a negative control (neg. ctrl.). S: supernatant, P: pellet.

Figure 2: DRG1 interacts with the microtubule lattice in distinct binding modes

(a) Kymographs showing three different binding modes (*fast diffusion, slow diffusion, immobile*) of eGFP-DRG1 over four different concentrations (0.08 nM, 0.4 nM, 4 nM, 40 nM). Every kymograph represents a microtubule on its horizontal axis observed over time (vertical). The proportions **(b)** and interaction times **(c)** of the different DRG1 binding populations are shown at aforementioned concentrations. Color scheme: fast diffusion (magenta), slow diffusion (cyan), immobile (green).

Figure 3: Different DRG1 domains interact with microtubules

(a) Scheme of DRG1 indicating the different domains. **(b)** Full-length and truncated versions of *Xenopus laevis* DRG1 were incubated and co-sedimented with taxol-stabilized MTs as in Figure 1c. **(c)** Full-length DRG1 and its truncated versions lacking both the HTH and TGS domains were incubated and co-sedimented with taxol-stabilized MTs. **(d)** Structure prediction of *Xenopus* DRG1 modeled with Swiss-Model⁴⁸. Blue color represents the positively charged surface and red the negative charges (± 5 kT/e). Lower structure shows a cartoon representing the different domains using the color code from **(a)**. **(e)** Taxol-stabilized MTs were digested by the protease subtilisin and employed in the co-sedimentation assay with full-length DRG1.

Figure 4: DRG1 bundles and polymerizes microtubules *in vitro*

(a/b) 0.3 μM taxol-stabilized, Cy-3 labeled MTs were incubated with 1 μM DRG1, BSA or buffer for 10 min at RT. Samples were analyzed by confocal microscopy **(a)** or electron microscopy **(b)**. **(c)** 5 μM tubulin (mixed in a 1:4 Cy3 labeled:unlabeled ratio) were incubated with 1 mM GTP and 1 μM DRG1, BSA or buffer for 30 min at 37 °C, fixed with BRB80 buffer containing 0.25 % glutaraldehyde, 10 % glycerol and 0.1 % Triton X-100, spun down on coverslips and post-fixed with cold methanol. Samples were analyzed by confocal microscopy. MT only polymerized if DRG1 was present. **(d)** Light-scattering experiments were carried out by mixing 2.5 μM tubulin, 1 mM GTP and 1 μM DRG1 in a

96-well plate which was followed by immediately measuring absorbance at 340 nm every 38 seconds for 2:10 hours.

Figure 5: DRG1 stabilizes microtubules in the cold

(a) 12 μM tubulin was polymerized in the absence or presence of 5 μM DRG1 for 1 h at 37 °C and placed on ice for 30 min. MTs were then pelleted by centrifugation, while free tubulin stays in the supernatant. Pellet and supernatant were analyzed by SDS-PAGE. **(b)** Western blotting shows that DRG1 was knocked-down in HeLa cells stably expressing histone H2B-mCherry and eGFP-tubulin by siRNA 72h post-transfection. **(c)** siRNA treated HeLa cells were placed 72 hrs after transfection on ice for 1 hour to induce MT disassembly. Warm medium was then added to the cells which were fixed with 4 % PFA at indicated time points. Maximum intensity projections of Z-stacks from representative prometaphase cells at the given time points are shown. **(d)** The spindle size in voxels was quantified in 20 random prometaphase cells (from 2 independent experiments) per time point and siRNA (mean and SD are plotted). *** 0.001<P; ** 0.01<P; * 0.01<P. Insert shows the spindle size at 0 min enlarged.

Figure 6:

Microtubule binding, bundling, polymerization and stabilization activity of DRG1 does not require GTP hydrolysis

(a) MT co-sedimentation was done as in figure 1 with DRG1 S78N and DRG1 P73V. **(b)** MT-polymerization assay was done as in figure 5 using 1 μM DRG1 WT, S78N and P73V. **(c)** MT bundling assay was done as in figure 5 using 1 μM DRG1 WT, S78N and P73V. **(d)** DRG1 S78N and DRG1 P73V were employed in the microtubule stabilization assay as in figure 6.

Figure 7: DRG1 regulates mitotic progression and spindle assembly in cells

(a) HeLa cells stably expressing histone H2B-mCherry and tubulin-eGFP were transfected with siRNA oligonucleotides against DRG1 or a control. The cells were imaged every 3 min for 48 h starting at 24 h post-transfection. **(b)** A cumulative histogram of the timing from prophase to anaphase onset based on chromatin morphology (based on H2B-mCherry) and **(c)** of the timing from aster formation to anaphase spindle (based on eGFP-tubulin) are shown. Mean and SD from 3 independent experiments containing more than 150 cell trajectories per siRNA and experiment are plotted.

Figure 8: DRG1 plays a role in spindle dynamics *in vivo*

(a) HeLa cells were seeded on glass coverslides and transfected with DRG1 or control siRNA oligonucleotides. 72 h post-transfection cells were incubated with 70 μM monastrol with or without 2 nM taxol for 3 h³⁴, fixed and stained with antibodies against α -tubulin (green) and anti-human centromere (magenta). DAPI in blue. **(b/c)** Quantitation of cells with asymmetric asters. Z-Stacks

from five to eight random positions per condition were acquired and quantified (4 independent experiments for monastrol treatment **(b)** and two independent experiments (represented by the two dots/squares) for monastrol treatment with rescue by taxol **(c)**). Between 15 and 98 cells with monopolar spindles were evaluated per siRNA knockdown per experiment. Mean and SD are plotted. *** 0.001<P; ** 0.01<P; * 0.05<P.

Figure 2

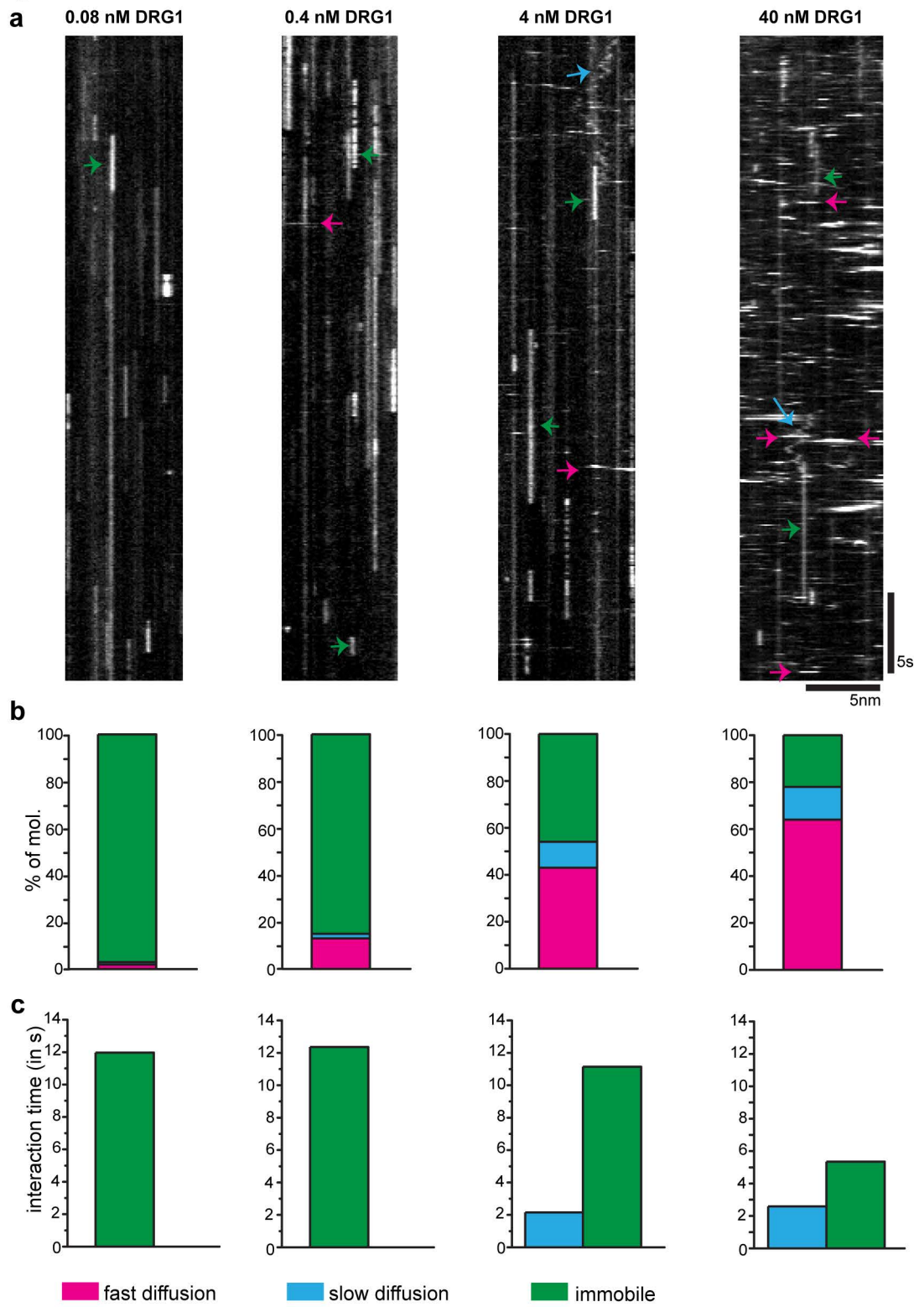


Figure 3

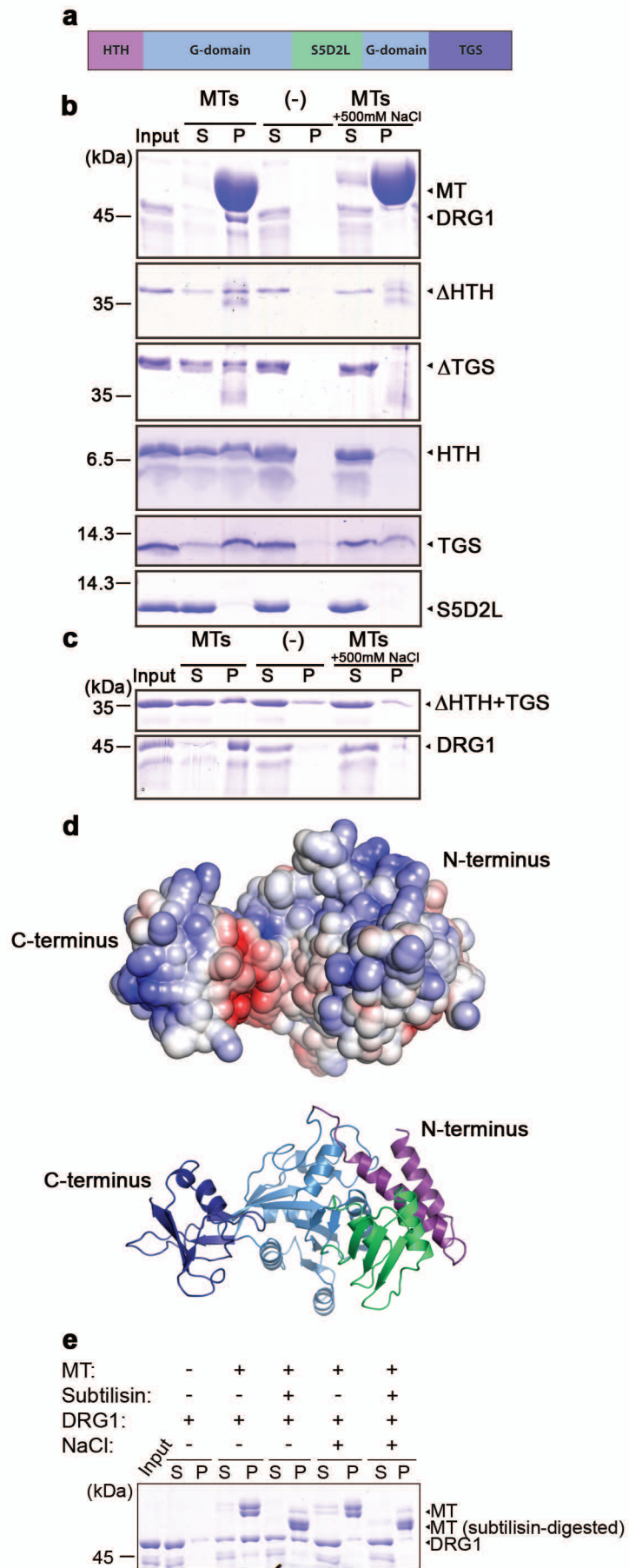


Figure 4

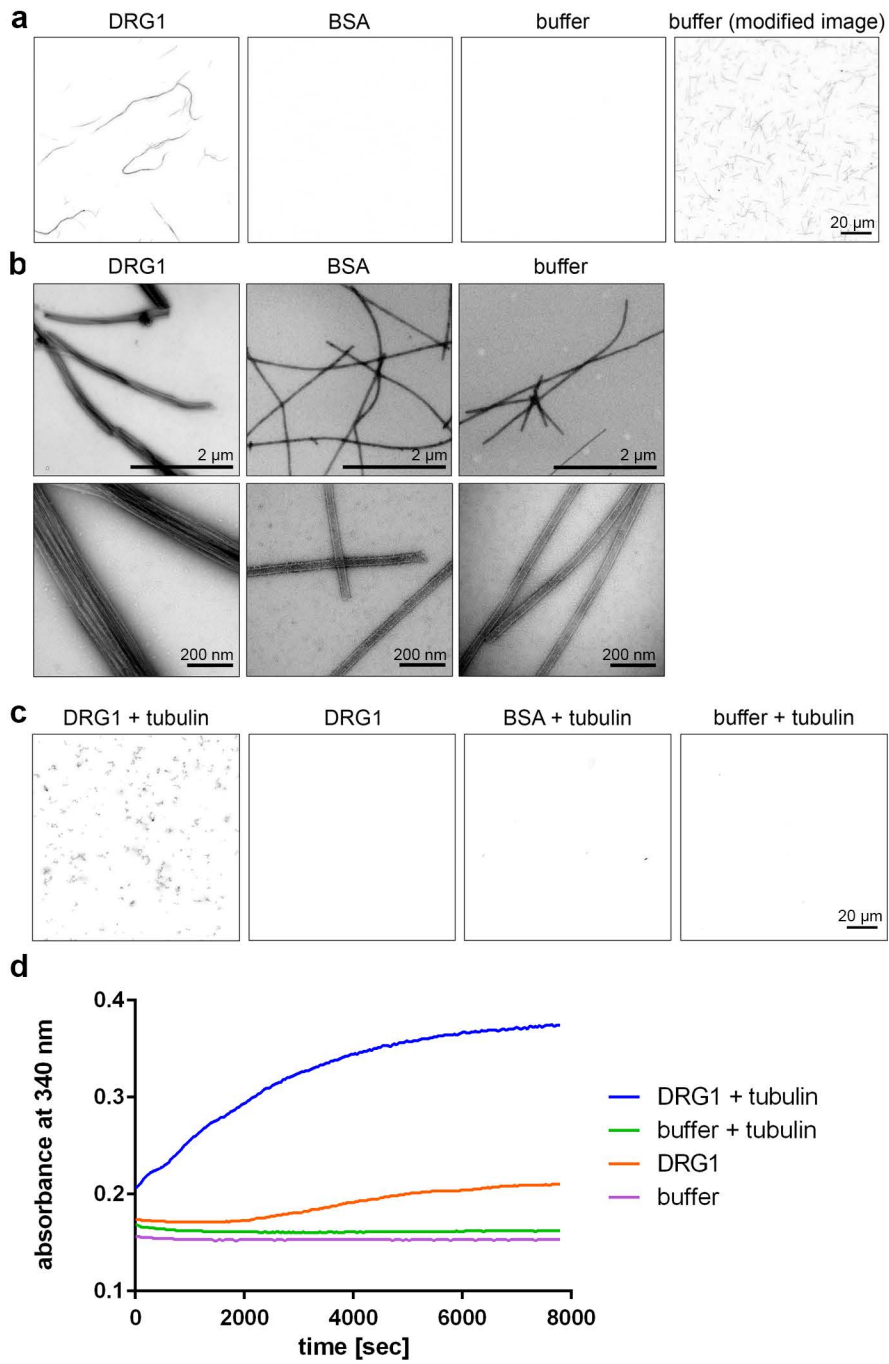


Figure 5

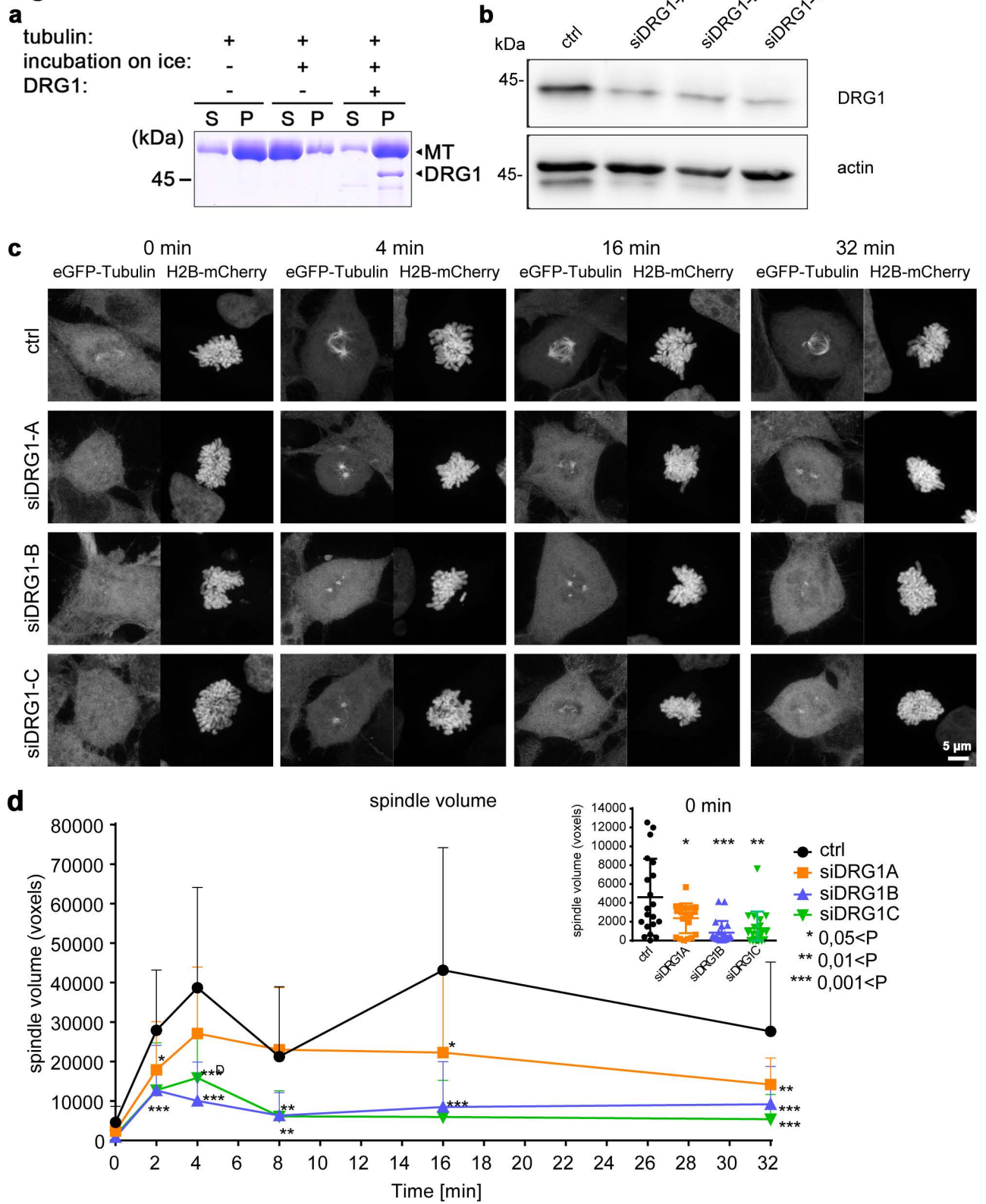


Figure 6

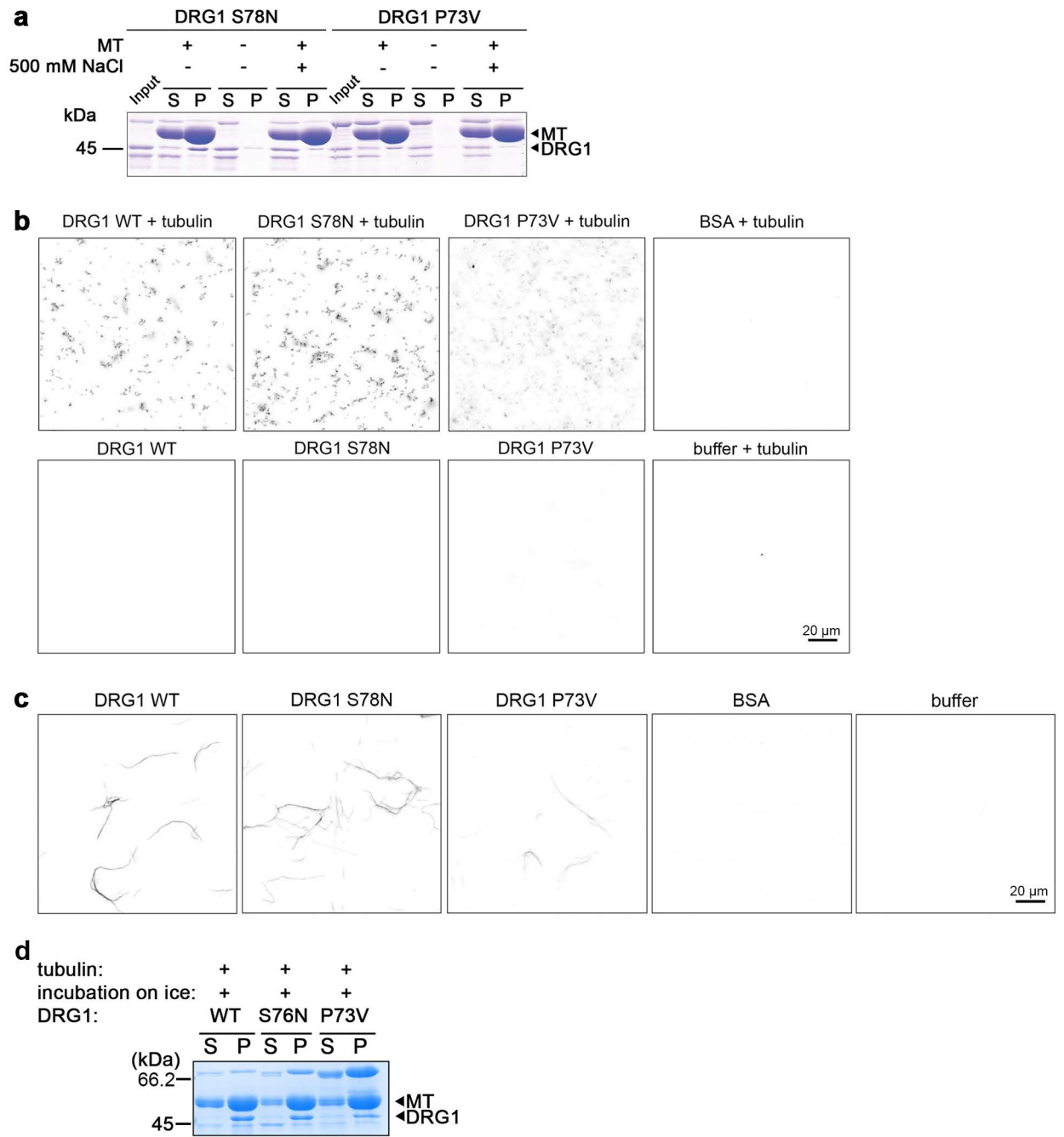


Figure 7

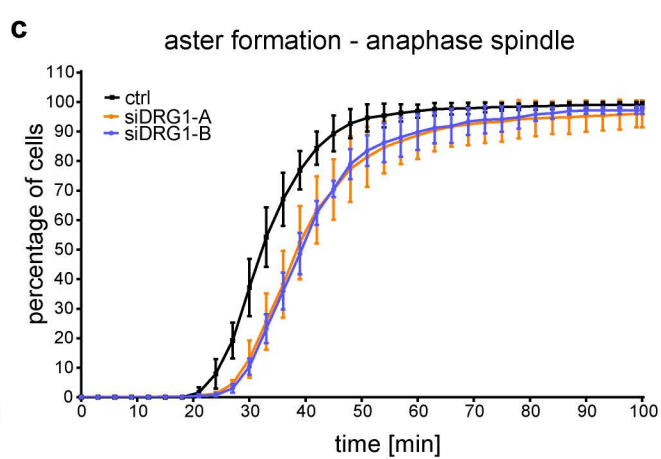
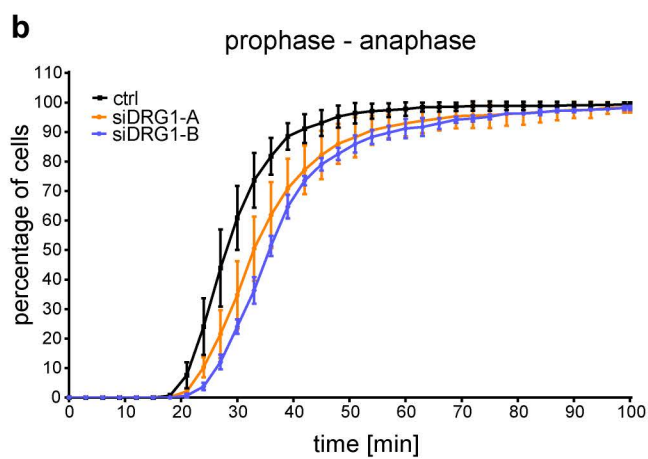
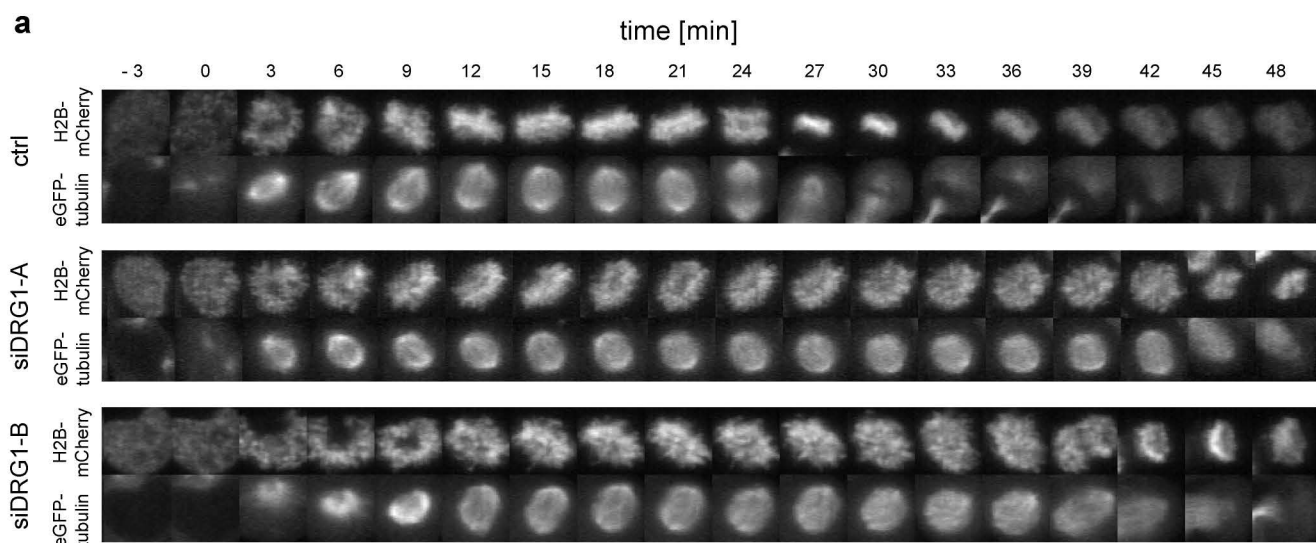
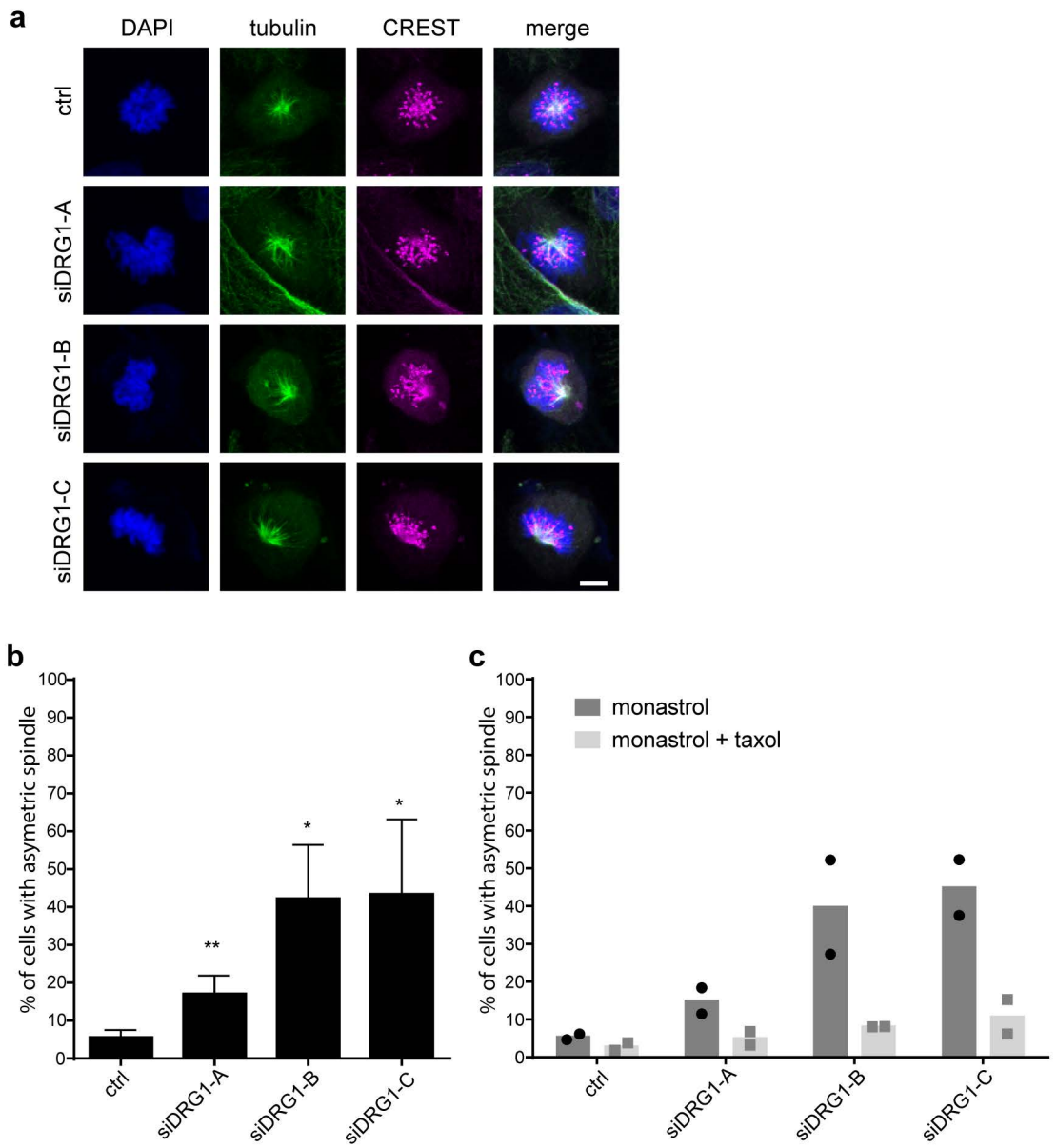


Figure 8



Developmentally Regulated GTP binding protein 1 (DRG1) controls microtubule dynamics

Anna Katharina Schellhaus (1, 2), Daniel Moreno-Andrés (1, 2), Mayank Chugh (3), Hideki Yokoyama (1, 2), Athina Moschopoulou (1), Suman De (3), Fulvia Bono (4), Katharina Hipp (4), Erik Schäffer (3), Wolfram Antonin* (1, 2)

*corresponding author

Supplemental material:

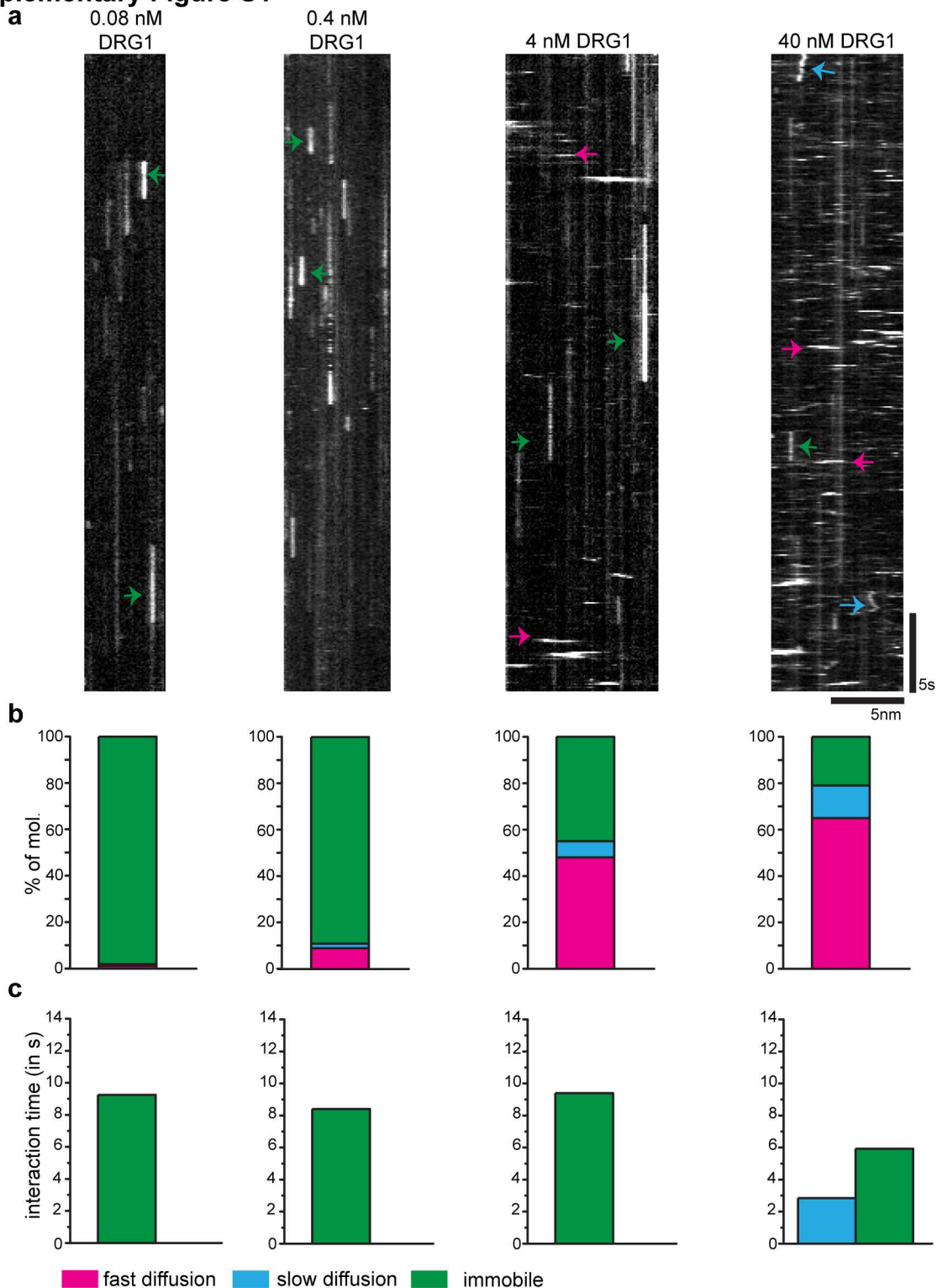
Supplementary Figure S1: The different microtubule-binding modes of DRG1 exist also in the presence of GTP γ S

Motility assays were repeated as in figure 2 but in the presence of GTP γ S. **(a)** Kymographs representing different binding modes (*fast diffusion, slow diffusion, immobile*) of eGFP-DRG1 over four different concentrations (*0.08 nM, 0.4 nM, 4 nM, 40 nM*). The proportions **(b)** and interaction times **(c)** of the different DRG1 populations are shown at aforementioned concentrations. Color scheme: fast diffusion (magenta), slow diffusion (cyan), immobile (green).

Supplementary Figure S2: Full-length DRG1 is necessary to bundle, polymerize and stabilize MTs

Truncated DRG1 versions were tested in the MT bundling **(a)** and polymerization **(b)** and stabilization **(c)** assay.

Supplementary Figure S1



Supplementary Figure S2

